# EVALUATION OF AAV8 AS A GENE THERAPY VECTOR TO DELIVER NT-3 AND $shRNA_{RhoA}$ TO INJURED DORSAL ROOT GANGLION NEURONES

by

STEVEN JOHN JACQUES

A thesis submitted to the
University of Birmingham
for the degree of
DOCTOR OF PHILOSOPHY

Molecular Neuroscience Group

School of Clinical and Experimental Medicine

College of Medical and Dental Sciences

University of Birmingham

# Abstract

Two major reasons for the failure of central nervous system axon regeneration are (i) lack of neurotrophic factors available to CNS neurones and (ii) the presence of molecules that inhibit the growth of axons. In this study a gene therapy approach using adeno-associated virus 8 (AAV8) was used to manipulate these two factors.

The following major aims were addressed: (i) confirm the bioactivity of transgenes that would be packaged into the AAV8 vector; (ii) assess the cellular tropism of AAV8 in the dorsal root ganglion (DRG); (iii) evaluate the inflammatory responses of the nervous system to AAV8 after intra-DRG and intrathecal injection; (iv) determine the axon regenerative effect of AAV8-mediated delivery of *nt-3* (a neurotrophic factor) and $shRNA_{RhoA}$ (a disinhibitory therapy) to dorsal root ganglion neurones after spinal cord injury in the rat.

Delivery of the *nt-3* transgene *in vitro* resulted in production of high levels of NT-3 protein. Transfection of $shRNA_{RhoA}$-containing plasmids into cell lines resulted in a marked decrease in the amount of RhoA detectable in cell lysates. AAV8 was found to preferentially transduce large diameter, proprioceptive DRG neurones (DRGN) but in the context of a significant inflammatory response after intra-DRG injection 28d following intra-DRG injection. Axon regenerative effects of AAV8-mediated transgene delivery before lesioning were ambiguous and further work need to be undertaken to clarify this matter.

# Dedication

This thesis is dedicated to my Dad, Paul Jacques and my late Nan, Mary Jacques. Without these two people I sincerely believe that I would not have entered academia (or gone to university, for that matter). They taught me that it is worthwhile trying to do something with your life.

Thankyou

# Acknowledgements

Science is a highly social pursuit, and exquisitely dependent upon teamwork and co-operation between workers. Thus, I would like to acknowledge (in alphabetical order) the contributions of some particularly influential people who have served to inspire, reassure, assist or instruct me. Additionally, I would like to thank the International Spinal Research Trust for funding my work.

**Ana Gonzalez** Ana is always happy to spend as much time as it takes to help you out. Her dedication to teaching and the correct practice of science have given me great inspiration.

**Andy Thewles** As the first renal physiologist on the moon (he never really talks about it), Andy knows a thing or two about science. In order to keep him happy, Thewles requires just four things: cakes, chocolate, Lasagne and empty red crates.

**Ann Logan** The long-suffering supervisor who helped me to keep my head down, and convinced me that I *would* eventually get this thing written!

**Anna Forbes** A highly competent BMedSci student who made important contributions to the analysis of the intrathecal injection experiments. She'll go far in medicine, I'm sure.

**Daljeet Mahay** A lovely person to have around in the lab, always willing to help you out. Provider of amazing samosas, but don't ask her to make you a cup of tea, though – a few too many spices in it for my taste!

**Debby Gordon** You can always tell when Debs is approaching down the corridor – the sound of army boots on linoleum is unmistakeable! Joking aside, the lab would definitely suffer if Debby (and 'mini-Debs', Chloe) was not around to sort stuff out!

**Jenna O'Neill** Hard working, but laid back, Jenna is a great example of what the correct attitude to science should be. Also, a very high threshold for frustration (as evidenced by her patience with Photoshop!)

**Kevin Morrison** A truly inspiring character and a pleasure to work with in the lab. Hilarious, kind and absolutely brimming with ideas, no lab should be without a Kev. Hail Dawkins!

**Lois Jacques** My wonderful wife who has stood patiently by my side, through the good times and bad. Thanks for being so tolerant. And yes, I *will* decorate the kitchen when this is handed in! xxx

**Martin Berry** A bona-fide representative of the 'old school' but still working at the cutting edge. Inspirational neuroanatomist and a fine role model for any budding scientist.

**Michael Douglas** Hard core clinician-scientist who is always willing to offer invaluable pearls of wisdom served with lashings of common sense.

**Sam Prince** Probably the most curious person I know. Great company on long walks home. Immensely funny with a keen analytical mind, Sam's unique "Geordie-Cornish" blend will be missed.

**Zubair Ahmed** Last, but not least Zubair. If he's got the time (i.e. not eating or at the gym) he'll always gladly help you out with anything.

Not listed above, but still endlessly inspiring we have: Barbara Lorber, Martin Read, Richard Blanch, Ruth Seabright, Wendy Leadbeater and everyone else who is a member of the Molecular Neuroscience Group at Birmingham. Additionally, there are all those people who, though not directly connected with my work, have made life that little bit more fun such as Martin Vreugdenhil and his cringe-worthy LENS meeting introductions, Darren Arbon (grower of vegetables, wearer of shorts), the ubiquitous and seemingly omnipotent Trevor Hayward and all the other people I've had the pleasure of knowing over the last 4 years.

# Table of Contents

# List of Figures and Tables

**Page numbers refer to the page that the figure comes after**

**Tables**

# Abbreviations

| | |
|---|---|
| AAV | Adeno-associated virus |
| Ad | Adenovirus |
| ADP | Adenosine diphosphate |
| AGIL | Axon growth inhibitory ligands |
| APC | Antigen-presenting cell |
| APS | Ammonium persulphate |
| ATP | Adenosine triphosphate |
| BBB | Blood-brain barrier |
| BDNF | Brain-derived neurotrophic factor |
| BSA | Bovine serum albumin |
| cAMP | Cyclic adenosine monophosphate |
| CMV | Cytomegalovirus |
| CNS | Central nervous system |
| CSF | Cerebro-spinal fluid |
| CSPG | Chondroitin sulphate proteoglycan |
| CST | Cortico-spinal tract |
| CTB | Cholera toxin B |
| DC | Dorsal column |
| d | Days |
| DAPI | 4',6-diamidino-2-phenylindole |
| DMEM | Dulbecco's modified Eagle medium |
| DMSO | Dimethylsulphoxide |
| dpl | Days post-lesion |
| DNA | Deoxyribonucleic acid |
| dNTP | Deoxyribonucleotide triphosphates |
| DREZ | Dorsal root entry zone |
| DRG | Dorsal root ganglia |
| DRGN | Dorsal root ganglion neurones |
| DSCT | Dorsal spino-cerebellar tract |
| dsDNA | Double-stranded DNA |
| ECL | Enhanced chemiluminescence |
| ECM | Extracellular matrix |
| ELISA | Enzyme linked immunosorbent assay |
| EtBr | Ethidium bromide |
| FasL | Fas Ligand |
| FBS | Foetal bovine serum |
| 5-FDU | 5-fluorodeoxyuridine |
| GAP | GTPase-activating protein |
| GDP | Guanosine diphosphate |
| GEF | Guanine-nucleotide exchange factor |
| GFAP | Glial fibrillary acidic protein |

| | |
|---|---|
| GFP | Enhanced green fluorescent protein (protein) |
| *gfp* | Enhanced green fluorescent protein (gene) |
| GTP | Guanosine triphosphate |
| h | Hours |
| HEK | Human embryonic kidney cells |
| hrGFP | Humanised Renilla green fluorescent protein (protein) |
| *hrgfp* | Humanised Renilla green fluorescent protein (gene) |
| HRP | Horseradish peroxidise |
| ICC | Immunocytochemistry |
| IFN | Interferon |
| IHC | Immunohistochemistry |
| ITR | Inverted terminal repeat |
| LB | Lysogeny broth |
| LIMK | LIM-domain containing protein kinase |
| LINGO-1 | Leucine-rich repeat and Ig domain containing |
| LMR | 67kDa laminin receptor |
| LV | Lentivirus |
| mAb | Monoclonal antibody |
| MAG | Myelin-associated glycoprotein |
| MAPK | Mitogen activated protein kinase |
| MCS | Multiple cloning site |
| MHC | Major histocompatibility complex |
| miRNA | MicroRNA |
| MLC | Myosin light chain |
| MLCK | Myosin light chain kinase |
| MOI | Multiplicity of infection |
| mRNA | Messenger RNA |
| MSC | Marrow stromal cells |
| mTOR | Mammalian target of rapamycin |
| NBA | Neurobasal-A medium |
| NDS | Normal donkey serum |
| NGF | Nerve growth factor |
| NgR | Nogo receptor |
| NT-3 | Neurotrophin 3 (protein, generic) |
| *nt-3* | Neurotrophin 3 (gene) |
| NT-4 | Neurotrophin 4 |
| NTF | Neurotrophic factors |
| NT | Neurotrophins |
| OCT | Optimal cutting temperature |
| OEPCR | Overlap extension PCR |
| OMgp | Oligodendrocyte-myelin glycoprotein |
| pAb | Polyclonal antibody |
| PBS | Phosphate buffered saline |
| PBST | PBS with Triton X-100 |
| PC12 | Rat phaeochromocytoma cells |

| | |
|---|---|
| PCR | Polymerase chain reaction |
| pDC | Plasmacytoid dendritic cell |
| PDL | Poly-D-lysine |
| PirB | Paired immunoglobulin-like receptor B |
| PKC | Protein kinase C |
| PLC | Phospholipase C |
| PNS | Peripheral nervous system |
| PVDF | Polyvinylidene fluoride |
| RGC | Retinal ganglion cell |
| rhNT-3 | Recombinant human neurotrophin 3 (protein) |
| Rho-GDI | Rho-GDP dissociation inhibitor |
| RISC | RNA-induced silencing complex |
| RNA | Ribonucleic acid |
| RNAi | RNA interference |
| ROCK | Rho-associated kinase |
| rt | Room temperature |
| s | Seconds |
| SCI | Spinal cord injury |
| SDS | Sodium dodecyl sulphate |
| SDS-PAGE | SDS-polyacrylamide gel electrophoresis |
| shRNA | Short hairpin RNA |
| siRNA | Small interfering RNA |
| ssDNA | Single-stranded DNA |
| STT | Spino-thalamic tract |
| TACE | TNFα converting enzyme |
| TBS | Tris buffered saline |
| TBST | Tris buffered saline with Tween-20 |
| TEMED | Tetramethylethylenediamine |
| TGF-β | Transforming growth factor β |
| TID | Trypsin inhibitor cocktail |
| TLR | Toll-like receptor |
| TMB | 3,3´,5,5´-tetramethylbenzidine |
| Trk | Tropomyosin-like receptor kinase |
| TROY | TNFRSF expressed on the mouse embryo |
| TTBS | Tris buffered saline with Tween-20 |
| WB | Western blot |
| YFP | Yellow fluorescent protein |

# Chapter 1

# Introduction

## 1.1 Spinal cord injury – defining the problem

Spinal cord injury (SCI) is an important source of chronic morbidity and mortality in the developed and developing world. It is such an important problem because the majority of SCI patients were previously fit, healthy young people who frequently become condemned to a life of disability, pain, loss of dignity and inability to work.

Worldwide, around 3 million individuals are living with a spinal cord injury, with an estimated incidence of 130 000 new cases per year (ICCP 2010). Around 80% of cases of SCI are in men, with the peak age being 30-50 years. In the developed world the majority of cases are due to road traffic accidents as opposed to the developing world, where falls account for the majority of injuries to the spinal cord (Chiu, Lin et al.).

### 1.1.1 The extent of the problem

SCI is not merely a physical problem. It affects all aspects of the patient's life, with significant psychological, social and economic implications. Patients with SCI frequently are not able to work and consume a significant proportion of the health service budget. Current treatments are predominantly based around rehabilitation and symptom control, offering only minimal functional improvements over what the patient would experience spontaneously. Having said this, however, the mortality rate from SCI has fallen considerably over the last 100 years as the multifactorial and highly complex nature of this condition has been increasingly recognised (Tremblay 1995).

#### 1.1.1.1 Mechanisms of injury

The brain and spinal cord are protected from injury by the robust axial skeleton, composed of the skull and vertebrae. The bony components of this structure are anchored to each other by strong ligaments and thick layers of muscle. Thus, injury to the spinal cord typically results from high energy impacts such as road traffic accidents and falls from some height. These injuries lead to fractures and/or dislocations of vertebrae, with resultant compression, twisting or pulling of the cord.

As well as traumatic aetiologies, SCI can be caused by a variety of other pathologies including tumours, degenerative and inflammatory conditions, infections and ischemia (McDonald and Sadowsky 2002). Regardless of the mechanism, however, functional deficits will often ensue after even relatively mild insults to the cord.

#### 1.1.1.2 At-risk groups and prevalence of morbidity

SCI typically affects men in their twenties or thirties, with a much lower incidence in children and older age groups. This pattern is usually attributed to the fact that young men are at a higher risk of engaging in activities such as outdoor pursuits and reckless driving. Another important cause of SCI in young men is violent crime, seen at relatively high rates in some sectors of the community. Having said that, the paediatric and elderly groups also contribute to the burden caused by central nervous system (CNS) injuries due to conditions such as cerebral palsy, strokes and falls.

The effects of SCI, however, are much more wide-ranging than paralysis; so much so that SCI can be considered as a systemic disease with effects on almost all systems

of the body. Long-term sequelae affect the cardiovascular, respiratory and genitor-urinary systems, leading to pathologies such as pneumonia, urinary tract infections and bedsores (Zeilig, Dolev et al. 2000).

#### 1.1.1.3 How SCI research can inform other areas

Some may argue that SCI, despite its grave consequences, is a relatively uncommon condition and so may not warrant very high levels of research funding. This point of view, in the author's opinion, fails to acknowledge the far-reaching and eclectic impact of CNS regeneration research. For example, work on myelin neutralisation therapies is showing considerable promise in stroke – a common and devastating illness (Gillani, Tsai et al. 2010). Also, advances in the understanding of Rho proteins are being used in developing treatments for cancers and the modulation of angiogenesis (Merajver and Usmani 2005).

### 1.1.2 Spinal cord injury in more detail

One of the major illustrations of how research into SCI can inform other areas, such as stroke or cerebral palsy, is that the injury response of the CNS is fairly uniform across different regions such as the optic nerve, brain and spinal cord. It is this generic response to CNS damage that the following section is devoted to. The reader is referred to section 1.1.2.3.2.2 for more specific details concerning the dorsal column (DC) crush model.

#### 1.1.2.1 The CNS injury response to penetrating trauma

One of the best characterised models for examining CNS injury responses employs the cerebral stab method, whereby the brain is exposed and the cortex penetrated using a scalpel blade mounted in a stereotactic instrument (Logan, Green et al. 1999). This model has been used extensively to study the basic mechanisms of the CNS injury response, as well as to examine the efficacy of anti-scarring reagents. The phenomenology of the injury response using this model can be successfully extrapolated to the DC crush model (used as the experimental paradigm in the present study), since both breach the meninges, both involve sharp transection, both sever axons and both lead to extensive glial activation and scar formation.

Three stages of the CNS injury response have been defined in adult rat models, based on time after lesioning: the acute (0-3 days post-lesion (dpl)), sub-acute (3-8 dpl) and consolidation (8-20 dpl) phases. The reader is referred to an excellent, although no longer current, volume describing the changes discussed below in much greater detail (Berry and Logan 1999).

***The acute phase***

The acute phase is characterised by extensive haemorrhage into the lesion site, with breach of the blood-brain barrier (BBB), the blood-cerebrospinal fluid (CSF) barrier and the brain-CSF barrier. Blood and CSF are known to contain many components, both cellular and acellular, which are involved in initiating and modulating the CNS injury response. For example, platelets carry Transforming Growth Factor β (TGF-β), which is known to have a significant role in scar-tissue formation. Monocytes

deposited in the lesion become transformed into active macrophages. Additionally, serum and CSF carry a number of growth factors which can lead to macrophage activation and fibroblast recruitment. The influx of these molecules initiates a molecular cascade which serves to initiate, modulate and perpetuate the injury response. Modification of this 'cytokine cascade' is an active area of SCI research.

***The subacute phase***

The subacute phase is characterised by the clearance of necrotic debris from the lesion site by macrophages, and the increasing recruitment and activation of glial cells. The lesion core becomes walled off (and hence the BBB restored) by an accessory glia limitans, orchestrated by activated astrocytes at the wound margin. Meningeal fibroblasts begin to invade the lesion core, depositing extracellular matrix (ECM) components such as collagens, chondroitin sulphate proteoglycans (CSPGs) and laminin, which will form the bulk of the glial scar.

***The consolidation phase***

This phase, variable in length, is characterised by contraction of the lesion core and a decreased level of glial activation. The accessory glia limitans becomes increasingly thick and organised, and the number of cells within the lesion core decreases, leaving a collagen, CSPG and fibronectin-rich scar. Axons are seen not to traverse the lesion core or to accumulate in great numbers at the lesion margins. Thus, the CNS injury response is complete, and the lesion can be said to have entered the chronic stage.

#### 1.1.2.2 Immediate *versus* late responses to CNS injuries

With respect to most human cases of SCI, the events described above constitute only a small fraction of the length of time the patient is alive post-injury. It is known that a number of additional events take place in the months to years following CNS injuries. Some of these processes are advantageous to the patient (e.g. neural plasticity leading to limited spontaneous functional recovery), but most lead to further problems, and can be progressive unless treated, such as post-traumatic syringomyelia (Brodbelt and Stoodley 2003) and progressive demyelination (Blight 1985). Particularly worrying for the researcher hoping to use reparative growth factors as therapeutics is the possibility of exacerbating post-SCI neuropathic pain, a condition which is known to lead to significant morbidity within the spinally injured community.

#### 1.1.2.3 Injury models

Animal models of CNS injuries have been in use for well over 100 years, and they continue to provide valuable new insights. However, it must be born in mind that no single model of SCI currently in use is perfectly suited to answering all of the questions that remain to be answered. Each model is particularly suited to answering a particular set of questions, and comes with its own unique strengths and limitations which must be considered when interpreting research data. Furthermore, technical aspects of experimental design, such as species used, animal numbers, controls and outcome measures, have a vital bearing on the applicability of results to human SCI. The reader is referred to two excellent review articles from the groups of

Tetzlaff and Tessier-Lavigne concerning technical aspects of *in vivo* SCI experimental design (Kwon, Oxland et al. 2002; Steward, Zheng et al. 2003).

#### 1.1.2.3.1 A brief survey of SCI models

Animal models of SCI can be categorised as either sharp or blunt, which can be further split into complete or partial. To perform competently, all require a great deal of technical skill and high quality apparatus to ensure that results are maximally valid and animal suffering is kept to a minimum.

##### 1.1.2.3.1.1 Complete transections

Experiments employing complete transections of the cord form a relatively small proportion of all published reports of SCI work. This is probably due to a number of factors, both technical and translational. Firstly, most human SCI is partial due to the fact that the spinal cord is well protected within the vertebral column, and dislocations of the spine adequate to fully transect the cord are rare. Thus, any results from complete transection models are unlikely to extrapolate to the SCI patient community as a whole. Having said that, any axon regeneration seen using such a model is likely to be indicative of a highly robust treatment effect which would certainly warrant further investigation.

From a technical point of view, complete transections tend to be much more labour intensive, and hence more costly, than partial lesions, due to the intensive care animals require after injury (e.g. manual voiding, locomotor problems). However, this additional cost may be abrogated by the probable requirement for smaller animal

numbers, since complete lesions are inherently less variable in extent than partial ones.

Another problem experienced with complete transections is that the two ends of the cord tend to naturally separate from one another after lesioning. Such a situation almost certainly leads to a highly inhospitable environment for regenerating axons, and means that such experiments are likely to require bridging strategies to demonstrate any effect of a therapeutic on axon regeneration.

Finally, ethical reasons must be considered when planning which kind of lesion to perform in animals. Complete transections lead to significant loss of function, and animals need much more intensive care after such lesions. Partial lesions tend to have much less profound functional consequences on experimental animals and are preferred from an ethical point of view.

#### 1.1.2.3.1.2 Partial transections

These are by far the most popular type of lesion performed in the experimental spinal cord injury research community. They are more representative of human SCI and do not necessitate bridging strategies or intensive postoperative care. However, experiments using partial transection models require a highly rigorous design, and are frequently open to criticisms concerning the plausibility of any axon regeneration seen.

Partial transections usually involve a specific, defined tract or tracts within the white matter of the spinal cord. This is advantageous, and such lesions lend themselves to neuroanatomical tract tracing methods, behavioural outcome measures and neurophysiological testing. However, confounding factors abound in such experiments due to the phenomena of axon sparing and synaptic plasticity.

Axon sparing refers to the preservation of some axons within a lesion. This may be due to a lesion being incomplete (e.g. only transecting 1mm of a 1.5mm tract), or that axons within the core of the lesion have just been disrupted rather than transected (e.g. by applying an inadequate compressive force). Either way, one may see axons distal to the lesion and conclude that they have regenerated. It is possible to account for this if the experiment is designed rigorously.

Before conducting any experiments, one must ensure that the lesion will transect all of the axons in question in an animal of a particular species at a particular age. Thus, one requires an appreciation of the location and physical dimensions of the tract of interest, its developmental dynamics and any interspecies neuroanatomical variation. Ideally, the lesion should be performed using a mechanical device, appropriately calibrated, or at the very least by hand by an experienced operator with graduated instruments to ensure consistent lesion size.

Axon sparing may be excluded at the analysis stage of an experiment by looking for the presence of an anterograde tracer at the distant target of the transected axon. For example, in the DC crush model (described below), cholera toxin B (CTB) is

injected into the sciatic nerve 2d before killing the animal. This is adequate time to completely fill a large proportion of transected axons. Providing that the time frame is appropriate (see below), no CTB should be seen in the gracile nucleus. From this, one can conclude that the lesion was complete.

As mentioned above, the amount of time between lesion and tracer injection/sacrifice must be chosen carefully (Steward, Zheng et al. 2003). Killing the animal too soon after lesioning may give a spurious negative result, since axons are likely to require some time to recover after injury whether they ultimately regenerate or not. In the case of an efficacious treatment where axons regenerate to their distant targets, waiting too long post injury may lead one to incorrectly conclude that the lesion was incomplete.

Synaptic plasticity as a confounding factor in partial SCI models, tends to mainly affect experiments with behavioural outcome measures. Virtually all spinal cord injuries, whether in man or other animals, show some degree of spontaneous recovery. Even after complete transections, rats can walk with appropriate training and pharmacological intervention (Kwon, Oxland et al. 2002). Of course, such effects can be controlled for, but one must be mindful of treatments given to stimulate axon regeneration but which are also able to affect plasticity. Axon regeneration and plasticity are closely related phenomena (Cafferty, McGee et al. 2008).

#### 1.1.2.3.1.3 Contusions

The majority of blunt transections are performed by transiently compressing the exposed spinal cord using a known force (contusion). Such injuries usually employ sophisticated pieces of apparatus which are capable of delivering a precisely controlled amount of energy, for example the New York University Impactor (Kwon, Oxland et al. 2002). Spinal cord contusion models reflect human pathology very closely, not only in their mechanism of injury but also in the pathological features seen. They are able to produce remarkably consistent and reproducible injuries, the effects of which can be monitored successfully using behavioural techniques. However, they are limited with respect to assessing anatomical axon regeneration since, although the clinical effects are consistent, specific tracts cannot be precisely and completely transected. Thus, one is left with the issue of spared axons discussed above.

#### 1.1.2.3.1.4 Sharp transections

Models using sharp transection techniques can deliver well-defined anatomical lesions to given white matter tracts, lending themselves to the use of neuroanatomical techniques to monitor axon regeneration. Performed correctly, such lesions display minimal variability in extent. However, there are a number of disadvantages to using these models. Firstly, there is the issue that only a minority of human SCI is due to sharp transections (e.g. stabbing). Thus, any experiments employing such techniques may need to be repeated using a more appropriate model (e.g. contusion). Secondly, these lesions are often technically demanding requiring detailed knowledge of neuroanatomy. In order to perform a sharp

transection, one must usually penetrate the dura and arachnoid maters, leaving a CSF leak which may confound experiments.

#### 1.1.2.3.2 The DC crush model

The model used in this study to examine the axon regenerative effects of therapeutics is the DC crush. This can be classified as a sharp, partial transection of the spinal cord. Despite the term 'crush', axons are seen to have been immediately transected after lesioning (see section 2.2.3). This lesion transects two well defined white matter tracts and has been used previously in studies of cellular responses to injury and axon regeneration (Dusart and Schwab 1994; Lagord, Berry et al. 2002; Alto, Havton et al. 2009).

##### 1.1.2.3.2.1 Anatomy relevant to the DC crush model

The reader is reminded that further detail concerning rat and human neuroanatomy is available from a number of sources (Craigie, Innes et al. 1963; Standring and Gray 2008; Watson 2009). Unless otherwise stated, all neuroanatomy described is that of *Rattus norvegicus*.

***Spinal cord***

At its most fundamental level, the spinal cord can be described as a segmented, cylindrical extension of the brain containing a central core of grey matter surrounded by an outer layer of white matter. The grey matter of the spinal cord is composed mainly of lower motor neurone cell bodies, directly innervating muscles; and second order sensory neurone cell bodies projecting to the thalamus. The white matter of

the spinal cord contains descending projections which act to modulate the activity of lower motor neurones and sensory neurones, and ascending projections, which can be either from first or second order sensory neurones. Furthermore, the spinal cord is known to contain many interneurones, which travel within propriospinal pathways. The white matter can be subdivided into three major regions (dorsal, lateral and ventral funiculi), containing defined subpopulations of neuronal projections (Figure 1.1 A).

The boundaries of the dorsal funiculus are the pial surface of the spinal cord dorsally, the dorsal horns laterally and the central grey matter containing the central canal ventrally. In the rat, the dorsal funiculus contains two major axonal populations: the ascending dorsal columns and the descending corticospinal tracts. In man, the corticospinal tracts are found in the lateral and ventral funiculi.

Strictly speaking, a lesion of the dorsal funiculus has been performed in this study, since a lesion depth of 1.5 mm includes dorsal columns, corticospinal tracts and grey matter adjacent to the central canal (see section 2.2.3). However, the author refers to a 'DC lesion', since it is the neurones of the DC that have been examined for any evidence of axon regeneration.

***DRG and dorsal roots***

Each spinal cord segment has two corresponding dorsal root ganglia (DRG), connected to it by a pair of dorsal roots (Figure 1.1 B). In simple histological preparations, one is able to observe many dorsal root ganglion neurones (DRGN),

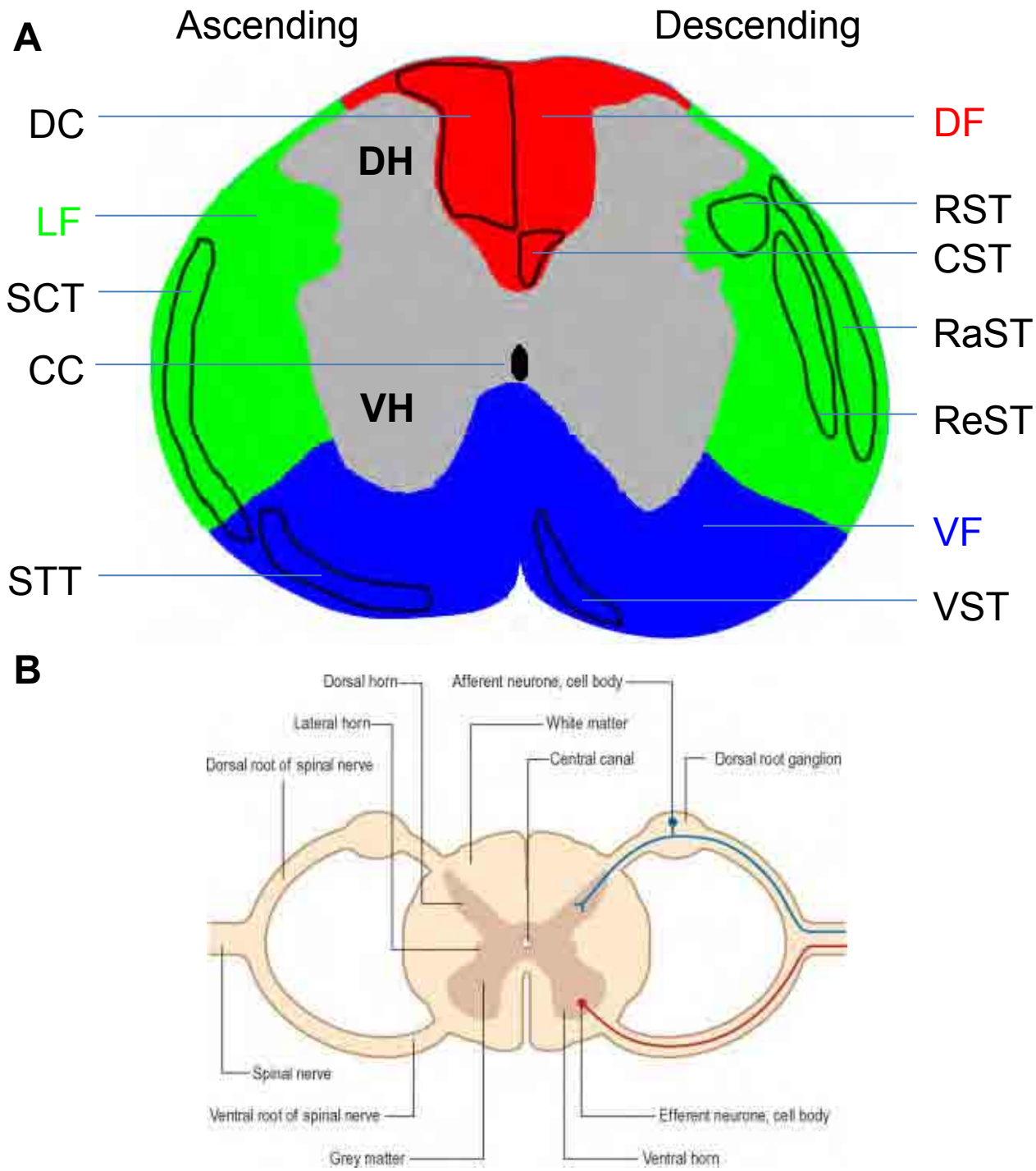


**Figure 1.1**. Arrangement of the white matter and immediate peripheral connections of the rat spinal cord. **A**. Transverse section at the L1 cord level, showing the funiculi and ascending and descending tracts. CC: central canal, CST: corticospinal tract, DC: dorsal column, DF: dorsal funiculus, LF: lateral funiculus, RaST: raphespinal tract, ReST: reticulospinal tract, RST: rubrospinal tract, SCT: spinocerebellar tracts, STT: spinothalamic tract, VF: ventral funiculus, VST: vestibulospinal tract. Dorsal funiculus in red, lateral funiculus in green and ventral funiculus in blue. Adapted from figure 14.1, Watson 2009. **B**. Schematic of a transverse section through the lumbar cord, roots, DRG and spinal nerve showing the arrangement of white and grey matter and the trajectory of DRGN and motor neurone axons. From Standring 2008.

each surrounded by a layer of satellite cells (Figure 1.2). Also present are myelinated and unmyelinated fibres, blood vessels, connective tissue components and very occasional macrophages. DRGN contact sensory end-organs and are of considerable interest since, despite the fact that they are part of the peripheral nervous system (PNS), they have projections to both CNS and PNS (see section 1.4.4.2 for further details).

DRGN are a heterogeneous population, and have been classified by many different and often overlapping methods such as size, protein expression, sensitivity to toxins and electrophysiology (Willis and Coggeshall 2004). The commonest classification splits DRGN into small and large cell body diameter populations, with large diameter DRGN tending to have large, fast-conducting axons and small DRGN having small, slower conducting axons (Harper and Lawson 1985). Fast-conducting axons are associated with functions such as proprioception and discriminative touch, whilst nociceptive fibres tend to have small, slow-conducting axons (Willis and Coggeshall 2004).

Satellite cells are by far the most common resident cell of the DRG (Landon 1976). They surround DRGN cell bodies and the initial segment of DRGN axons, usually in single layers (Pannese 1994). The function of satellite cells is yet to be fully elucidated, although a large amount of data point towards roles in regulation of the extracellular milieu, responses to circulating substances, responses to injury and barrier functions (Hanani 2005). See Chapter 4 for a more in-depth discussion of some of these points.

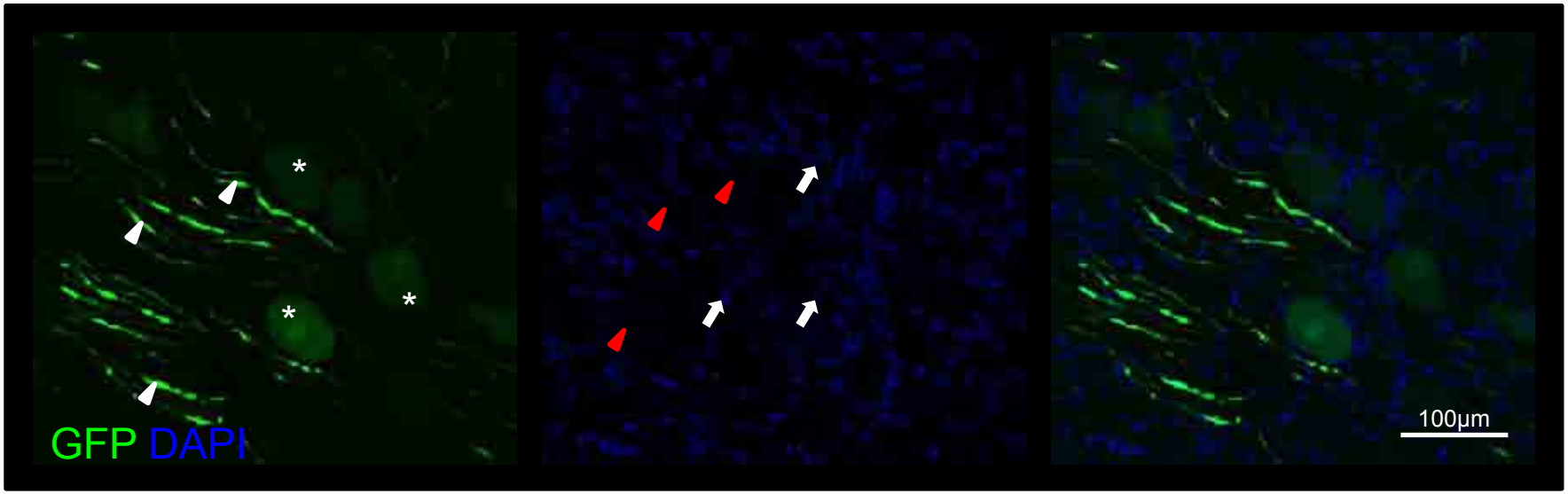


**Figure 1.2**. Confocal microscopic appearance of the adult rat DRG after intra-DRG injection of AAV8$_{egfp}$. GFP$^{+}$ DRGN cell bodies (*) and axons (white arrowheads) are clearly visible, with associated nuclei of perisomatic satellite cells (white arrows) and periaxonal Schwann cells (red arrowheads).

The dorsal roots contain central projections of DRGN, destined for the dorsal horn or DC. Axons are myelinated by Schwann cells, surrounded by a connective-tissue layer. The point of transition to CNS tissue, where axons are myelinated by oligodendrocytes, is at the dorsal root entry zone (DREZ), directly adjacent to the spinal cord.

***Spinal nerves***

The peripheral projections of DRGN, emanating from the DRG, converge with the ventral root just proximal to the intervertebral foramina and emerge as the spinal nerves. Spinal nerves usually enter plexuses such as the sacral plexus, ultimately forming major branches such as the sciatic nerve (Figure 1.3). Within spinal nerves, axons are myelinated by Schwann cells and there is a functional blood-nerve barrier which serves to protect the enclosed axons from chemical insults. Spinal nerves regenerate damaged axons readily, although function is often not completely restored.

It is not known why regeneration is less successful in the CNS compared with the PNS, although certain anatomical and molecular factors contribute including the presence of basal lamina tubes in the PNS along which axons can grow and differences in neuronal growth state and mechanisms of axon degeneration after PNS injury compared to CNS injury (Huebner and Strittmatter 2009).

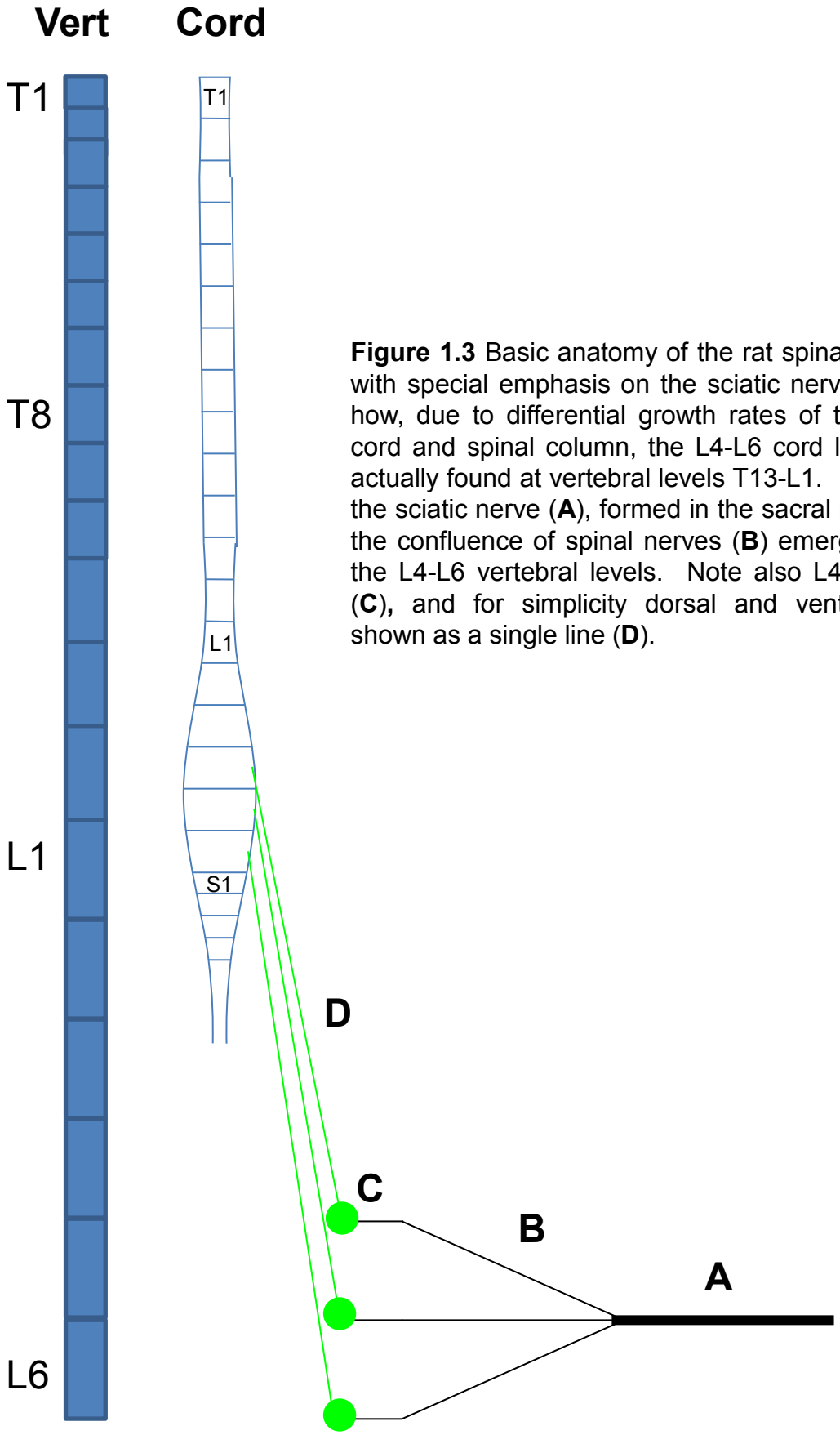


**Figure 1.3** Basic anatomy of the rat spinal column, with special emphasis on the sciatic nerve. Note how, due to differential growth rates of the spinal cord and spinal column, the L4-L6 cord levels are actually found at vertebral levels T13-L1. In the rat, the sciatic nerve (**A**), formed in the sacral plexus by the confluence of spinal nerves (**B**) emerging from the L4-L6 vertebral levels. Note also L4-L6 DRG (**C**), and for simplicity dorsal and ventral roots shown as a single line (**D**).

### *Central projections of DRGN*

Three major 'classic' pathways exist that convey afferent information from the periphery to the brain: the DC pathway (Figure 1.4), the spinothalamic tract (STT; Figure 1.5) and the dorsal spinocerebellar tract (DSCT; Figure 1.6). These pathways have been described in great detail elsewhere (Craigie, Innes et al. 1963; Willis and Coggeshall 2004; Standring and Gray 2008). In addition to these there are a plethora of other pathways whose roles have not yet been elucidated comprehensively (Willis and Coggeshall 2004). The following section aims just to describe the central projections of the first order neurone (i.e. the DRGN) in these pathways, since it is these that are predominantly transected in the DC crush model.

First order projections of all three major pathways originate from sensory structures found in organs such as the skin (e.g. Pacinian corpuscles), joints (joint capsule endings), muscles (muscle spindles) and tendons (Golgi tendon organs). These structures are innervated by the peripheral projection of DRGN, the impulse being conveyed to the spinal cord *via* the central projection in the dorsal root. All first-order sensory neurones (i.e. DRGN) project ipsilaterally in the cord. In the STT and DC pathway, the second order neurone is found in the dorsal horn and the dorsal column nuclei, respectively. Second-order neurones decussate at approximately the level of entry of the first order neurone in the case of the STT, or in the internal arcuate fibres of the medulla in the DC pathway.

The DSCT takes its origin from second order neurones lying in Clarke's column, a group of cells found deep within lamina V of the dorsal horn, in the thoracic and

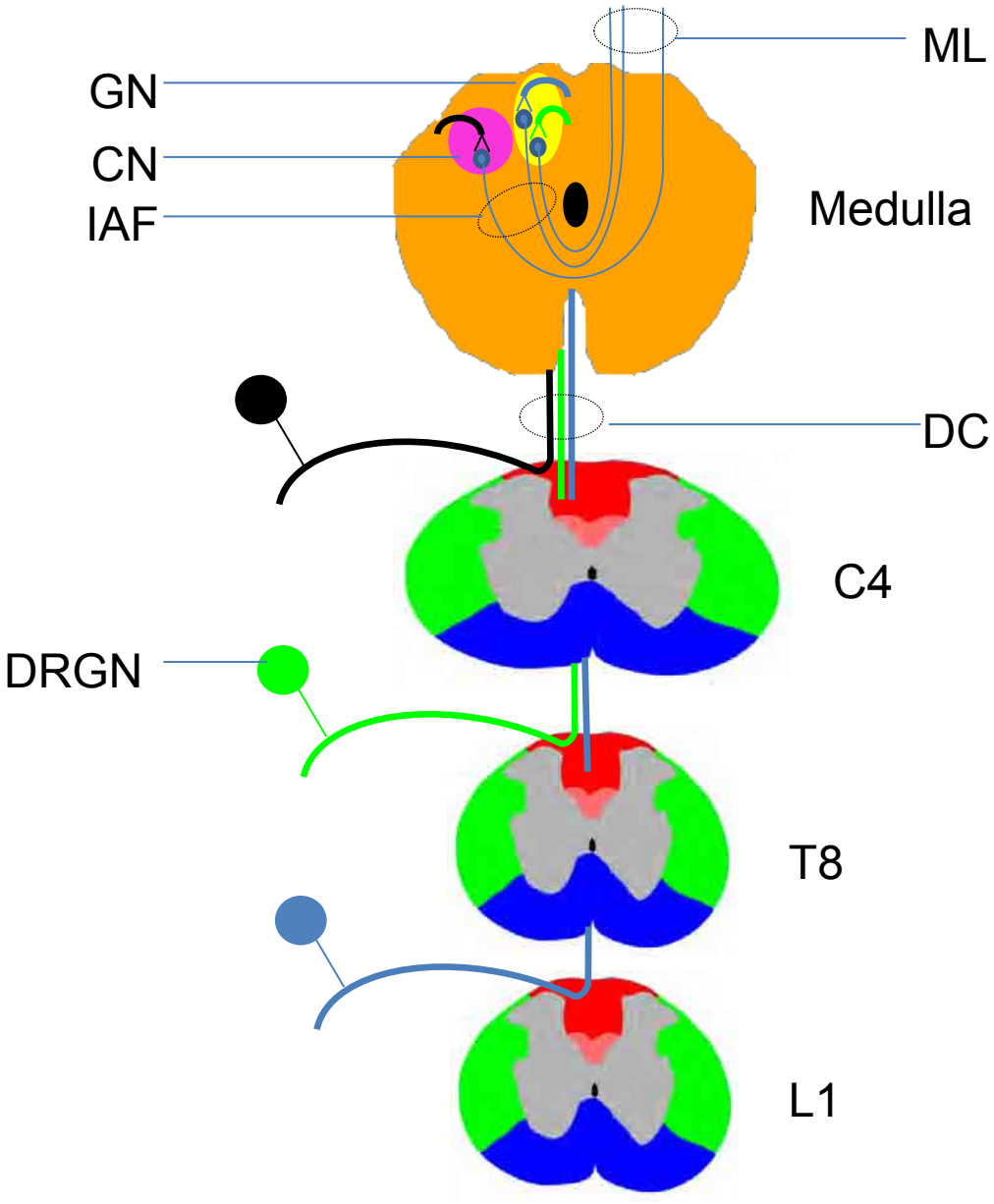


**Figure 1.4**. The dorsal column-medial lemniscus pathway. Note that (i) DC fibres arising from successively rostral cord segments are added *laterally* to the DC; (ii) within the cord, the DC pathway is entirely ipsilateral; (iii) second-order neurones reside within the GN for the lower half of the body and CN for the upper half; (iv) IAF project to the thalamus *via* the ML. CN: cuneate nucleus; DRGN: dorsal root ganglion neurone; DC: dorsal column; GN: gracile nucleus; IAF: internal arcuate fibres; ML: medial lemniscus. Dorsal funiculus in red, lateral funiculus in green, ventral funiculus in blue.

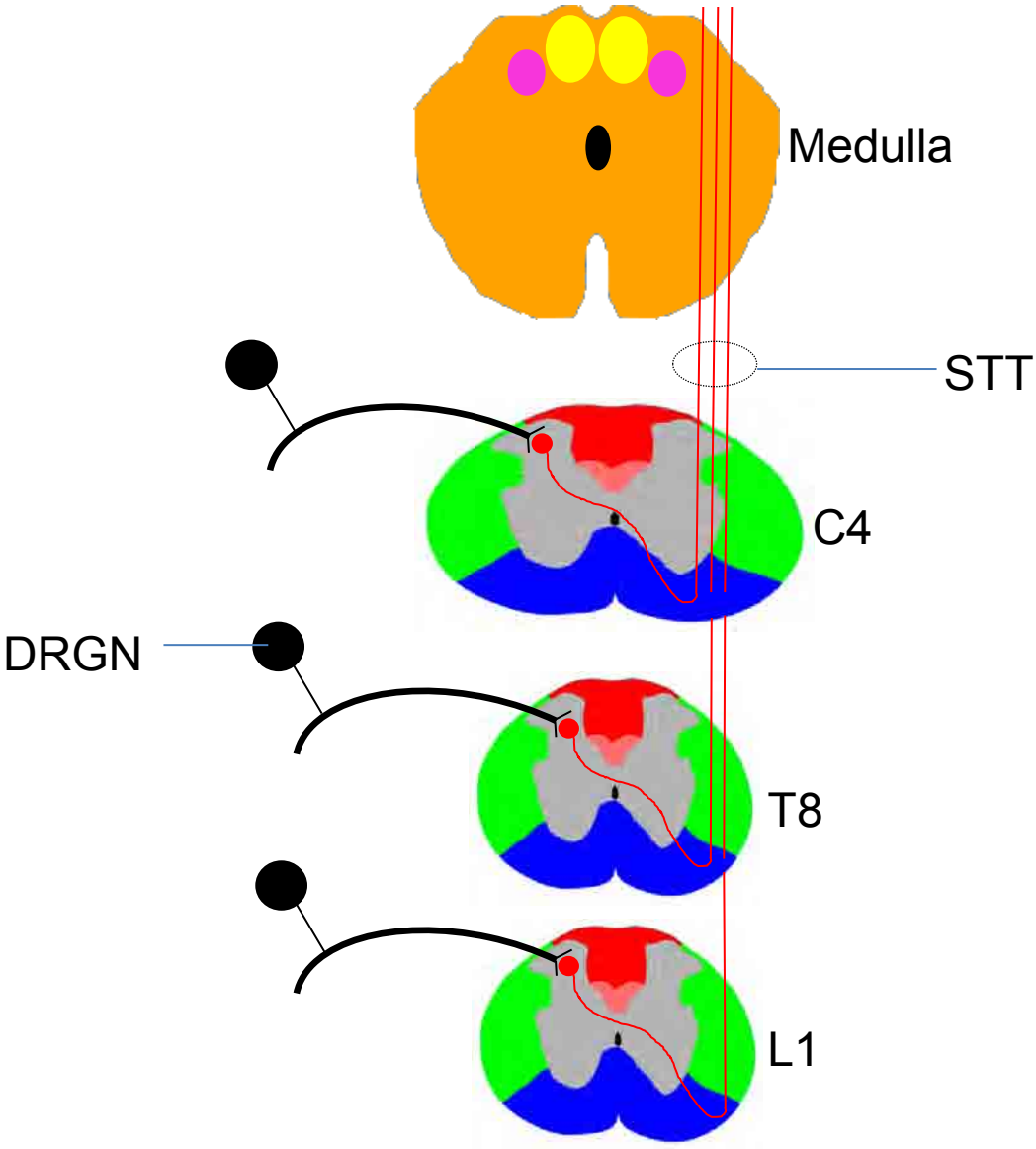


**Figure 1.5**. The spino-thalamic tract. Note that (i) Fibres arising from second-order neurones from successively rostral cord segments are added *medially* to the STT; (ii) within the cord, the STT is contralateral to first-order neurones; (iii) second-order neurones reside within the dorsal horn. DRGN: dorsal root ganglion neurone, STT: spino-thalamic tract. Colour scheme showing funiculi is as described in Figure 1.1.

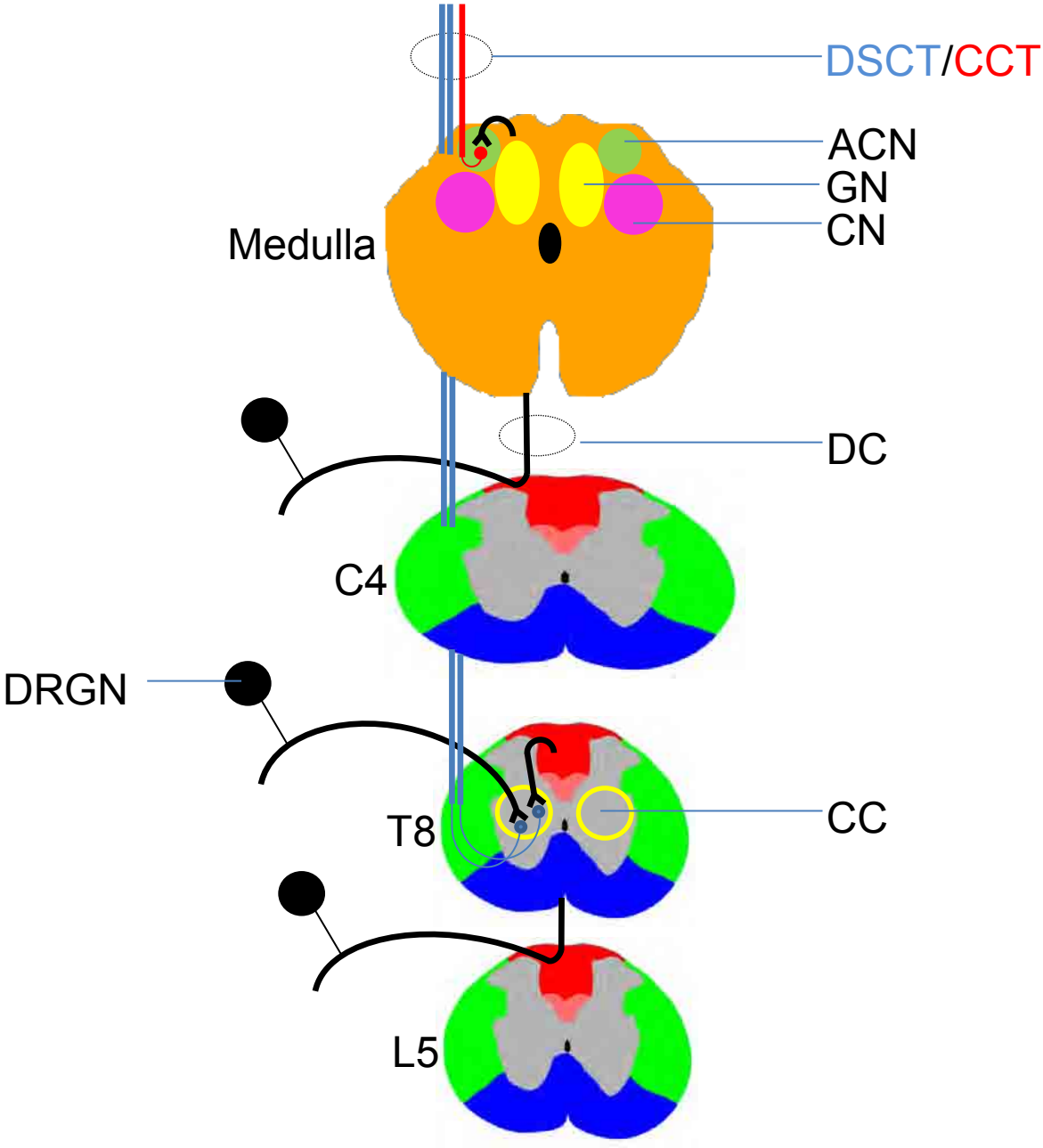


**Figure 1.6**. The dorsal spino-cerebellar tract. Note that (i) DRGN with central projections entering the lower lumbar cord ascend in the DC; (ii) CC is found in the lower cervical, thoracic and upper lumbar cord and contains second order neurones that project axons in the DSCT; (iii) DRGN whose central projections enter the upper and mid-cervical cord ascend in the DC to synapse with second-order neurones of the ACN in the medulla; (iv) Neurones of the ACN project medial to the DSCT to the cerebellum. ACN: accessory cuneate nucleus; CC: Clarke's column; CCT: cuneocerebellar tract; CN: cuneate nucleus; DC: dorsal column; DRGN: dorsal root ganglion neurone; DSCT; dorsal spinocerebellar tract; GN: gracile nucleus. Colour scheme showing funiculi is as described in Figure 1.1.

upper lumbar segments. First order neurones project to Clarke's column within the dorsal funiculus; thus DC lesions transect first order neurones of both the DC pathway and projections to Clarke's column.

Finally, it must be born in mind that there is considerable diversity in the central projections of DRGN. For example, not all ascend once entering the spinal cord – a significant minority *descend* 2 or 3 segments before synapsing. Also, there is considerable collateralisation within these pathways, such as branches to the ventral horn, lateral horn and higher structures.

#### 1.1.2.3.2.2 Cellular responses seen after DC crush

DC crush leads to a set of cellular responses very similar to any other CNS injury, involving axons, glia, inflammatory cells and the extracellular matrix. See Figure 1.7 for characteristics of the lesion used in this study.

##### *Axons and neuronal cell bodies*

From as early as one day post lesion (1 dpl) axons are seen to be absent from the lesion core, indicating a complete transection. At 28 dpl, axonal debris is seen in macrophages in the degenerating DC rostral to the lesion (Lagord, Berry et al. 2002). CNS axons do attempt to regenerate in the early stages after a lesion by producing short sprouts, but they fail to enter the lesion core and form so-called 'dystrophic endballs' at their tips, thought initially by Cajal to be unresponsive and quiescent, but now recognised to be capable of further growth (Ramon y Cajal 1991; Yiu and He 2006).

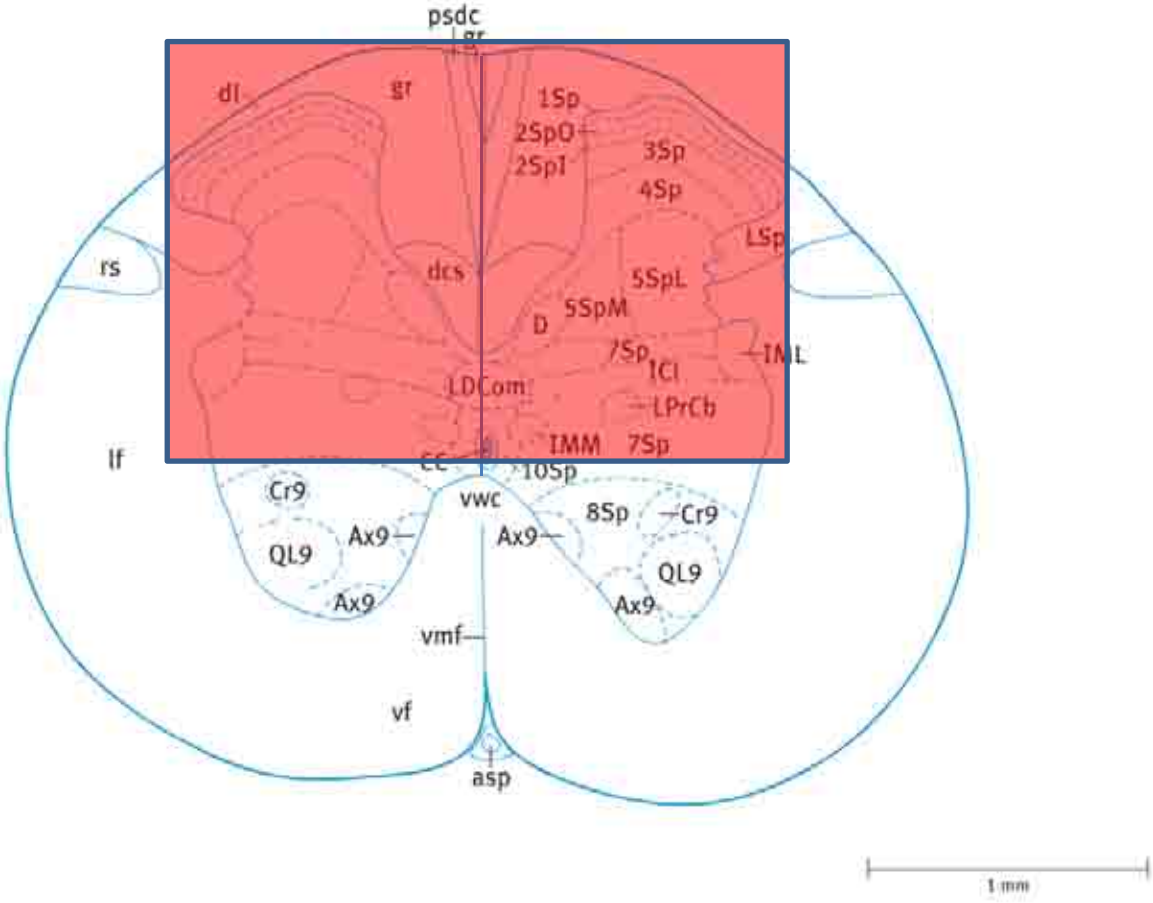


**Figure 1.7** The extent of the DC lesion used in this study. The lesion has a dorsal/ventral dimension of 1.5mm extending to the central canal, bounded laterally by the dorsal root entry zones. Spinal cord regions disrupted in this lesion include the dorsal funiculus (containing ascending dorsal column and descending corticospinal axons), the dorsal horns and part of the ventral horns. Image adapted from Watson , 2009.

Available data indicate that there is minimal DRGN cell death after transection of the central process, contrasting with the large amount of apoptotic death occurring after transection of DRGN peripheral processes (Shi, Tandrup et al. 2001; Chew, Leinster et al. 2008). This is possibly due to the large amount of peripherally derived neurotrophic factors acting upon DRGN.

***Glia***

The three major glial types found in the CNS are astrocytes, microglia and oligodendrocytes. Astrocytes have diverse roles in the normal and pathological nervous system, including regulating synaptic transmission, maintaining the blood-brain barrier and maintenance of extracellular ion concentrations (Verkhratski and Butt 2007). Additionally, astrocytes respond to injury by up-regulating expression of glial fibrillary acidic protein (GFAP), developing thicker processes and laying down ECM components such as CSPGs (Properzi, Asher et al. 2003).

Activated astrocytes are seen surrounding the lesion site from the first week post lesion, occasionally extending processes into the lesion by 3 weeks (Dijkstra, Geisert et al. 2000). By 56 dpl astrocytes are seen lining the lesion cavity, and any cysts that may have formed.

Microglia are the resident phagocytes of the CNS, derived from blood-borne monocytes that invaded the CNS parenchyma early in development (Verkhratski and Butt 2007). They actively survey the CNS environment with their motile processes and respond to injury by developing shorter, thicker processes and up-regulating

their expression of phagocytic markers such as CD68 and CD11b (Ransohoff and Perry 2009).

From the first week post lesion, activated microglia are seen surrounding the lesion site, with increasing numbers found rostral to the lesion by 21 dpl (Lagord, Berry et al. 2002; Agudo, Robinson et al. 2005).

Oligodendrocytes are the myelinating cells of the CNS, with each oligodendrocyte contributing to the myelin sheath of up to 30 axons (Verkhratski and Butt 2007). After CNS lesions, oligodendrocytes become dissociated from axons and develop fine processes that become ramified between degenerating axons (Berry and Logan 1999).

By 4 dpl, 2,3-cyclic nucleotide 3'-phospho-diesterase positive oligodendrocytes have disappeared from the lesion site, but are still found in the degenerating rostral tract (Lagord, Berry et al. 2002). Oligodendrocyte numbers decline in the DC rostral to the lesion well into the chronic period, as Wallerian degeneration progresses (Almad, Sahinkaya et al. 2011).

***Inflammatory cells***

Haematogenous macrophages are seen from early time points after DC crush, migrating into the blood-filled core of the lesion, alongside lymphocytes and monocytes. By 20 dpl, numerous macrophages are seen both within and rostral to the lesion site, and are probably actively involved in removing axonal and myelin debris (Lagord, Berry et al. 2002).

***Scarring and cavitation***

During the first 3 dpl, fibroblasts positive for ECM components such as fibronectin can be detected in the lesion core. At 7 dpl, this fibrotic region becomes capped by a laminin positive layer derived from meningeal fibroblasts (Lagord, Berry et al. 2002).

At the lesion site from 4 dpl, a large cavity is seen filled with blood derived cells and cellular debris. This cavity is seen to extend as time progresses, with secondary cavitation extending up to a total distance of around 4mm (Figure 1.8). Cavities are typically filled with macrophages, fibroblasts, laminin fibronectin and collagen, and are lined by astrocytes constituting the accessory glia limitans (Lagord, Berry et al. 2002). .

### 1.1.3 Why is CNS axon regeneration so limited?

At this point, it is prudent to clarify what is meant by the term 'regeneration' as it is encountered in this work. The Oxford English Dictionary defines 'regeneration' in its biological sense as "the formation of new animal tissue; the natural replacement of lost parts or organs". In the nervous system, it is important to differentiate between regeneration due to the replacement of lost cells (e.g. neurogenesis or replacement of lost glial cells) and regeneration due to the growth of existing cells (i.e. regrowth of a severed axon, axonogenesis). In this study, regeneration will be discussed with respect to the process of axonogenesis.

It has been known for centuries that compared with the PNS, the CNS has only a very limited capacity for axon regeneration. Consequently, many researchers have

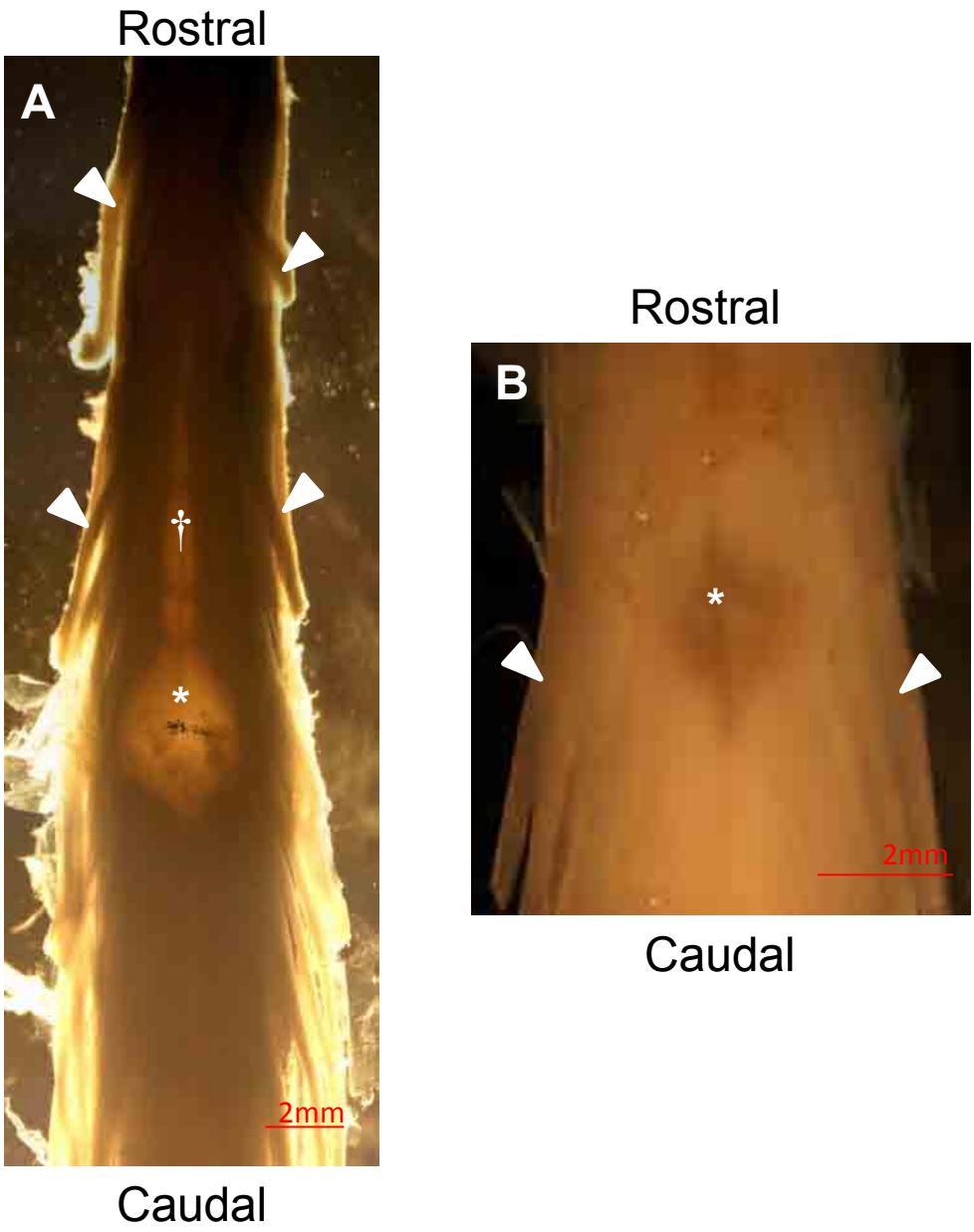


**Figure 1.8.** Comparison of the gross appearance of the lesioned rat spinal cord 1 and 3 months post injury. Details of lesioning technique can be found in section 2.2.3. **A**. 3 months post DC lesion at T8 cord level. Note the large, fluid-filled cystic cavity at the primary lesion site indicated by ink staining of the meninges (*) and the degenerating dorsal columns rostral to the lesion (†). Arrowheads indicate dorsal roots. **B**. 1 month post DC lesion at L1 cord level. Note the much smaller primary lesion cavity than in **A**, filled with cells and debris. There is no gross evidence of rostral degeneration or cavitation in the DC.

focussed on the essential differences between the two major divisions of the nervous system in terms of responses to injury and molecular characteristics. Furthermore, it is known that in certain 'lower' phylogenetic groups (e.g. fishes, amphibians), axon regeneration occurs readily in the CNS. Many workers, the author included, believe that this could hold a vital key to achieving CNS axon regeneration in mammals.

Four major factors are thought to contribute to the lack of CNS axon regeneration seen in mammals. These are: lack of endogenously synthesised neurotrophic factors (NTF) in the CNS, the presence of axon growth inhibitory ligands (AGIL), the presence of a glial scar in CNS lesions and the death of CNS neurones after axotomy.

***Insufficient NTF synthesis in the CNS***

Three major lines of evidence converge on the conclusion that there are lower levels of NTF synthesis in the CNS compared with the PNS. Firstly, the results of the intravitreal peripheral nerve grafts of Berry et al. (see below) show that by providing a rich source of NTF to CNS neurone cell bodies, axon regeneration can be achieved (Berry, Carlile et al. 1996). Thus, it seems likely that levels of NTF in the intact or injured CNS are insufficient to elicit axon regeneration. Secondly, studies on peripheral nerve regeneration have shown that NTF are released in appropriate temporal and spatial gradients in a way that is conducive to PNS axonal regeneration (Boyd and Gordon 2003). Finally, a recent study demonstrates directly that CNS tissue contains lower titres of NTF than PNS tissue (Du, Yang et al. 2010).

However, it must be stressed that the CNS does contain abundant NTF, including NT-3, derived from target tissues such as skeletal muscle and sensory receptors (Zhou and Rush 1994; Curtis, Tonra et al. 1998; Hiltunen, Laurikainen et al. 2005; Wang, Meng et al. 2008). However, the concentrations provided by endogenous sources are clearly not sufficient to stimulate axon regeneration on their own, necessitating the need to deliver higher concentrations to activate the growth state of axotomised neurones.

***AGIL***

In 1982, Berry was the first to hypothesise the existence of molecules found within CNS neuropil that are capable of inhibiting the growth of axons (Berry 1982). This idea arose from the observation that retinal ganglion cell (RGC) axons transected within the retina (an environment devoid of myelin) are capable of profuse growth. Furthermore, all of the studies employing peripheral nerve grafts to connect two CNS regions never showed axonal penetration of the CNS neuropil despite extensive growth within the graft.

The first demonstration that specific protein fractions from myelin contained an inhibitory activity came from Martin Schwab's group, who followed this lead up extensively culminating in the demonstration that the molecule that they named Nogo was a key player in axon growth inhibition (Caroni and Schwab 1988; Zorner and Schwab 2010). Many other AGIL, derived from both myelin and the glial scar, have been identified since including myelin-associated glycoprotein (MAG)

(Mukhopadhyay, Doherty et al. 1994), oligodendrocyte-myelin glycoprotein (OMgp) (Wang, Koprivica et al. 2002) and a variety of CSPGs (Galtrey and Fawcett 2007).

***Scarring***

As has already been mentioned in section 1.1.2.2, the final stage in the evolution of many CNS injuries is the formation of a dense glial scar. Windle proposed that the scar acted as a simple mechanical barrier to axon growth, but this has failed to stand up to evidence accumulated over the last 20 years (Windle and Chambers 1950). It has since become clear that the glial scar contains many molecules with inhibitory effects on growth cones, such as CSPG, semaphorins and ephrins (Fitch and Silver 2008). Interestingly, some controversy still remains with respect to glial scarring, particularly surrounding the dynamics of scar deposition and its interactions with regenerating axons (Ahmed, Dent et al. 2005).

***Neuronal death***

An important consequence of axotomy in the CNS is neuronal death, and is currently the subject of intense research activity in translational SCI research. CNS lesions lead to high levels of neuronal death which occurs in varying degrees depending on the level of collateralisation in the lesioned system (collateralisation correlates with the amount of target-derived neurotrophic support a neurone is receiving). For example in the visual system, more than 90% of RGCs have died by apoptosis 14d after intra-orbital transection of the optic nerve (Berkelaar, Clarke et al. 1994). RGCs

are particularly susceptible to cell death after transection of their axons, since no collaterals emerge from the optic nerve.

DRGN, in part due to their possession of both central and peripheral projections (see section 1.1.2.3.2.1), are more robust than most CNS neurones with respect to cell death after axotomy. Although relatively little studied, it seems clear that transection of the DRGN central processes does not lead to significant DRGN apoptosis (Chew, Leinster et al. 2008). Transection of the peripheral process, however, is seen to lead to around a 40% loss of DRGN (Tandrup, Woolf et al. 2000). The conclusion from these studies is that DRGN are more dependent upon growth factors derived from their peripheral targets than those from their central targets. Furthermore, this is consistent with the evidence supporting a relative paucity of NTF in the CNS environment.

### 1.1.4 Reasons to be optimistic about regenerative therapies

In the period after Cajal's coining of the phrase "abortive regeneration", the neuroscience community felt resigned to what they believed was the inherent impossibility of CNS axon regeneration (Ramon y Cajal 1991). However, it was the serendipitous discovery by Windle in the early 1950s that a bacterial polysaccharide could stimulate regeneration of axons in the transected spinal cord that led many researchers to reconsider what Cajal had proposed (Windle 1955).

### *CNS neurones are capable of extending axons*

In the 1980s, work from the laboratory of Albert Aguayo showed that axons from the spinal cord and optic nerve were able to grow readily for considerable distances into peripheral nerve grafts, refuting the dogma that CNS axons are incapable of further growth (Richardson, McGuinness et al. 1980; Aguayo, Vidal-Sanz et al. 1987). Thus, it became a worthwhile pursuit looking for ways to attain axonal growth in the injured CNS.

### *CNS neurones can regenerate axons if stimulated appropriately*

Two major possibilities arose from Aguayo's work. CNS axons could have grown into the PNS graft because (i), there was a higher concentration of growth factors in the graft than in the adjacent CNS neuropil or (ii), the graft had a more permissive environment for axon growth than CNS neuropil. Partly to address these hypotheses, Berry et al. inserted fragments of live and freeze-thawed peripheral nerve into the vitreous humour of eyes which had had their optic nerves transected (Berry, Carlile et al. 1996). The result was a large number of regenerating axons found in the grafted animals, particularly those receiving a live graft. Indeed, it has been shown that that Schwann cells are capable of synthesising a number of NTF (Funakoshi, Frisen et al. 1993). These results demonstrated that CNS neurones are capable of extending axons when given appropriate neurotrophic stimulation.

### *Regenerating CNS axons can navigate to appropriate targets*

Having demonstrated successful axon regeneration of CNS neurones, researchers became anxious to show whether these axons were capable of following the

developmental signposts that had guided them during embryogenesis. To address this, Berry et al. examined the trajectories of regenerating axons in the optic nerve as they decussate at the chiasm (Berry, Carlile et al. 1999). They were able show that regenerating RGC axons did indeed recapitulate the paths that they had taken during development. This was an extremely exciting result, since it suggested that, providing axon regeneration was sufficiently robust, appropriate functional connections may be restored.

### 1.2 Neurotrophic factors

The term NTF refers to a number of small polypeptide molecules which have functions relevant to neuronal growth, differentiation and survival. This should be contrasted with the term *neurotrophins* (NT) which refers to a family of molecules that are themselves NTF but which act specifically through a particular type of receptor.

#### 1.2.1 The neurotrophins

This group of NTF contains four members found in mammals: nerve growth factor (NGF), brain-derived neurotrophic factor (BDNF) (Barde, Edgar et al. 1982), neurotrophin-3 (NT-3) (Kaisho, Yoshimura et al. 1990) and neurotrophin-4 (NT-4) (Hallbook, Ibanez et al. 1991). NT-4 is also known as NT-4/5 or NT-5. These molecules all act *via* the tropomyosin-like receptor kinases (Trks), which come in three subtypes: NGF binds TrkA; BDNF binds TrkB; NT-3 binds TrkC as well as TrkA and TrkB with lower affinity and NT-4 binds TrkB. In addition to Trk receptors, NT are also able to act directly *via* the $p75^{NTR}$ receptor (Reichardt 2006).

In mammals, NT are widespread in the CNS, although their relative concentrations and detailed spatial distribution may differ according to developmental stage or presence of disease states (Heumann, Lindholm et al. 1987; Tanis, Newton et al. 2007). Since the remit of this project is axon regeneration of DRGN, the remainder of the discussion will focus on NT and Trk receptor distribution in DRG and spinal cord in the intact adult animal and following injury, with particular emphasis on NT-3. There have been a number of excellent reviews of this area, so a brief overview will be presented, emphasising those aspects believed to be of particular importance (Patapoutian and Reichardt 2001; Huang and Reichardt 2003; Reichardt 2006; Blochl and Blochl 2007).

#### 1.2.1.1 NT receptors and signalling cascades

*In vivo*, NT exist as non-covalently bound homodimers, each monomer being capable of binding with high affinity to the membrane-proximal region of a single Trk molecule (Reichardt 2006). Signalling is initiated by homodimerisation of Trk receptors after NT binding and subsequent transphosphorylation of intracellular tyrosine residues by tyrosine kinase domains (Jing, Tapley et al. 1992). The phosphorylation of intracellular domains of Trk receptors provides docking sites at membrane-proximal and membrane-distal sites for a number of adaptor proteins, with the ultimate effect of activating one of three major pathways. The major effectors of these pathways are Protein Kinase C (PKC), PI3-kinase/Akt and mitogen activated protein kinase (MAPK) (Figure 1.9). A further, important downstream effector of NTF signalling is the mammalian target of rapamycin (mTOR), which has important functions in

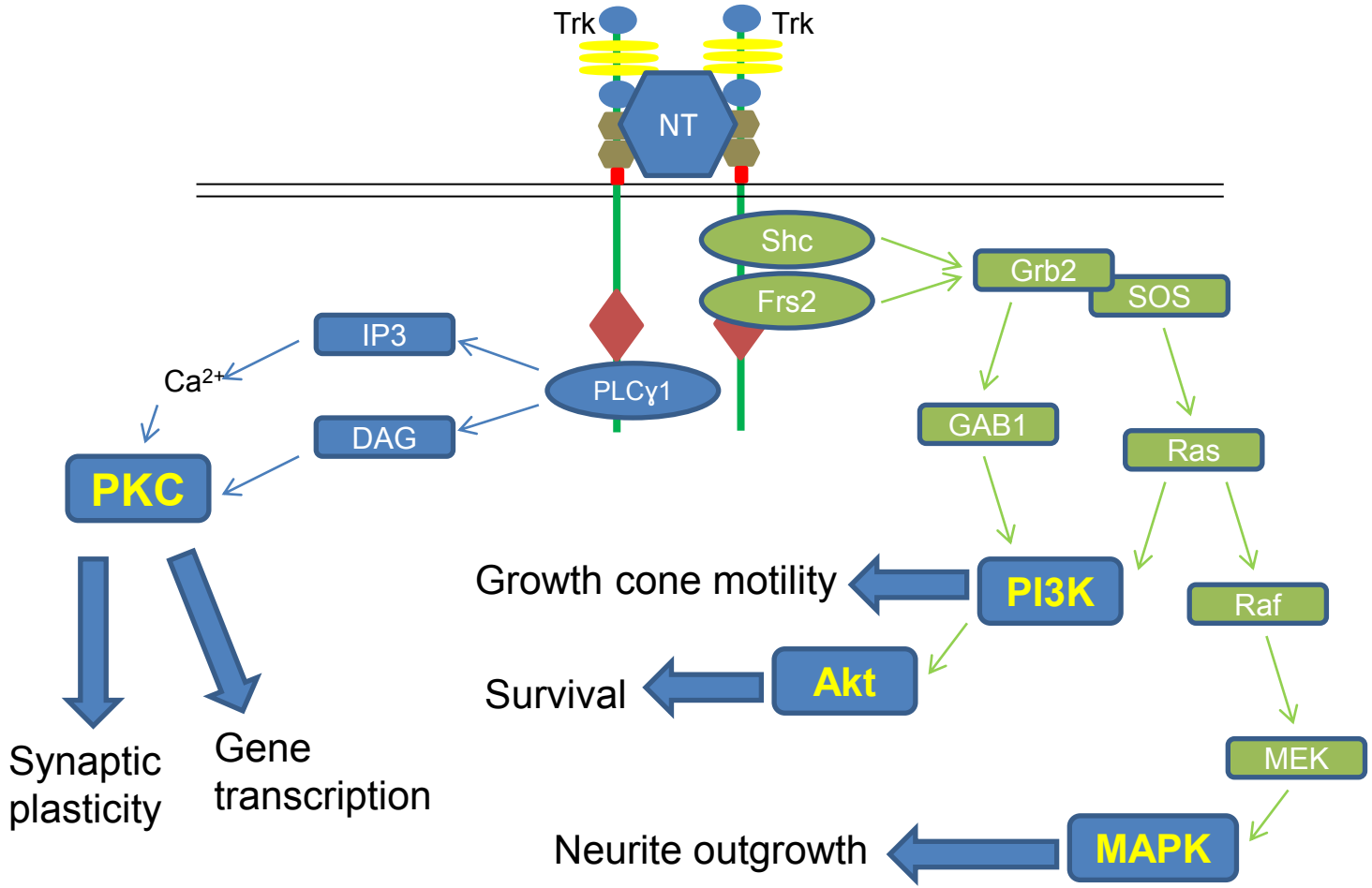


**Figure 1.9**. The major neurotrophin signalling pathways activated by binding of NT. The Trk receptors control three important signalling pathways. Activation of MAPK following recruitment of the Ras pathway by Shc, Frs2 and Grb2/SOS augments neurite outgrowth. PI3K, activated by the same upstream regulators as the Ras pathway but also involving GAB1, enhances growth cone motility and, through Akt, neuronal survival. Recruitment of PLCγ1 to the distal segment of the Trk intracellular domain leads to the generation of IP3 and DAG, with the subsequent activation of PKC leading to changes in synaptic plasticity and gene transcription.

sensing the availability of raw materials and trophic factors and regulating the growth responses of the cell (Park, Liu et al. 2010).

$p75^{NTR}$ was the first receptor for NT to be identified, however its true significance to NT signalling is only now becoming fully apparent. This receptor binds NT with a low but similar affinity across all subtypes, and has three main regions: the extracellular domain ($p75^{ECD}$) which interacts with ligands, the intracellular domain ($p75^{ICD}$) and a transmembrane domain (Reichardt 2006). The intracellular domain can be enzymatically cleaved, and is able to initiate apoptosis – hence its alternative name of the 'death domain'. Unlike Trk receptors, the $p75^{NTR}$ does not have any inherent catalytic activity, its signals being transduced by association with intracellular molecules such as Traf6, neurotrophin receptor interacting protein and Rho-GDP dissociation inhibitor (RhoGDI). Additionally, $p75^{NTR}$ has been shown to augment the affinity and specificity of NT interactions with Trk (Chao 1994)

#### 1.2.1.2 Biological effects of neurotrophins

The cellular effects of $p75^{NTR}$ activation include effects on growth-cone motility *via* Rho GTPases as well as causing cell survival or apoptosis dependent upon the other receptors present on the cell surface (Blochl and Blochl 2007). Binding of proneurotrophins to the $p75^{NTR}$ receptor has been shown to stimulate apoptosis *via* an interaction with sortilin, a molecule involved in protein trafficking (Lee, Kermani et al. 2001; Teng, Teng et al. 2005).

As mentioned above, Trk phosphorylation leads ultimately to activation of one of three major effector systems: PKC, PI3-kinase/Akt and MAPK. Between them, these pathways impinge upon gene transcription, cell survival, neurite outgrowth and growth cone motility. For further details please refer to either of these excellent reviews (Huang and Reichardt 2003; Reichardt 2006).

***PKC***

Upon binding of phospholipase C-ɣ1 (PLC-ɣ1) to membrane-distal phosphotyrosine residues, it is itself phosphorylated and hence activated by the Trk tyrosine kinase domain. Once activated, this important enzyme is able to convert the substrate PtdIns(4,5)$P_2$ into IP3 and diacylglycerol (DAG). IP3 causes release of $Ca^{2+}$ from intracellular stores which activates many $Ca^{2+}$ -dependent kinases, and DAG activates various isoforms of PKC. Additionally, $Ca^{2+}$ release itself activates other PKCs leading to almost all isoforms of PKC becoming activated. The major effects of activation of this pathway are *via* the nucleus through changes in gene transcription, particularly those for ion channels.

***PI3-kinase/Akt***

The recruitment of Shc and Frs2 to membrane-proximal phosphotyrosine residues leads to activation of the Grb2/SOS complex. Grb2/SOS is able to activate PI3K by a Ras-dependent pathway or one involving GAB1. Active PI3-kinase generates 3-phosphoinositides which, *via* PDK-1 activate the protein kinase Akt, which has substrates involved in cell survival and the cell cycle. Additionally, the 3-phosphoinositides generated by PI3-kinase are able to recruit small GTPases such

as Cdc-42, Rac and Rho which, when active, can directly affect the cytoskeleton and hence cell motility including that of growth cones.

***MAPK***

Active Ras, generated by the events described in the previous section, is able to activate Raf, and in turn MEK leading to the activation of a variety of MAPK subtypes. MAPKs can activate intermediates such as CREB, ultimately affecting gene expression *via* transcription factors such as *Egr-1*, which have been shown to stimulate neurite outgrowth in phaeochromocytoma-12 (PC12) cells after application of NGF.

### 1.2.1.3 The relevance of NT-3 to spinal cord injury

Transcript for the major NT-3 receptor, TrkC, is seen in around 15-20% of neurones in the dorsal root ganglion of intact adult rats, the majority of these being of medium to large diameter (Kashiba, Noguchi et al. 1995; Kashiba, Ueda et al. 1996). This pattern of expression, alongside *in vitro* data showing expression of TrkC in neuronal cell lines can lead to neurite outgrowth in the presence of NT-3, has led a number of investigators to examine the potential therapeutic effects of administering NT-3 in spinal cord injured animals (Tsoulfas, Soppet et al. 1993). The following account focuses on studies examining the effects of NT-3 administration on axon regeneration of sensory neurones projecting to the spinal cord of adult animals. However, the reader should be made aware that many other studies have looked at other CNS pathways including the motor and auditory systems (Schnell, Schneider et al. 1994; Gharabaghi and Tatagiba 2005; Fortun, Puzis et al. 2009; Petruska, Kitay et

al. 2010). Also, much of the preliminary work showing NT-3 to be important was performed using immature animals, whose neurones are much more dependent upon NT for survival.

NT-3 has been shown to have a number of roles in the developing nervous system, particularly with respect to the development of proprioceptive axons and synaptic plasticity of primary afferent synapses (Mendell, Munson et al. 2001; Taylor, Vancura et al. 2001; Taylor, Vancura et al. 2001; Wright, Williams et al. 2002; Taylor, Holdeman et al. 2005).

One of the first reports that NT-3 has axon regenerative activity in adult animals *in vivo* was from Tuszynski's group, who injected NT-3 expressing fibroblasts into the central grey matter of the rat spinal cord (Nakahara, Gage et al. 1996). In the absence of any previous injury, it was seen that a large number of sensory axons projected into the fibroblast grafts. This study demonstrated not only that NT-3 is axogenic *in vivo*, but also that neurones retain the ability to respond to NTF into adulthood.

NT-3 was shown to be active in promoting axon regeneration in a study employing the dorsal root injury model. Adenoviral-mediated delivery of NT-3 promoted the regeneration of sensory neurones not only across the DREZ, but into the grey matter of the cord towards the site of injection (Zhang, Dijkhuizen et al. 1998). Thus, NT-3 was shown to act both to promote axon regeneration and to guide axon growth, effects which would be further exploited in future studies.

The logical next step was to examine the effect of NT-3 delivery on regeneration of axons within a white matter tract. This was performed by Bradbury et al. using a DC crush model and continuous infusion of recombinant NT-3 for 4 weeks at the lesion site (Bradbury, Khemani et al. 1999). Compared with control and other growth factors tested, NT-3 led to many axons sprouting into, and some beyond, the lesion site within the spinal cord.

Despite these promising results, it remained clear that NT-3 was unlikely to be viable as a monotherapy for SCI since the number of regenerating axons seen was typically modest. Also, no study ever saw axons regenerating all the way to their distant targets (but see experimental design section 1.1.2.3).

### 1.3 Axon growth inhibitory ligands

As mentioned in section 1.1.3, it has been known for more than 20 years that a number of molecules exist that are capable of inhibiting axon growth, specifically by causing the collapse of growth cones. Since this realisation, a tremendous amount of work has been carried out examining the roles of these molecules in normal and pathological situations, particularly with respect to their molecular signalling mechanisms and potential neutralisation strategies.

#### 1.3.1 The growth cone

It is believed that Cajal was the first to describe “concentration[s] of protoplasm of conical form, endowed with amoeboid movements”; entities that we now refer to as growth cones (Ramon y Cajal 1890). Growth cones have major roles in development

when the nervous system is being built, but also into adulthood in the processes of axon regeneration and neuronal plasticity. The modern view of growth cones is that they are highly dynamic structures, capable of integrating a whole host of molecular signals leading to a relatively simple decision: whether to collapse or not, whether or not to grow, and if so in which direction and how fast. Growth cone collapse is an active process, and is not simply growth cone stasis. Collapsed growth cones shrink considerably and become quite refractory to stimuli.

The signals which growth cones use for guidance are highly diverse, ranging from attractive substances such as neurotrophins, repulsive substances such as semaphorins and collapsing substances such as Nogo. The following section will focus on the role of myelin-derived AGIL (Nogo, OMgp and MAG), their signalling pathways and distribution in the intact and injured CNS. The reader is referred to a comprehensive review for further details (Sandvig, Berry et al. 2004).

### 1.3.2 Expression of myelin-derived AGIL in the normal and injured CNS

In the majority of reports, myelin-derived AGIL are found within the myelin sheaths of axons, and in the cell bodies of oligodendrocytes (Sandvig, Berry et al. 2004). However, their mere presence may not necessarily be sufficient to inhibit the growth of axons. An interesting study conducted through collaboration between Jerry Silver and Geoff Raisman demonstrated that adult DRGN, when atraumatically transplanted into the CNS are able to extend neurites through white matter for distances of around 6mm (Davies, Fitch et al. 1997). Their conclusions focussed primarily on the glial scar, however the results of this study quite clearly show that

intact white matter is not inhibitory to adult DRGN. The explanation for this may be that myelin-derived AGIL must be solubilised in order to interact with receptors such as nogo receptor (NgR) on the growth cone. Such solubilisation is likely to occur through primary and secondary effects of the lesion such as tissue disruption and Wallerian degeneration.

A second, seemingly paradoxical observation is that some neurones express AGIL themselves, and are even seen at the growth cone (Hunt, Coffin et al. 2002). The significance of this neuronal AGIL expression is not yet fully appreciated, although it is probable that molecules such as Nogo have roles in growth cone guidance and the inhibition of formation of inappropriate connections (Llorens, Gil et al. 2011).

***Expression of Nogo in the intact and injured spinal cord***

Of the three different Nogo subtypes, Nogo-A is believed to have the most important role in the CNS. In the spinal cord, Nogo-A protein is seen in motor neurones and oligodendrocytes – particularly in their cells bodies and myelin sheaths, particularly in the myelin adjacent to axons (Huber, Weinmann et al. 2002).

Very little modulation of Nogo-A is seen after SCI, although this is not necessarily evidence that Nogo-A has a limited role in CNS axon regenerative failure (Huber, Weinmann et al. 2002).

***Expression of MAG in the intact and injured spinal cord***

MAG is found in the myelin sheaths of both the CNS and PNS, and has been detected in a soluble form in degenerating tracts post injury (Sandvig, Berry et al. 2004).

***Expression of OMgp in the intact and injured spinal cord***

It has recently been demonstrated that OMgp is found in both neurones and oligodendrocytes of the spinal cord, and that there is an increase in mRNA and protein levels after injury (Guo, Li et al. 2007; Dou, Huang et al. 2009).

### 1.3.3 Myelin-derived AGIL signalling

Nogo-A, MAG and OMgp all signal through Nogo Receptor 1 (NgR1), and MAG is known also to bind to NgR2 (Tuszynski and Kordower 2008). Additionally, all known myelin-derived AGIL bind to paired immunoglobulin-like receptor B (PirB), a molecule known to have roles in neural plasticity and the immune system (Atwal, Pinkston-Gosse et al. 2008). Regardless of the AGIL, the common downstream signalling molecule responsible for growth cone collapse is RhoA. Since most is known about NgR1 signalling to RhoA and the cytoskeleton, this will be the focus of the following discussion.

NgR1 is expressed on the surface of neurones, including growth cones, and is thought to be the major receptor mediating myelin-derived AGIL induced growth cone collapse (Fournier, GrandPre et al. 2001). Alone, NgR1 is not able to transduce signals to the growth cone cytoskeleton since it does not possess an intracellular signalling domain. In order for signal transduction to occur, NgR1 associates with a

number of membrane-spanning proteins including p75 $^{NTR}$ (Wang, Kim et al. 2002), leucine-rich repeat and Ig domain containing (LINGO-1) (Mi, Lee et al. 2004) and TNFRSF (tumor necrosis factor receptor superfamily) expressed on the mouse embryo (TROY) (Park, Yiu et al. 2005).

NgR1 forms a trimer with LINGO-1 and p75$^{NTR}$ or TROY, which is able to activate RhoA *via* p75$^{NTR}$ (Figure 1.10). RhoA exists in a dynamic equilibrium between and inactive GDP-bound (Rho-GDP) form and an active GTP-bound form (Rho-GTP). Guanine-nucleotide exchange factors (Rho-GEFs) activate RhoA by converting Rho-GDP to Rho-GTP, whilst GTPase activating proteins (Rho-GAPs) inactivate RhoA by converting ho-GTP to Rho-GDP. Rho-GDP (inactive) can be sequestered from Rho-GEFs by binding to Rho-GDI, taking it 'out of the loop' and impairing its activation. Binding of AGIL to NgR1 leads to displacement of Rho-GDI from Rho-GDP by creating a binding site on p75$^{NTR}$ with a higher affinity for Rho-GDI than Rho-GDP. Thus, Rho-GDP is released and can be activated by Rho-GEFs.

Activated RhoA is able to activate a number of pathways involved in growth cone arrest, turning and collapse *via* the important intermediate protein Rho-associated kinase (ROCK). There are at least two subtypes of ROCK, but for clarity and brevity they shall be considered together (Schmandke and Strittmatter 2007). ROCK has two major functions with respect to growth cone collapse and turning – inhibition of actin depolymerisation and formation of stress fibres.

Growth cones are highly dynamic structures, achieving this motility mainly by the co-ordinated formation of actin fibres and microtubules. All dynamic cytoskeletal

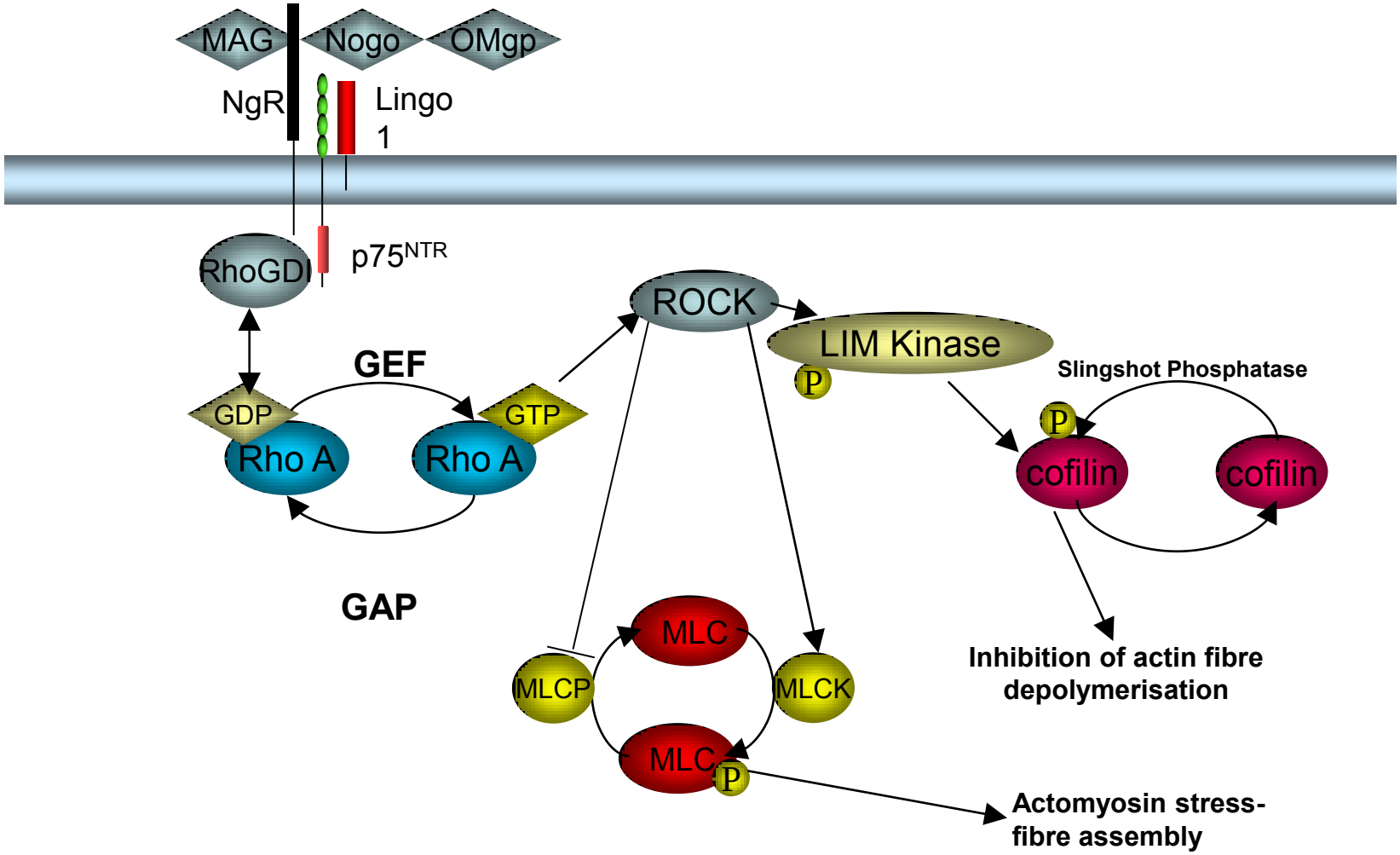


**Figure 1.10**. The major signalling cascade activated by NgR binding to myelin-derived AGIL. AGIL-binding leads to displacement of Rho-GDI from RhoA-GDP allowing activation of RhoA by GEF. Activated RhoA then activates ROCK, leading to (i) the formation of actomyosin stress fibres *via* activation of MLCK and inhibition of MLCP; and (ii) inhibition of actin fibre depolymerisation *via* LIMK and cofilin. The net effect of i and ii is growth cone collapse and inhibition of its motility. Adapted from an original figure provided by Professor Ann Logan and adapted by by Dr Kevin Morrison.

elements are maintained by the balance between formation and destruction. In the case of actin, an equilibrium exists between the free, globular or G-actin and the filamentous F-actin (Geraldo and Gordon-Weeks 2009). Actin polymerisation is regulated by many pathways; one of the most important involves LIM-domain containing protein kinases 1 and 2 (LIMK) and cofilin (Schmandke and Strittmatter 2007). ROCK activation leads to phosphorylation of LIMK, which in turn deactivates cofilin by phosphorylation. Normally, cofilin is an important catalyst for depolymerisation of F-actin which is vital for actin turnover and cytoskeletal motility. This 'actin paralysis' is not sufficient, however, to explain growth cone collapse. Myosin light chains (MLC) associate with actin fibres to generate contractile forces, which are able to lead to growth cone collapse (Zhao and Manser 2005). ROCK is able to directly phosphorylate MLC and to inhibit the activity of myosin light chain phosphatase, allowing stress fibres to form.

***A note on the subtlety of growth cone dynamics***

The picture painted above is one of an ostensibly simple story, leading to a logical choice of therapeutics. However, it must be stressed that the events occurring within the growth cone are phenomenally complex. It is the opinion of the author that a single therapeutic intervention (e.g. knocking down a single molecule in the AGIL signalling cascade) is unlikely to be successful. Furthermore, examination of any recent review will highlight some contradictions and new directions that may be of importance, such as the growth-promoting effects of RhoA activation *via* mDia and the enigmatic citron kinase (Schmandke and Strittmatter 2007).

### 1.3.4 Disinhibitory therapies

As discussed in section 1.3, engagement of AGIL to cell-surface receptors such as NgR1 and NgR2 result in activation of the small GTPase RhoA and its downstream effector ROCK. In order to dissect the role of these molecules in the pathway, much work has been done in the last decade to examine the effects of inhibiting or activating various components on axon regeneration both *in vitro* and *in vivo*.

#### 1.3.4.1 Knockout studies

Experiments examining the axon regenerative effects of genetic deletions (i.e. gene knockouts) can be highly informative, but must be interpreted with a great deal of caution. This is mainly due to the fact that knockout animals have undergone development in the presence of the deletion, meaning that normally redundant systems could come into play and have a significant, confounding role. Also, it is not always possible to conduct knockout studies if the gene under scrutiny is essential to life.

##### *NgR1 knockouts*

Knocking out the NgR1 receptor has been shown to have, at best, a modest effect on axon regeneration *in vivo* (Kim, Liu et al. 2004; Zheng, Atwal et al. 2005). This is in the context of a comparatively more robust effect of Nogo inhibitors such as the antibody IN-1 (Teng and Tang 2005). The conclusion of these studies as a whole seemed to be that another receptor for Nogo existed, since inhibiting the ligand had a

greater effect than inhibiting its (known) receptor. This prediction was borne out in 2008 when Tessier-Lavigne's group reported that a new receptor for AGIL had been identified – PirB (Atwal, Pinkston-Gosse et al. 2008).

### *RhoA knockouts*

At the time of writing, no reports of RhoA knockdown could be found. This is probably due to embryonic lethality of total RhoA deletion, since this molecule is believed to be a crucial intermediary in regulating development of the nervous system.

### *ROCK knockouts*

By deleting *ROCKII*, the major nervous system ROCK isoform, Strittmatter's group were able to show modest increases in the amount of axon regeneration seen in the raphespinal and corticospinal tracts (Duffy, Schmandke et al. 2009). However, the nature of this regeneration must be considered carefully: spontaneous regeneration of raphespinal fibres is a recognised phenomenon, and no corticospinal tract (CST) axons were seen traversing the lesion site (Kiernan 1979). Thus, *ROCKII* knockout is unlikely to be sufficient to effect axon regeneration on its own. Irrespective of these caveats however, the genetic deletion experiments described above did indeed show that ROCKII has a role to play in axon regenerative failure.

### 1.3.4.2 Knockdown studies

RNA interference (RNAi) has made genetic dissection of pathways increasingly accessible, but its advantages are far greater than merely eliminating the need for knockout animals. RNAi can be delivered either as RNA molecules directly to the cytoplasm (small-interfering RNA, siRNA) or within a plasmid to the nucleus, which is then transcribed into an RNA molecule (short hairpin RNA, shRNA). This technology allows genes to be 'deleted' in fully developed, adult animals. The crucial advantage to this is that, unlike in a knockout, the animal has not had the opportunity to bring into play redundant pathways. Also, RNAi is usually delivered to a specific tissue so lethality, even when knocking down crucial genes, is not a significant issue.

However, there are disadvantages including lack of specificity of knockdown, unpredictable effects on cellular metabolism and the need to deliver RNAi constructs to the appropriate cellular compartment (Ehlert, Eggers et al. 2010; Olejniczak, Galka et al. 2010).

#### *NgR1 knockdown*

The consensus is that knockdown of NgR1 leads to augmentation of neurite outgrowth in the presence of myelin-derived AGIL *in vitro*, although the precise mode of action of this effect is debatable (Ahmed, Dent et al. 2005; Chivatakarn, Kaneko et al. 2007). Chivatakarn et al. propose that NgR1 has a role in acute growth-cone collapse but not in chronic inhibition of neurite outgrowth when presented as a substrate. Ahmed et al. show, however, that DRGN neurite outgrowth *is* disinhibited by NgR1 knockdown (equivalent to the 'chronic inhibition' described above). For

technical reasons, the two studies are not easy to reconcile but provide the same basic conclusion – NgR1 knockdown is capable of augmenting regeneration *in vitro*.

***RhoA knockdown***

RhoA is a pivotal protein in the AGIL pathway (see section 1.3.3). Targeting this molecule holds much promise as it is an important nodal point, integrating signals from most of the AGIL.

RNAi-mediated knockdown of RhoA has been demonstrated to lead to disinhibited neurite outgrowth in DRGN and rat PC12 cells by two independent groups (Ahmed, Dent et al. 2005; Fan, Pang et al. 2008; Suggate, Ahmed et al. 2009).

***ROCK knockdown***

At the time of writing, no reports of the effects of RNAi-mediated knockdown of ROCK on neurite outgrowth have been reported in the literature. This is probably due to the availability of the pharmacological inhibitor Y27632 (see section 1.3.4.3).

**1.3.4.3 Peptide and small molecule inhibitors of the AGIL signalling pathway**

It is the ultimate goal of SCI research to develop therapies which are highly efficacious and which can be delivered non-invasively. Therapies based on small molecules may offer this, since they offer the potential for oral administration and long-term delivery. Part of the development of small molecule inhibitors involves the generation of peptide-based agents, which have themselves shown some promise in animal models of SCI and stroke.

### *NgR1 inhibitors*

As of writing, no small molecule inhibitors of NgR have been reported in the literature. However, a number of workers have described peptide inhibitors of NgR which they employed during studies of NgR signalling. These include the NEP-1 peptide, comprising the first 40 amino acids of Nogo-66 (GrandPre, Li et al. 2002); and the NgR(310)ecto-Fc molecule (Fournier, Gould et al. 2002). NEP-1 antagonises NgR by competing with Nogo for the ligand-binding domain, and has been shown to stimulate axon regeneration in the injured CST. NgR(310)ecto-Fc acts a soluble NgR, effectively 'mopping up' and sequestering any soluble myelin-derived AGIL, and has also been shown to improve regeneration of severed axons in the CST (Li, Liu et al. 2004).

### *RhoA inhibitors*

A membrane-permeable form of the bacterial enzyme C3-transferase has been shown to have efficacy in animal models, and is now undergoing phase I/II clinical trials with promising results (Lord-Fontaine, Yang et al. 2008; Fehlings, Theodore et al. 2011). C3-transferase works by Adenosine diphosphate (ADP)-ribosylation of the RhoA effector domain, rendering RhoA unable to activate its downstream targets such as ROCK (Winton, Dubreuil et al. 2002).

### *ROCK inhibitors*

The ROCK inhibitor Y27632 has a strong disinhibitory effect on cortical neurones *in vitro* and the CST *in vivo*, but requires the presence of NTF to stimulate outgrowth from RGCs exposed to myelin *in vitro* (Dergham, Ellezam et al. 2002; Ahmed, Berry et al. 2009). Despite the fact that ROCK inhibitors are being used in many areas of

biomedical research, there were no published clinical trials describing its use at the time of writing.

### 1.4 Therapeutic delivery technologies

Regenerative agents are usually delivered to the CNS by direct injection into neural tissues such as the brain, spinal cord or DRG. Such injections tend to be hampered by the fact that the CNS is extremely well protected by bone and tough meningeal layers. Agents injected into the circulation are frequently prevented from entering the CNS neuropil by the presence of the BBB and the blood-cerebrospinal fluid barrier. Furthermore, the friable nature of the brain and spinal cord mean that they are liable to injury during injections.

However, there are certain advantages of the CNS as a target, including the fact that it has a relatively attenuated immune response compared with the periphery. Thus, delivery of an immunogenic agent such as a virus or protein is likely to lead to only a very slow rate of clearance by the immune system. Additionally, the anatomy of CNS is very well characterised in most species meaning that lesions and injections can be performed very precisely using stereotactic instruments if available. Such knowledge also facilitates tracing of regenerated fibres.

Whatever the method of delivery, the agent must be supplied for a prolonged period of time if one is to achieve long tract regeneration. It is this problem which has led many groups to use gene therapy as a way of achieving sustained delivery of their therapeutic of choice. Whereas peptides delivered by single injections have only very short half-lives (around 30 min) *in vivo* (Krewson and Saltzman 1996), peptides

produced by gene delivery can be detected many months following the initial injection of the gene (Wu, Meyer et al. 2005). Thus, one must either deliver a peptide by continuous infusion which is difficult and costly, or generate a (usually) viral vector containing the gene of interest. The most common gene therapy vectors used in the nervous system are described below, with particular emphasis on adeno-associated viral (AAV) vectors, which were used in this study.

### 1.4.1 Non-viral gene delivery methods

Non-viral gene delivery may be desirable if, for example one is concerned about potential pathological effects of viral vectors, illustrated tragically by the case of Jesse Gelsinger, the first person to die in a gene therapy trial (Raper, Chirmule et al. 2003). However, these methods have a number of serious limitations, yielding low levels of gene expression which tend to decrease rapidly compared with viral vectors. This is due to the fact that non-viral deoxyribonucleic acid (DNA) payloads are cleared quickly from tissues, especially those containing many dividing cells (Glover, Lipps et al. 2005).

Three major methods exist for the non-viral delivery of genes – naked DNA, cationic polymers and liposomes. Naked DNA can be introduced in a number of ways, usually employing physical methods such as microinjection, ballistic delivery or electroporation (Glover, Lipps et al. 2005). Naked DNA has been successfully used in the CNS, giving high, sustained levels of expression in the brain (Yurek, Fletcher et al. 2009).

Cationic polymers and liposomes exploit the phenomenon that DNA is able to form highly condensed complexes when mixed with polymers or lipids containing many, repeated positively charged sites (Elsabahy, Nazarali et al. 2011). Upon contacting the cell membrane, these complexes become endocytosed, subsequently entering the nucleus and leading to gene expression. However, these technologies yield very low transfection rates in neurones, since they rely on the breakdown of the nuclear envelope during mitosis to gain entry to the nucleus (Barrett, Berry et al. 2004).

### 1.4.2 AAV based vectors

AAV vectors were originally discovered serendipitously, co-purifying with adenovirus (Ad), and have been used in gene therapy for more than twenty years in a large variety of tissues including the CNS (Chamberlin, Du et al. 1998). AAVs belong to the parvovirus family, and are small (25nm) polyhedral encapsidated, non-enveloped particles which are highly dependent upon other viruses for their normal life-cycle (Daya and Berns 2008). The genomes of all AAV-based vectors are composed of single stranded DNA (ssDNA), containing an expression cassette spanned by inverted terminal repeats (ITRs), usually from AAV2 (Figure 1.11). Capsid proteins from serotypes other than AAV2 are able to assemble around AAV2 ITRs, forming a so-called transencapsidated vector. Such vectors are described by giving the origin of the ITRs followed by the origin of the capsid genes (e.g. AAV2 ITRs with AAV8 capsid is designated AAV2/8). The capsid proteins expressed determine the interaction of the vector with its host cells, and hence the majority of its tropism. However, it is known that other factors downstream of viral entry, can contribute to differential expression of delivered transgenes (Duan, Yue et al. 2000). In this study,

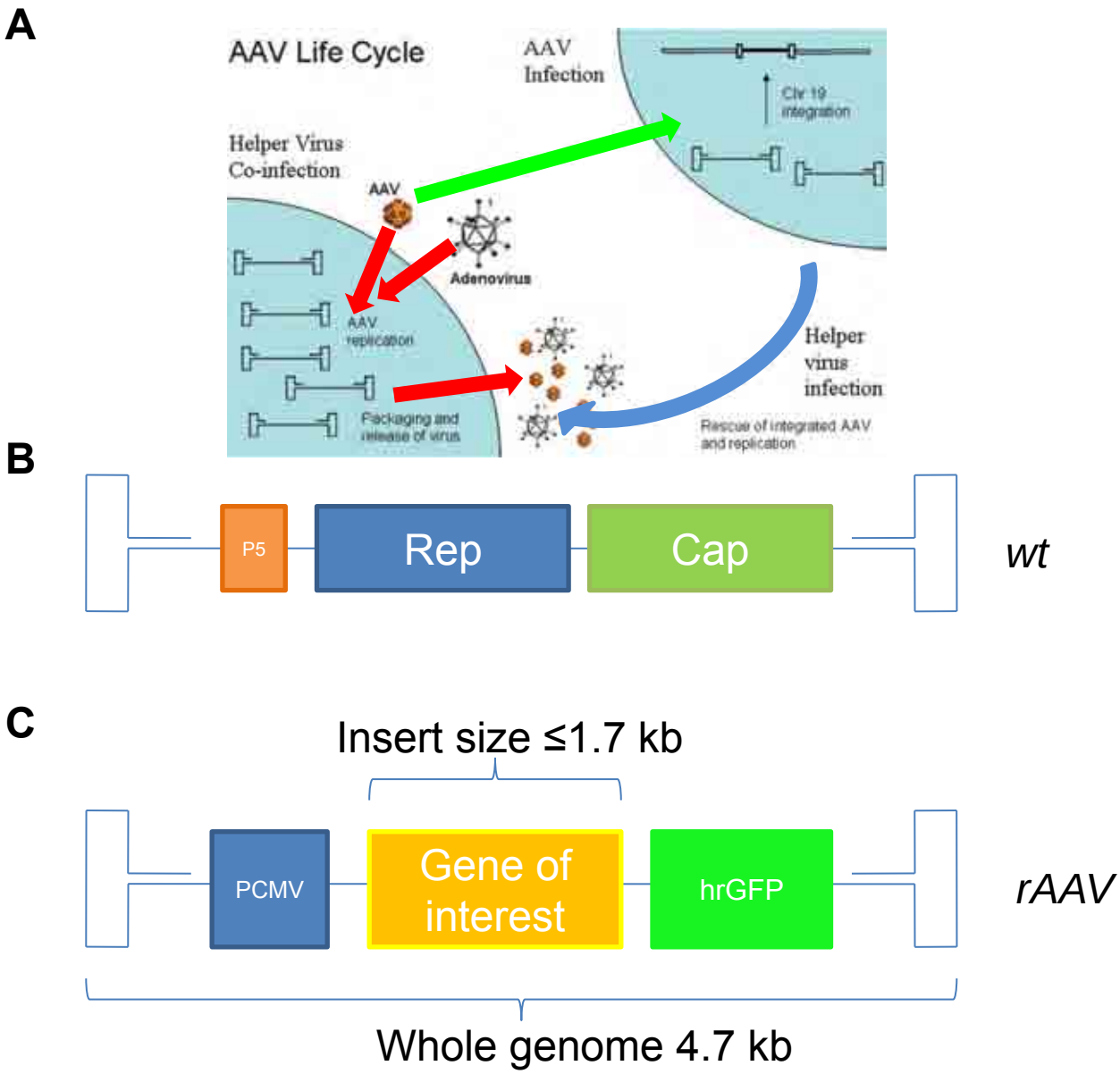


**Figure 1.11**. Life cycle and genome structure of AAV and AAV-based vectors. **A**. Infection of cells by wtAAV particles can lead to (i) a lytic phase involving replication of AAV particles and lysis of infected cells in the presence of helper viruses such as adenovirus (red arrows) or (ii) integration of AAV genomes into the host genome in the absence of helper viruses (green arrow). Subsequent infection of cells with integrated AAV genomes can lead to reactivation of the lytic phase (blue arrow). Adapted from Daya 2008. **B**. Genome structure of wild-type AAV. The P5 region and some genes found in the Rep complex are involved in viral integration. The rest of the Rep genes facilitate replication of the genome. The Cap region encodes the serotype-specific capsid proteins. **C**. Generic structure of the genome of recombinant AAV vectors used in this study. To generate these vectors, the wild type virus is genetically 'gutted', leaving space for inserts of up to 1.7kb in the presence of the CMV promoter and an hrGFP reporter gene.

for clarity, AAV2/8-based vectors (which are used throughout) will be referred to as AAV8.

#### 1.4.2.1 AAV vector manufacture

AAV vectors can be manufactured in a variety of ways, but all rely upon the presence of three key elements (Goncalves 2005). Further details can obtained from the comprehensive review by Goncalves et al. Firstly, one requires the viral genome containing the transgene of interest spanned by ITRs. Secondly, the genes encoding the appropriate capsid and Rep proteins must be supplied. Thirdly, since AAV requires 'helper' genes to be supplied for successful replication, these must also be supplied. Helper genes are typically involved in facilitating AAV genome replication, and work by interacting with proteins encoded by the *rep* complex. These elements are usually transfected into an appropriate cell line (such as human embryonic kidney (HEK) cells). The cells take up the transgenes and produce AAV vector particles, which can be purified from the medium. Originally, helper genes were supplied by including Ad in the medium, which when it infects cells produces proteins that can assist AAV replication: E1A, E1B, E2A, E4ORF6 and VA . However, this posed a number of challenges to purification since AAV and Ad are very similar in their molecular characteristics. The inability to get a highly pure, Ad-free AAV preparation led workers to deliver the helper genes not by Ad infection, but by transfecting them into cells within a so-called 'helper plasmid'.

The triple-transfection technique described above is a laborious method, using large volumes of culture medium and yielding relatively low levels of viral particles. In response to this, insect cells which are highly efficient at generating recombinant proteins, were employed to manufacture AAV particles (Urabe, Ding et al. 2002). See Chapter 3 for more details on AAV manufacture in insect cells.

Regardless of the method of production, viral particles must be purified from the cell culture medium. This is most commonly achieved by caesium chloride density ultracentrifugation, where the vector accumulates as a single band which can be aspirated. However, with greater insights into AAV biology, more selective and efficient methods are being developed such as column chromatography which can exploit the capsid's natural affinity for a receptor (Goncalves 2005).

#### 1.4.2.2 AAV vector advantages

AAV has a number of distinct advantages over many other viral vectors. It is not associated with any known human diseases and, at least in the case of AAV2, has been shown to be well tolerated when injected into the human CNS (Marks Jr, Ostrem et al. 2008). Part of its lack of pathogenicity is due to the inability of AAV vectors to integrate into the genome. Wild-type AAV contains two gene complexes designated *rep* and *cap* (Figure 1.11). The *rep* complex is involved in viral replication and integration into the host genome, and the *cap* complex contains genes encoding capsid proteins. If a wild-type AAV infects a cell in the absence of a helper virus such as Ad, then it may integrate into chromosome 19, ready to start replicating if conditions become more favourable (infection by Ad, cellular stress etc.). Current

AAV vectors lack this ability, since *rep* and *cap* have been removed to allow insertion of an expression cassette (Daya and Berns 2008). In future, AAV vectors may be designed that are capable of integrating, to give long-term gene expression. However, the side-effects of genome integration must be examined thoroughly to avoid potentially fatal adverse events such as neoplasia.

Another advantage of AAV vectors over many others is the great diversity of serotypes, and hence cellular tropisms, available to work with. The tropism of an AAV particle is determined largely by the capsid proteins encoded by the *cap* gene complex. To date, 12 human serotypes have been identified, showing a wide variety of tropisms which often overlap. For example, AAV2 has a predilection for RGCs whereas AAV5 has been shown to transduce DRGN (Harvey, Hellstrom et al. 2009; Mason, Ehlert et al. 2010). Not only are researchers restricting themselves to the available serotypes, they are also increasingly modifying *cap* genes to yield vectors with even more finely tuned tropisms (White, Mazur et al. 2008).

The third major advantage of AAV vectors over many others is that they are able to effect long-term and high level transgene expression (Lo, Qu et al. 1999). This is particularly pertinent to the treatment of CNS injuries, since it is known that regenerating neurones require prolonged growth stimulation for them to successfully re-innervate distant targets.

#### 1.4.2.3 AAV vector disadvantages

When working with AAV vectors, several limitations must be borne in mind, many of which are the subject of intense research. Firstly, AAV vectors can only accept relatively small inserts meaning that very large genes such as dystrophin cannot be expressed in a single vector (although AAV vectors are being deployed for muscular dystrophy, using a variety of ingenious methodologies (Miyagoe-Suzuki and Takeda 2010)). Conveniently, the genes used in this study fall well under the ~4kb maximum capacity for an AAV genome.

A second limitation to AAV vectors is that the kinetics of expression from most serotypes is slow, resulting from the need to convert the ssDNA AAV genome into double-stranded DNA (dsDNA) from which genes can be transcribed (Ferrari, Samulski et al. 1996). With most AAV serotypes in DRGN, it typically takes 2-4 weeks for expression to reach maximal levels (Mason, Ehlert et al. 2010). When using AAV vectors in acute models of CNS injury, this usually necessitates injecting the viral vector *before* performing the lesion. Clearly, this is not appropriate for therapeutic use in humans, leading to a number of methods of modifying AAV vectors to give faster expression kinetics (McCarty, Monahan et al. 2001).

### 1.4.3 Adenoviruses

Ads are polyhedral, encapsidated non-enveloped viruses that contain a linear dsDNA genome (Verma and Weitzman 2005). Despite the fact that they are responsible for

a diverse range of human diseases, they have been deployed as successful gene therapy vectors for many years. There are over 50 serotypes of Ad capable of infecting humans, with tropisms for most body tissues including the CNS.

Ads can accommodate an insert of around 8kb, around twice that of AAV (Verma and Weitzman 2005). However, their expression kinetics are quite different to AAV: a rapid onset of high-level expression, which is seen to decay over the course of a few weeks (Xu, Mizuguchi et al. 2005). Thus, from the point of view of CNS axon regeneration, Ad based vectors are likely to be less useful in the context of chronic injuries and more useful in the acute setting. A large component of the transience of Ad expression is due to clearance by the immune system. A number of groups have developed ways to circumvent this, such as by coating the particles to evade immune recognition (Sims, Ahmed et al. 2009).

### 1.4.4 Lentivirus

In contrast to AAV and Ad, lentivirus (LV) is a retrovirus, possessing an RNA genome surrounded by core proteins and a lipid envelope (Verma and Weitzman 2005). LVs include Human Immunodeficiency Virus and Simian Immunodeficiency Virus. After reverse transcription of their genomes, LV are able to integrate into the host genome giving a long duration of expression. Despite the fact that LV only exist in a limited number of serotypes, they lend themselves well to pseudotyping and have been employed successfully in the nervous system, including SCI models (Alto, Havton et al. 2009; Cannon, Sew et al. 2011).

## 1.5 Combinatorial therapies

Possibly with the exception of AG1478, no feasible monotherapy to date has resulted in convincing axon regeneration in the CNS (Koprivica, Cho et al. 2005). When the mechanisms of action of successful single interventions are examined in detail, it frequently becomes clear that multiple pathways are being manipulated. AG1478 was found, by an unknown mechanism, to stimulate the release of multiple NTF from retinal cells and to increase the level of cyclic adenosine monophosphate (cAMP) within RGC (Douglas, Morrison et al. 2009). It was already known from experiments employing intravitreal peripheral nerve grafts that multiple NTF could elicit axon regeneration in the optic nerve by activating the 'growth state' of RGC in addition to causing the release of scar-dissolving enzymes from growth cones (Berry, Carlile et al. 1996; Ahmed, Dent et al. 2005; Ahmed, Suggate et al. 2006). These observations, and many others, have led the CNS regeneration community to the conclusion that combinatorial therapies are probably the most promising approaches to this most difficult of biomedical problems (Lu and Tuszynski 2008).

### 1.5.1 Multiple NTF

It has been shown in the injured optic nerve, using two different delivery strategies, that NTF act synergistically leading to increased RGC survival and axon regeneration (Berry, Gonzalez et al. 2001; Logan, Ahmed et al. 2006). That multiple NTFs should have effects over and above the total of the effects for each individual NTF should not come as a surprise, since most growth factors tend to converge on the same

second messenger systems. Thus it is likely that multiple NTF would bring a large number of neurones above a 'trophic threshold' necessary for growth and survival.

### 1.5.2 NTF plus disinhibitory therapies

One of the earliest reports of the effect of combining NTF delivery with disinhibition came from Schwab's laboratory (Schnell, Schneider et al. 1994). In this study, NT-3 was delivered as a single injection just rostral to a DC lesion alongside continuous intrathecal delivery of the IN-1 antibody. It was shown that elongation of CST fibres beyond the lesion site was significantly enhanced by the combined treatment, compared with the effect of delivering each singly. NT-3 alone resulting in short distance sprouting, whereas IN-1 alone resulted in a modest amount of elongation compared with the combined treatment. Schwab's group went on to replicate this experiment in the same injury model, but in the chronic situation (von Meyenburg, Brosamle et al. 1998). Similar findings have also been demonstrated in the auditory system (Tatagiba, Rosahl et al. 2002).

*In vitro, s*trong synergistic effects have also been shown when fibroblast growth factor 2 (FGF-2) and the TNFα converting enzyme (TACE) are delivered in the presence of CNS myelin to DRGN (Ahmed, Mazibrada et al. 2006). TACE disinhibits neuronal growth by digesting $p75^{NTR}$, effectively abolishing a major component of the AGIL signalling pathway. Each treatment alone resulted in very little growth promotion.

### 1.5.3 NTF containing bridges

An important challenge in the treatment of SCI, particularly in the chronic stage, is the presence of a significant gap between the proximal and distal cord stumps and cavities within the remaining peri-lesion tissue (see section 1.1.2.3.2.2). Such spaces impair regeneration since axons are unable to grow in the absence of a suitable substrate. To overcome this problem, a number of cell and bioengineering approaches have been taken, often incorporating NTF in an attempt to stimulate axon growth into the graft.

A report from Tuszynski's group demonstrated the efficacy of BDNF-expressing marrow stromal cell (MSC) grafts inserted into acute DC lesion cavities (Lu, Jones et al. 2005). Compared to control GFP-expressing MSC grafts, BDNF expressing grafts were invaded by large numbers of DRGN central projections, but only limited numbers of CST axons. Unfortunately, this study showed no convincing behavioural improvement in any of the grafted animals. This is probably due to the fact that, like in many other similar grafting experiments, axons penetrate the MSC grafts by never leave them. This effect is probably due to the BDNF-expressing grafts forming a 'neurotrophin sink', keeping axons in the lesion by positive chemotaxis. The authors mentioned that such problems may be overcome by using approaches to deliver a gradient of NTF, encouraging regenerating axons to enter CNS tissue adjacent to the graft.

### 1.5.4 Manipulation of the neuronal growth state

Despite the optimism generated by Aguayo's peripheral nerve grafting experiments (see section 1.1.4), it was still apparent to many that CNS neurones seemed to have a poorer intrinsic growth capacity than their peripheral counterparts. This was formally demonstrated in a study from Fawcett's group, where the rate of regeneration of RGCs was compared with that of DRGN *in vitro* (Chierzi, Ratto et al. 2005). Fewer RGCs regenerated than DRGN, and in those that did RGCs regenerated three times more slowly than DRGN.

The growth state of neurones is determined by a complex gene network with multiple points of regulation. Factors which can influence the neuronal growth state in a positive way are diverse, including: presence of NTF, neuronal injury, perineuronal inflammation, intracellular cAMP and the presence of suitable substrates for growth (Tuszynski and Kordower 2008). These signals are integrated by a number of metabolic pathways including mTOR, PI3-kinase and MAPK ultimately impinging on neuronal transcription factors such as cAMP response element binding, c-Jun and activating transcription factor 3 (Liu, Tedeschi et al. 2011).

#### *DRGN and the conditioning effect*

DRGN possess a peculiar anatomical feature unique to primary sensory neurones – they have peripheral and central axonal processes, projecting to peripheral sense organs and the cord, respectively (Willis and Coggeshall 2004). This leads to an

inevitable, and seemingly paradoxical situation where the same single neurone possesses one axon which is capable of regeneration (peripheral) and one axon which is not (central). This simple observation has, through some ostensibly simple experiments, led to a number of important discoveries.

It has been known for almost 40 years that if a peripheral nerve is transected (the 'conditioning' lesion), and then re-transected some days later between the original lesion and the DRG, regeneration of DRGN peripheral processes is enhanced in the peripheral nerve (McQuarrie and Grafstein 1973). Furthermore, if such a conditioning lesion is performed prior to a spinal cord lesion containing a peripheral nerve implant, regeneration of DRGN *central* processes is enhanced into the peripheral nerve graft (Richardson and Issa 1984). The culmination of this work came when Neumann and Woolf demonstrated that conditioning lesions enhanced regeneration of DRGN central processes in the *absence* of any permissive grafts in the spinal cord (Neumann and Woolf 1999). The conclusion of these experiments, taken together, is that the conditioning lesion activates the growth program of DRGN allowing their central processes to regenerate. It has since become clear that increased levels of neuronal cAMP and inflammatory responses within the DRG have important roles in the conditioning effect, although some anomalies still exist such as the lack of a conditioning effect from lesions to the dorsal root (Silver 2009).

### 1.5.5 Putting it all together – the state of the art of combinatorial therapies

Unsurprisingly, researchers have attempted extensive combinatorial treatments in animal models of SCI. One of the most interesting examples is from Tuszynski's

group, where three treatments were combined in animals receiving a high cervical (C1) DC lesion: a conditioning lesion was performed, a MSC graft was inserted into the lesion site and a LV expressing NT-3 was injected rostral to the lesion (Alto, Havton et al. 2009). Axons regenerated across the MSC graft and into the medulla, and electron-microscopic (although not electrophysiological) evidence of synapses was observed. The results of this study are encouraging, but still of limited usefulness in the clinical setting since the synapses are not functional and the conditioning lesions are unfeasible (and unethical) in human subjects.

There are still many obstacles that need to be crossed before SCI can be effectively treated in human subjects. Axon regenerative therapies have been so unsuccessful over the last 100 years that some researchers feel that this may have become a sterile field, and that the community as a whole should put the majority of its energy into rehabilitative measures. However, the author hopes that the preceding pages and those to come will provide at least some evidence that spinal cord axon regeneration is indeed worthwhile pursuing from the points of view of both clinical and basic research.

### 1.6 Rationale, hypothesis and aims

It is clear from the literature that combinatorial approaches, providing neurotrophic support to neurones and targeting AGIL, are likely to provide successful therapies for SCI. This study aims to examine the effect of AAV8-mediated delivery of NT-3 and $shRNA_{RhoA}$ on axon regeneration in the lesioned DC of adult rats.

### 1.6.1 Main hypothesis

AAV8$_{hrgfp\text{-}nt3\text{-}shrna\text{-}rhoa}$ and AAV8$_{hrgfp\text{-}nt3}$ transduction of DRGN *in vivo* mediates neurone disinhibited regeneration of DC axons

### 1.6.2 Main aims

- To generate and evaluate plasmids that contain NT-3 and shRNA$_{RhoA}$, that will ultimately be used to generate the vectors AAV8$_{hrgfp\text{-}nt3\text{-}shrna\text{-}rhoa}$ and AAV8$_{hrgfp\text{-}nt3}$
- To examine the cellular tropism of AAV8 in the DRG
- To assess the glial and inflammatory responses to AAV8-mediated delivery of GFP in the DRG and spinal cord
- To examine the effect of AAV8-mediated delivery of NT-3 and shRNA$_{RhoA}$ on axon regeneration in the lesioned DC of adult rats

# Chapter 2

# Materials and methods

## 2.1 *In vitro* methods

### 2.1.1 Preparation of dissociated DRG cultures

Adult male Sprague-Dawley rats (weight 150-250g) were killed by cervical dislocation. The whole spinal column from cervical to sacral levels was removed and kept on ice. Paraspinal musculature was removed and the spinal cord and DRG visualised by cutting through the pedicles with rongeurs and removing the lamina of each vertebra. Lumbar DRG from L2-L5 were removed under direct vision at 20X magnification and kept in ice cold Neurobasal A medium (NBA; Gibco, Paisley, UK).

When the dissection was complete DRG were washed in warm NBA, then placed in 0.125% collagenase (Sigma-Aldrich, Poole, UK) in NBA, snipped in half and incubated for 2 hours (h) at 37°C, 5% $CO_2$ in a humidified atmosphere. DRG were then washed in NBA to remove excess collagenase, and resuspended in 2ml of warmed NBA. They were then triturated 15-20 times through a cut-off 500µl pipette tip followed by a further 15-20 triturations through an intact pipette tip. Each 1ml of the cell suspension was then carefully layered onto 2ml of warm 15% bovine serum albumin (BSA) in NBA and spun at 120g for 10min at room temperature. The supernatant was carefully removed and the resulting pellet resuspended in 100µl warmed trypsin inhibitor cocktail, from which 10µl was taken for cell counting. Cells were finally resuspended in an appropriate amount of NBA supplemented with 2% B27 supplement, 200mM L-glutamine and 0.2% gentamycin before plating. Cells were plated onto 8-well chamber slides at a density of 500 DRGN per chamber in a volume of 300µl.

### 2.1.2 COS-1 cell culture

COS-1 cells, originally derived from the kidney of the green monkey, were used for the expression of recombinant NT3 and NT3-FLAG proteins (Gluzman 1981). COS-1 cells were maintained as monolayers in 75cm$^2$ and 175cm$^2$ tissue culture flasks (Sarstedt, Leicester, UK) in Dulbecco's modified Eagle medium (DMEM, GIBCO) supplemented with 10% foetal bovine serum (FBS) and containing 1% penicillin/streptomycin. Cells were split at a ratio of 1:10 using 0.05% trypsin in sterile PBS, and never maintained beyond passage number 10 (all reagents above from Gibco).

### 2.1.3 Transfection of cells using Lipofectamine 2000

#### 2.1.3.1 Principles

Cationic lipids are established vectors for the introduction of plasmid DNA into eukaryotic cells. Purified plasmid DNA is mixed with Lipofectamine 2000 at a given ratio, resulting in the formation of micelles, containing the DNA enclosed between an inner core and outer shell of lipid. These micelles enter cells by endocytosis, and, by mechanisms which are not fully understood, their DNA payload enters the cytosol. Once in the cytosol, the DNA enters the nucleus by passive diffusion, facilitated in dividing cells by the transient breakdown of the nuclear envelope during prometaphase. (Elsabahy, Nazarali et al. 2011)

### 2.1.3.2 Protocol

COS-1 cells were plated at a density of 500 000 cells/well of 6-well plates in DMEM with 10% FBS and 1% penicillin/streptomycin and allowed to settle for 24h. The medium was removed and replaced with 2ml serum and antibiotic free DMEM. In the meantime, for each well, 4µg plasmid DNA and 10µl Lipofectamine 2000 (Invitrogen) were diluted in 250µl DMEM at room temperature (rt) and allowed to equilibrate for 5min. The diluted Lipofectamine 2000 was added to the diluted plasmid DNA and incubated at room temperature (rt) for 20min to allow lipid-DNA complexes to form. The complexes were added to cells, and incubated for 5h in a humidified atmosphere at 37°C, 5% $CO_2$. After this, the medium was removed and replaced with 2ml DMEM supplemented with FBS and penicillin/streptomycin. If COS-1 cells were being grown on for 6 days (d) to produce recombinant protein, an additional 1ml of medium was added after 3d.

### 2.1.3.3 Production of conditioned medium

COS-1 cell were transfected with appropriate plasmids and maintained under appropriate conditions for 7d. After 7d, conditioned medium was removed from cells and spun at 13000G for 5min. The resulting supernatant was decanted and stored at -18ºC.

### 2.1.4 Histological techniques

Immunocytochemistry (ICC) and immunohistochemistry (IHC) are used to detect cellular antigens in dissociated cell preparations by exploiting the ability of antibodies to bind strongly and specifically to a given protein antigen. These so-called primary

antibodies can be either monoclonal (usually derived from mouse, specific for a single epitope from a single protein) or polyclonal (from a number of species, specific to multiple epitopes from the same protein). A secondary antibody, usually with a conjugated fluorophore is applied to enable visualisation of the location of the antigen-bound primary antibody.

In the present study, every experiment using ICC or IHC included a control where the primary antibody was omitted in order to exclude binding of secondary antibodies to the tissue or cells. Unless stated otherwise, no staining was observed in tissue or cells exposed to secondary antibody alone. Other, relevant controls for ICC and IHC include looking for a similar staining pattern with a different antibody, Western blotting using the antibody of interest (fewer bands on a tissue lysate indicate higher antibody specificity) and incubation of the primary antibody with a blocking peptide to demonstrate specificity. These additional controls were not usually carried out in the present study, since the Molecular Neuroscience Group has extensive experience of using these antibodies in the spinal cord, brain and optic nerve. Hence, their specificity was well established.

#### 2.1.4.1 Protocol for βIII-tubulin immunocytochemistry on DRG cultures

Mixed DRG cultures grown in 8-well chamber slides for 2d on poly-D-lysine (PDL) with and without laminin were removed from the tissue culture incubator and allowed to cool at rt for 5min. Medium was removed and each well fixed in 500µl 4% formaldehyde (TAAB Laboratories, Aldermaston, Berkshire, UK) for 15min. Wells were washed 5min x3 with 500µl phosphate buffered saline (PBS) before adding

500µl blocking solution to each well for 10min at rt (blocking solution contained 3% BSA (Bio-Rad, Hertfordshire, UK) and 0.1% Triton X-100 (Sigma) in PBS). Antibodies were diluted in antibody diluting buffer containing 3% BSA and 0.05% Tween-20 (Sigma). The antibodies used are listed in Table 2.1. To each well 100µl primary antibody was added and incubated at rt with gentle shaking for 1h. Three 5min washes were then performed with PBS followed by addition of 100µl diluted secondary antibody. This second incubation was done in the dark to avoid bleaching of the fluorophore. After 3 washes in PBS the plastic chambers were removed followed by the addition of Vectashield with 4',6-diamidino-2-phenylindole (DAPI, Vector laboratories Ltd., Peterborough, UK) and application of a coverslip prior to microscopic examination.

#### 2.1.4.1.1 Quantification of neurite outgrowth and neuronal survival from dissociated DRG cultures

After immunocytochemistry, each individual chamber from chamber slides was split into 9 equal areas in 3x3 grid. Within each of these areas, three randomly selected fields of view were photographed at x10 magnification thus yielding 27 micrographs representing a sample of the DRGN population in that specific chamber. At least 2 chambers were used per condition.

The number of DRGN per image were counted, as well as the length of the longest neurite per DRGN using ImagePro software (Media Cybernetics Inc., Maryland, USA). Neurites less than a cell body's diameter were not measured.

| Primary antibody | Source | Species | Concentration for ICC | Concentration for IHC | Concentration for WB |
|---|---|---|---|---|---|
| CD68 | Serotech | Mouse | N/A | 1:200 | N/A |
| CD11b | Serotech | Mouse | N/A | 1:200 | N/A |
| GFAP | Sigma | Mouse | N/A | 1:500 | N/A |
| PV | Sigma | Rabbit | N/A | 1:8000 | N/A |
| eGFP | AbCam | Rabbit | 1:4000 | 1:4000 | N/A |
| βIII-tubulin | Sigma | Mouse | 1:200 | 1:1000 | N/A |
| 3X FLAG | Sigma | Mouse | N/A | N/A | 10µg/ml |
| CTB | List | Goat | N/A | 1:100 | N/A |
| **Secondary antibody** | | | | | |
| AlexaFluor 488 anti-mouse IgG | Molecular Probes | Goat | 1:200 | 1:500 | N/A |
| AlexaFluor 594 anti-mouse IgG | Molecular Probes | Goat | 1:200 | 1:500 | N/A |
| AlexaFluor 488 anti-rabbit IgG | Molecular Probes | Goat | 1:200 | 1:500 | N/A |
| AlexaFluor 594 anti-rabbit IgG | Molecular Probes | Goat | 1:200 | 1:500 | N/A |
| Anti mouse IgG HRP | GE Healthcare | Sheep | N/A | N/A | 1:1000 |
| Anti rabbit IgG HRP | GE Healthcare | Donkey | N/A | N/A | 1:1000 |
| AlexaFluor 594 anti goat | Molecular Probes | Donkey | N/A | 1:400 | N/A |

**Table 2.1**. Antibodies used in this study**.** Abbreviations: ICC Immunocytochemistry; IHC Immunohistochemistry; WB western blotting; HRP Horseradish peroxidise; N/A not applicable

### 2.1.4.2 Protocol for immunohistochemistry

In order to perform IHC, four major steps must be performed. First, tissue must be dissected, fixed and embedded; secondly the embedded tissue must be cut into sections; thirdly, the sections must be stained using appropriate primary and secondary antibodies; finally, stained tissue must be visualised and quantified, if appropriate.

#### 2.1.4.2.1 Preparation of tissue

Animals were sacrificed by $CO_2$ narcosis and transcardially perfused with 4% formaldehyde (TAAB laboratories, Aldermaston, Berkshire, UK) in PBS. L4/L5 DRG, dorsal and ventral roots, spinal cords (separated into segments containing L4/L5 DREZ, rostral lumbar segments of the cord, thoracic cord, cervical cord and lesion sites with 5mm rostral and caudal to the lesion) and medullas were removed and post-fixed in 4% formaldehyde in PBS overnight at 4ºC. Tissue specimens were cryo-preserved by equilibration in sucrose at 10, 20 and 30% w/v concentration, embedded in optimal cutting temperature (OCT) mounting medium, and stored at -80ºC.

#### 2.1.4.2.2. Tissue sectioning

Frozen tissue sections were cut at a thickness of 15µm or 25µm (lesion sites) using a Bright cryostat. DRG sections were cut in a longitudinal orientation, parallel to the axis of entry of roots and exit of spinal nerves of the ganglion. Dorsal and ventral roots were cut in the transverse plane, the spinal cord cut in both coronal and horizontal planes and medullas cut in the coronal plane at the level of the gracile

nucleus. Lesion sites were cut in the sagittal plane, and sections approximately 200µm to the left of the midline were examined using IHC.

#### 2.1.4.2.3 Immunostaining

Thawed sections were washed X2 for 5min in PBS, X1 for 5min in PBS+0.1% triton X-100 or PBS+1% triton X-100 (PBST) and then incubated in a humidified chamber for 1h at room temperature (rt) in either 3% bovine serum albumin (BSA; Sigma, Poole, UK), or 2% BSA+10% normal donkey serum (NDS) in PBST, incubated overnight at 4ºC with either primary antibody (Table 2.1) diluted in 3% BSA, or 2% BSA in PBST, washed X3 for 5min in PBST and then incubated with secondary antibody (Table 2.1) diluted in 3% BSA in PBST for 1h at rt, washed X3 for 5min in PBST, and mounted in Vectashield mounting medium with DAPI (Vector laboratories Ltd., Peterborough, UK).

#### 2.1.4.2.4 Visualisation and quantification

Sections were photographed throughout using a Zeiss Axioplan 2 microscope connected to a PC running AxioVision 4.6 software (Carl Zeiss Ltd., Hertfordshire, UK).

##### 2.1.4.2.4.1 Analysis of enhanced green fluorescent protein (GFP) expression in DRG allowing assessment of transduction rate

For analysis of AAV8$_{gfp}$ tropism in the DRG, approximately 35 fields of view per DRG section were captured using the x10 objective and merged to create a single composite image using the Photomerge feature in Adobe Photoshop CS3 (Adobe

Systems Incorporated). For analysis of GFP expression, DAPI and FITC channels were converted to greyscale and examined using ImagePro image analysis software (Media Cybernetics Inc., Maryland, USA). DRGN were identified in the DAPI channel as large, round cell bodies visible as empty areas with large, round pale DAPI+ nuclei, encircled by satellite cells with small elongated DAPI+ nuclei. DRGN were identified during 4 passes of each composite image at 25% and 100% digital zoom levels. The diameters and positions of each GFP+ DRGN were recorded and saved as a mask which was then applied to the FITC channel to compute frequencies and diameters. Assessment of the total number of DRGN in each section allowed estimation of the percentage transduction of DRGN by AAV8 (the transduction rate). The same procedure was used to analyse parvalbumin+ DRGN using the rhodamine and DAPI channels.

#### 2.1.4.2.4.2 Analysis of coronal sections of spinal cord

Coronal sections of the spinal cord were examined by producing composite images in Photomerge using fields of view taken through a X10 objective lens. Grey matter was demarcated using tissue auto-fluorescence and images were contrast adjusted to demonstrate GFP+ axons.

#### 2.1.4.2.4.3 Analysis of glial activation

Coronal sections of rostral lumbar cord from intact, intra-DRG PBS injected and intra-DRG AAV8$_{gfp}$ injected animals were stained for either GFAP, or CD11b as described above and photographed under identical conditions. For each animal, two micrographs (ipsilateral and contralateral) were taken from one of three regions

within the rostral lumbar cord – the dorsal column, the superficial dorsal horn and the deep dorsal horn. Using Adobe Photoshop CS3, the threshold level at which CD11b and GFAP staining disappeared was determined in three intact animals for the regions specified and a mean value determined. This value was then used to threshold micrographs from experimental animals, so that any staining observed could be attributed to up-regulation of CD11b or GFAP. The number of pixels in these images after thresholding was counted, giving a measure of glial activation.

#### 2.1.4.3 Oil-Red-O staining

Oil-Red-O staining was used to visualise myelin breakdown products. Signal is obtained when myelin degenerates, leading to the deposition of red staining lipid droplets. Horizontal sections of spinal cord were thawed, rinsed in 60% isopropanol, stained in freshly prepared Oil-Red-O for 15min at rt, rinsed in 60% isopropanol, counterstained with haematoxylin for 10sec, rinsed in distilled water and mounted in Vectamount (Vector Laboratories).

### 2.1.5 Sodium dodecyl sulphate polyacrylamide gel electrophoresis (SDS-PAGE) and western blotting

#### 2.1.5.1 Principles of protein electrophoresis and western blotting

It is possible to separate proteins based upon their molecular mass by denaturing them, giving them a known negative charge and then passing them through a polyacrylamide gel of known density. The gel itself can be stained for total protein using a reagent such as Coomassie blue, and the size of protein bands determined

by comparison with standards of known molecular weight. Alternatively, if one wishes to probe for a specific protein, the contents of the gel can be transferred to a nitrocellulose membrane which can then be incubated with an antibody of choice and visualised using a secondary antibody linked to an appropriate reporter.

### 2.1.5.2 Protocol for protein electrophoresis and Western blotting

#### 2.1.5.2.1 Gel casting and running SDS-PAGE

All apparatus for gel casting, running and transfer were from Invitrogen (Paisley, UK) and all reagents were from Sigma (Poole, UK), unless otherwise stated.

Gels composed of 12% polyacrylamide were cast in 1mm disposable cassettes. Each resolving gel was composed of 2.75ml Protogel (Geneflow, Fradley, UK), 1.65ml 1.5M Tris-HCl pH 8.8, 2.2ml water, 66µl 10% SDS, 23.1µl 10% ammonium persulphate (APS) and 9.9µl Tetramethylethylenediamine (TEMED, VWR International, Lutterworth, UK). Layering of 70% ethanol onto the resolving gel excluded air during polymerisation. Each stacking gel was composed of 0.4ml Protogel (Geneflow), 1.85ml 0.5M Tris-HCL pH 6.8, 0.75ml water, 30µl 10% SDS, 15µl 10% APS, 7.5µl TEMED (VWR International). A 1mm comb was inserted and the gel allowed to polymerise at rt.

Samples were prepared by first adjusting the protein concentration by dilution in MilliQ water if appropriate, followed by addition of an equal volume of 2X sample loading buffer, containing 2-mercaptoethanol (Sigma). The diluted samples were boiled for 4min at 90°C, and 20µl was added to each well. A volume of 10µl of pre-

stained protein ladder (Invitrogen) was added to assigned wells. Gels were run at 125V, 18mA, 2.1W for 1h 50min under buffer containing 25mM Tris-base, 192mM glycine and 0.1% SDS.

#### 2.1.5.2.2 Western blotting

When the samples had run an appropriate distance, the gel was released from its cassette and transferred onto a Polyvinylidene difluoride (PVDF) membrane, which had been activated by soaking in 100% methanol for 1min followed by a 1min wash in water. Gel and membrane were kept in close opposition using foam pads, the transfer process being carried out at 25V for 2h in a chilled buffer containing 25mM Tris-base, 192mM glycine, 20% methanol and 0.02% SDS.

All subsequent washes were carried out in TTBS (10mM Tris-base, 150mM NaCl, 0.05% Tween-20) and all blocking/antibody steps carried out in either 5% Marvel, or 3% BSA in TTBS, depending on the antibody used.

After transfer, the membranes were soaked in TTBS for 5min then incubated in blocking solution for 1h at rt. The blocking solution was removed and primary antibody added at an appropriate concentration followed by incubation at 4°C overnight. The membranes were washed x3 for 10min each before the addition of appropriate secondary antibody and incubation at rt for 1h. Membranes were washed as described above, dried gently on blotting paper and incubated for 1min at rt in 2ml enhanced chemiluminescence (ECL) solution. Excess ECL was blotted off, the membranes placed in bags and exposed onto Kodak Biomax film (Kodak).

### 2.1.6 Enzyme linked immunosorbent assay (ELISA)

#### 2.1.6.1 Principles

ELISA is a highly sensitive, quantitative assay for determining the concentration of a specific protein. There are many variations, but all involve the adsorption of an antibody or antigen to a sample plate followed by the addition of further antibodies. The final antibody is usually an horseradish peroxidase (HRP) conjugate allowing a colorimetric assay to be used for quantification. The ELISA used in the experiments described here to detect NT-3 was the NT-3 $E_{max}$ Immunoassay System (Promega, Madison, WI, USA). The NT-3 $E_{max}$ kit exploits the technique known as 'sandwich ELISA' in which a sample plate is coated with a polyclonal antibody against NT-3. After coating, samples were placed in appropriate wells and following a washing step a monoclonal antibody against NT-3 from mouse was added. Antibody-bound NT-3 was quantified by the addition of an HRP-conjugated secondary antibody which oxidised 3,3´,5,5´-tetramethylbenzidine (TMB) to a coloured product, which was measured colorimetrically using absorbance at 450nm. To get accurate estimations of concentration in each unknown sample, multiple dilutions were performed as well as a standard curve where absorbances of known concentrations of recombinant NT-3 were measured.

#### 2.1.6.2 Protocol

All reagents were from Promega unless otherwise stated. All antibodies, standards and Block and Sample Buffer were provided in the NT-3 $E_{max}$ Immunoassay System

(Promega, Madison, WI, USA). Quantities used were for a single Nunc Maxisorp 96-well plate (Thermo Fisher, Waltham, MA, USA).

Anti-human NT-3 polyclonal antibody (pAb) was diluted to a concentration of 1µg/ml in carbonate coating buffer (0.025M sodium bicarbonate, 0.025M sodium carbonate adjusted to pH 9.7) and 100µl added to each well. The plate was sealed with Parafilm M (Pechiney Plastic Packaging Company, Chicago, IL, USA) and incubated at 4°C overnight. The contents of each well were then flicked out and the plate washed once by filling all wells with TBST wash buffer (20mM Tris-HCL, 150mM NaCl, 0.05% Tween-20, pH 7.6).

The plate was blocked by adding 200µl 1X Block and Sample Buffer (exact composition proprietary), followed by incubation at rt for 1h. After blocking, the plate was washed once with TBST and samples and standards were added at appropriate dilutions in duplicate in a volume of 100µl per well. Typically, the initial dilution of each sample was 1:4 with serial 1:2 dilutions. The concentrations of the NT-3 standard ranged from 300pg/ml to 4.7pg/ml by serial 1:2 dilutions, with an additional set of wells containing no standard.

The plate containing samples was incubated at rt for 6h with shaking at 500rpm. After this, the wells were washed x5 with TBST and 100µl anti-NT3 monoclonal antibody (mAb) at a dilution of 1:4000 was added to each well before incubating at 4°C overnight. Wells were washed x5 with TBST and 100µl anti-mouse IgG HRP conjugate added to each well at a dilution of 1:100. The plate was incubated at rt

with shaking at 500rpm for 2.5h followed by 5 washes with TBST. Each well received 100µl TMB One solution (containing TMB, exact composition proprietary information) followed by incubation with shaking at rt for 15min. After this, the reaction was stopped by adding 100µl 1N HCl to each well. The absorbance of the plate was read at 450nm within 30min of addition of HCl on a Victor$^3$ Multilabel counter (Perkin-Elmer, Waltham, Massachusetts, USA).

Each plate was analysed by deriving a linear regression line from the standard curve, re-arranging the equation for this line to give concentration of NT-3 in terms of absorbance and applying this to the unknown values (Figure 2.1). Only sample absorbances which lay within the range seen on the standard curve were used to ensure that accurate estimates were obtained. Initial and serial dilutions were accounted for, and the value derived was taken as the mean of the most appropriate duplicate for each sample.

### 2.1.7 Molecular cloning

#### 2.1.7.1 Principles of molecular cloning

The term ‘cloning’ refers to a set of techniques used to precisely manipulate nucleic acid molecules. Such manipulations include transferring a sequence of DNA from one vector to another (the vector usually being a plasmid), introducing mutations at specific points in a DNA sequence and producing ‘libraries’ of genes from a specific tissue.

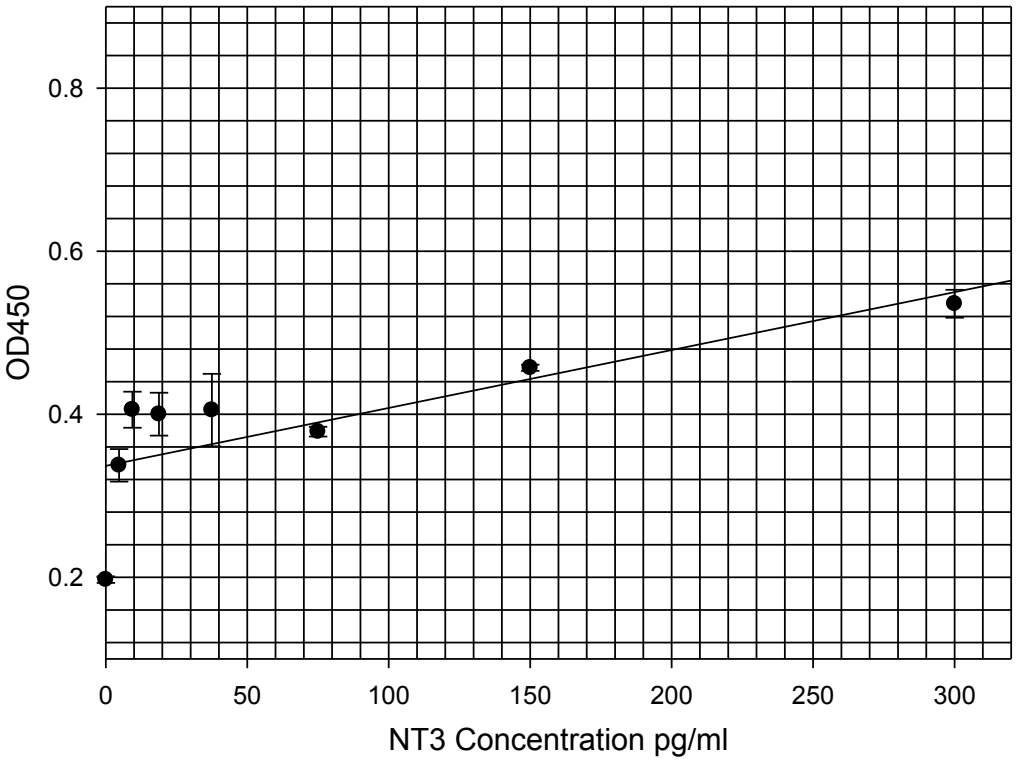


**Figure 2.1** A typical standard curve for NT-3 ELISA using the $E_{max}$ kit. The line of best fit was generated by Sigmaplot v.10 software, which also generated a linear equation allowing estimation of unknown concentrations.

Fragments of DNA can be cut at specific sites ('digested') with restriction endonucleases, often termed 'restriction enzymes'. These enzymes have allowed not only the accurate and reproducible digestion of DNA molecules, but have also allowed DNA sequences to be mapped, given a knowledge of the actual and predicted sites of cleavage by a chosen enzyme or enzymes.

After cleavage of DNA by restriction enzymes, fragments can be separated using agarose gel electrophoresis and visualised with ethidium bromide (EtBr). Such separation enables DNA fragments to be isolated, allowing further manipulations to be performed.

Cleaved pieces of DNA can be re-attached using DNA ligases that can join overlapping ('sticky') ends or non-overlapping ('blunt') ends of DNA fragments. This is commonly performed when inserting a fragment into a recipient plasmid during the process of sub-cloning.

Another commonly performed procedure is the polymerase chain reaction (PCR). This technique uses short oligonucleotide primers to amplify a segment of DNA defined by the position of the forward and reverse primers. In addition, PCR can be used to introduce mutations into DNA sequences using a variety of techniques. All of these methods of site directed mutagenesis use primers which contain a mutation. Since it is part of the primer, the mutation will be included in all of the amplified segments. The mutated segment can then be sub-cloned into an appropriate vector.

### 2.1.7.2 Protocol for restriction digestion of DNA

In a typical restriction digest, 1µg of plasmid DNA was digested using 10 units of restriction enzyme in the presence of the appropriate buffer, with or without BSA at 37ºC for 2h. All enzymes used in cloning are listed in Table 2.2. The products of each reaction were usually run on a 0.7% agarose gel.

### 2.1.7.3 Protocol for dephosphorylation of restriction digest products

If a plasmid was to become the recipient for a sub-cloning procedure, following its digestion, it was dephosphorylated to ensure that its own sticky ends did not ligate together. The resulting self-ligation results in a high level of vector background, as well as decreasing the efficiency of any sub-cloning procedure. Dephosphorylation was achieved by adding 5 units of antarctic phosphatase per microgram of DNA, along with an appropriate amount of antarctic buffer (both supplied by New England Biolabs, Ipswich, MA, USA) and incubating at 37ºC for 30min. The resulting dephosphorylated fragments were then run on an agarose gel, purified and stored for future use.

### 2.1.7.4 Protocol for agarose gel electrophoresis

Agarose (0.7%) was dissolved by heating in TAE-EtBr (2M Tris-acetate, 100mM $Na_2EDTA$ (Geneflow), 1µg/ml ethidium bromide (Promega)) before pouring into a gel casting unit, and inserting a comb. Samples were diluted in 6X gel loading buffer, and up to 20µl of sample loaded into each well alongside an appropriate DNA ladder. The gels were run at a current of 50mA for 60-90min, or until the bands were seen to

| Enzyme | Supplier | Sequence cut | Buffer | BSA |
|---|---|---|---|---|
| BamHI | NEB | 5'-GGATCC-3'<br>3'-CCTAGG-5' | 3 | 100µg/ml |
| NotI | NEB | 5'-GCGGCCGC-3'<br>3'-CGCCGGCG-5' | 3 | 100µg/ml |
| ScaI | NEB | 5'-AGTACT-3'<br>3'-TCATGA-5' | 3 | Not required |
| SnaBI | NEB | 5'-TACGTA-3'<br>3'-ATGCAT-5' | 4 | 100µg/ml |
| XhoI | NEB | 5'-CTCGAG-3'<br>3'-GAGCTC-5 | 4 | 100µg/ml |
| T4 DNA ligase | Promega | N/A | Ligase buffer | Not required |
| Taq polymerase | Roche | N/A | PCR buffer 2 | N/A |

**Table 2.2** Enzymes used in molecular cloning. Buffer 3: 100 mM NaCl, 50 mM Tris-HCl, 10 mM $MgCl_2$, 1 mM Dithiothreitol, pH 7.9 @ 25°C. Buffer 4: 50 mM potassium acetate, 20 mM Tris-acetate, 10 mM Magnesium Acetate, 1 mM Dithiothreitol, pH 7.9 @ 25°C. Ligase buffer: 300mM Tris-HCl (pH 7.8 at 25°C), 100mM $MgCl_2$, 100mM DTT and 10mM ATP. Composition of PCR buffer 2 not available.

have migrated a sufficient distance. Progress of each run was monitored using the Multigenius gel documentation system (Syngene, Cambridge, UK).

### 2.1.7.5 Protocol for ligation of DNA fragments

Purified fragments of interest, resulting from restriction enzyme digests of 1µg of plasmid (the insert) were inserted into dephosphorylated plasmid backbones (the vector) by incubating in the presence of T4 DNA ligase (Promega, Madison, WI, USA). Insert was usually incubated with vector in the presence of ligase buffer at the ratios of 0:1, 1:1 and 3:1 at rt for 30 min or overnight at 4ºC. After this, 5µl of the ligation mix was gently mixed with 50µl of XL10 competent cells (Agilent Technologies, Santa Clara, CA, USA). The cells were incubated on ice for 30 min followed by a heat shock at 42ºC for 45s then placed on ice for 2 min. After this, cells were spread on lysogeny broth (LB) agar plates with ampicillin and incubated at 37ºC overnight. Colonies were picked and used for preparation of plasmid DNA the following morning.

If the ligation efficiency was low, cells were subjected to a 'rescue step', where they were cultured for 1h in 5ml antibiotic-free LB broth before being spread on LB agar plates.

### 2.1.7.6 Polymerase chain reaction

Primers were designed by Dr Michael Douglas, and synthesised by Alta Biosciences (Birmingham, UK), see Table 2.3. Primers were diluted in 0.22 µm filtered MilliQ

| Primer name | Sequence (5'-3') |
|---|---|
| SnaBIfor | CAT-CTA-CGT-ATT-AGT-CAT-CGC-TAT-TAC-CAT-G |
| NotIOL2 | GCC-CGG-GCT-AGA-GCG-CGC-GCC-ACC-GCG-GTG-GA |
| NotIOL1 | TCC-ACC-GCG-GTG-GCG-CGC-GCT-CTA-GCC-CGG-GC |
| LONGpAAVrev | TGC-CAA-AAG-ACG-GCA-ATA-TGG-TGG |

**Table 2.3** Primers used in PCR reactions

water to a working stock concentration of 20 pmol/µl. Reactions were performed in a volume of 50µl in a Bio-Rad i-Cycler PCR machine (Bio-Rad).

#### 2.1.7.6.1 PCR on plasmid DNA

PCR reactions were performed using the Expand High Fidelity PCR System (Roche Diagnostics, West Sussex, UK). Plasmid DNA (20-30ng) was mixed with 40 pmol forward primer and 40 pmol reverse primer in the presence of 80µM deoxyribonucleotide triphosphates (dNTP) and 1X PCR buffer 2 at a total volume of 50µl. The reactions were performed using a melting temperature of 96ºC, an annealing temperature of 50ºC and an extension temperature of 72ºC. Extension was allowed to proceed for 1 – 1.5 min and the cycle repeated 14-18 times. When complete, the PCR mix was run on a gel and the appropriate band selected and purified (see section 2.1.7.8).

#### 2.1.7.6.2 Overlap extension PCR

Overlap extension PCR (OEPCR) uses three PCR reactions to introduce a point mutation into a defined region of a DNA sequence. The first two reactions (PCR1 and PCR2) use primers spanning the region to be mutated and overlapping primers containing a single point mutation at their centres. Thus, PCR1 and PCR2 will yield amplicons containing overlapping, mutated regions at one of their ends which will be complementary to one another. The full-length mutated sequence is created in PCR3 when the products of PCR1 and PCR2 are mixed in the presence of the terminal primers. The PCR reactions described below used reagents and apparatus described in section 2.1.7.6.

**PCR1**

The reaction mixture contained 28ng plasmid DNA, 2µl SnaB1for, 2µl NotIOL2, 2µl 2mM dNTP, 5µl PCR buffer 2, 1µl Taq polymerase and 37µl water. The reaction mixture was melted at 96ºC, annealed at 50ºC, extended at 72ºC for 1 min for 14 cycles.

**PCR2**

The reaction mixture contained 28ng plasmid DNA, 2µl NotIOL1, 2µl LONGpAAVrev, 2µl 2mM dNTP, 5µl PCR buffer 2, 1µl Taq polymerase and 37µl water. The reaction mixture was melted at 96ºC, annealed at 50ºC, extended at 72ºC for 1 min for 14 cycles.

The products of PCR1 and PCR2 were run on a 0.7% agarose gel. The bands were identified under UV light and purified as in section 2.1.7.8.

**PCR3**

The reaction mixture contained 1µl purified PCR1 product, 1µl purified PCR2 product, 2µl SnaBIfor, 2µl LONGpAAVrev, 5µl PCR buffer 2, 1µl Taq polymerase and 37µl water.

The products of PCR3 were run on a 0.7% agarose gel. The bands were identified under UV light and purified as in section 2.1.7.8.

### 2.1.7.7 Preparation of purified plasmid DNA from *E.coli*

Plasmid DNA was prepared at three different scales, depending upon its intended use. Standard kits of three sizes were used – QIAprep Spin Miniprep Kit and QIAfilter Midi and Maxi kits (QIAGEN, Crawley, West Sussex, UK). Minipreps were used to produce small amounts of plasmid DNA for analysis; midipreps were used for moderate amounts of plasmid DNA for testing and maxipreps were used to produce large amounts of DNA for routine use. The specific protocols for each of these are publicly available from www.qiagen.com so a general overview of the protocol will be provided followed by the detailed protocol for the QIAfilter Maxi kit.

Preparation of plasmid DNA can be split into five main stages. Firstly, transformed *E.coli* must be cultured in selective medium (usually LB Broth + ampicillin) to provide a sufficient amount of plasmid DNA. Following a successful ligation, a colony was aspirated using a P200 pipette tip and used to inoculate an appropriate volume of broth. The broth was then incubated in a rotary shaker at 37ºC overnight.

The next stage involved pelleting the cells by centrifugation and then resuspending them in an appropriate buffer. Resuspension must be complete as any lumps will not lyse efficiently. Lysis buffer was added and the mix was agitated gently. Lysis buffer contains SDS which breaks down cell walls and membranes allowing cell contents, including plasmid DNA to escape. After lysis, a third buffer was added which precipitates out bacterial cell walls and genomic DNA, leaving a solution containing plasmid DNA.

The precipitate was filtered out or pelleted and the resulting supernatant was passed through an equilibrated ion-exchange column which binds plasmid DNA. After washing, the plasmid was eluted off of the column and then precipitated out in isopropanol. The precipitated DNA was pelleted and then gently washed in 70% ethanol. Finally, the DNA pellet was air dried and resuspended in an appropriate buffer.

#### 2.1.7.7.1 Protocol for preparation of plasmid DNA using a QIAfilter Maxi kit

Five hundred millilitres of an overnight LB culture were centrifuged at ~6000g for 15 min at 4ºC. The resulting pellet was homogenously resuspended in 10ml buffer P1 (containing 50 mM Tris·Cl, pH 8.0, 10mM EDTA and 100µg/ml RNAse A) and placed in a 50ml Falcon tube. Buffer P2 (200mM NaOH, 1% SDS, 10ml) was added and the solution mixed by inversion until homogenous then incubated at rt. After 5 min, 10ml chilled buffer P3 (3M potassium acetate, pH 5.5) was added and the solution thoroughly mixed. The resulting solution, containing a white precipitate, was poured into the barrel of a QIAfilter cartridge and allowed to stand upright for 10 min. During this incubation, a QIAGEN tip 500 was equilibrated by passing 10ml buffer QBT (750 mM NaCl; 50 mM MOPS, pH 7.0; 15% isopropanol (v/v); 0.15% Triton® X-100 (v/v) through it. After equilibration of the QIAGEN tip, the cap was removed from the QIAfilter cartridge and the plunger inserted. The filtrate was applied directly to the equilibrated QIAGEN tip and allowed to pass through by gravity flow. Once all filtrate had passed though the QIAGEN tip, it was washed by passing 2x30ml buffer QC (1.0M NaCl, 50mM MOPS, pH 7.0, 15% isopropanol) through it. It was ensured that waste was not able to touch the end of the QIAGEN tip. Plasmid DNA was eluted

from the washed QIAGEN tip by applying 15ml buffer QF (1.25M NaCl, 50mM Tris-Cl, pH 8.5, 15% isopropanol) and collecting the eluate in a sterile tube. DNA within the eluate was precipitated by the addition of 10.5ml isopropanol at rt followed by gentle mixing. The precipitated DNA was pelleted by centrifugation at ~11000g for 30 min at 4ºC. The supernatant was discarded and the resulting pellet washed in ~1ml 70% ethanol, then transferred to a 1.5ml Eppendorf tube. The washed pellet was spun again at ~15000g for 10 min. The supernatant was removed and the pellet air-dried for ~10 min, then resuspended in an appropriate volume of buffer (usually 500µl buffer EB (10mM Tris-Cl, pH 8.5)).

### 2.1.7.8 Extraction of DNA from agarose gels

Gel extraction was performed using the QIAEXII gel extraction kit (QIAGEN), which contained all necessary reagents. The basic principle of this process was to melt the gel in a suitable buffer, hence releasing and solubilising a DNA fragment. DNA-binding beads were added to the mixture which were then washed and finally the DNA was eluted from them into a suitable buffer.

DNA bands were visualised within agarose gels under ultraviolet light and cut out as accurately as possible using a clean razor blade. The isolated band, containing a fragment of DNA of a given weight was then placed in a sterile 1.5ml Eppendorf tube. The gel sample was resuspended in 750µl buffer QXI in the presence of 10µl QIAEXII bead suspension. The mix was heated at 50ºC and vortexed for 5 min until the gel was dissolved. Then, 5 cycles of heating at 50ºC for 2 min followed by vortexing briefly were carried out. After this, the solution was centrifuged at ~5000g

for ~30 s. The resulting supernatant was poured off and the beads resuspended in 750µl buffer QXI (exact composition unknown). This was repeated twice but on the second time the beads were resuspended in 500µl buffer PE (exact composition unknown), which was repeated once. All buffer PE was removed and the beads allowed to air dry with the tube lid open for 5 min. Once dry, the beads were resuspended in 20-30µl buffer EB and heated at 50ºC for 5 min. The solution was centrifuged at ~5000g for ~30 s and the supernatant, containing a purified DNA fragment, carefully decanted.

### 2.2 *In vivo* methods

Groups of 3-6 adult male Sprague-Dawley rats (Charles River; 200-220g) were operated upon under license by Professor Martin Berry according to the UK Animal Act 1986 guidelines. Anaesthesia was induced with 4% isoflurane and maintained at 2% throughout the procedure. Buprenorphine, at a dose of 0.03mg/kg was used for analgesia, given at the start of the procedure and twice daily for a further 2d following surgery as required. After the procedure, animals were allowed to recover on a heated table. Aseptic conditions were used throughout.

#### 2.2.1 Intra-DRG injection

Injections were performed using a modification of a method previously described (Xu, Gu et al. 2003). Rats were placed on a heat pad in a custom-made stereotactic apparatus allowing the whole animal to be moved through all degrees of freedom, ensuring that the spine was kept rigid at all times. A 2cm incision was made in the midline over the lumbar region and held open with a retractor. The ligamentous

insertions of erector spinae were visualised and a small mark made on the contralateral side at the level of L4. A 2cm paramedian incision was made, with L4 as its midpoint, around 1mm to the left of the spinous processes down to the articulating surfaces of the facet joints. Ligamentous attachments to the articular surfaces were severed, followed by further blunt dissection to reveal the lateral vertebral processes which were removed to reveal the underlying ventral L4/L5 rami, which were dissected proximally to expose the L4/L5 DRG in the intervertebral foramina. Haemorrhage was stopped using Spongostan gel foam (Ferrosan, Soeborg, Denmark).

A solution of $10^{10}$ AAV2/$8_{eGFP}$ viral genomes (vg) in a volume 10µl, diluted in sterile PBS was injected into each DRG using a pulled borosilicate glass micropipette (Harvard apparatus, external diameter 1.5mm, internal diameter 0.86mm) attached to a 20ml syringe containing air. Injection was deemed successful if the DRG was observed to swell. The muscle was closed using catgut and the skin closed with staples. Animals were observed closely post-operatively until they recovered from anaesthetic, and then checked daily for any signs of autotomy.

### 2.2.2 Intrathecal injections

Perioperative care was identical to the above Injections were performed using a modification of a procedure described by De la Calle et al. (De la Calle and Paíno 2002) . Rats were placed in the prone position, and a 2cm incision made between the L5 and S1 vertebrae. The L6/S1 interspinous ligament was incised, allowing the L6 spinous process to be removed and reflected rostrally, allowing direct visualization

of the ligamenta flava. A blunt 25G needle was inserted between the ligamenta flava into the lumbar cistern at an angle of 60º to the horizontal. Access to the intrathecal space was confirmed by CSF in the needle cup, and the presence of a tail flick. CSF could also be expressed by gentle tail traction. The injectate (vehicle or $10^{12}$ vg in 30µl PBS) was pipetted into the needle cup, and injected gently with air from a 5ml syringe. See Figure 2.2 for intra-operative images.

Alternatively, injections were performed using pulled glass micropipettes. The surgical exposure was identical to that described above. A pulled glass micropipette was filled with 10µl PBS or $10^9$ or $10^{12}$ vg $AAV8_{gfp}$ in 10µl PBS. The tip of the micropipette was inserted through the ligamentum flavum and into the subarachnoid space. Successful access to the subarachnoid space was confirmed by entry of CSF into the micropipette by capillary action. Injection was performed by connecting a 20ml syringe filled with air and gently injecting until all of the injectate was introduced into the subarachnoid space. The micropipette was left *in situ* for 10s and then withdrawn. Closure and post-operative care were identical to that described previously.

### 2.2.3 Dorsal column crush

In light of the results discussed in Chapter 4, it was decided to perform a DC crush at the L1 cord level in order to maximise the number of transected axons belonging to AAV2/8 transduced DRGN, since most AAV2/8 transduced DRGN project to Clarke's column which extends to approximately the T13 cord level (Figure 2.3).

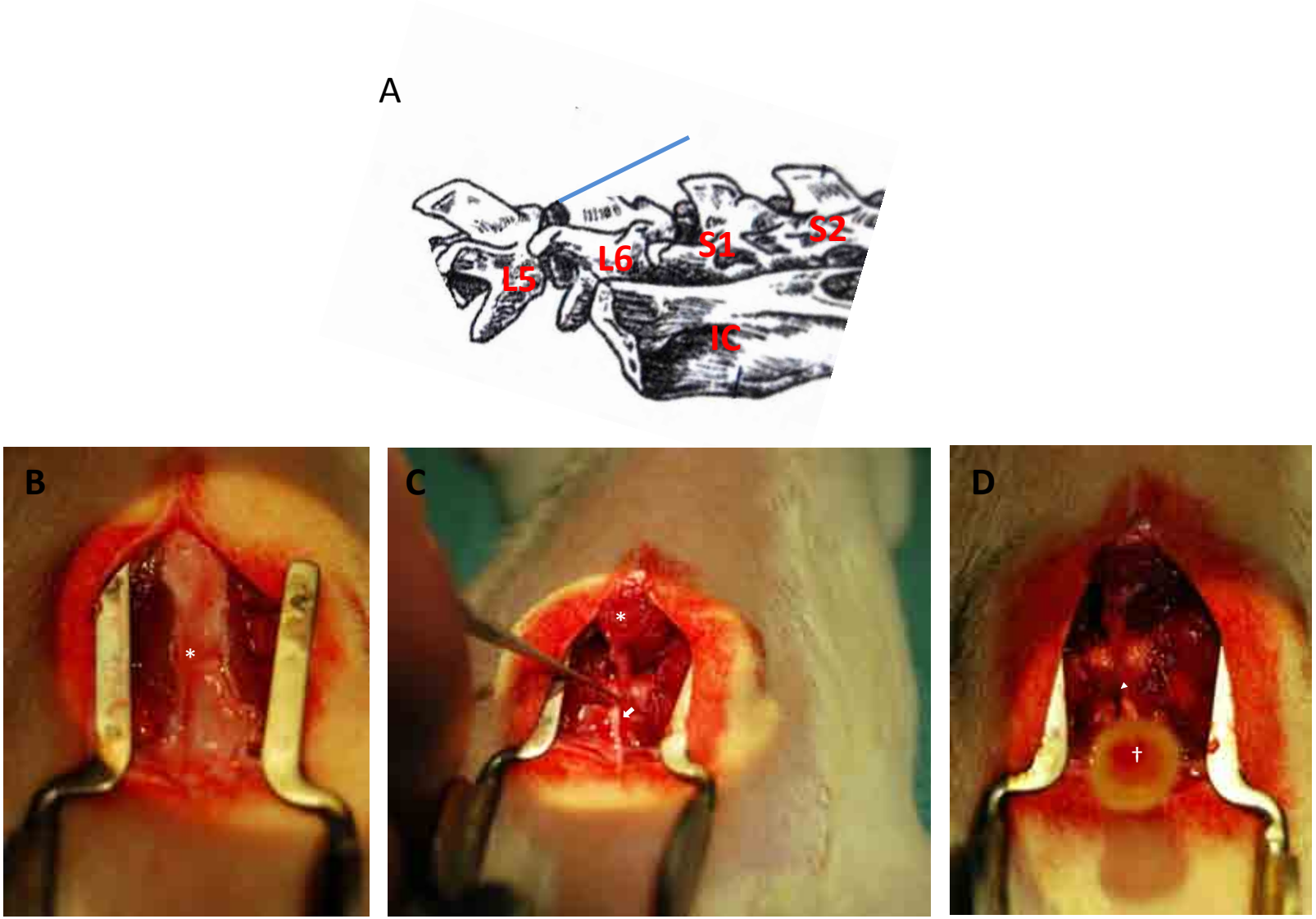


**Figure 2.2** Intra-operative images of intrathecal injection into an adult rat using a 25G needle. **A**. Bony anatomy of the region of interest in the rat, labels indicating vertebrae. Spinal cord ends at approximately the L1 vertebral level **B**. A 2cm incision in the skin has been performed followed by deeper incisions in the parasagittal plane just lateral to the spinous processes. The asterisk marks the L5 spinous process. **C**. Forceps pointing to the exposed ligamentum flavum. Arrowhead indicates L6 spinous process. **D**. 25G needle inserted through ligamentum flavum. Blood-stained CSF (†)is visible in the needle cup.

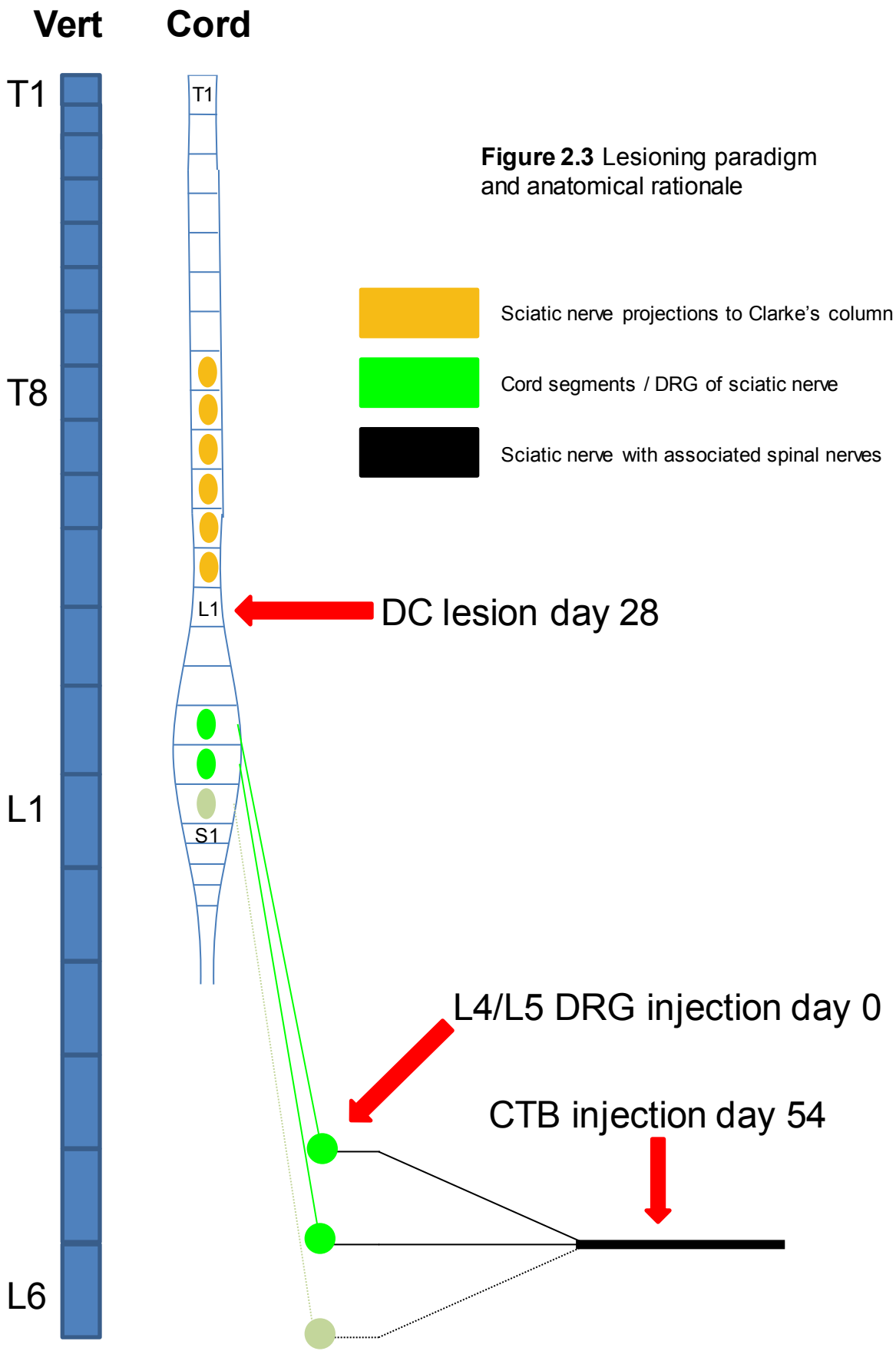


**Figure 2.3** Lesioning paradigm and anatomical rationale

In the adult rat, the L1 cord level is found at approximately the T12 vertebral level. The T13 vertebra was identified by palpating the 13$^{th}$ rib and hence the T13 spinous process. T12 could then be easily located allowing an approximately 1.5cm mid-line skin incision to be made over the T11, T12 and T13 spinous processes. Two parasagittal incisions just lateral to the T11-T13 spinous processes and extending down to the laminae were made in the erector spinae muscles, which were then retracted laterally. As much muscle as possible was removed from the T12 lamina before it was removed using fine rongeurs. Removal of the lamina revealed the spinal cord overlain by the arachnoid and dura mater. A 25G needle was inserted through the meninges at the location of each L1 dorsal root entry zone. The tips of a pair of fine watchmakers forceps which had been calibrated appropriately, were inserted through the meningeal puncture holes into the cord to a depth of 1.5mm. The blades were fully closed for 2s to create a complete lesion of the DC. After withdrawal of the forceps, the lesion could be visualised easily as a grey area between the dural puncture sites. Closure of the erector spinae muscles was achieved with absorbable sutures and the overlying skin using staples.

### 2.2.4 Injection of sciatic nerve with CTB

Approximately 2d before sacrifice the sciatic nerve was exposed by making a 5mm incision in the left posterior thigh inferior to the greater trochanter. The gluteal muscles were split and a retractor inserted to reveal the underlying nerve. A suture was tied around the distal portion of the nerve before 2µl of a 1% solution of CTB (Sigma-Aldrich, Poole, UK) was injected using a glass micropipette attached to a 20ml syringe containing air. The micropipette was inserted around 10s before

injection and left in for 10s after injection to minimise leakage. Injection was deemed successful if the nerve was seen to swell. The skin was closed using staples.

### 2.3 Statistical methods

All statistical analyses were performed using SPSS version 15. Multiple comparisons were analysed using one-way ANOVA or multiple t-tests with application of the Bonferroni correction (carried out by dividing the usual value for alpha, 0.05, by the number of comparisons performed). Before each test, homogeneity of variance and normality of the data set was assessed. If variances differed significantly, a Games-Howell post-hoc test was applied. Otherwise, Dunnett's post-hoc test was applied. Single comparisons were performed using a t-test, and assumptions above tested before the test was performed.

Non-parametric data were analysed using different methods, specifically the Mann-Whitney U-test was performed to compare the size distributions of total and GFP+ DRGN using data pooled from all injected animals.

# Chapter 3

# Production and validation of AAV constructs

## 3.1 Introduction

The context in which NT-3 and myelin neutralisation therapies for SCI find themselves has already been discussed in sections 1.2.1.3 and 1.3.4. The reader is directed to Chapter 6 for more detail on the use of AAV vectors to deliver the neurotrophin 3 gene (*nt-3*) and myelin neutralisation therapies to the injured spinal cord. This chapter concentrates on the validation of *nt-3* and $shRNA_{RhoA}$ constructs *in vitro* and then describes the mechanics of the production of plasmids containing these sequences for production using a baculoviral system. In this context, the use of the term 'construct' refers to a plasmid that will be used to generate an AAV-based gene therapy vector. Thus, if activity of the construct can be shown, it is likely that the viral vector made using it will display a similar activity.

Before proceeding, the reader is reminded of the convention whereby proteins are referred to in capital letters, whereas genes are referred to in lower case italics. Plasmids are named pABCDEF, with the genes contained within them written in capitals (mainly for clarity of reading). Genes for shRNAs are referred to here without italicisation, also for the purposes of clarity. rhNT-3 is a recombinant human NT-3, used as a positive control in experiments looking at biological activity of NT-3. Use of the term "NT-3" refers either to neurotrophin-3 in its generic sense or neurotrophin-3 that has been produced from transfection of cells using a particular plasmid. Also, two types of green fluorescent protein have been used in this study – "GFP" and "hrGFP". Strictly speaking, "GFP" is enhanced green fluorescent protein (eGFP) but the e has been dropped for clarity. hrGFP is humanised Renilla green fluorescent protein, derived from the sea pansy *Renilla reniformis*.

### 3.1.1 Demonstrating neurotrophic activity *in vitro*

Before describing more contemporary work, it is worth putting NTF into some historical context, particularly since the discovery of many NTF relied upon first the study of *in vivo* phenomenology followed by rigorous *in vitro* experiments to show particular aspects of neurotrophic activity. The emphasis in this chapter is on demonstrating neurotrophic activity *in vitro*.

It was in the laboratory of Viktor Hamburger that a number of important discoveries concerning the developmental control of the nervous system were made. In 1934, Hamburger demonstrated that removal of the wing bud from a chick embryo resulted in hypoplasia of motor and sensory neurones supplying the excised appendage (Hamburger 1934). It was thought that this phenomenon could be explained by two hypotheses. Either an influence from the limb bud cells was keeping existing neurones alive, or there was an effect on the recruitment of neuronal precursors. Further work in the Hamburger lab was inspired by experiments done by Bueker who implanted mouse sarcoma tissue into chick embryos (cited in (Levi-Montalcini 1987)). The results of these experiments showed invasion of the tumour grafts by sensory neurones and increase in size of DRGs supplying the tumour. Continuing this work, Levi-Montalcini observed increased innervation in organs distant from the graft in animals implanted with mouse sarcoma cells. This suggested the presence of a soluble factor, being released from the sarcoma and stimulating nerve growth.

This activity was demonstrated *in vitro*, using chick DRG explants. A robust neurite outgrowth response was observed in explants placed near to sarcoma tissue (Levi-

Montalcini, Meyer et al. 1954). Following on from this, a nucleoprotein fraction of the sarcoma tissue was identified as containing the active component. Attempts to degrade the nucleic acid component with snake venom, which contains phosphodiesterases, resulted in a paradoxical increase in neurite outgrowth promoting activity which led to the serendipitous discovery that mammalian salivary glands produce the so-called *nerve growth factor* in large amounts (snake venom glands are homologous to mammalian salivary glands). Following this work, the sequence of NGF was determined in 1971 (Cohen 1960; Angeletti and Bradshaw 1971).

The above account illustrates that NTF can have potent effects both *in vitro* and *in vivo*. Most of the published work looking at NTF activity has incorporated *in vitro* methods, mainly because these techniques allow experiments to be performed that tend to be cheap, convenient, versatile and more easily interpreted compared with *in vivo* experiments.

### 3.1.2 Protein knock-down using RNA interference

In order to understand how therapeutic RNAi works, it must first be appreciated that there are endogenous RNAi pathways at work in most organisms that are responsible for regulating gene expression. RNAi was discovered by Craig Mellow and Andrew Fire in the late 1990s following a series of confusing experimental results in plants. They went on to be awarded the Nobel Prize in 2006, having generated a significant amount of interest in most areas of biological science.

The basic concept of RNAi is of small RNA sequences, complementary to the mRNA of interest, that are able to inhibit transcription. The following describes the endogenous pathway for RNAi (i.e. that which occurs physiologically in organisms), and the reader is referred to a useful review aimed at neuroscientists for an accessible description of RNAi (Boudreau and Davidson 2010).

Endogenous RNA interference is mediated by so-called microRNAs (miRNAs) that are encoded in the genome. Newly transcribed miRNA molecules are known as primary miRNAs, with hairpin-loop structures arising as a consequence of self-complementarity within the single-stranded miRNA molecule. Within the nucleus, the enzyme Drosha trims the primary miRNA to a length of 60-70 nucleotides, which is now termed a pre-miRNA. The pre-miRNA is exported from the nucleus to the cytoplasm, where it is acted upon by the enzyme Dicer. Dicer removes the hairpin loop, generating a mature miRNA duplex consisting of a sense and an antisense strand (sense referring to the sequence of the messenger RNA (mRNA) in question, antisense being the complementary sequence to that). The antisense sequence of the miRNA duplex is fed into the RNA-induced silencing complex (RISC), which mediates silencing of mRNA translation. If the miRNA has a high level of complementarity to the target mRNA sequence, then degradation of the transcript ensues. Lower levels of complementarity lead to translational inhibition without degradation of the transcript.

With knowledge of these events, scientists have been able to exploit this pathway using two major types of synthetic miRNA: siRNAs and shRNAs. shRNA can be

thought of as an exogenous pre-miRNA. Thus, any method used to deliver shRNA must be able to access the nucleus. siRNA can be thought of as an exogenous mature miRNA duplex, necessitating delivery to the cytoplasm. shRNAs are processed identically to pre-miRNAs, ultimately forming a mature miRNA duplex that is fed into the RISC complex. Cytoplasmically delivered siRNAs enter the RISC complex immediately to mediate gene silencing.

Superficially it would seem that siRNA and shRNA are functionally equivalent. However, it has to be borne in mind that siRNAs must be delivered to the cytoplasm for them to work. This usually involves complexing the siRNA with a non-viral gene therapy vector (e.g. Lipofectamine, a cationic lipid). Once in the cytoplasm, the siRNA has a relatively short half-life precluding prolonged treatment effects. Conversely, shRNA can be delivered using viral vectors, some of which are known to be capable of mediating expression over months and even years. Thus, shRNA-based therapies are likely to hold more promise in the treatment of diseases that require prolonged treatment effects such as SCI.

### 3.1.3 The importance of testing gene therapies *in vitro*

Before proceeding to experiments *in vivo*, it is necessary to test reagents (specifically, plasmids that will be used to generate viral vectors) *in vitro* for three major reasons: technical, ethical and financial.

Any plasmid containing transgene(s) that will be used to produce a viral vector should be tested to show that it is capable of mediating the expression of the transgene(s). Testing ideally involves transfection of the plasmid into an appropriate

cell line and demonstration of the biological activity of the transgene payload. In plasmids containing the gfp gene (*gfp*) or other reporter genes, the first step usually involves observation of reporter gene expression in transfected cells. This confirms that the plasmid has entered cells and is mediating protein expression. One must then look for evidence of production of other transgenes of interest within the plasmid (e.g. by Western blotting or ELISA). Failure of expression of a transgene may be due, for example, to a mutation within the plasmid (it is often not practicable to sequence an entire plasmid). Once transgene expression has been confirmed, biological activity should ideally be assessed, and compared with a suitable positive control such as a commercially available recombinant protein. If the transgene is being expressed, it is unlikely that its biological activity has been compromised, however this cannot be guaranteed and is particular relevant to scenarios where the transgene has been tagged with an additional sequence that could potentially affect its biological activity.

From an ethical point of view, it is necessary to test gene therapies *in vitro* before going *in vivo* in order to minimise animal use and any potential animal suffering. It is not desirable to inject gene therapies *in vivo* when no knowledge of their activity has been gained. The same argument applies to the financial point of view. Production of a recombinant AAV vector costs around £2000 per virus. Thus, plasmids need to be tested first before this costly investment is made.

### 3.1.4 Baculoviral production of AAV vectors

Experience in our lab has shown that in-house production and purification of AAV8 is challenging and not cost-effective. This is due mainly to the time-consuming and costly need to optimise all steps of the viral production process, since a commercially available kit for production of AAV8 is not available. Thus, it was decided that it would be more cost- and time-effective to outsource AAV8 production. The author would like to thank at this point Dr Michael Douglas who, as well as giving invaluable advice and supervision for the entire project, generated pAAV-CMV-NT3-IRES-hrGFP and pAAV-CMV-NT3-FLAG-IRES-hrGFP; designed the primers used in the following series of experiments and performed the second (successful) ligation of the NotI mutant sequence into the pAAV backbone.

#### 3.1.4.1 Background to the baculoviral expression system as a means of producing AAV

Due to difficulties in manufacture of AAV8 viruses in house, it was decided to outsource the viral manufacture to the Gene Transfer Vector Core at the University of Iowa, USA. This facility makes use of a baculoviral system which is capable of producing high titres of AAV8 particles with relatively little plasmid DNA (Urabe, Ding et al. 2002). AAV vectors can be produced by transducing Sf9 cells (of insect origin) with three separate baculoviruses containing the AAV rep and cap gene complexes, adenoviral helper genes and the AAV ITR-spanned coding region (pFBGR, see below). In order to generate baculoviruses, the coding regions described above must first be subcloned into a baculoviral donor plasmid, where they are spanned by Tn7 elements allowing transposon-mediated insertion into an engineered baculoviral

genome ('bacmid') within *E.coli*. The resulting recombinant bacmid is then purified and transfected into insect cells where baculoviral particles containing the appropriate AAV construct are manufactured. The three resulting baculoviruses are then co-infected into insect cells, resulting in production of high titres of recombinant AAV which can be purified using standard protocols. See Figure 3.1 for summary of the above.

#### 3.1.5.1 Specific hypotheses

- Delivery of *nt-3* to DRGN *in vitro* augments survival and stimulates neurite outgrowth
- Knockdown of RhoA by transfection of an shRNA against RhoA will lead to diminution of RhoA protein levels and disinhibited neurite outgrowth

#### 3.1.5.2 Specific aims

- To generate plasmid constructs suitable for use in baculoviral-based production of AAV8. These constructs will contain *gfp*, *hrgfp*, *nt-3* and $shRNA_{RhoA}$ in various combinations
- To demonstrate an effect of rhNT-3 on survival and neurite outgrowth of DRGN *in vitro*
- To demonstrate biological activity of NT-3 produced from the plasmids of interest
- To demonstrate that the $shRNA_{RhoA}$ construct is capable of knocking down RhoA *in vitro*

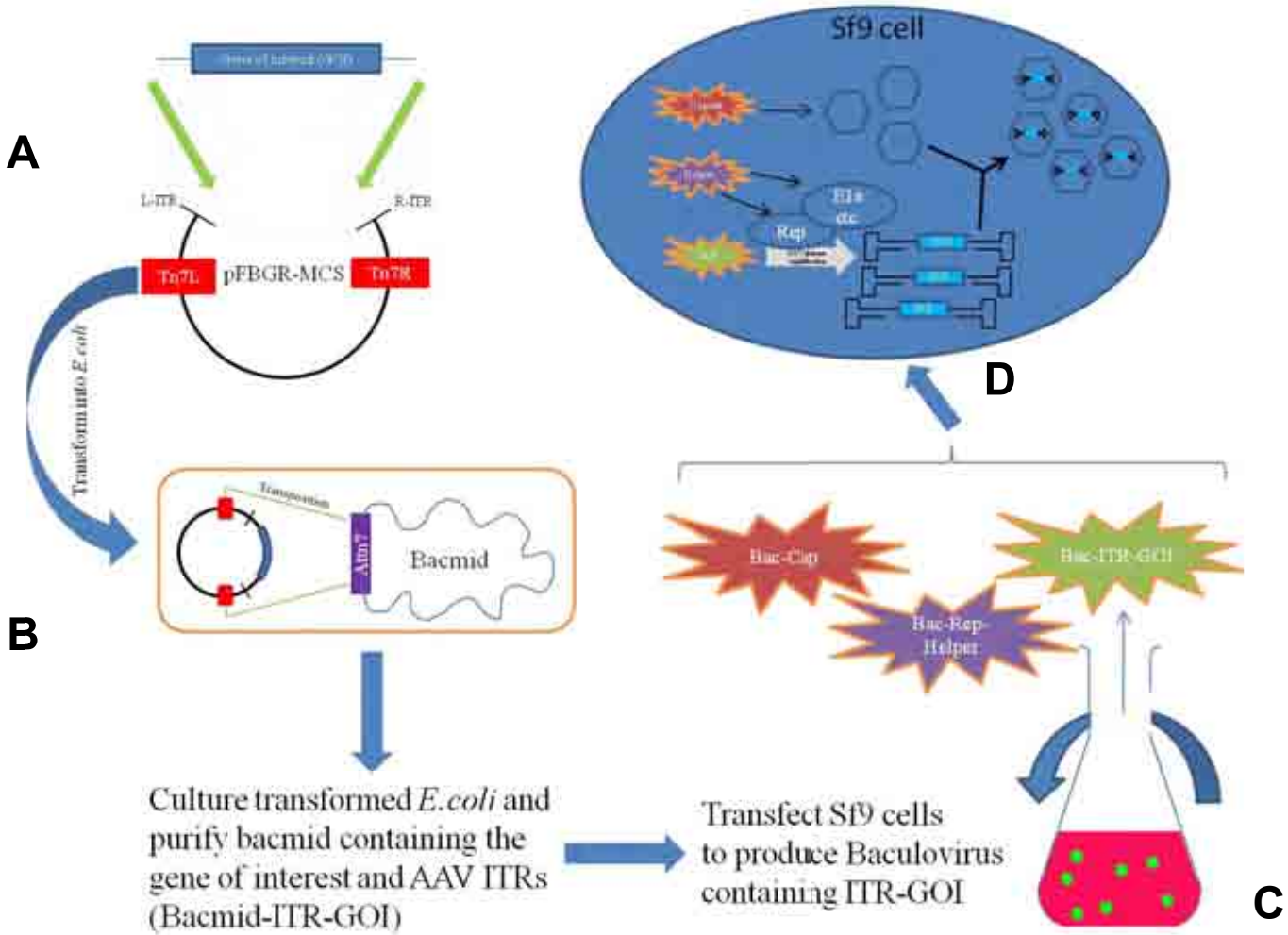


**Figure 3.1**. Basic principles of AAV production using the baculoviral method. **A**. The gene of interest is cloned into the baculoviral ITR-containing plasmid, pFBGR-MCS. **B**. pFBGR-GOI is transformed into *E.coli* containing the *Attn7* site, which is able to accept transposons spanned by Tn7L and Tn7R (shown in red). **C**. The purified, transposed bacmid is transfected into Sf9 cells, resulting in the production of a baculovirus containing the ITR-spanned AAV genome sequence with the gene of interest (Bac-ITR-GOI). **D**. Transduction of Sf9 cells with Bac-ITR-GOI alongside baculoviruses containing capsid proteins specific to the serotype (Bac-cap) and helper genes (Bac-Helper) results in the formation of mature rAAV particles which can be subsequently harvested and purified from Sf9 conditioned medium and lysate.

### Section 3.1.6 Brief description of methods

Dissociated cultures of adult rat DRG were prepared and exposed to recombinant NT-3 or conditioned media comtaining human NT-3. Briefly, conditioned media were generated by transfecting COS-1 cells with plasmids either containing GFP alone, or containing the *nt-3* gene. COS-1 cells were left for 7d before harvesting conditioned media. DRG cultures exposed to NT-3 were stained immunocytochemically for beta-III tubulin, allowing quantification of neuronal survival and neurite outgrowth.

Additionally, conditioned media were analysed for the presence of NT-3 using Western blotting, ELISA and silver staining of SDS-PAGE gels.

Plasmids containing *nt-3* and *shRNA* constructs were generated using standard molecular biology techniques including restriction enzyme digestion, DNA ligation, PCR and plasmid amplification and purification.

# Results

### 3.2.1 rhNT-3 supported survival but not neurite outgrowth of adult rat DRGN *in vitro*

A dose-response experiment was performed examining the effects of rhNT-3 on survival and neurite outgrowth of adult rat DRGN. Concentrations used were between 1 and 50ng/ml, which lie in the range of values reported to be used *in vitro* in the literature (Mohiuddin, Fernandez et al. 1995; Kimpinski, Campenot et al. 1997). At a concentration of rhNT-3 of 10ng/ml, approximately twice as many DRGN survived compared to control (Figure 3.2A; one-way ANOVA, p=0.013). The dose-response curve displayed a bell-shaped appearance, with the highest concentration giving a lower amount of survival compared with the optimal dose.

Surprisingly, there was no effect of rhNT-3 on the size of the longest DRGN neurite *in vitro* (Figure 3.2B). All doses led to approximately the same level of neurite outgrowth, the differences not reaching statistical significance.

### 3.2.2 The addition of a mitotic inhibitor had no effect

It was possible that NTF produced by satellite cells present in the mixed DRG cultures was causing maximal growth stimulation of DRGN, leading to the lack of an effect of additional rhNT-3. To counter this, the mitotic inhibitor 5-fluorodeoxyuridine (5-FDU) was added to the cultures to suppress the proliferation of cells including satellite cells and Schwann cells (Ahmed, Mazibrada et al. 2006). In the pilot experiment performed, 5-FDU was seen both to fail to uncover an effect on neurite outgrowth of rhNT-3 and to abolish the survival effect of rhNT-3 on DRGN *in vitro*

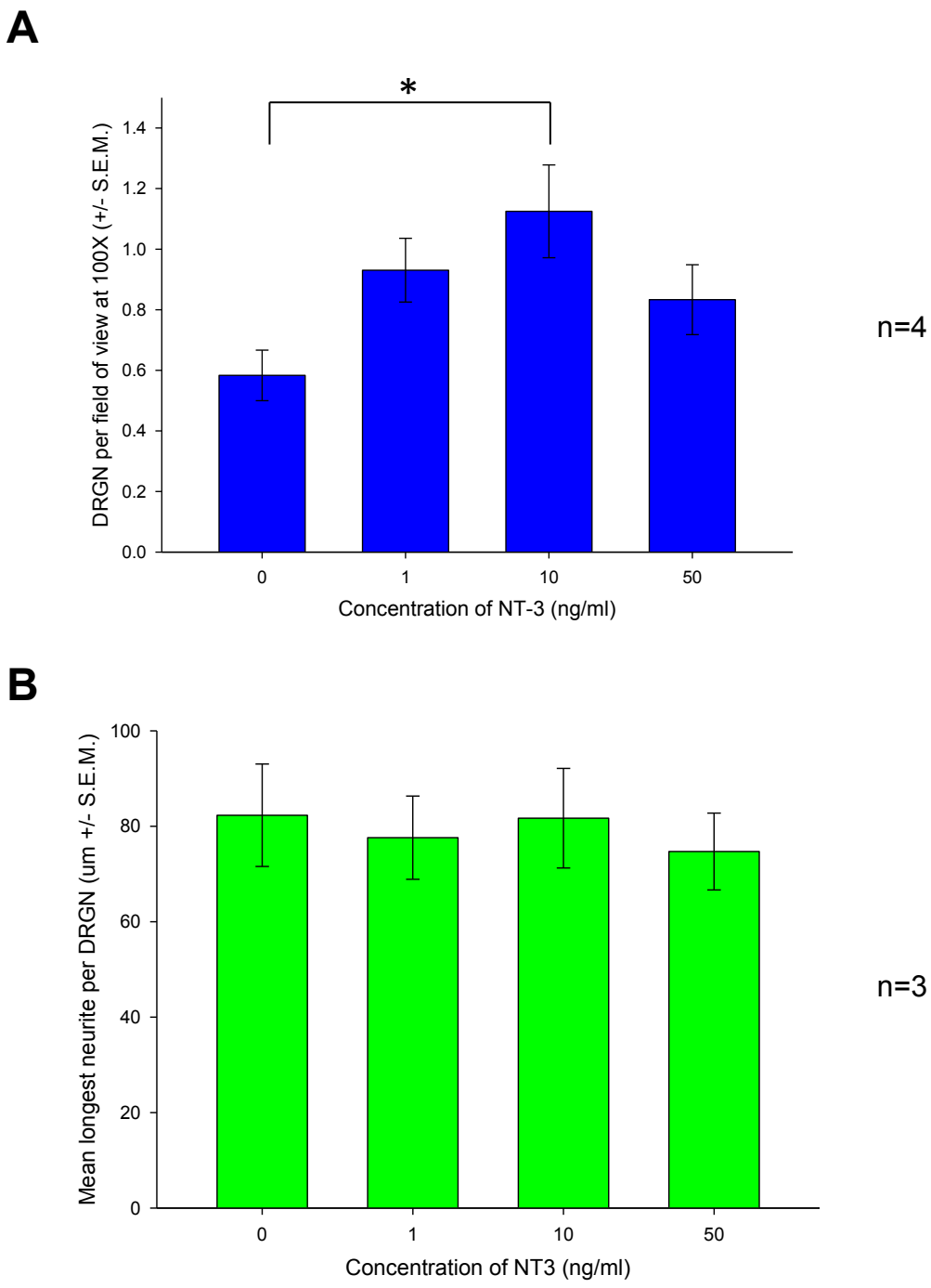


**Figure 3.2** The effect of rhNT-3 on growth and survival of adult rat DRGN after 2d *in vitro*. **A**. rhNT-3 supports maximal survival of DRGN at a concentration of 10ng/ml (one-way ANOVA, p=0.013). **B**. There is no effect of rhNT-3 on neurite outgrowth *in vitro* (one-way ANOVA, p=0.705). * represents post-hoc Dunnett's test p=0.003

(Figure 3.3). Due to the apparent lack of promise of this approach, this experiment was not repeated.

### 3.2.3 Demonstration of biological activity of NT-3 produced by transfection of COS-1 cells with pAAV-CMV-NT3-FLAG-IRES-hrGFP was difficult

Having shown that rhNT-3 is able to lead to a biological effect in DRGN, it was decided to attempt to show this using NT-3 produced 'in-house' from transfection of COS-1 cells using various plasmids either containing *nt-3* or containing *gfp* as a control. The basic aim of the experiments described below was to first show that NT-3 had been produced after transfection of COS-1 cells, then to attempt to apply it to DRGN *in vitro* (either as raw conditioned medium or purified) in order to show that it had similar effects to rhNT-3, which has already been shown to support DRGN survival.

#### 3.2.3.1 FLAG-tagged NT-3 was detected by both Western blotting and ELISA

In order to facilitate both purification and detection, it was decided to tag *nt-3* using a commonly used system – the FLAG tag. Genes inserted into the multiple cloning site (MCS) of pAAV-IRES-hrGFP are transcribed with a FLAG-tag by default, unless a stop codon is inserted before the FLAG coding region. The FLAG tag can be detected using highly specific commercially available antibodies.

A high proportion of COS-1 cells were transfected by all of the plasmids used in this study, as shown by their strong expression of GFP (Figure 3.4Aii). The cells appeared grossly normal, and grew readily *in vitro* after transfection.

**A**

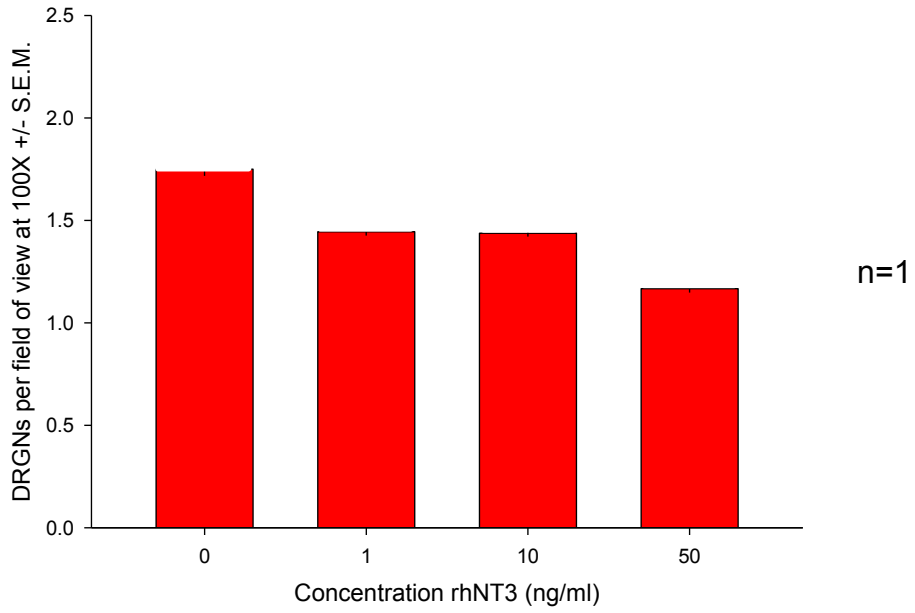


**B**

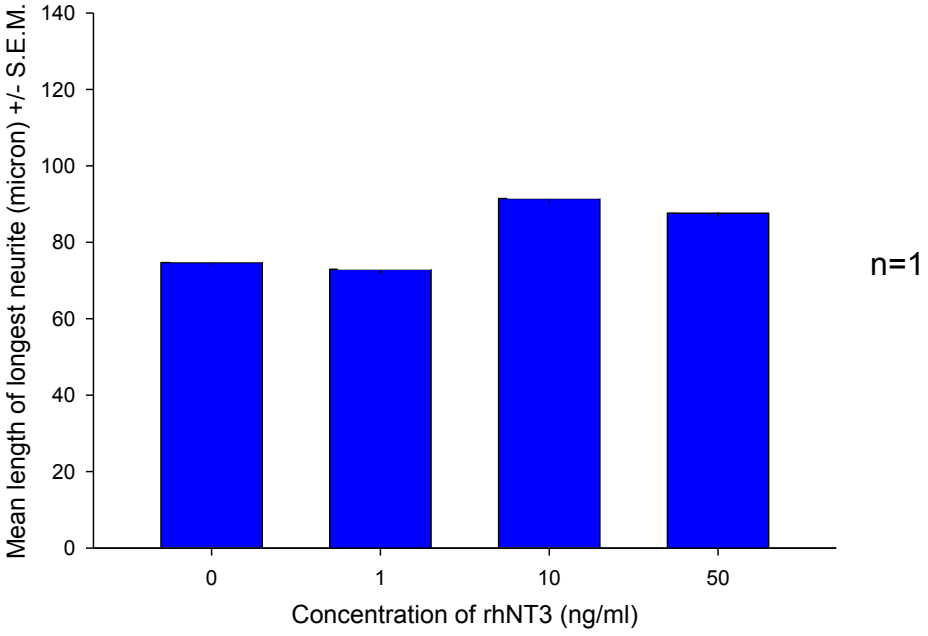


**Figure 3.3** Effects of rhNT-3 on survival (**A**) and neurite outgrowth (**B**) of DRGN *in vitro* in the presence of 30μM 5-FDU.

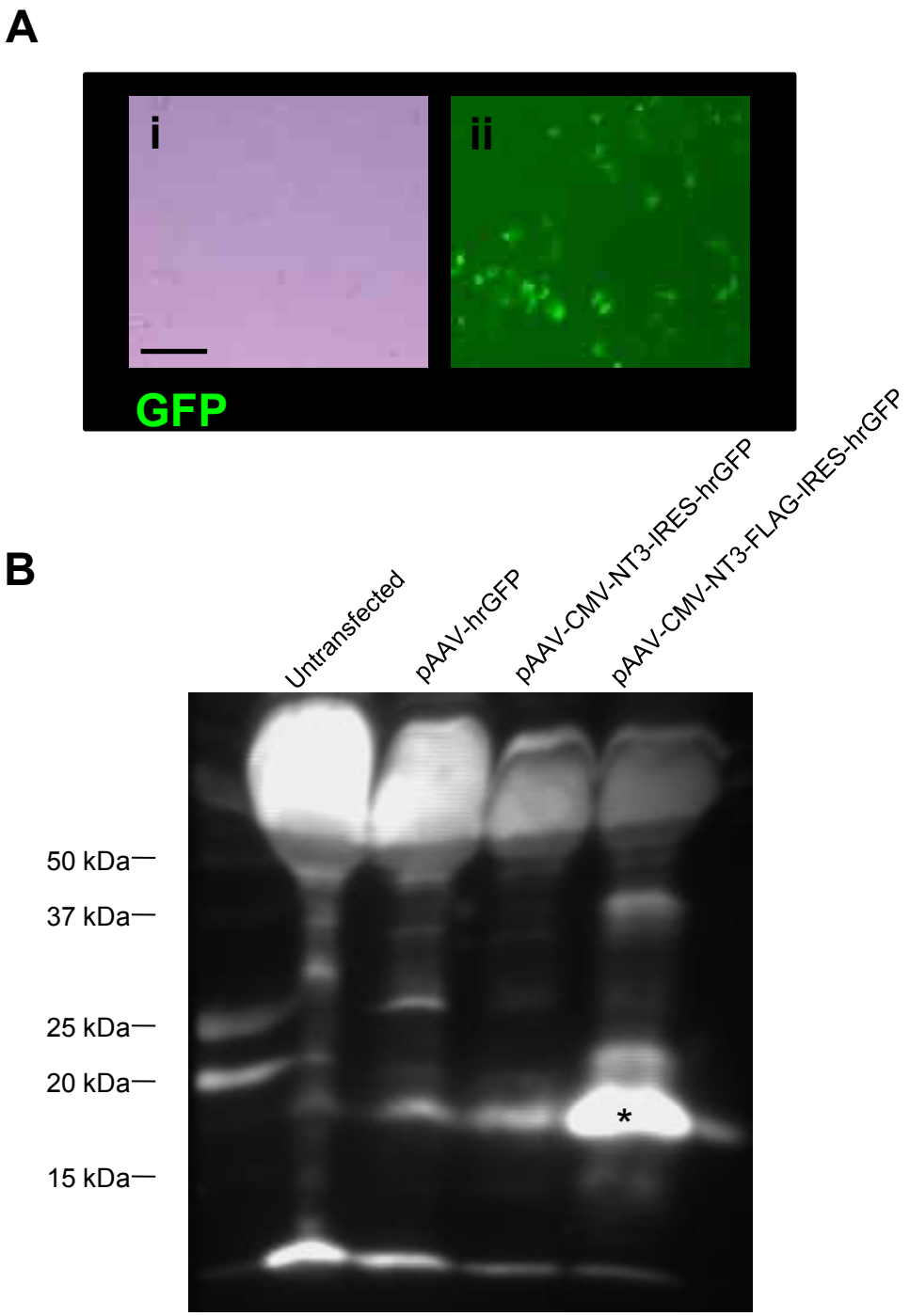


**Figure 3.4** COS-1 cells transfected with plasmids encoding *nt3-flag* produced readily detectable quantities of NT-3. **A**. Since all plasmids used contained gfp, transfected COS-1 cells were identifiable by their expression of GFP. A high percentage of COS-1 cells were GFP+. (i) Phase-contrast image showing COS-1 cells; (ii) fluorescence microscopy (FITC channel) image of the same field of view as in (i). Scale bar 10μm. **B**. Western blot on samples of conditioned medium from COS-12 cells transfected with various plasmids including an untransfected control, stained using the anti-FLAG antibody to detect NT3-FLAG. A strong band at ~17kDa (*) demonstrates the presence of a large quantity of NT3-FLAG in conditioned medium from COS-1 cells transfected with pAAVCMV-NT3-FLAG-IRES-hrGFP.

COS-1 cells transfected with the *nt3-flag* containing construct produced readily detectable quantities of NT3-FLAG. Western blotting using an anti-FLAG antibody revealed a prominent band in conditioned medium from COS-1 cells transfected with pAAV-CMV-NT3-FLAG-IRES-hrGFP (a plasmid yielding NT3-FLAG) at the predicted weight of NT3-FLAG (17kDa; Figure 3.4B). A subsequent ELISA assay on the same batch of conditioned medium revealed a concentration of NT3-FLAG of 64ng/ml. No NT-3 was detected in conditioned media from untransfected COS-1 cells or those transfected with pAAV-IRES-hrGFP.

#### 3.2.3.2 No conclusive biological effect could be attributed to NT3-FLAG conditioned medium

Dissociated cultures of adult rat DRG were prepared as usual and allowed to settle overnight before supplemented Neurobasal-A medium, DMEM with 10% FBS and 1% penicillin/streptomycin or conditioned media were used to replace their usual medium (supplemented Neurobasal-A). The conditioned media were from untransfected, pAAV-GFP, pAAV-CMV-NT3-IRES-hrGFP or pAAV-CMV-NT3-FLAG-IRES-hrGFP transfected COS-1 cells left for 3d. The DRG cultures were left for 48h and then the survival of DRGN was assessed by immunocytochemistry and microscopy. Figure 3.5A shows the results of the experiment described above. Although very little can be gleaned from an experiment using cells from only a single animal, two major features are worthy of comment. Firstly, there appears to be a certain degree of toxicity to DRGN associated with COS-1 cell conditioned media, particularly when COS-1 cells were untransfected or transfected with pAAV-IRES-hrGFP. Secondly, it appears that COS-1 cell conditioned media that contain NT-3

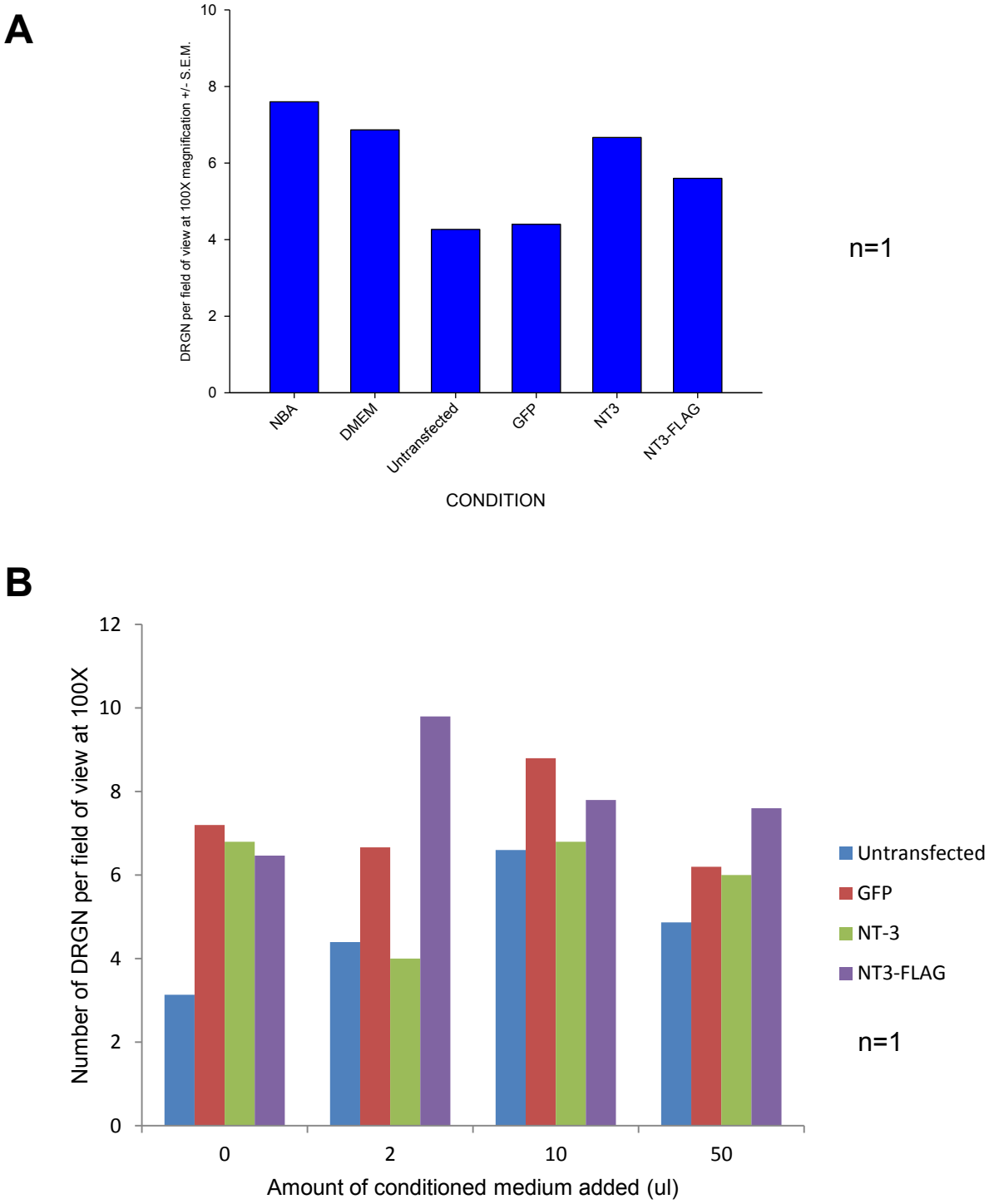


**Figure 3.5** A pilot experiment showing the effect of various conditioned media on DRGN survival *in vitro*. **A**. Effect of whole conditioned media from COS-1 cells transfected with various plasmids on adult rat DRGN survival. **B**. Dose-response characteristics of 10X concentrated conditioned media on survival of adult rat DRGN *in vitro*.

are able to rescue DRGN from toxicity, since the amount of survival is similar when using conditioned media from COS-1 cells transfected with pAAV-CMV-NT3-IRES-hrGFP or pAAV-CMV-NT3-FLAG-IRES-hrGFP.

In response to the apparent toxicity of conditioned media in general, it was decided to concentrate the conditioned media by a factor of 10 in a 10 000 Da cut-off micro-concentrator. Concentrating the samples has two major effects on the composition of conditioned media – it increases the concentration of NT-3, and should decrease the amount of small-molecule toxins since they would pass through the filter and be removed as waste. A pilot dose-response experiment, on a culture from one animal, was performed using between 0 and 50µl of 10X concentrated conditioned media covering a range of approximately 0-100ng/ml (Figure 3.5B). The results of this experiment are difficult to interpret (see discussion), although some findings may be relevant: (i) conditioned media containing NT3-FLAG always yielded greater DRGN survival than media from untransfected COS-1 cells; (ii) NT3-FLAG containing media always gave higher levels of DRGN survival than NT-3 containing media and (iii) there was little correspondence between the experiment using whole conditioned media compared with that using concentrated media. The results which make this experiment difficult to interpret are: (i) when no conditioned media were added to DRG cultures, survival should have been the same in all. Instead, the DRG cultures 'exposed' to 0µl of untransfected COS-1 cell medium showed considerably less survival than the other groups and, (ii) in all cases, conditioned media from COS-1 cells transfected with *gfp*-only containing constructs led to more survival than

conditioned media from COS-1 cells transfected with pAAV-CMV-NT3-FLAG-IRES-hrGFP.

#### 3.2.3.3 Purification of NT3-FLAG from conditioned media was not efficient enough to yield usable quantities of NT3-FLAG

As should be apparent from the results described above, the use of conditioned media in assessing the efficacy of NT-3 generated from transfection of COS-1 cells with *nt-3* is not simple. Given these problems, it was decided that a useful approach may be to purify the NT3-FLAG from the conditioned media and then directly apply this pure preparation to DRG cultures, thus directly replicating the experiment described in section 3.4.1. The most suitable approach to this problem was by immune-affinity chromatography.

The approach employed used a FLAG-affinity column, where conditioned medium was passed through a column containing beads coated with anti-FLAG antibody, allowing NT3-FLAG to bind to the beads and then be eluted off (Figure 3.6). Whole conditioned medium from pAAV-CMV-NT3-IRES-hrGFP transfected COS-1 cells was passed through a FLAG-affinity column and the effluent collected for analysis. Elution was performed using a low pH solution, yielding a very faint band at ~17kDa, the predicted weight of NT3-FLAG. A positive control, 1µg rhNT-3, gave a strong band at ~14 kDa.

Despite the success of purification of NT3-FLAG by the above method, it was felt that this method was probably far from ideal due to two major factors. First, acid elution

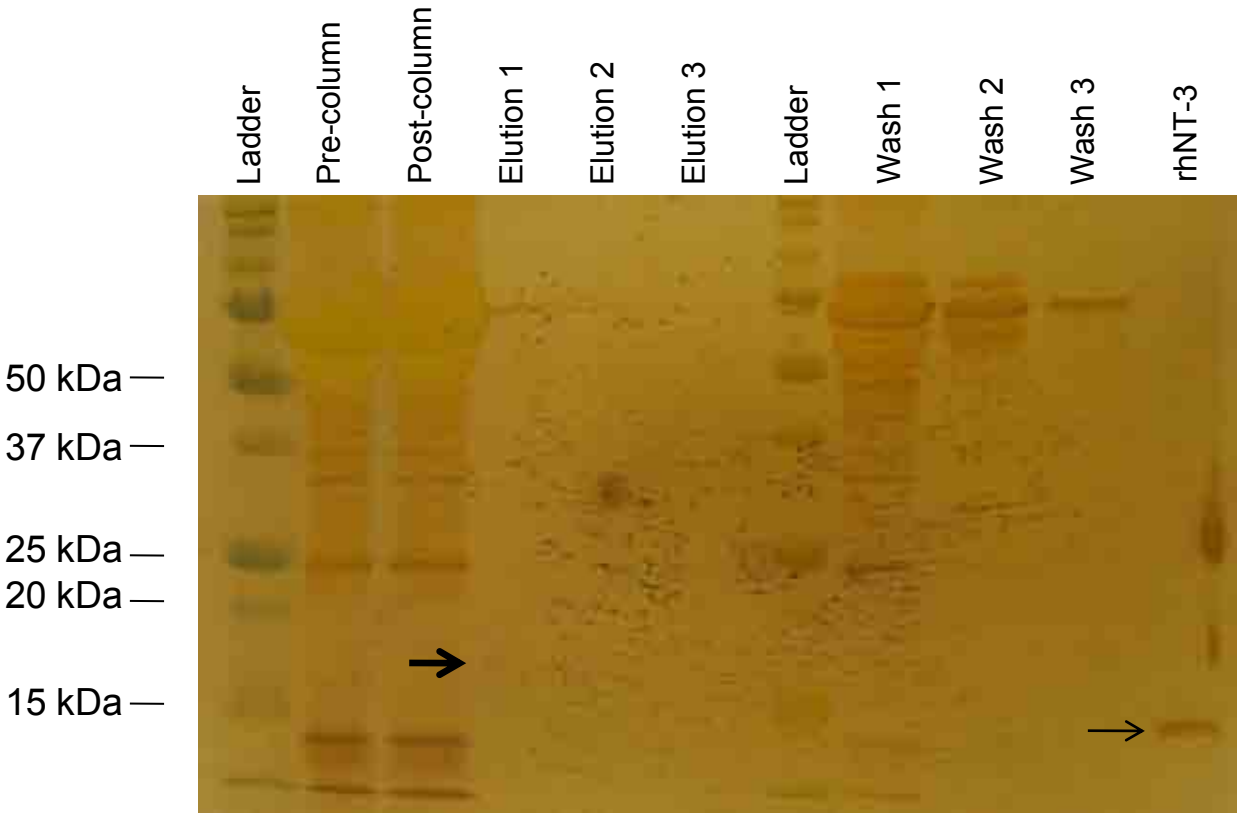


**Figure 3.6** Purification of NT3-FLAG from COS-1 cell conditioned medium by immunoaffinity chromatography. Silver-stained gel showing samples from an entire experiment. Whole conditioned medium (Pre-column) was passed through a FLAG-affinity column and the effluent collected (Post-column). The column was washed three times (Wash 1, 2, 3) before being eluted three times (Elution 1, 2, 3). A sample of rhNT-3 was added as a positive control, and can be seen clearly on the gel (light arrow). The band corresponding to NT3-FLAG (dark arrow) is barely visible at around 17kDa.

had the risk of denaturing the eluted NT-3 thus rendering it unusable in bioassays. Secondly, the quantities produced by the method were very small and unlikely to yield enough NT-3 to use in assays. To overcome the potential acid denaturation problem, competitive elution using a FLAG peptide was performed. Unfortunately, this proved unsuccessful as the NT3-FLAG would not dissociate from the beads, even with heating and varying concentrations of peptide.

## 3.2.4 Production of human NT-3 containing constructs

### 3.2.4.1 The starting materials

Primers were designed to enable amplification of the human *hnt-3* gene (*hnt-3*), including its signal sequence and pre- and pro-domains from an existing plasmid containing the full-length human form designated "*nt-3* gene" (Maisonpierre, Belluscio et al. 1990). These primers also contained XhoI and BamHI restriction sites, allowing sub-cloning into pAAV-IRES-hrGFP, yielding pAAV-CMV-NT3-IRES-hrGFP, and were performed by Dr Michael Douglas (Figure 3.7). Note that pAAV-CMV-NT3-IRES-hrGFP contains a stop codon, preventing a 3X FLAG tag being conjugated to the C-terminal of *hnt-3*. pFBGR, provided by Dr Maria Scheel of the Gene Transfer Vector Core, is the plasmid that receives the construct of interest allowing a baculovirus to be produced that can be used to manufacture AAV8 in insect cells (see introduction).

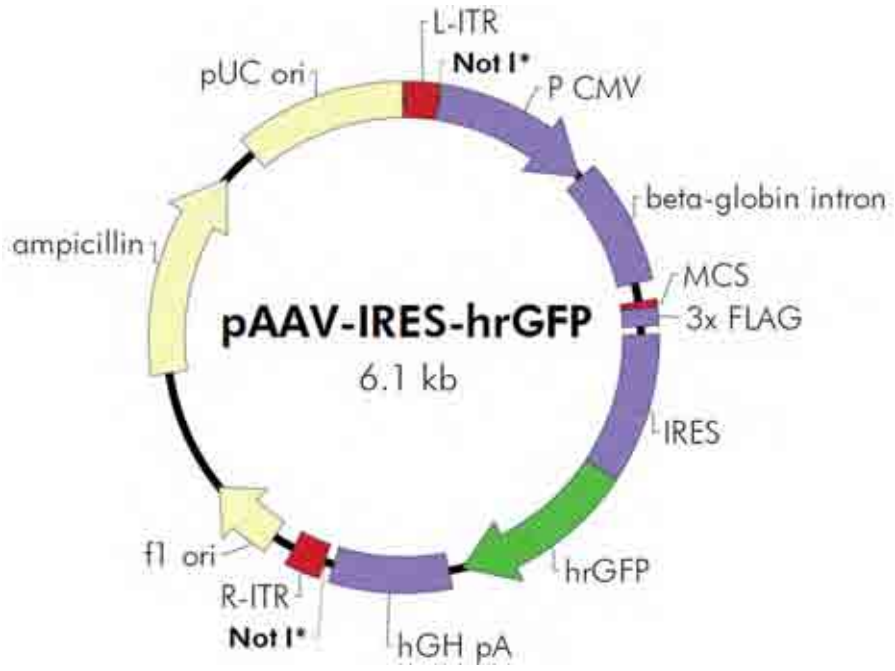


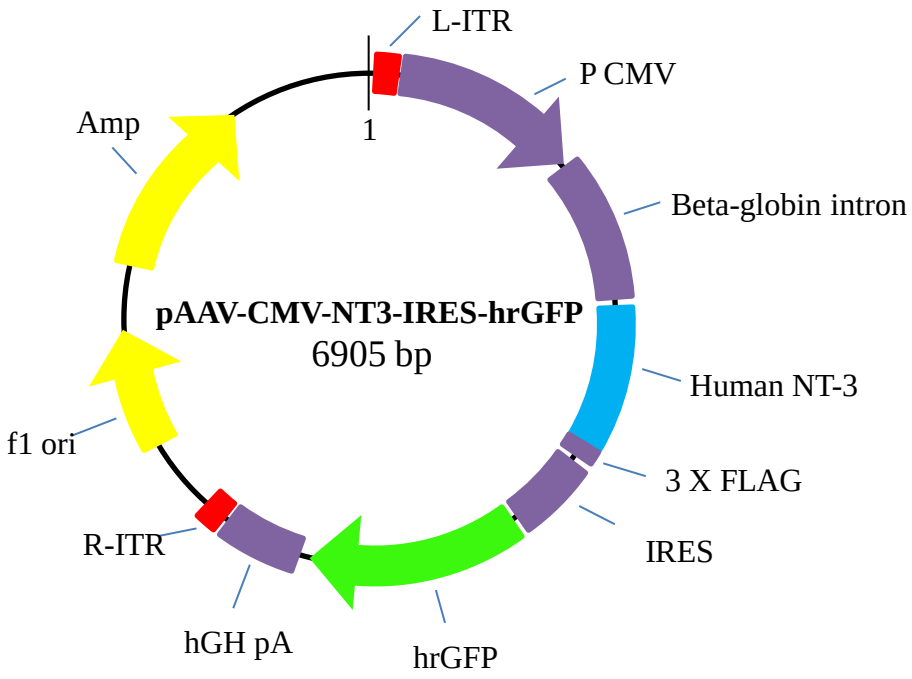


**Figure 3.7** Map of pAAV-IRES-hrGFP (A) and after insertion of human NT-3 sequence (B). pAAV-CMV-NT3-IRES-hrGFP does not express NT3-FLAG due to the inclusion of a stop codon. pAAV-IRES-hrGFP map courtesy of Stratagene.

### 3.2.4.2 The AAV sequence from pAAV-CMV-NT3-IRES-hrGFP could not be inserted into pFBGR by a simple cut-and-paste approach

On examination of the plasmid maps it seemed most reasonable to subclone the NotI spanned fragment from pAAV-CMV-NT3-IRES-hrGFP into the NotI spanned region of pFBGR, preserving the ITRs. Digestion of pFBGR with NotI and subsequent dephosphorylation of the 4963bp fragment was successful, yielding a product called "pFBGR vector". However, digestion of pAAV-CMV-NT3-IRES-hrGFP with NotI yielded one smaller fragment at 1.2kb containing the cytomegalovirus (CMV) promoter and beta-globin intron, and 2 unresolvable overlapping bands at 2.8kb, one containing the *nt3-ires-hrgfp* segment and the other containing the rest of the pAAV-CMV-NT3-IRES-hrGFP backbone (Figure 3.8). Thus, in order to resolve the *nt-3* containing segment from the backbone segment, it was decided to digest this doublet band of 2.8kb with ScaI, which is known to cut in the ampicillin resistance gene. However, digestion of pAAV-CMV-NT3-FLAG-IRES-hrGFP and pAAV-CMV-NT3-IRES-hrGFP (data not shown) with ScaI yielded two fragments, showing that ScaI is not a unique site in these plasmids, and so not useful for resolving the overlapping 2.8kb bands. Indeed, digestion of the 2.8kb bands resulting from digestion of pAAV-CMV-NT3-IRES-hrGFP and pAAV-CMV-NT3-FLAG-IRES-hrGFP resulted in complex sets of digestion products which were too difficult to interpret for use in subsequent cloning.

Since the above problems were caused by the presence of an additional NotI site within pAAV-CMV-NT3-IRES-hrGFP, it was decided to use a site-directed mutagenesis approach to ablate the additional NotI site, allowing straight-forward

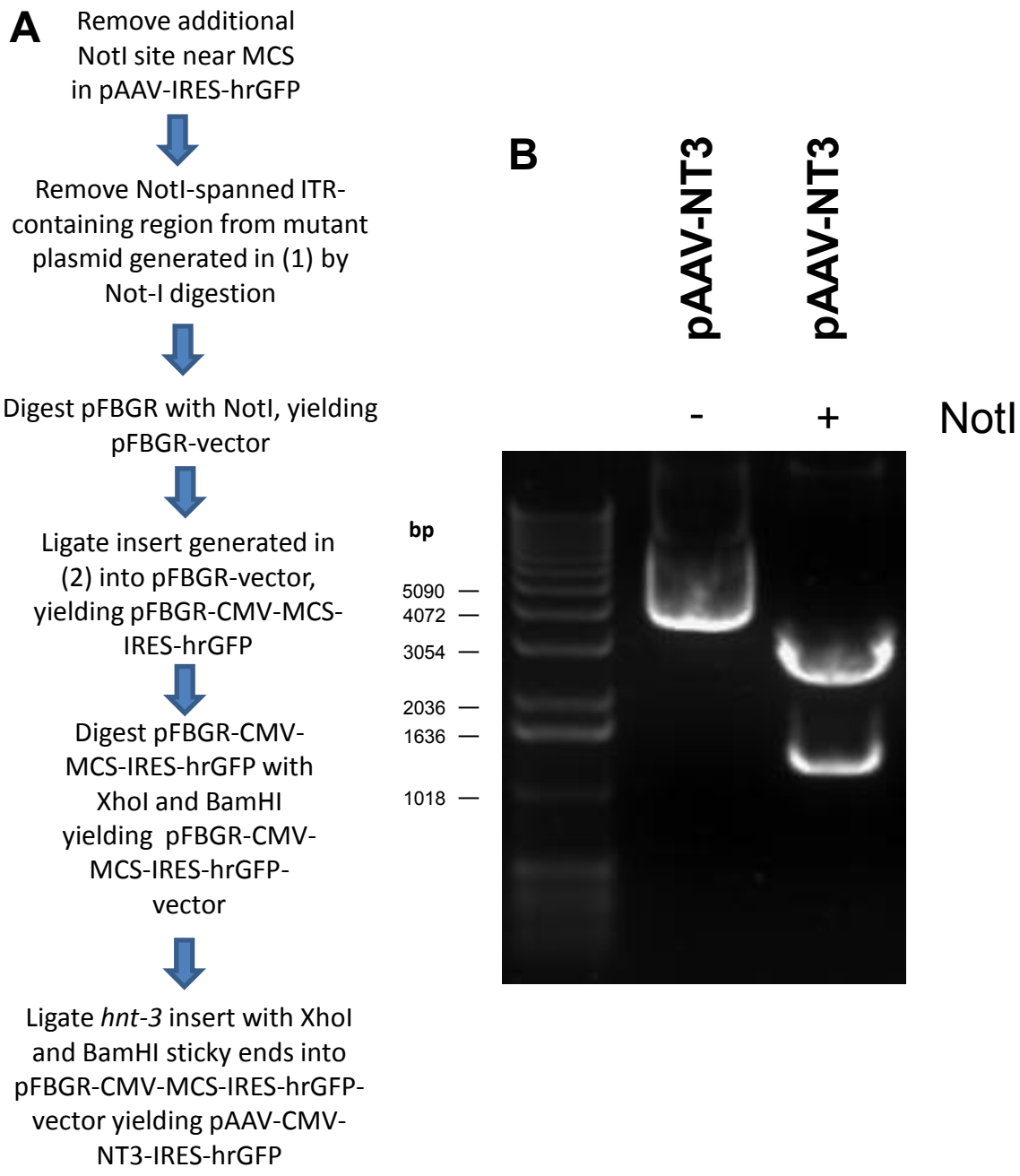


**Figure 3.8**. A. Schematic showing the steps involved in producing pAAV-CMV-NT3-IRES-hrGFP. **B**. Digestion of pAAV-CMV-NT3-IRES-hrGFP (pAAV-NT3) with NotI yields 3 fragments, 2 of which are unresolvable at ~2.8kb.

sub-cloning of the NotI site spanned MCS-containing segment of pAAV-IRES-hrGFP into “pFBGR vector”, to yield a pFBGR-IRES-hrGFP-MCS plasmid, into which the *hnt-3* sequence could be subsequently sub-cloned.

### 3.2.4.3 Production of pFBGR-IRES-hrGFP-MCS

The following section is split into three main parts. Firstly, site-directed mutagenesis of the additional NotI site in pAAV-IRES-hrGFP. Secondly, insertion of the mutated cassette back in pAAV-IRES-hrGFP. Thirdly, sub-cloning of the mutated cassette from pAAV-IRES-hrGFP(NotI mut) into pFBGR.

#### 3.2.4.3.1 Optimisation of overlap extension PCR

OEPCR was performed in three stages, involving three separate PCR reactions. The first PCR (PCR1) used a forward primer of designed using the sequence spanning an SnaBI site within the CMV promoter region (SnaBIfor). That this site was unique within pAAV-IRES-hrGFP was confirmed by restriction digest of pAAV-IRES-hrGFP with SnaBI (Figure 3.9). The reverse primer for PCR1, based around the additional NotI site near the MCS of pAAV-IRES-hrGFP contained a single mutation within the NotI site itself (NotIOL2, Figure 3.10A).

The second PCR (PCR2) employed a forward primer which was complementary to NotIOL2 (NotIOL1) and a reverse primer based upon a sequence at the 5’ end of the IRES sequence within pAAV-IRES-hrGFP (LONGpAAVrev, Figure 3.10A).

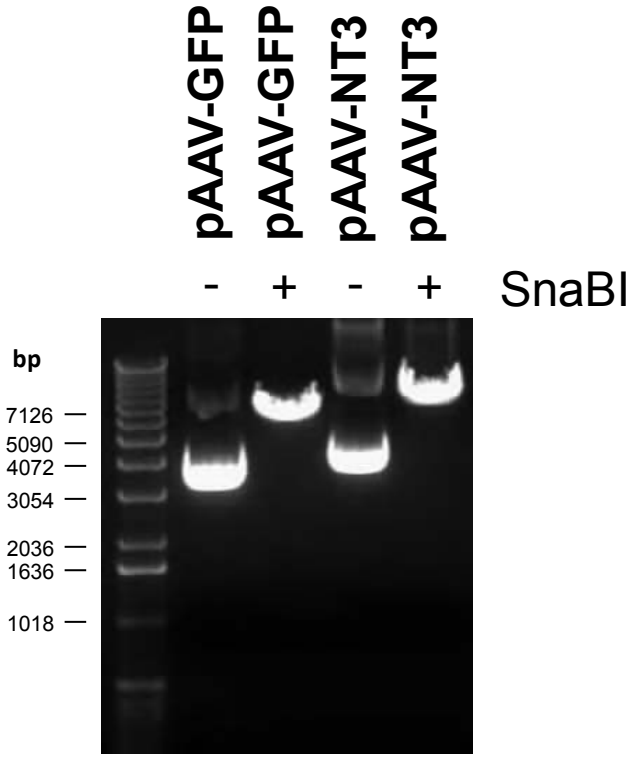


**Figure 3.9**. Digestion of pAAV-IRES-hrGFP (pAAV-GFP) and pAAV-CMV-NT3-IRES-hrGFP with SnaBI shows that the SnaBI site is unique in these plasmids

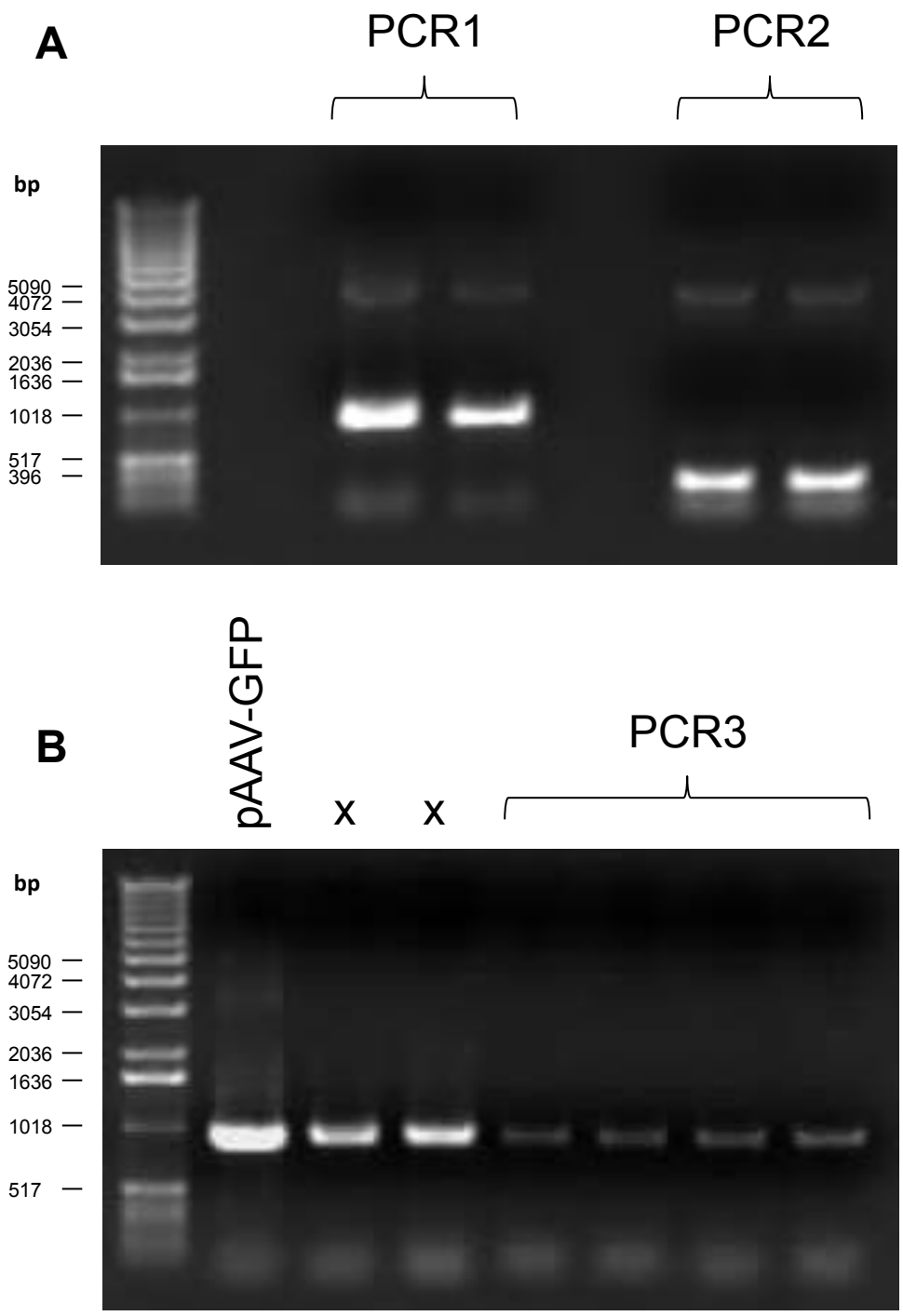


**Figure 3.10**. Overlap extension PCR to ablate a NotI site in pAAV-IRES-hrGFP (pAAV-GFP). **A**. PCR1 (template pAAV-GFP, primers SnaBIfor and NotIOL2) and PCR2 (template pAAV0GFP, primers NotIOL1 and LongpAAVrev). **B**. PCR3 (template PCR1+PCR2 products, primers SnaBIfor and XhoIrev). Lane "pAAV-GFP" was a positive control using primers for PCR3. "x" refers to lanes used to amplify products from a previous, inefficient PCR3.

In PCR3 the products of PCR1 and PCR2 were gel purified and combined together along with SnaB1for and LongpAAVrev. A successful result would yield an amplicon of ~1200bp. Unfortunately, PCR3 failed to yield any products.

In order to increase the efficiency of PCR3, two strategies were assessed. First, dimethylsulphoxide (DMSO, which is known to linearise DNA secondary structures) was added to the PCR mix. Secondly, a primer designed around the XhoI site within the MCS of pAAV-IRES-hrGFP was used. This primer would yield a shorter product in PCR3, with the intention of decreasing secondary structure within the amplicon. The use of XhoIrev resulted in a low level of amplification in PCR3, necessitating further optimisation in the form of increased number of cycles (from 14 to 18) and the addition of extra magnesium to the PCR mix. Figure 3.10B shows the successful product of PCR3.

#### 3.2.4.3.2 Reconstitution of pAAV-IRES-hrGFP containing the NotI mutation

The product of PCR3 was digested with SnaBI and XhoI to yield a fragment (designated NotImut Insert) with 'sticky' ends for ligation into pAAV-IRES-hrGFP, which had been digested with these same enzymes and subsequently dephosphorylated (designated pAAV vector, Figure 3.11). After gel purification, ligation of NotImut Insert into pAAV vector at a volume ratio of 1:1 and 3:1 was performed. The negative control plate (i.e. 1µl vector to 0µl insert) had 1 colony, the 1:1 ligation plate had 1 colony and the 3:1 ligation plate had 3 colonies. Thus, despite a low 'background' in the negative control plate, the ligation failed with at

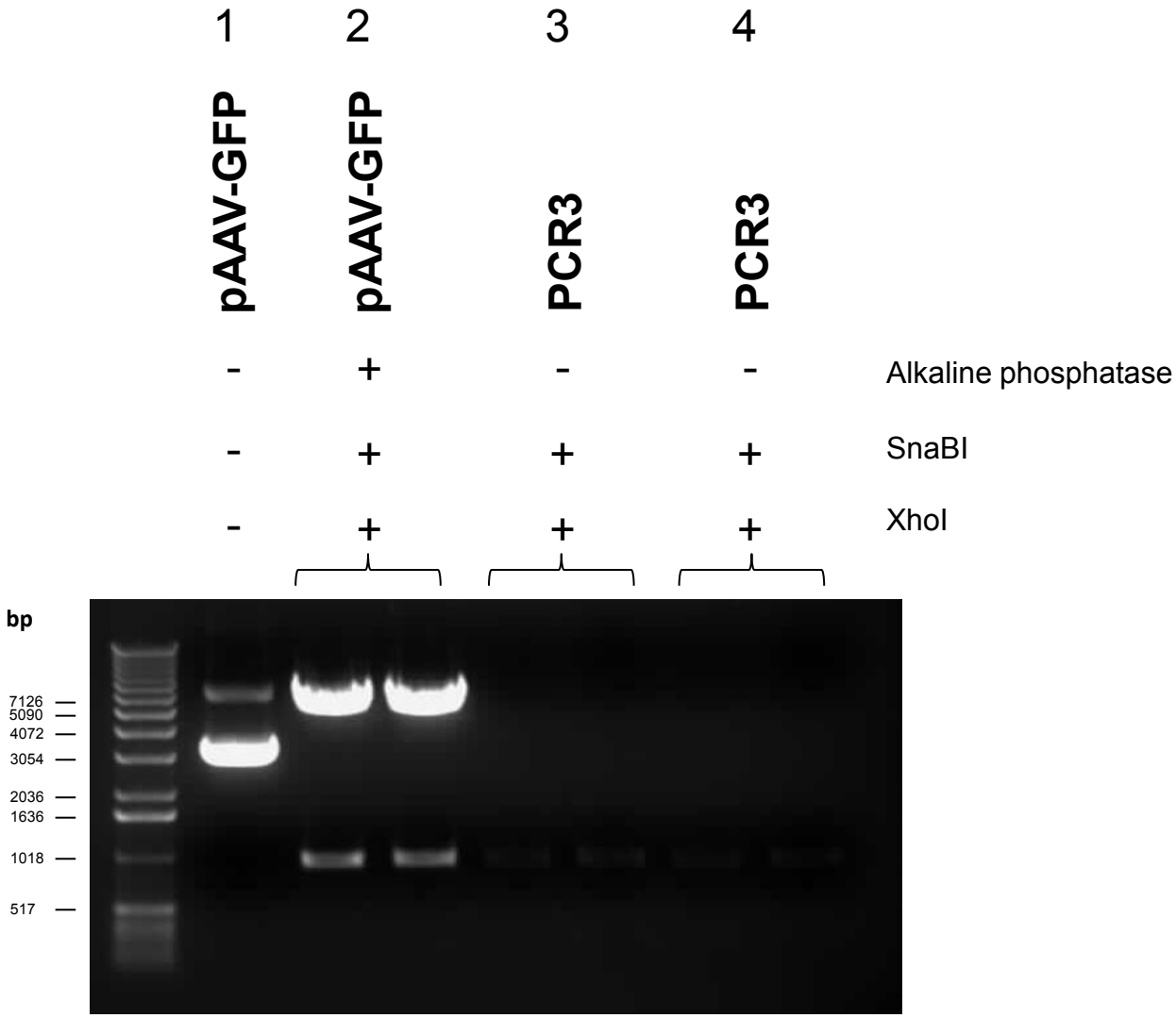


**Figure 3.11**. Production of pAAV-IRES-hrGFP (pAAV-GFP) vector and NotI mutant insert by digestion with SnaBI and XhoI. **1**. Undigested pAAV-GFP. **2**. Digestion and dephosphorylation of pAAV-GFP yielded a vector fragment at ~7100bp. **3** and **4**. Two individual digestions of the PCR3 amplicon spread across 4 lanes.

least 10X fewer colonies than expected. Higher insert-to-vector ratios, up to 15:1 were performed, yielding similar results.

More NotImut Insert was prepared following the steps described above and the ligation repeated using 1:1 and 3:1 insert to vector ratios. This yielded 0 background colonies, 2 colonies on the 1:1 plate and 1 colony on the 3:1 plate. Given that this ligation appeared to be of low efficiency it was decided to miniprep all colonies and screen for the presence of insert by digestion with SnaBI and XhoI. No colonies contained the insert. The next step was to repeat the ligation but to increase the transformation efficiency by performing a rescue step. The rescued ligation yielded 4 colonies on the background, 6 colonies on the 1:1 plate and 12 colonies on the 3:1 plate. Screening of 8 colonies from the 3:1 plate by restriction digest showed that none of the ligations had been successful.

One reason for the poor efficiency of ligation may have been that SnaBI cut the product from PCR3 inefficiently. In order to increase the efficiency of SnaBI digestion, a primer was designed to replace SnaBIfor which binds 5' from the SnaBI site, yielding an amplicon from PCR3 with a longer 'cap' segment 5' to the SnaBI site. Digestion of this amplicon, subsequent ligation and miniprepping of colonies yielded 1 successful ligation out of 6 (Figure 3.12). This plasmid, designated pAAV-IRES-hrGFP(NotImut) was sequenced, confirming the presence of the mutation.

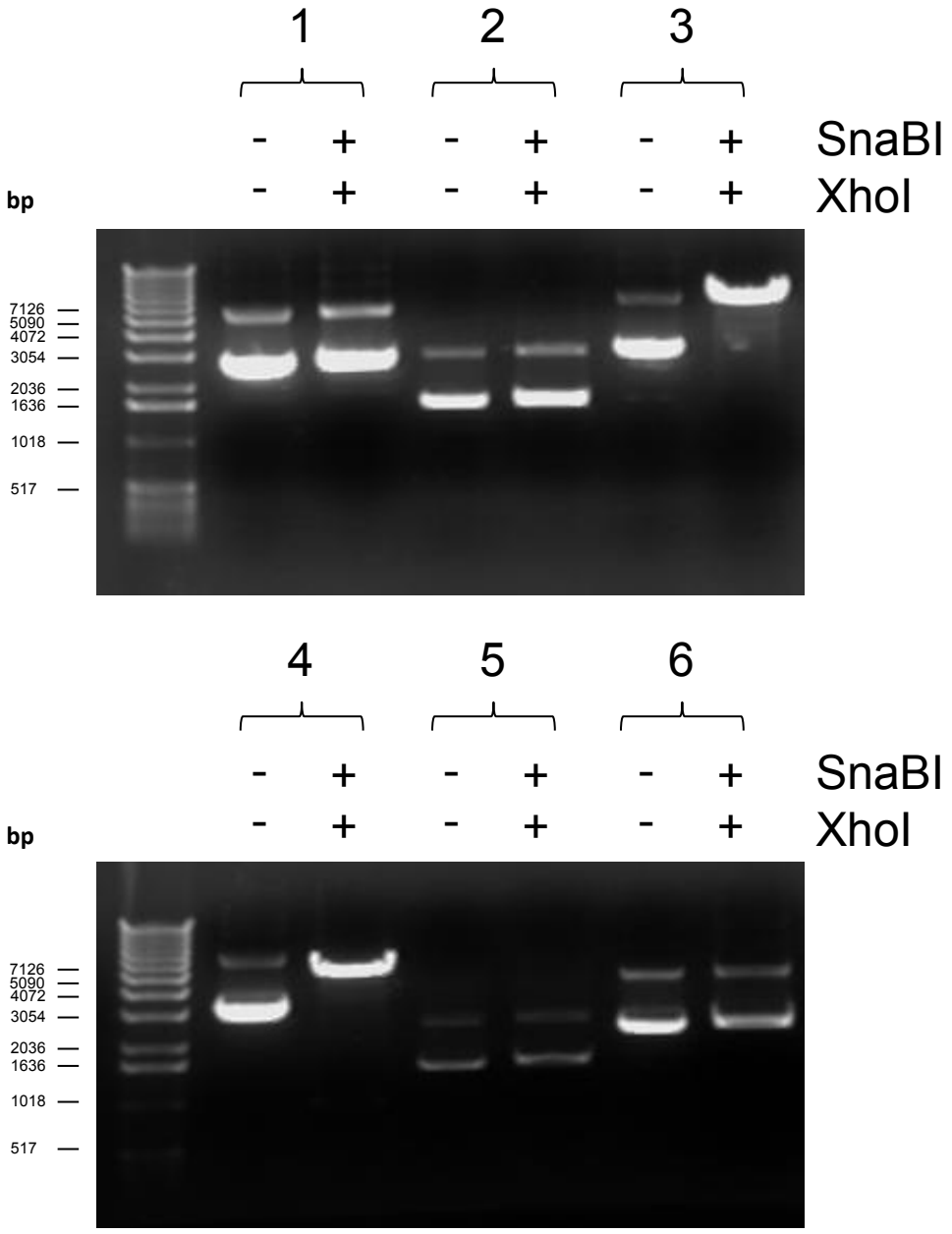


**Figure 3.12**. One miniprep out of 8 (very dim band at ~1000bp in number 4) contained the insert carrying the mutated NotI site.

#### 3.2.4.3.3 Sub-cloning the NotI mutant cassette from pAAV-IRES-hrGFP(NotImut) into the NotI sites of pFBGR

By means of confirmation, pAAV-IRES-hrGFP(NotImut) was digested with NotI. As expected, digestion of pAAV-IRES-hrGFP yielded 3 fragments while pAAV-IRES-hrGFP(NotImut) yielded two fragments (Figure 3.13A). Unfortunately, the two fragments from the latter digest were too close to resolve. This problem was overcome by digestion of pAAV-IRES-hrGFP(NotImut) with both NotI and ScaI, resulting in the conversion of the larger unresolvable fragment into two smaller, resolvable fragments and allowing the fragment of interest (designated pAAV-NotImut Insert) to be isolated (Figure 3.13B).

pAAV-NotImut Insert was ligated into the NotI sites of the pFBGR backbone (pFBGR vector) at ratios of 1:1 and 7:1. This ligation, under standard conditions, was unsuccessful, but yielded 20 colonies in the 7:1 ratio after a rescue step. Three of these 20 colonies were midiprepped and subjected to NotI digestion (Figure 3.14). Two clones out of three were found to be positive for insert and were designated pFBGR-IRES-hrGFP-MCS.

### 3.2.4.4 Sub-cloning the *hnt-3* sequence into pFBGR-IRES-hrGFP-MCS yielded a functional plasmid

pFBGR-IRES-hrGFP-MCS and pAAV-CMV-NT3-IRES-hrGFP were digested with BamHI and XhoI yielding a 'vector' and 'insert' respectively (Figure 3.15). Ligation followed by a rescue step yielded 8 colonies on the 3:1 plate, which were screened for the presence of the *hnt-3* insert by digestion with BamHI and XhoI (Figure 3.16).

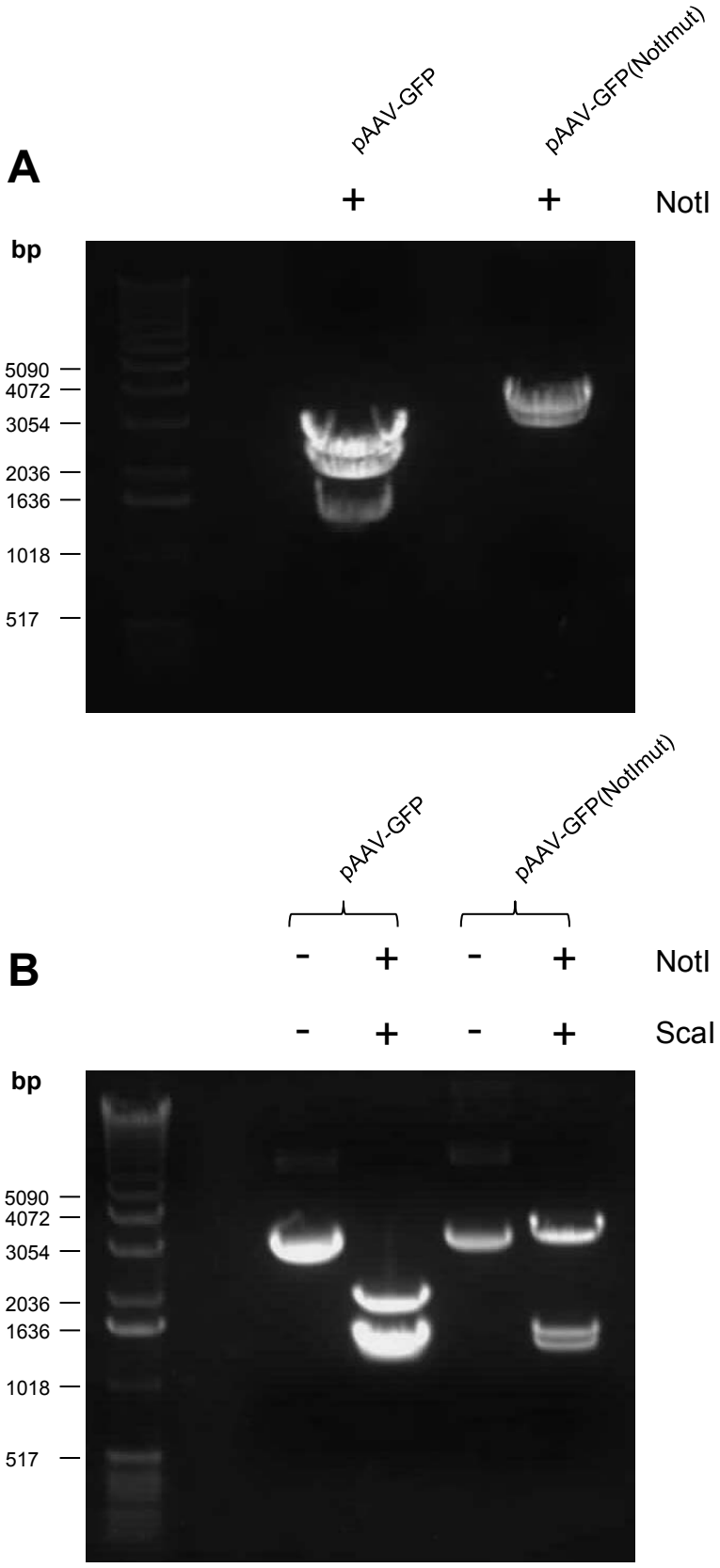


**Figure 3.13**. **A**. Digestion of pAAV-IRES-hrGFP(NotImut) with NotI yields 2 unresolvable fragments, compared with 3 fragments from the unmutated plasmid. **B**. The NotI mutated cassette, spanned by NotI sites, can be isolated at ~3500bp by digestion with NotI and ScaI.

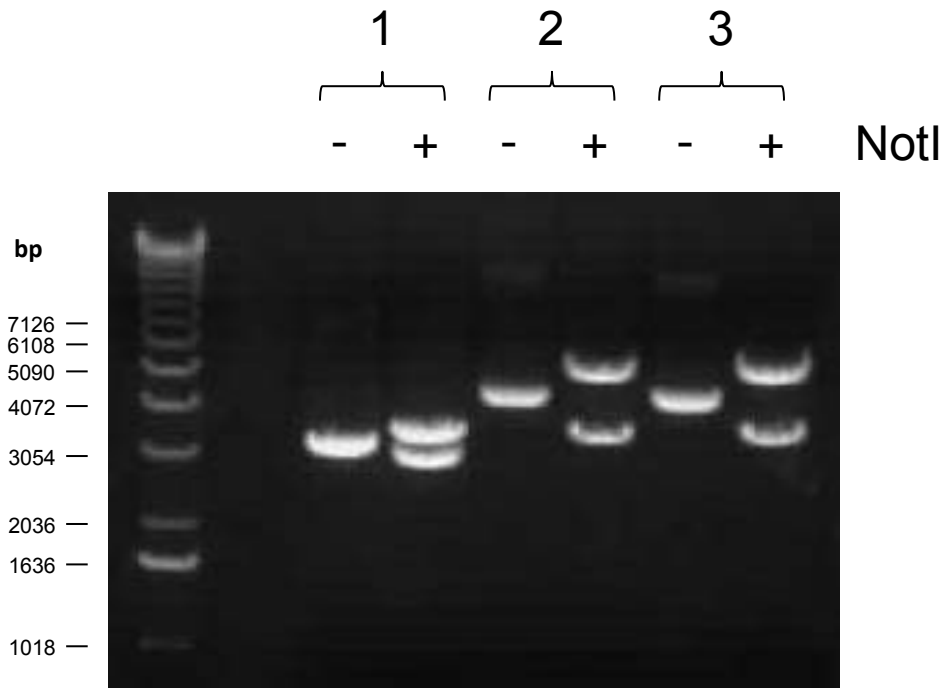


**Figure 3.14**. Clones 2 and 3 were positive for the presence of the pAAV-NotImut insert. Clone 2 was kept and designated pFBGR-IRES-hrGFP-MCS

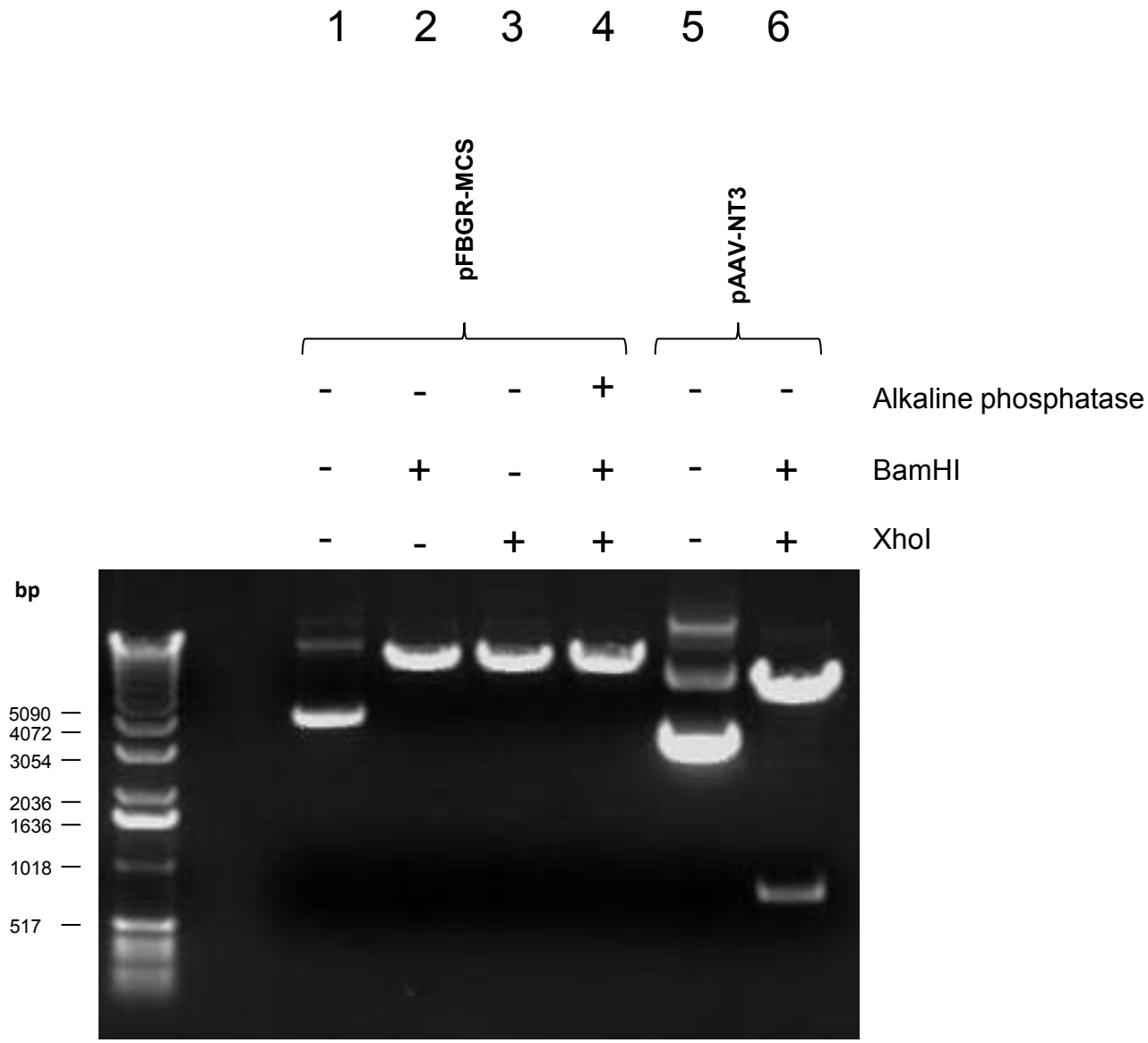


**Figure 3.15**. Preparation of vector from pFBGR-IRES-hrGFP-MCS (pFBGR-MCS) and insert from pAAV-CMV-NT3-IRES-hrGFP (pAAV-NT3). **1, 2 and 3**. BamHI and XhoI are single cutters in pFBGR-MCS. **4**. The dephosphorylated pFBGR-MCS vector. **5 and 6**. The ~700bp hNT-3 containing insert is easily isolated.

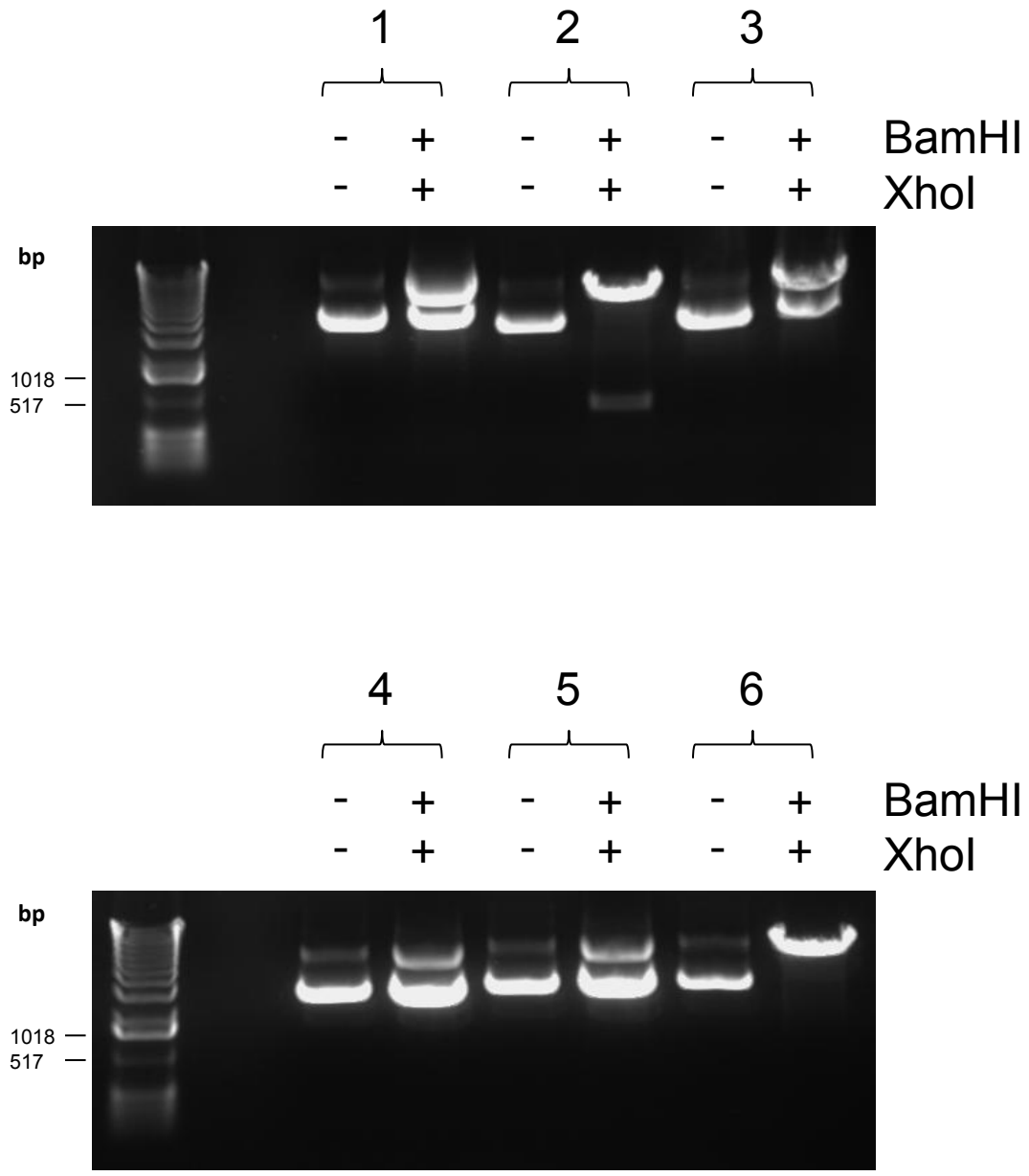


**Figure 3.16**. One clone out of 6 (number **2**) contained the hNT-3 insert, spanned by BamHI and XhoI sites.

Clone 2 contained the insert, and was designated pFBGR-CMV-NT3-IRES-hrGFP (Figure 3.17). Transfection of pFBGR-CMV-NT3-IRES-hrGFP into COS cells resulted in strong GFP expression in ~90% of cells and very high levels of NT-3 in the conditioned medium, as determined by ELISA. The levels of NT-3 could not be accurately quantified as the highest dilution of conditioned medium had a higher concentration than the top standard in the ELISA assay.

## 3.2.5 Production of $shRNA_{RhoA}$ containing constructs

### 3.2.5.1 The starting materials

As well as kindly supervising all of the following, Dr Michael Douglas provided the $shRNA_{RhoA}$ sequence (driven by a mouse U6 promoter) within pAAV-U6-$shRNA_{RhoA}$-CMV-CNTF-IRES-hrGFP and designed the primers to determine the orientation of the $shRNA_{RhoA}$ insert. The biological activity of the $shRNA_{RhoA}$ sequence used in this study was confirmed by Dr Douglas by transfecting a plasmid containing the sequence into COS-1 cells that overexpressed rat RhoA. Western blotting of the lysate from these cells at an appropriate time-point revealed effective knockdown of RhoA compared with two published sequences (Ahmed, Dent et al. 2005; Pille, Denoyelle et al. 2005) and a GFP shRNA (Figure 3.18)

### 3.2.5.2 Generation of pFBGR-IRES-hrGFP-NT3-$shRNA_{RhoA}$

pFBGR-IRES-hrGFP-NT3-$shRNA_{RhoA}$ was produced in three main steps. The $shRNA_{RhoA}$ sequence designed by Dr Michael Douglas was released from pAAV-IRES-hrGFP-$shRNA_{RhoA}$ and ligated into pFBGR-IRES-hrGFP-NT3 at an MluI site found between the 5' ITR and the NotI site. After this, the orientation of the insert

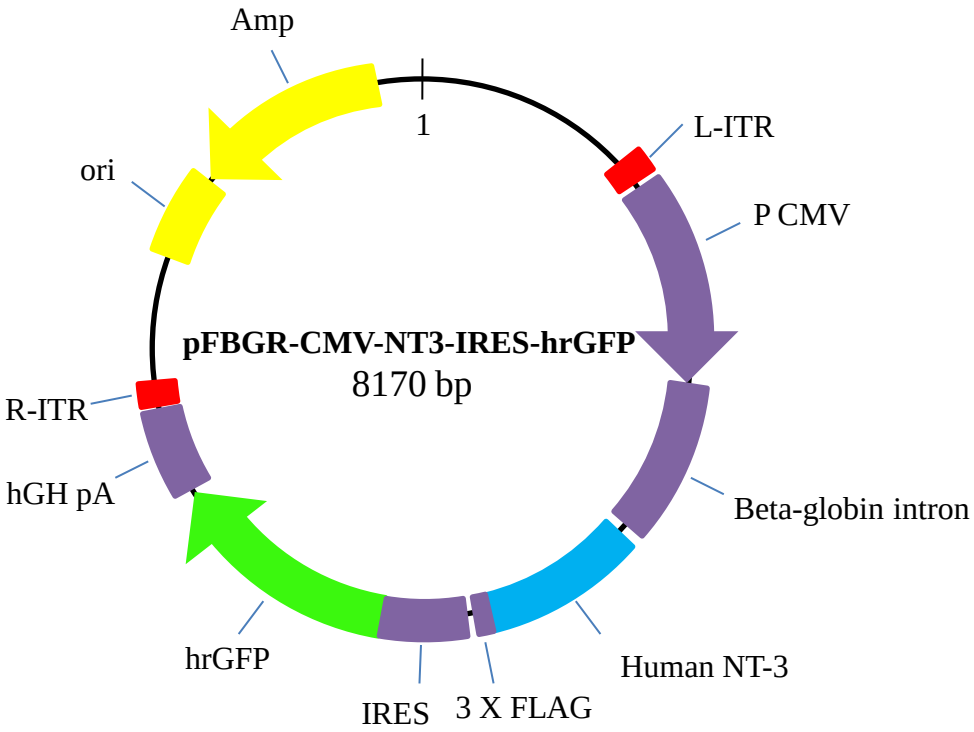


| Feature | Nucleotide position |
|---|---|
| L-ITR† | 662-837 |
| CMV promoter* | 859-1521 |
| Beta-globin intron* | 1529-2021 |
| Human NT-3 | 2101-2870 |
| 3 X FLAG* | 2879-2950 |
| IRES* | 2986-3572 |
| hrGFP* | 3570-4286 |
| hGH pA* | 4344-4822 |
| R-ITR† | 4866-5041 |
| Amp / ori† | 5042-8170 |
| NotI cleavage site | 852, 5041 |

*From pAAV-IRES-hrGFP
†From pFBGR

**Figure 3.17**. Map of pFBGR-CMV-NT3-IRES-hrGFP

Pille et al. 5'-GACATGCTTGCTCATAGTC*TT*-3'

Ahmed et al. 5'-AAGGATCTTCGGAATGATGAG-3'

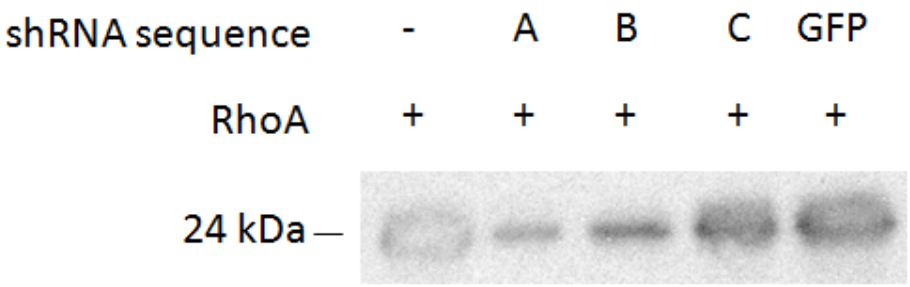


**Figure 3.18**. Preliminary validation of shRNA constructs performed by Dr M. Douglas. Sequence **A**, giving maximal knockdown, was designed by Dr M. Douglas (sequence unavailable). Sequences **B** and **C** were based on published sequences (see Pille 2005 and Ahmed 2005, respectively).

was confirmed by PCR to ensure that transcription of the $shRNA_{RhoA}$ occurred from the same strand as *hrgfp* and *nt-3*. Production of pFBGR-IRES-hrGFP-$shRNA_{RhoA}$ was unsuccessful for unknown reasons.

#### 3.2.5.2.1 Ligation of the $shRNA_{RhoA}$ insert into pFBGR-CMV-NT3-IRES-hrGFP was successful, but attempts at producing an $shRNA_{RhoA}$ only plasmid failed

pAAV-IRES-hrGFP-$shRNA_{RhoA}$ was digested with MluI to release the $shRNA_{RhoA}$ sequence (spanned by MluI sites, designated "shRNA insert"), and pFBGR-IRES-hrGFP-MCS and pFBGR-CMV-NT3-IRES-hrGFP were digested and dephosphorylated to prepare vectors designated "pFBGR-MCS vector" and "pFBGR-NT3 vector" (Figure 3.19).

The shRNA insert was ligated into pFBGR-MCS and pFBGR-NT3 vectors, and transformed into *E.coli*. Four colonies were picked from each plate and miniprepped, followed by digestion with MluI to confirm presence of insert (Figure 3.20).

In order to establish that both the shRNA and *hrgfp* or *hrgfp-nt3* expression cassettes would be transcribed from the same strand, primers were designed based upon the AAV ITR sequence (pAAVITRf) and the MluI sequence (MluIrev). PCR screening of the successful ligation products with these primers yielded one positive (i.e. correctly orientated) clone amongst the NT-3 containing constructs, whilst none of the pFBGR-IRES-hrGFP-MCS constructs had the shRNA in the correct orientation (Figure 3.21). A number of further ligations were attempted to generate a correctly orientated pFBGR-IRES-hrGFP-MCS, to no avail.

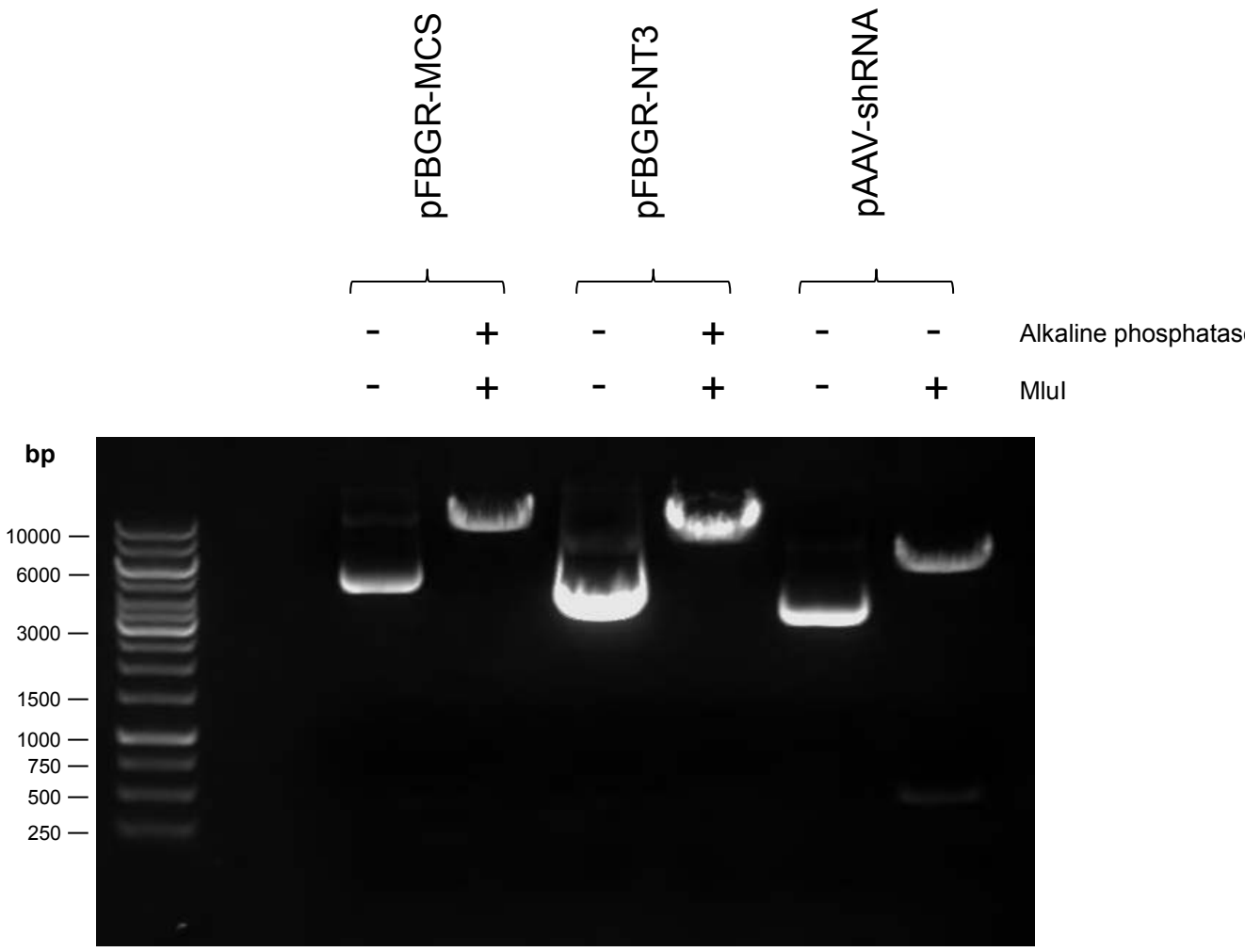


**Figure 3.19**. pFBGR-IRES-hrGFP-MCS (pFBGR-MCS) and pFBGR-CMV-NT3-IRES-hrGFP (pFBGR-NT3) were digested with MluI and dephosphorylated. The $shRNA_{RhoA}$ construct was released from pAAV-IRES-hrGFP-$shRNA_{RhoA}$ (pAAV-shRNA) for sub-cloning into the pFBGR vectors.

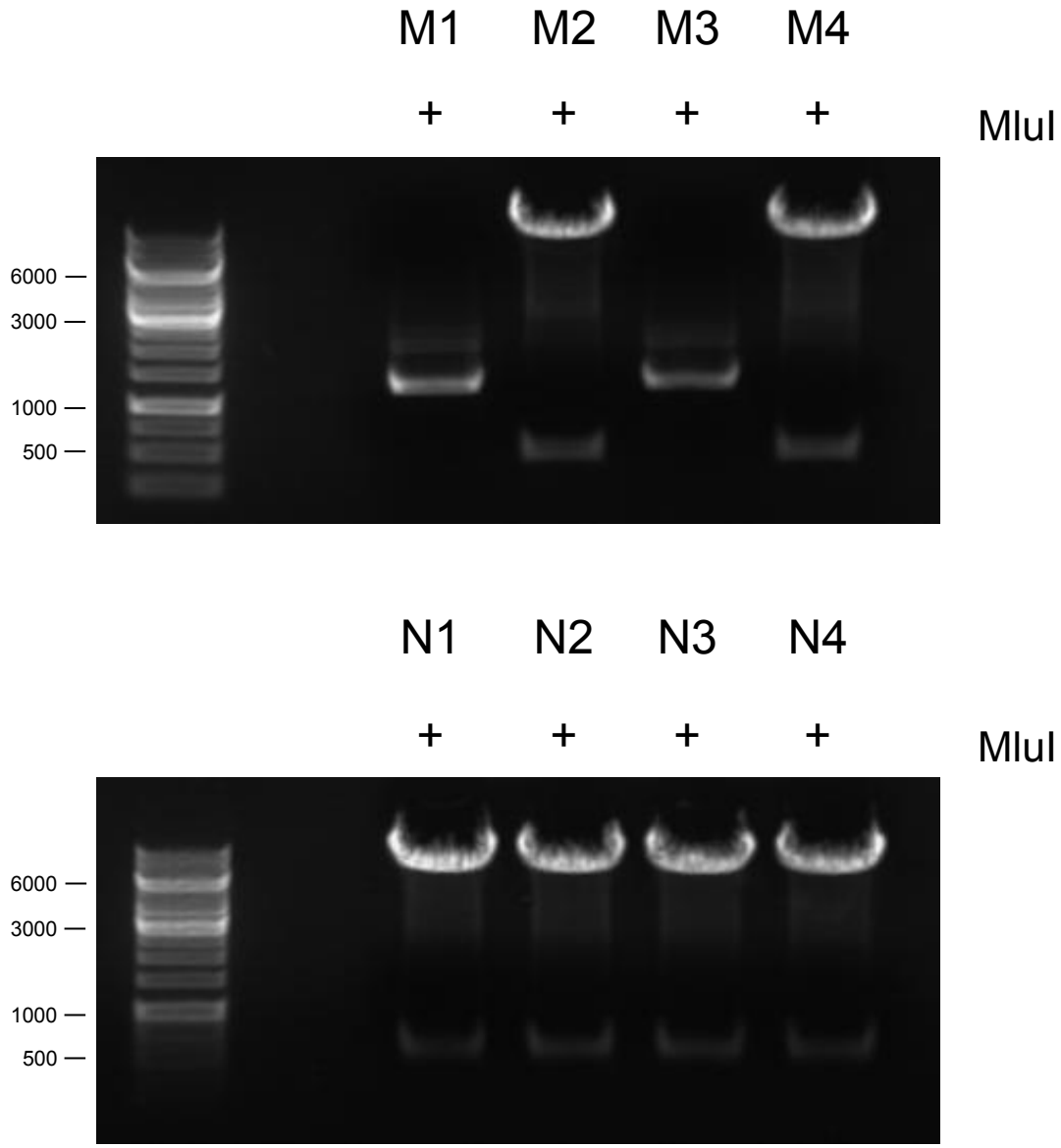


**Figure 3.20**. Restriction digest to confirm the presence of the $shRNA_{RhoA}$ insert. Positive colonies from ligation of $shRNA_{RhoA}$ insert into pFBGR-MCS vector (**M1-M4**) and pFBGR-NT3 vector (**N1-N4**) were picked and miniprepped, then digested with MluI to detect the ~500bp insert, which was present in M2, M4 and N1-N4.

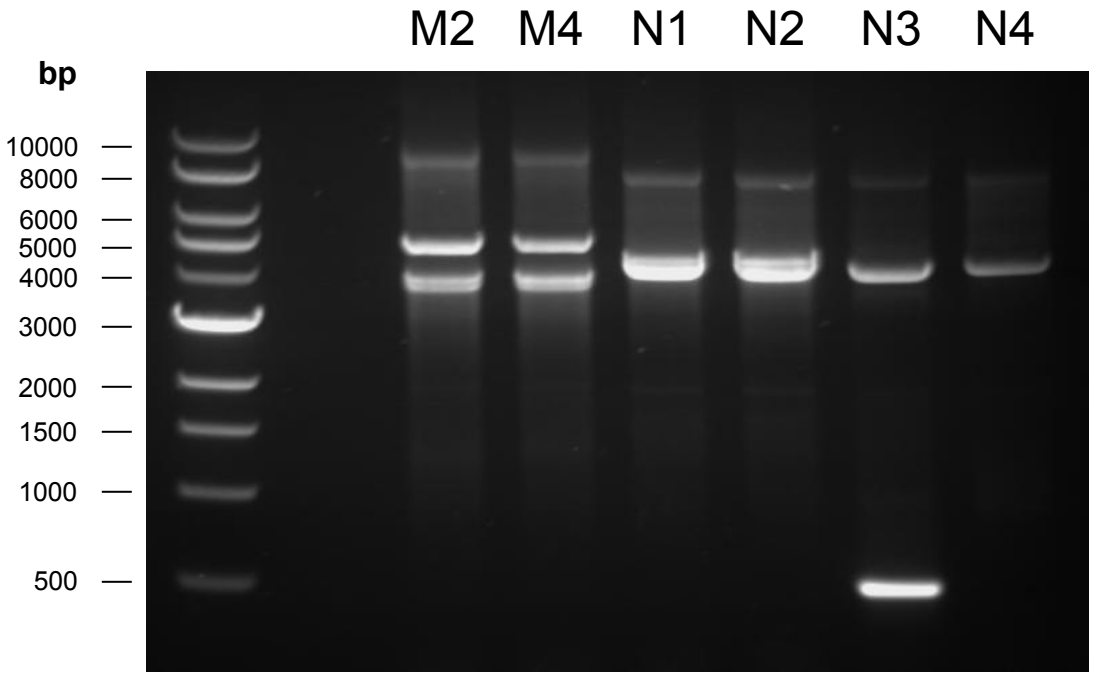


**Figure 3.21**. Determination of $shRNA_{RhoA}$ insert orientation. **N3** was the only correctly oriented clone, giving a PCR product at the expected ~500bp size.

# Discussion

### 3.3.1 Biological activity of rhNT-3 *in vitro*

rhNT-3 bioactivity was confirmed by the demonstration of a DRGN survival promoting effect. This is a known effect of NT-3 on neurones, and has been shown to be the result of stimulation of the Akt pathway (Liot, Gabriel et al. 2004). In the study by Liot, the dose that was found to give the maximal survival was 10ng/ml, identical to the optimum concentration found in this study. However, it must be born in mind that Liot did not report the effect of any doses higher than 10ng/ml and used a serum-deprivation paradigm.

It is interesting that rhNT-3 did not promote neurite outgrowth of DRGN in the experiments described above. On examination of the literature, the neurite growth promoting activity of NT-3 appears to be a topic of some controversy. Most reports showing positive effects of NT-3 on neurite outgrowth employ explants, usually from embryonic or early post-natal animals (usually rat and chick). A PubMed search using the terms “nt-3 neurite outgrowth” yielded 108 hits, with only 3 papers describing results from experiments using dissociated adult rat DRG cultures (Mohiuddin, Fernandez et al. 1995; Kimpinski, Campenot et al. 1997; Gavazzi, Kumar et al. 1999). The paper by Mohiuddin et al. used dissociated cultures of DRG from adult Wistar rats exposed to rhNT-3, and showed a positive effect on neurite outgrowth from DRGN at a concentration of 10ng/ml. However, Gavazzi et al. showed no effect of rhNT-3 on neurite length in dissociated DRG cultures, whilst Kimpinski et al. showed no neurite growth promotion in dissociated DRG cultures grown in a compartmented culture system.

Closer examination of the papers described above reveals that the way in which they quantify neurite outgrowth is different. Kimpinski et al. used a non-conventional dissociated culture system, and so will be excluded from the following discussion. Mohiuddin et al. used a method based upon neurite density, applying a Weibel grid to micrographs of cultures and then counting the number of intersections of DRGN neurites with gridlines. Gavazzi et al. measured three separate parameters relating to neurite outgrowth by conventional means: percentage of process-bearing DRGN, length of the longest neurite per DRGN (i.e. the single longest neurite) and total neurite length per DRGN (i.e. the sum of the lengths of all neurites for a given DRGN). The measure used by Mohiuddin et al. is most closely correlated with 'total neurite length' used by Gavazzi et al. At a concentration of 50ng/ml rhNT-3, Mohiuddin et al. showed 4 times greater neurite outgrowth compared with control. At the same concentration of rhNT-3, Gavazzi et al. also showed an increase in total neurite length but only of small magnitude (~1.5 times greater compared with control) and restricted to medium-diameter DRGN. Thus it appears that the parameter used to quantify neurite outgrowth in the present study was inappropriate for demonstrating an effect of NT-3 on neurite outgrowth. However, the fact remains that biological activity of rhNT-3 in DRG cultures *was* demonstrated, and agreed with reports already published in the literature.

The failure of the mitotic inhibitor 5-FDU to reveal an effect on neurite outgrowth is clear following the discussion above. Recalling that the rationale for adding 5-FDU was to remove NT produced by non-neuronal cells in DRG cultures, it is also interesting to note that just after the experiment being discussed here was

performed, it was discovered by Zubair Ahmed and the author that conditioned medium from dissociated DRG cultures does not actually contain detectable or physiological levels of NT (Ahmed, Jacques et al. 2009). This result is likely to be due to failure of DRG cultures to synthesise NT-3 but could be caused by sequestration of NT-3 by the ECM.

### 3.3.2 Detection of NT3-FLAG

The major aim of the experiments described in section 3.5.1 was to demonstrate that NT-3 was in fact produced when cells were transfected with pAAV-CMV-NT3-IRES-hrGFP. That NT-3 was detected came as no surprise given that the sequence of the NT-3 coding region of the plasmid was known to be correct. Two points will be discussed in further detail below: (i) the concept of experimental repetition and, (ii) the relevance of the concentration of NT-3 found *in vitro*.

The author acknowledges that the Western blot and ELISA for NT3-FLAG should have been repeated at least three times. Three major factors contributed to this inadequacy, namely cost, time and the questionable relevance of the concentration of NT-3 found in conditioned medium. To run a single $E_{max}$ ELISA plate costs in excess of £100, not to mention the cost of producing the conditioned medium. Additionally, to run such an ELISA plate required a three day protocol to be performed. Finally, it must be stressed that it was known that COS-1 cells do not produce NT-3 (Farhadi, Mowla et al. 2000). Thus, any NT-3 detected in COS-1 cell conditioned media must have been from an exogenous source, resulting in the experimental question becoming not one of how much NT-3 is produced by

transfected *versus* untransfected COS-1 cells but rather whether NT-3 is produced *at all* after transfection with an NT-3 containing construct. Finally, it must be stressed that NT-3 production by COS-1 cells transfected with pAAV-CMV-NT3-FLAG-IRES-hrGFP has been shown in three independent trials employing three different techniques: Western blotting (Figure 3.4B), ELISA and immunoprecipitation (Figure 3.6).

It was found, in one batch of conditioned medium from COS-1 cells transfected with pAAV-CMV-NT3-FLAG-IRES-hrGFP, that the concentration of NT-3 was 64ng/ml. Superficially, this appeared to be an encouraging result showing that a biologically active amount of NT-3 is produced by transfection of cells with a particular plasmid. However, it must be borne in mind that such *in vitro* experiments employing plasmids have many limitations and must only be extrapolated to the *in vivo* situation with caution. First, recall that it was pFBGR-CMV-NT3-IRES-hrGFP that was used to manufacture the viral vector $AAV8_{hrGFP\text{-}NT3}$, not pAAV-IRES-hrGFP (the plasmid used in the experiments discussed above). This was due to there needing to be a change of strategy relatively late on in the project in order to produce the viral vectors. The pFBGR plasmids were constructed, but there was insufficient time to test them. NT-3 production by pFBGR-CMV-NT3--IRES-hrGFP was shown by ELISA, however. Secondly, how can the concentration of NT-3 in conditioned medium be extrapolated to the concentration of NT-3 *in vivo*? Such extrapolation is impossible, since *in vitro* a transfected, proliferating cell line from a green monkey (COS-1 cells) is being grown in 2 dimensions in an enclosed compartment in a specified volume of medium. *In vivo*, transduced non-proliferating cells (DRGN) are growing in 3 dimensions in a

complex and varying milieu with the added complications of the immune system etc. The only comment that can be made about the value of 64ng/ml of NT-3 in COS-1 cell conditioned medium is that it is a lot, and would *probably* correspond to a lot being made *in vivo* using a viral vector. Further experiments must be performed to show how much additional NT-3 is produced *in vivo*.

### 3.3.3 The biological activity of NT3-FLAG was not convincingly demonstrated

The attempts to show biological activity of NT3-FLAG represented an arduous and frustrating time for the author. Given the successful reports in the literature demonstrating the activity of virally delivered or recombinant NT-3, these experiments were embarked upon with great optimism (Dijkhuizen, Hermens et al. 1997; Blits, Oudega et al. 2003). Closer examination of these reports, however, reveals some essential differences that may explain the difficulties faced in this study.

Blits et al. applied conditioned media to embryonic DRG explants, and used neurite outgrowth from the explant as their main measure for NT-3 activity. In the present study, conditioned media were applied to dissociated adult rat DRG cultures, using survival to demonstrate rhNT-3 activity. Blits et al. demonstrated positive effects on DRGN neurite outgrowth in the presence of rhNT-3 and NT-3 applied in conditioned media with an apparent absence of toxicity. In the present study, no strong positive biological effects of NT-3 containing conditioned medium were demonstrated; in fact, conditioned media appeared to be toxic. Three factors may explain the failure of the present study compared with Blits et al. Firstly, Blits et al. used DRG explants, compared with the dissociated cultures in this study. Explants are likely to be more

biologically relevant than dissociated cultures, since the DRG tissue is intact. Dissociated cultures were used by the author since this is the technique that the Molecular Neuroscience Group is most familiar with. Also, the author attempted to perform some experiments using explants which failed, due to them becoming detached from the culture dish. The use of explants by Blits et al. may have protected the DRGN within from toxic agents within the conditioned media, since the DRG capsules would presumably have been intact. Dissociated DRG cultures may be more susceptible to toxicity since DRGN are in direct contact with culture medium.

The second factor likely to have a role is the age of the neurones used in experiments. The Molecular Neuroscience Group has historically used adult neurones in cell culture experiments. The use of cells from adult animals makes good sense from the point of view of translation, since most of the pathologies that are the subject of intense research in the neurodegeneration/repair field affect adults predominantly. A survival effect of NT-3 on DRG cultures may not have been observed due to the fact that adult neurones are less dependent on NTs than their embryonic counterparts (Snider and Silos-Santiago 1996).

Finally, it may be possible that the way in which conditioned media were prepared could have a bearing on the failure of the experiments described here. Conditioned media used in the experiments described above had been prepared by leaving transfected COS-1 cells for 7d, compared with 3d in the case of Blits et al. Over 7d, many toxic compounds are likely to have accumulated in the conditioned media including small molecules such as urea and ammonia. Additionally, nutrients will

have been depleted from the media. It is likely that the conditioned media, used by Blits et al. were less nutrient depleted and contained lower concentrations of metabolites than those used in the present study.

### 3.3.4 NT3-FLAG could not be purified in sufficient quantities allowing assessment of biological activity

Given the apparent toxicity of whole conditioned media it was decided to attempt to purify the FLAG-tagged NT3 by using immunoaffinity chromatography. Acid elution yielded a (barely) detectable amount of NT3-FLAG, and FLAG peptide elution failed.

At this point, the issue of *why* so much emphasis was placed upon demonstrating biological activity of NT3-FLAG must be discussed. The presence of a FLAG tag is beneficial mainly from the point of view of ease of detection. Neurotrophins are notoriously difficult to detect, particularly on Western blots (personal communications, various sources). By FLAG-tagging them, NTs can be detected easily with the well validated anti-FLAG monoclonal antibody. However, whenever a tag is applied to a protein it must always be borne in mind that there exists a theoretical possibility that the activity of the tagged protein may differ from the untagged state (Terpe 2003). Despite the fact that most tag sequences are small, they may still have the potential to interfere with protein-protein interactions, and in the case of NT-3 they may interfere with its interaction with TrkC.

As a consequence of the failure to demonstrate that NT3-FLAG has identical biological activity, it was decided to instead produce an AAV8 vector containing

untagged NT3. This was not ideal, since using this virus renders it impossible to differentiate between endogenous and exogenous NT3, since the sequences of the human and rat proteins are identical.

### 3.4 Further work

Much additional work is required to complete the investigations discussed above. This work was not completed by the author due mainly to time constraints within the project framework. The following described the major additional experiments the author would like to perform. Additionally, the author would like to increase the n numbers in those experiments described with less than three replicates.

#### Further characterisation of DRGN neurite outgrowth parameters affected by NT-3

As mentioned in the discussion, it is likely that the measure of neurite outgrowth employed in this study was inappropriate for demonstrating NT-3 bioactivity. Thus, it would be informative to measure additional parameters such as number of neurites per DRGN, total neurite length and branching. Assessment of these parameters may reveal an effect of NT-3 (or indeed any of the conditioned media) on neurite outgrowth.

#### Optimisation of NT3-FLAG purification

It would be beneficial to spend more time attempting to maximise the yield of NT3-FLAG. This could possibly be achieved by increasing the concentration of FLAG peptide used for elution, altering the conditions of elution (e.g. increasing the

temperature during elution, agitation, alteration of pH) or by employing a different type of affinity tag.

### *In vitro* testing of the $shRNA_{RhoA}$ sequence

Despite the fact that knockdown of overexpressed rat RhoA in COS-1 cells was shown by Dr Michael Douglas, it would be useful to examine the effect of this shRNA sequence on neurones grown in the presence of an inhibitory substrate. This could be achieved by transfecting DRGN with a plasmid containing the $shRNA_{RhoA}$ sequence and then exposing these neurones to an inhibitory substance such as myelin. The Molecular Neuroscience Group has an established inhibitory assay that could be used (Ahmed, Dent et al. 2005). The major difficulty with such an experiment would be in transfecting the DRGN, since they are post-mitotic and hence refractory to traditional transfection reagents such as Lipofectamine. One technique that could be employed is electroporation, where neurones are exposed to plasmids in the presence of an electrical field. This has been shown to be successful in both retinal ganglion cells and DRGN (Leclere, Panjwani et al. 2005).

### Generation of a plasmid enabling manufacture of an shRNA-only containing AAV8 vector

It remains unclear why it proved impossible to generate a plasmid containing the shRNA construct alone. Further work is required, probably involving greater numbers of ligations and optimisation of ligation conditions.

# Chapter 4

# Assessment of the cellular tropism of AAV8 in the DRG using two different delivery methods

# Introduction

### 4.1.1 Viral tropism in the DRG

Viral tropism has been defined as the ability of a virus to infect a particular cell type, tissue or host. To a virologist interested in tropism, 'infection' occurs if the virus is able to enter the proliferative phase of its life cycle (McFadden, Mohamed et al. 2009). However, from the point of view of gene therapy, lytic infection is not usually desirable, so tropism in this context refers to the ability of a given virus to transduce (i.e. mediate the expression of a transgene such as *gfp*) a particular cell, tissue or host. The focus of the following account will be on *cellular* tropism of AAV8 in the DRG.

The importance of assessing the tropism of a given gene therapy vector is paramount. Lack of knowledge of which cells or tissues a viral vector transduces renders one unable to predict the effects (or side effects) of a virally delivered transgene product. At the time that these studies were performed, no published reports existed that described the detailed neuronal tropism of AAV8 in DRG (recall that DRGN have been sub-classified, discussed below), although it was known that this vector was able to target sensory neurones in the PNS and a variety of neuronal types in the CNS (Klein, Dayton et al. 2006; Storek, Reinhardt et al. 2008).

### 4.1.2 Determinants of viral tropism

Viral tropism is determined by a diverse array of factors at various points in the life-cycle of the virus from attachment to the host cell membrane, to trafficking of the

particle in the cytoplasm and processing of the viral genome (McFadden, Mohamed et al. 2009). Additionally, the detection of a transduced cell depends upon that cell being capable of manufacturing the transgene product within the experimental timescale, and that product not being overtly toxic or immunogenic (i.e. a viral vector may be capable of transducing cells, but the transgene delivered may kill cells or be cleared by the immune system, leading to an artefactual negative result). Furthermore, the promoter driving the transcription of the transgene mRNA must be appropriate to the cell being targetted, for example using a neuron-specific promoter to give expression in neurones but not glia.

In the case of AAV8 *versus* other serotypes such as AAV2, relatively little is known of the precise mechanisms whereby the virus is able to enter cells. It was recently shown that the multi-functional 67 kDa laminin receptor (LMR) can act as a receptor for a variety of AAV serotypes, including AAV8 (Akache, Grimm et al. 2006). However, at the time of writing no other receptors for AAV8 have been identified. Given the roles of molecules such as LMR, heparan sulphate proteoglycans and integrins in AAV transduction, it seems likely that the ECM plays a role in determining viral entry and hence may influence cellular tropism (Pajusola, Gruchala et al. 2002; Daya and Berns 2008).

It is likely that AAV8 enters the cytoplasm in a clathrin-dependent manner, and is able to escape from endocytic vesicles by the enzymatic degradation of the vesicle membrane by capsid proteins (Daya and Berns 2008). However, the mechanism of

AAV trafficking from the cytosol to the nucleus still remains unclear, with even the role of the nuclear pore complex yet to be elucidated. It is probable that there are differences in the trafficking of different capsid proteins, which may impact upon cellular tropism.

In the case of standard recombinant AAV vectors, once in the nucleus, the viral genome must be released from the capsid proteins and gain access to the nuclear machinery where its ssDNA genome can be converted into dsDNA. This is thought to be a rate-limiting factor in AAV transduction and has led to the development of self-complementary AAV vectors, in which the second strand is reconstituted much more quickly than in standard recombinant (rAAV) vectors (Goncalves 2005). The above events may impinge upon the cellular tropism observed if different vectors are given different genome structures leading to differential processing within the nucleus. Additionally, different capsid proteins may traffic to the nucleus at different rates, meaning that the length of time between delivery and assessment of transduction rate is important – if a vector is slow to traffic, early time points may show spuriously poor transduction rates. Additionally, if different cell types traffic vectors differentially, tropism profiles may vary at different time points.

### 4.1.3 DRGN sub-populations

Classification of DRGN by size is one of the commonest and most convenient methods in use, and has yielded unimodal, bimodal and trimodal distributions (Willis and Coggeshall 2004). Bimodal size distributions are seen most commonly, leading

to the conclusion that DRGN can be split into two major classes – small and large cells (Schmalbruch 1987; McLachlan, Janig et al. 1993). However, there is a significant body of evidence showing that DRGN can in fact be split into three distinct groups based on size, and which correlate with neurophysiological parameters such as axon conduction velocity (Willis and Coggeshall 2004). DRGN have been separated into small, medium and large diameter populations in this study since much of the literature describes this classification (particularly in neurophysiology).

### 4.1.4 AAV based vectors in the nervous system

That AAV vectors are capable of transducing DRGN was first demonstrated 10 years ago by Fleming et al. who showed that an AAV2 vector expressing GFP could transduce all three of the major cell types of the DRG *in* vitro (Fleming, Ginn et al. 2001). This was followed by a report describing the delivery of an AAV2 vector to the DRG *in vivo* by Xu et al. who compared the transduction characteristics in the DRG after delivery by a variety of routes including intra-DRG and intrathecal injection (Xu, Gu et al. 2003). They showed strong preferential targeting of DRGN after intra-DRG injection, and also transduction of dorsal horn neurones but not DRGN after intrathecal injection.

The first description of AAV8 delivery to the nervous system was from Klein et al. who were able to deliver neurotoxic levels of proteins including GFP to the substantia nigra (Klein, Dayton et al. 2006). Soon, DRGN were shown also to be targetted by

AAV8, although no data were published showing preferential transduction of DRGN sub-types (Foust, Poirier et al. 2008; Storek, Reinhardt et al. 2008).

### 4.1.5 Intra-DRG versus intrathecal injection

The two delivery techniques employed in this study each have distinct advantages and disadvantages in the context of spinal cord repair. Intra-DRG injection allows localised delivery of relatively high concentrations of therapeutics to the DRG, whereas intrathecal injection is capable of delivering substances to the entire neuraxis, but usually at lower doses than intra-DRG injection (Fischer, Kostic et al. 2011). Surgically, intra-DRG injection is more traumatic and less well tolerated than the relatively non-invasive intrathecal injection. If viral vectors become commonplace in the clinic, either of these methods of delivery are likely to be used in different circumstances.

### 4.1.6 Some important assumptions

Given the above remarks, it becomes clear that the concept of cellular tropism is a difficult one to explicitly define in the complex *milieu* of the whole animal. Many factors contribute and interact, necessarily leading one to make certain assumptions to simplify the design of experiments and the interpretation of results. In the case of the experiments performed in this chapter, it has been assumed that the intracellular processing of AAV8 is the same in all sub-populations of DRGN. This is probably a reasonable assumption, since all DRGN share the same embryological origin and

hence probably process viruses in a similar manner. Using this assumption, one can then state that any differential expression of transgene delivered by AAV8 is due to differences either in the way the virus *accesses* DRGN or the way it *interacts* with DRGN. To control for the way AAV8 accesses DRGN, this study has employed two different delivery paradigms – one would predict that if the same cellular tropism is seen using more than one delivery method, it is likely that the tropism is due to how the virus interacts with cells and not how it gets to them.

The methods of delivery employed are described in detail in Chapter 2. Briefly, intra-DRG injection involved surgical exposure and injection under direct vision of the left L4 and L5 DRG. Intrathecal injection was performed by accessing the subarachnoid space in the lumbar cistern using a small needle and injecting virus into the CSF. $AAV8_{gfp}$ was kindly generated and provided by Dr. Ronald Klein. This virus encoded eGFP under the control of a hybrid CMV/β-actin promoter and contained the 3' enhancer woodchuck hepatitis virus posttranscriptional regulatory element.

#### 4.1.7.1 Specific hypotheses

- AAV8 transduces all subtypes of DRGN with equal frequency *in vitro* and *in vivo* regardless of delivery route – there is no cellular tropism
- Transduction of DRGN will correlate with the level of expression of LMR
- The central projections of DRGN will be completely filled with GFP

### 4.1.7.2 Specific aims

- To classify DRGN based on their diameters and assess which of these are GFP+ *in vitro*, and also *in vivo*, after intra-DRG and intrathecal injection
- To trace the central projections of $GFP^+$ DRGN and correlate the trajectories of these projections with those of known populations of DRGN
- To correlate GFP positivity in DRGN with the presence of LMR and parvalbumin *in vivo*

## Section 4.1.8 Brief description of methods

A total of 18 animals (200-220g) were used in this study: 6 intra-DRG injection of $AAV8_{gfp}$; 3 intra-DRG injection of PBS; 3 intrathecal injection of $AAV8_{gfp}$; 3 intrathecal injection of PBS; and 3 uninjected rats comprised controls.

The nine animals receiving intra-DRG PBS or $AAV8_{gfp}$ received injections of 10µl PBS alone or $10^{10}$ vg in 10µl PBS to the left L4 and L5 (L4/L5) DRG using a glass micropipette inserted into the DRG under direct vision, and were sacrificed 28d later, this being a timepoint when expression is likely to be at high levels due to the need for second strand synthesis (Ferrari, Samulski et al. 1996). Animals undergoing intrathecal injections received either 30µl PBS alone or $10^{12}$ vg $AAV8_{gfp}$ in 30µl PBS using a 25G needle inserted into the subarachnoid space in the lumbar spine.

GFP expression within DRGN was analysed by photographing entire sections of the DRG at an exposure time that demonstrated zero background staining in uninjected

animals. All DRGN were counted and their diameters' recorded. GFP positivity was also recorded, allowing assessment of the diameter of GFP+ DRGN.

LMR and PV expression were assessed using standard immunohistochemical techniques, with PV expression being quantified as above.

AAV8 was applied to dissociated DRG cultures *in vitro* at a given multiplicity of infection (MOI). The MOI refers to the number of viral particles delivered per neurone in each chamber of the culture dish. Cultures were left for 7d and then analysed using a similar technique to that described above.

# Results

### 4.2.1 AAV8 targeted DRGN independent of delivery route

After both intra-DRG and intrathecal injection, GFP expression (Figure 4.1A and B) was restricted to DRGN and their axons in DRG. No non-neuronal cells were transduced by $AAV8_{gfp}$. The mean transduction rate of DRGN after intra-DRG injection was 11.36 ± 1.63% compared to 1.48 ± 0.48% after intrathecal injection (Table 4.1). A small number of DRGN were GFP+ in uninjected contralateral DRG after intra-DRG injection (data not shown). The intrathecal injection experiment was repeated using a glass micropipette instead of a 25G needle. Unfortunately, there was no transduction of any DRGN. No GFP+ axons were seen in the cord or dorsal roots.

### 4.2.2 AAV8 preferentially transduced large-diameter, parvalbumin$^+$ DRGN

(i) After intra-DRG injection, only 2.04 ± 0.66% small diameter DRGN were GFP+, compared with 14.95 ± 1.98% medium diameter DRGN and 31.79 ± 10.55% large diameter DRGN (Figure 4.2 Bi), correlated with a significant shift to the right of the size distribution of $GFP^+$ DRGN (Figure 4.2 Bii; Mann-Whitney U test, $p=6 \times 10^{-36}$, n=6). Additionally, the method of Vulchanova et al. was used to analyse the proportion of GFP+ DRGN that were less than or above 22μm in diameter (Vulchanova, Schuster et al. 2010). This revealed that there were significantly more GFP+ DRGN with diameters greater than 22μm than GFP+ DRGN with diameters <22μm, implying that large-diameter DRGN were over-represented in the GFP+ population (t-test, $p=4.4 \times 10^{-7}$, n=6). (ii) Similar differences in transduction rates were recorded after intrathecal injection of 0.04 ± 0.04% for small diameter compared with

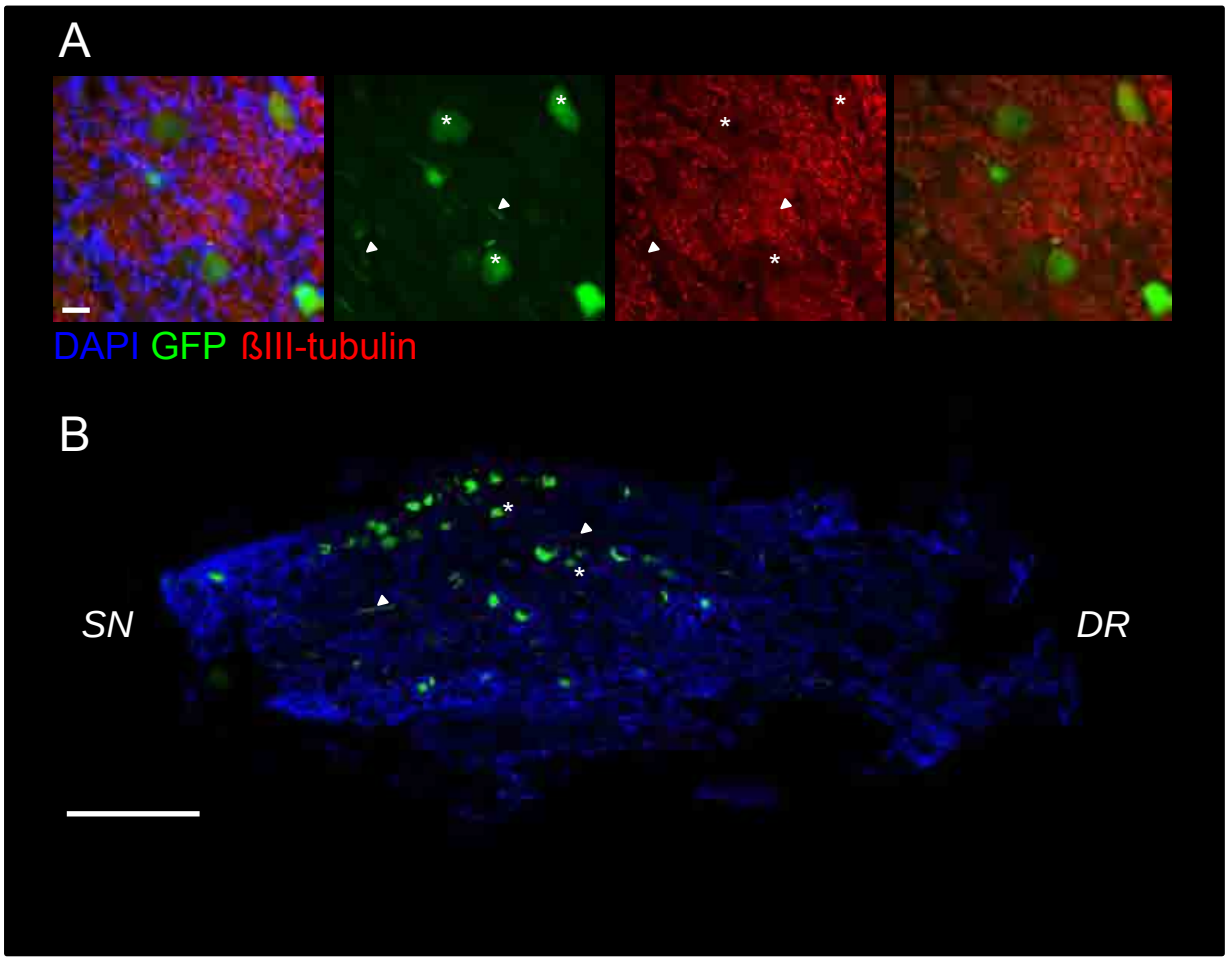


**Figure 4.1** Cells targeted by AAV8$_{gfp}$. **A**. Many GFP+/ßIII-tubulin+ DRGN cell bodies (asterisks) and their axons (arrowheads) were present in the DRG. (**B**) Low magnification view of a horizontal section through the centre of a DRG 28d after intra-DRG injection of AAV8$_{gfp}$. Note widespread DRGN transduction and minimal gross tissue disruption. (*SN*=spinal nerve, *DR*=dorsal root. Scale bar in **A** = 500µm, in **B** = 50µm).

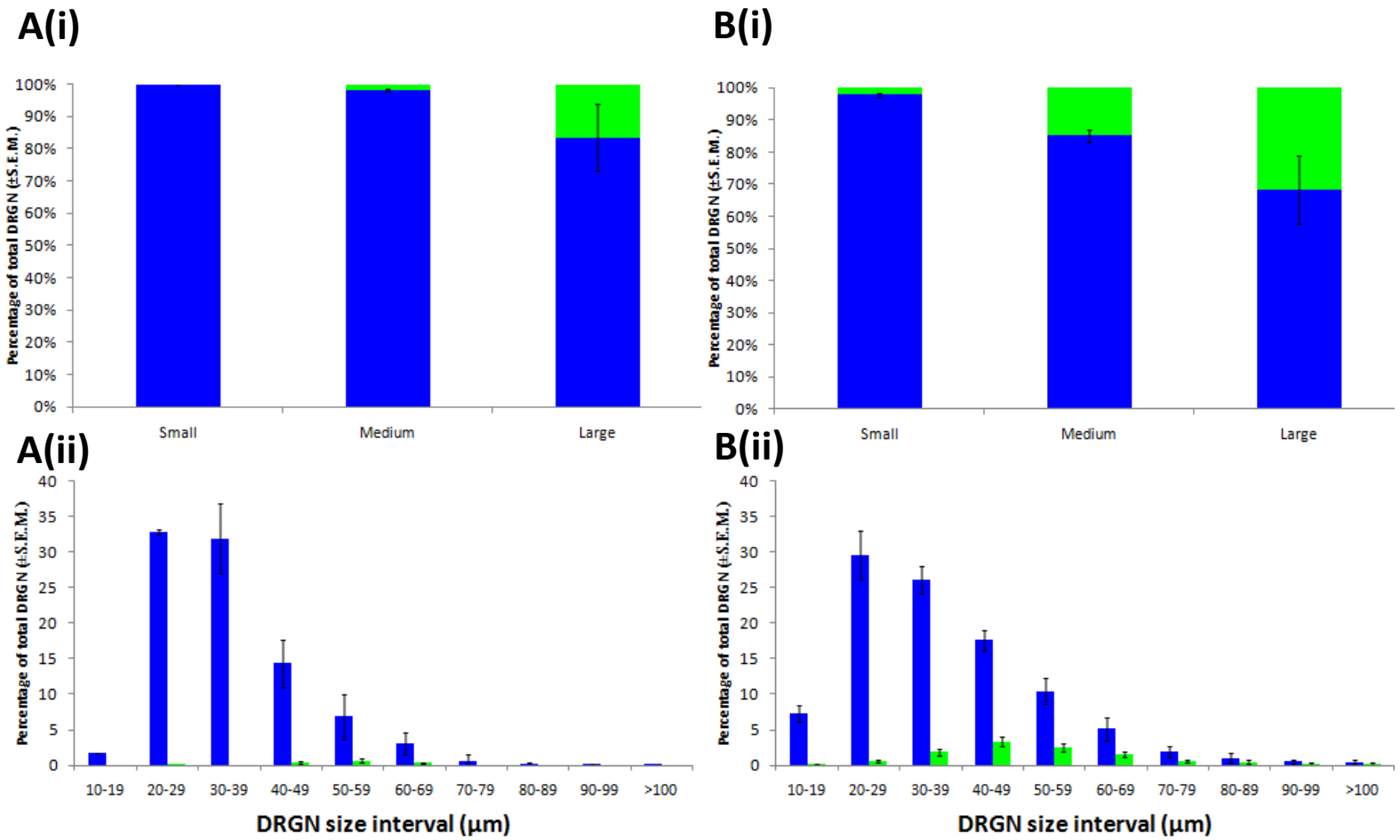


**Figure 4.2** Size distribution of GFP$^+$ and GFP$^-$ DRGN. Proportions (%) of small (0-29µm), medium (30-59µm) and large (>60µm) diameter (**A(i)** and **B(i)**) and size distribution (**A(ii)** and **B(ii)**) of GFP$^+$ DRGN (green bars= GFP$^+$; blue bars = total DRG population) after intrathecal (**A**) and intra-DRG injection (**B**), respectively. **A**: n=3, **B**: n=6

**A**

| | L4 | L5 | **L4** | **L5** | L4 | L5 | **L4** | **L5** | L4 | L5 | **L4** | **L5** | **Overall mean** |
|---|---|---|---|---|---|---|---|---|---|---|---|---|---|
| **% Transduction** | 12.1 | 5.4 | 13.7 | 9.4 | 14.0 | 16.3 | 10.3 | 23.1 | 5.9 | 8.1 | 2.5 | 15.5 | 11.36 |
| **Mean DRGN cell body diameter (µm)** | 33.5 | 28.4 | 37.8 | 35.2 | 53.5 | 57.4 | 36.0 | 37.6 | 31.8 | 36.2 | 34.3 | 33.7 | 38.0 |
| **Mean GFP+ DRGN cell body diameter (µm)** | 46.9 | 34.0 | 50.2 | 49.8 | 65.3 | 74.2 | 47.7 | 47.7 | 43.5 | 56.4 | 46.9 | 42.8 | 50.5 |

**B**

| | L4 | L5 | **L4** | **L5** | L4 | L5 | **L4** | **L5** | L4 | L5 | **L4** | **Overall mean** |
|---|---|---|---|---|---|---|---|---|---|---|---|---|
| **% Transduction** | 0.6 | 0 | 0 | 0.2 | 5.1 | 2.7 | 1.7 | 1.8 | 2.5 | 0.6 | 1.1 | 1.5 |
| **Mean DRGN cell body diameter (µm)** | 31 | 33 | 31 | 31 | 37.8 | 35 | 61 | 36 | 33 | 35 | 36 | 36.3 |
| **Mean GFP+ DRGN cell body diameter (µm)** | 51 | n/a | n/a | 26 | 54.8 | 52 | 53 | 51 | 54 | 54 | 59 | 50.5 |

**Table 4.1** Percentage transduction and diameters of total and GFP+ populations of DRGN after intra-DRG (**A**) and intrathecal (**B**) injection. Alternating bold and non-bold text refers to DRGs from different animals. In the intrathecal injection experiment one DRG was not analysed due to there being no ganglion tissue in any sections.

1.83 ± 0.52% medium and 16.53 ± 10.24% for large diameter DRGN (Figure 4.2Ai, ii; Mann-Whitney U, p=1,57 x $10^{-12}$; t-test, p=0.005, n=3). Of medium and large diameter DRGN, 17.4% were parvalbumin+, compared with 33.3% of GFP+ DRGN (t-test, p=0.046; Figure 4.3 A, B).

### 4.2.3 All DRGN were LMR$^{+}$

Qualitatively, all sizes of GFP+ and GFP- DRGN expressed LMR (Figure 4.4) suggesting that LMR may not be used exclusively by AAV8 to transduce DRGN.

### 4.2.4 The central projections of DRGN were labelled with GFP

*(i)* After intra-DRG injection (Figure 4.5), GFP+ axons entered the spinal cord at the DREZ, invaded the ipsilateral dorsal column and dorsal horn, and projected to the ventral horn, but none penetrated the contralateral grey matter, although a few were seen in the contralateral DREZ. GFP+ axons projected in the ipsilateral lumbar and thoracic gracile fasciculi (Figure 4.5 A, B), containing less GFP at more rostral levels (Figure 4.5 A-C). In longitudinal sections of the rostral lumbar cord, GFP+ axons exclusively projected in the ipsilateral gracile fasciculus (Figure 4.5 D). There were very faint GFP+ axons in the gracile fasciculus of the cervical cord, but none in the medulla at the level of the ipsilateral gracile nucleus (data not shown). No GFP+ neuronal somata were seen in either the spinal cord, or brainstem grey matter. (ii) After intrathecal injection, the central projections of large diameter DRGN at all levels of the cord were labelled (Figure 4.6 A-C). The dorsal roots and dorsal columns contained GFP+ axons at all cord levels, terminating in the deeper parts of the dorsal horn, particularly at lumbar (Figure 4.6 A) and thoracic (Figure 4.6 B) levels, with

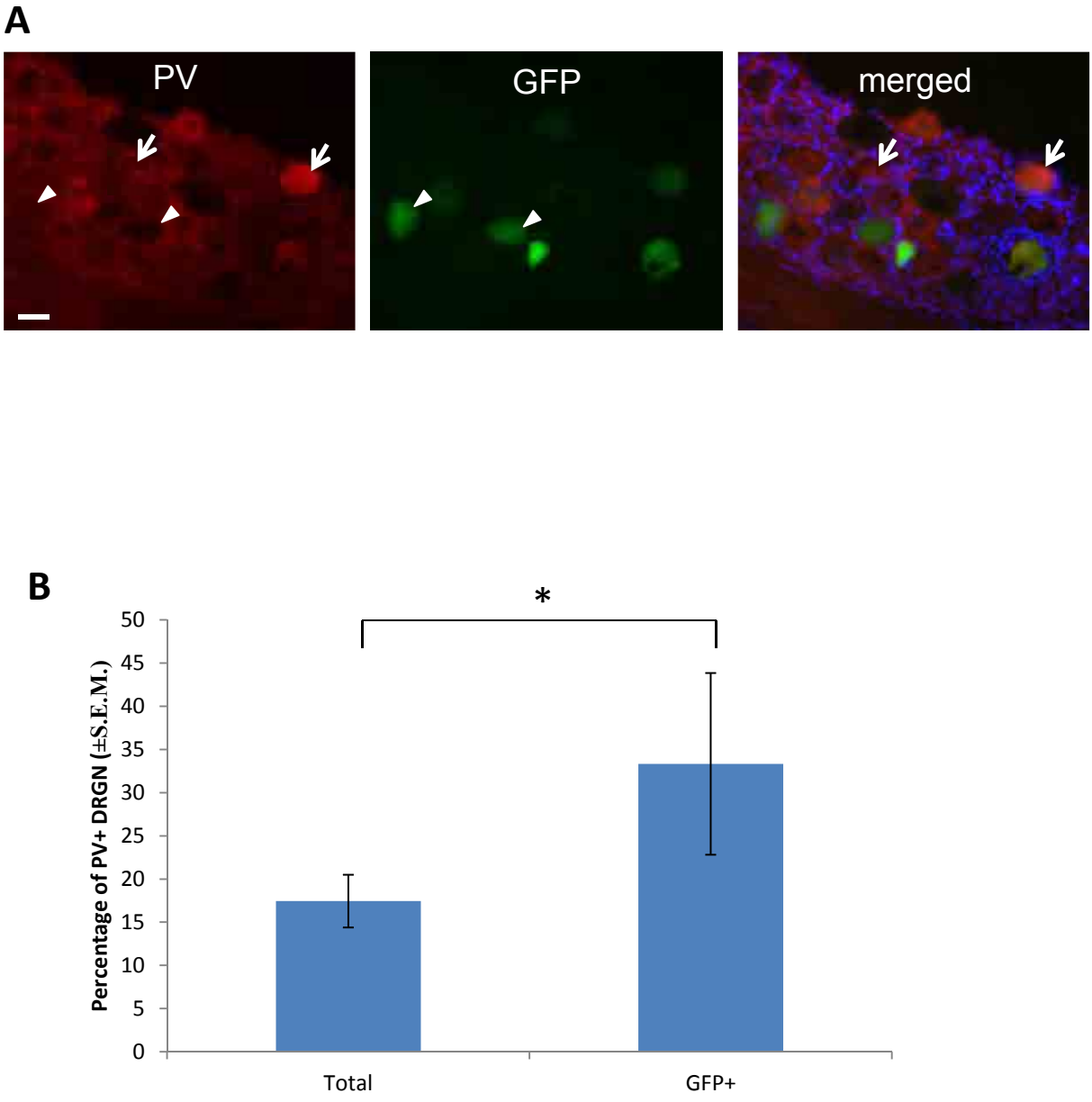


**Figure 4.3** Proportion of GFP$^+$/parvalbumin$^+$ DRGN after intrathecal injection. **A**. Expression of parvalbumin in GFP- (arrows) and GFP+ (arrowheads) DRGN. **B.** Proportion (%) of total parvalbumin+ DRGN compared with parvalbumin+/GFP+ DRGN after intrathecal injection; (t-test; p=0.046, n=3)

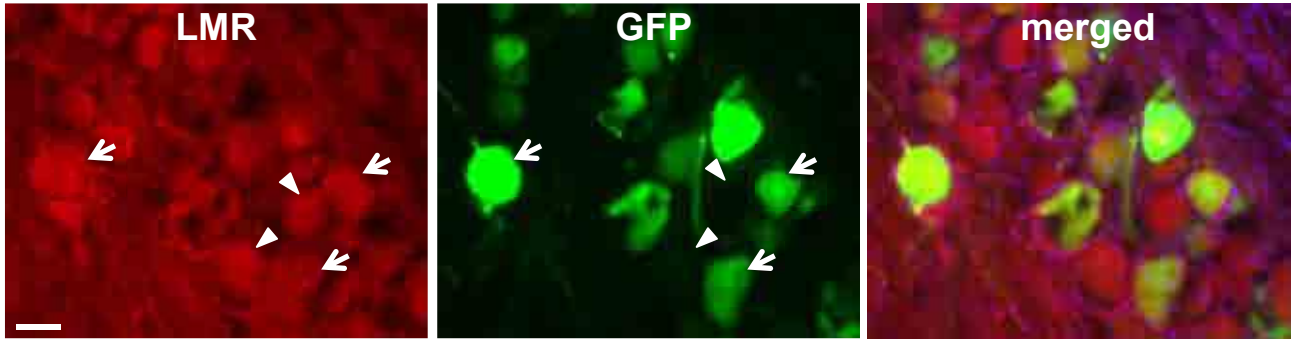


**Figure 4.4** 67 kDa laminin receptor expression in the DRG. Both GFP+ (arrows) and GFP- (arrowheads) DRGN expressed the LMR. Scale bar 50μm.

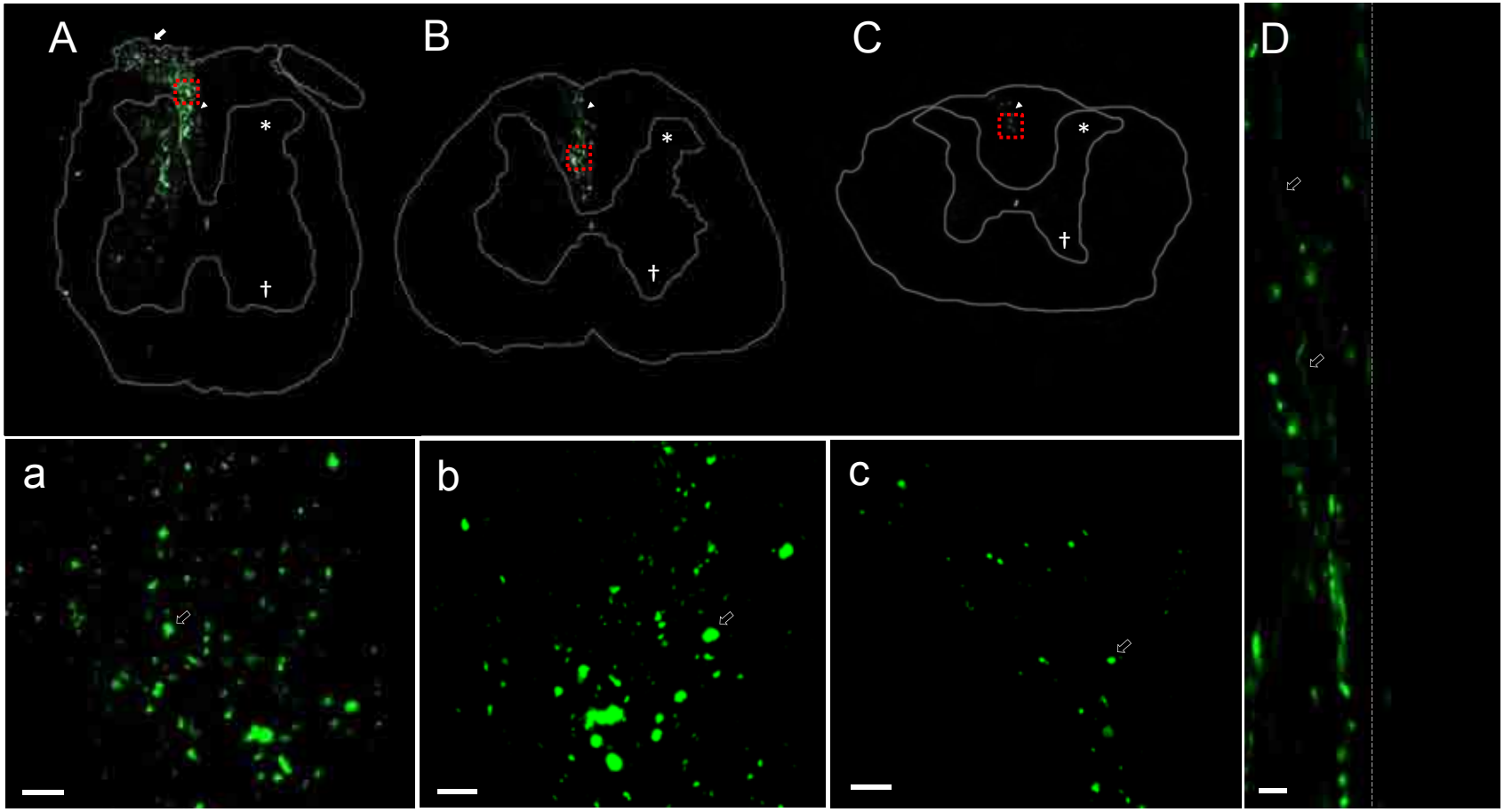


**Figure 4.5** The central projections of DRGN in the left gracile fasciculus were clearly labelled by GFP. **A**. L4 dorsal root entry zone; **B**. Rostral lumbar cord; **C**. Mid-thoracic cord (not to scale, composed of merged fields at 100X magnification). **D**. Longitudinal section of the rostral lumbar cord (dashed line represents dorsal median sulcus). **a-c** refer to insets demonstrated by the red boxes in **A**, **B** and **C**, respectively. DREZ=solid arrow; gracile fasciculus=arrow heads; GFP+ axons=open arrows; dorsal horn=asterisks; ventral horn=daggers. Scale bar 50μm.

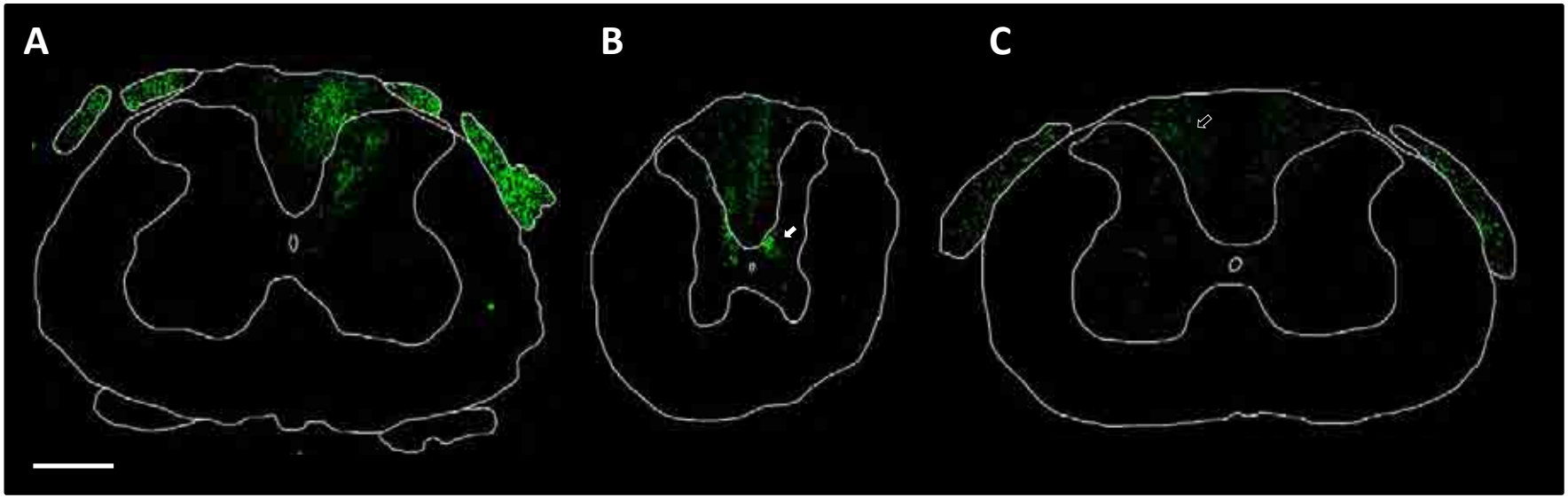


**Figure 4.6** The central projections of DRGN were clearly labelled with GFP after IT injection. **A**. Rostral lumbar cord. **B**. Mid-thoracic cord. **C**. Mid-cervical cord. Clarke's column=solid arrows; cuneate fasciculus=open arrows. Scale bar 500μm.

Clarke's column clearly defined in the latter. The intensity of labelling in the gracile fasciculus diminished in successively rostral segments, and very little was observed in the cervical cord (Figure 4.6 C).

### 4.2.5 Preferential transduction of large diameter DRGN is lost *in vitro*

At a multiplicity of infection (MOI) of 2 x $10^{10}$, 18.20% (S.E.M. 0.70%) of DRGN were GFP+. The lack of any significant shift in the size distribution of GFP+ DRGN compared with total DRGN demonstrated that there was no preferential targeting of DRGN by $AAV8_{gfp}$ *in vitro* (Figure 4.7 A. Mann-Whitney U; p=0.628). Furthermore, there was no significant difference in the survival of DRGN in cultures exposed to $AAV8_{gfp}$ compared with those exposed to PBS (Figure 4.7 B. t-test; p=0.744). In culture, GFP+ DRGN appeared grossly normal, with neuritic trees extensively filled with GFP (Figure 4.7 Ci). Additionally, Schwann cells (appearing fusiform *in vitro*) were also seen to be transduced in DRG cultures (Figure 4.7 Cii).

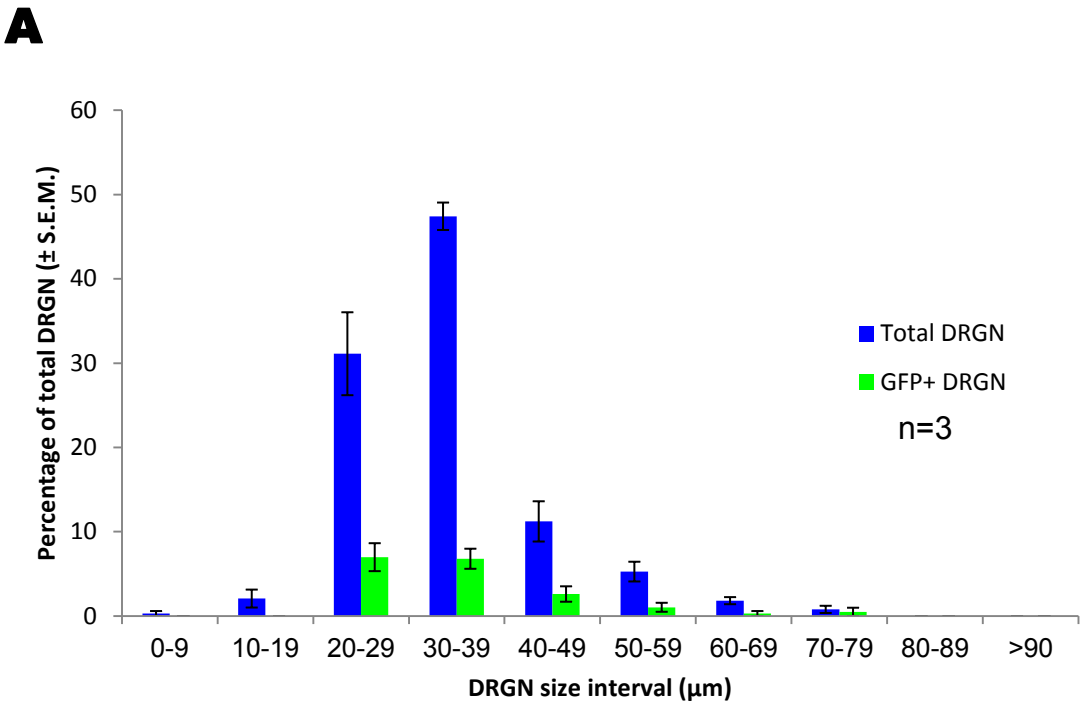


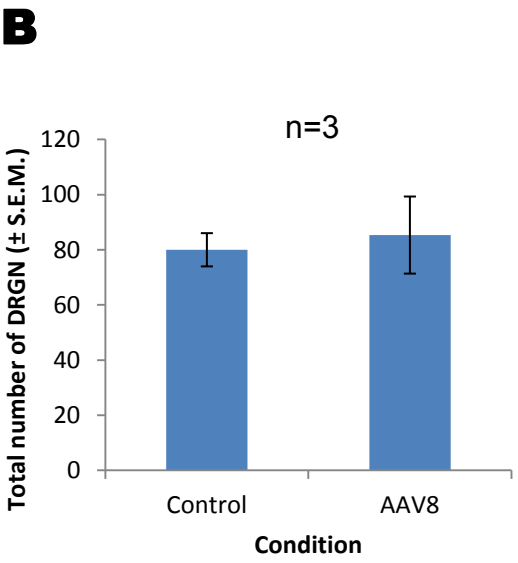


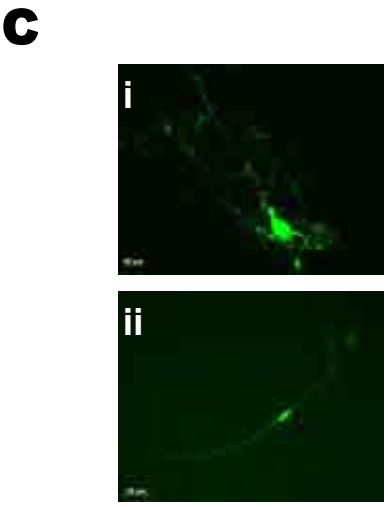


**Figure 4.7** Cellular tropism of AAV8$_{gfp}$ *in vitro*. **A.** Histogram showing the size distribution of all DRGN and GFP+ DRGN at an MOI of 2 x $10^{10}$. There was no significant difference between the distributions for total DRGN and GFP+ DRGN (Mann-Whitney U; p=0.628). **B.** Histogram showing survival counts of DRGN in cultures exposed to AAV8$_{gfp}$ or PBS as control. There was no significant difference between the two groups (t-test; p=0.744). **C.** The appearance of a large diameter GFP+ DRGN *in vitro* (**i**). Note the labelling of the neuritic tree. Targeting *in vitro* was much less specific than *in vivo*, with many transduced Schwann cells present in culture (**ii**).

# Discussion

### 4.3.1 DRGN transduced with AAV8$_{gfp}$ did not die

Although not definitive, the correspondence between the size distribution data from this study and other published accounts suggests that there was no DRGN death after both intra-DRG and intrathecal delivery AAV8$_{gfp}$ (McLachlan, Janig et al. 1993). These observations are further backed up by the lack of toxicity observed *in vitro*, where an extremely high multiplicity of infection (MOI) was employed. No evidence of gross damage was observed in the DRG after either delivery method, an observation in agreement with Mason (2010) who compared AAV gene delivery in the DRG across serotypes (Mason, Ehlert et al. 2010). There was no evidence of Wallerian degeneration in the dorsal columns.

The above findings are extremely interesting, given that neuronal death does occur when *gfp* is delivered to the CNS under the control of the CMV promoter (Klein, Dayton et al. 2006). In Klein's study, toxicity attributable to AAV8 was excluded by showing no detrimental effects of an empty AAV8 vector. Thus GFP may be less toxic to neurones of the PNS compared with those of the CNS since no cell death was observed in the DRG. However, it must be emphasised that stereological techniques were not used to establish definitive counts of surviving DRGN. See Chapter 5 for a more in-depth discussion of toxicity related to AAV8$_{gfp}$.

### 4.3.2 AAV8 targeted predominantly large diameter proprioceptive DRGN *in vivo* but not *in vitro*

Size distributions of adult rat DRGN reported in the literature correlate closely with the results from this study, with a positively skewed distribution and modal diameter

of ~30μm (Natalie, William et al. 2002; Gaudet, Williams et al. 2004; Lu, Zhang et al. 2006). Similar distributions have been reported in studies examining cell profile areas after a simple square root transformation of the data (Jamieson, Liu et al. 2005). Here, the first detailed comparison of the cellular tropism of AAV8 after intra-DRG and intrathecal injection is presented, which supports the assertion of preferential transduction by AAV8 of proprioceptive sensory neurones. These neurones are large diameter, LMR+, PV+ DRGN with central projections in the dorsal root, ventral and dorsal horn, and dorsal columns where axons terminate in Clarke's column to be relayed in the dorsal spinocerebellar tract. The diminution of dorsal column GFP labelling in successively rostral cord segments after intra-DRG injection is consistent with GFP+ axons leaving the dorsal column and terminating in the deep dorsal horn, predominantly Clarke's column in the thoracic and rostral lumbar cord. Given its tropism for large diameter, proprioceptive DRGN, AAV8 holds much promise for therapies directed at regaining locomotor function after SCI, since an essential factor for a normal gait is proprioceptive input to the spinal cord and brain which may be restored by therapies delivered using AAV8 vectors.

The mechanism of preferential transduction of large diameter DRGN by AAV8 is not known. Interaction of AAV8 with receptors differentially displayed on specific size classes of DRGN could explain the differential transduction of DRGN observed. The archetypal AAV serotype (AAV2) enters cells by exploitation of the heparan sulphate proteoglycans, integrins and fibroblast growth factor receptors (Goncalves 2005) and AAV8 transduces mouse hepatocytes *in vivo* after binding LMR (Akache, Grimm et al. 2006). However, this study failed to observe any relationship between the

expression pattern of laminin receptor and the transduction efficiency of AAV8, suggesting that laminin receptor is not necessary or sufficient for DRGN transduction by AAV8. The finding that preferential targeting of DRGN by AAV8 is lost *in vitro* has some interesting possible explanations. One compelling idea, consistent with what is already known about AAV in general, is that the ECM has a role in transduction of DRGN. *In vitro*, the ECM will be considerably different to that seen *in vivo*, possible leading to deficiency of ECM components necessary for transduction of large diameter DRGN by AAV8. However, the results of the *in vitro* experiment described must be interpreted carefully due to the high dose of AAV8 used. Such high concentrations of vector could possibly overcome a putative 'threshold' level for smaller diameter DRGN leading to the result obtained, although if this were true then one may just see even higher levels of transduction of large diameter DRGN than seen *in vivo*.

AAV8 based vectors are useful to research groups using the dorsal column injury model, since many of the axons comprising the dorsal column project from large diameter DRGN. The exclusion of small diameter DRGN as AAV8 targets would reduce the incidence of NGF-induced lowered pain thresholds after AAV8$_{ngf}$ therapeutic delivery (Dyck, Peroutka et al. 1997). Moreover, intracerebro-ventricular delivery of NGF stimulates sympathetic axon sprouting within DRG, which could also contribute to neuropathic pain (Nauta, Wehman et al. 1999).

An assessment of viral vector neuronal tropism is also important in the selection CNS injury models for gene therapy treatments. For example, mid-thoracic (T8) cord

transections are commonly used to evaluate the success of gene based therapeutics delivered to L4/L5 DRG in axon regeneration studies (Gonzalez, Berry et al. 2006). However, given that almost 50% of AAV8-transduced DRGN are PV+, whose dorsal column projections terminate in the caudal half of Clarke's column (LaMotte, Kapadia et al. 1991), a T8 lesion would fail to transect proprioceptive axons from L4/L5 DRG; a lesion placed more caudally (i.e., at L1) would be required to transect GFP+ proprioceptive axons in this paradigm (see Figure 2.3).

### 4.3.3 AAV8$_{gfp}$ transduces DRGN via the CSF

The transduction rate of DRGN after intrathecal delivery was low, and comparable to that seen in other reports (Vulchanova, Schuster et al. 2010).

Delivery of AAV8 successfully transduces neurones (Klein, Dayton et al. 2006) in, for example: (1), multiple brain regions including neocortex and striatum after intra-cerebral ventricular injection (Broekman, Comer et al. 2006); (2), the cord after intrathecal injection (Storek, Reinhardt et al. 2008); and (3), in DRG where DRGN become transduced after intramuscular (Zheng, Qiao et al. 2009), intravenous, and intraperitoneal injections Foust, 2008 #266}. These and our findings are consistent with AAV8 being unable to cross the ependyma, pia and blood-brain barriers.

The routes of access of AAV8 to DRG from the CSF are unknown, although diffusion across the arachnoid membrane is most likely since epidurally delivered HRP quickly enters DRG, probably by direct diffusion (Byrod, Rydevik et al. 2000). Diffusion may be facilitated at portals of entry where CSF and DRG neuropil are in continuity at: (1),

the DREZ where a sleeve of the relatively impermeable dorsal root sheath is open (Haller, Haller et al. 1972); and (2), the 'lateral arachnoid recess' of the DRG (an evagination of the arachnoid, usually filled with macrophages) (Himango and Low 1971). It is likely that, after intra-DRG injection of AAV8, these portals allow the egress of the vector into the CSF accounting for occasional transduction of DRGN in contralateral uninjected DRG.

The failure of the second intrathecal injection experiment where a pulled glass micropipette was used instead of a 25G needle is puzzling. An identical amount of AAV8 $_{gfp}$ was injected and confirmation of injection to the subarachnoid space was made by observation of CSF entering the glass capillary tube. Animals made an unremarkable recovery, and the dissected tissues (DRG, dorsal roots and cords) appeared no different from tissues from animals from the previous experiment. Two possible explanations arise: experimental error or some essential difference between injection with a metal needle compared with injection using a glass micropipette.

Experimental error seems unlikely in this case, since the author made up the appropriate dilution of AAV8 $_{gfp}$ in two batches on two separate days. These dilutions were, however, made using the same batch of undiluted virus. To determine if the original viral batch was active, some of this was applied to COS-1 cells *in vitro*. From 1-2 days post inoculation, COS-1 cells were seen to be GFP+ although no comparison was made with a 'gold-standard' batch of virus.

The second possible explanation could be that there is something about intrathecal injection using a metal needle that facilitates transduction of DRGN or something about injection using a glass micropipette that inhibits transduction. It is certain that needle injection is more traumatic to the animal than when using a glass micropipette. Both injections employ the same surgical approach, but the needle is advanced much further into the lumbar cistern than the glass micropipette. Much of the CSF refluxing into the needle cup was blood-stained compared with almost none of the CSF entering the glass micropipette. Perhaps trauma and/or subarachnoid haemorrhage facilitate transduction of DRGN by AAV8 $_{gfp}$? A study by Murata et al. showed that peri-DRG inflammation induced by application of nucleus pulposus led to increased permeability of the DRG capsule (Murata, Rydevik et al. 2005). Nucleus pulposus, the jelly-like material forming the core of intervertebral discs, is a commonly used pro-inflammatory substance injected into the tissues around the DRG. It is feasible that the use of a needle to inject AAV8$_{gfp}$ intrathecally could have led to inadvertent rupture of intervertebral discs, particularly because one of the signs of successful injection was a tail-flick caused by contact of the needle with ventral roots which lie close to the dorsal aspect of the intervertebral discs. Also, it is possible that the presence of blood in the CSF has similar pro-inflammatory effects to nucleus pulposus.

A second possibility is that the presence of blood within the CSF after needle injection could have sealed off the hole created in the meninges, inhibiting egress of the virus from the CSF into surrounding tissues. The lack of bleeding after glass micropipette injection may have left a hole in the meninges that did not seal. This

seems an unlikely explanation, since the glass micropipette was left *in situ* for around 10s after injection, to allow the injectate to distribute within the CSF. Also, one would expect *some* transduction since the probability of egress of all of the viral particles injected seems highly unlikely.

Additionally, there are potential technical issues surrounding the use of glass micropipettes, such as the possibility of AAV8 particles binding to the glass itself (Ann Logan, personal communication). However, this seems unlikely as an explanation here since glass micropipettes were used to perform intra-DRG injections which were successful.

### 4.3.4 Can the predilection of AAV8 for large DRGN be explained by the data presented above?

The evidence for AAV8 showing a preference for transducing large diameter DRGN is strong. That this phenomenology exists and can be replicated in a number of different delivery paradigms shows that it has great potential in a clinical setting. However, the question of *how* AAV8 does this remains a pertinent one from both the point of view of the basic scientist and that of the clinician who may wish to pseudotype other vectors to confer upon them a tropism for large DRGN. The mechanism of the cellular tropism described could be explained under one (or more) of the following headings: physical, chemical and artefactual.

Two major physical mechanisms that could have roles with respect to AAV8 and DRGN are surface area and volume. If it is assumed that in 100 DRGN within an hypothetical DRG, 20 are large diameter (say 60μm) and 80 are small diameter (say

10μm), then some simple calculations reveal that, despite the fact that the large diameter DRGN are in the minority, they actually possess some 90% of the surface area and 98% of the volume of the ganglion as a whole (excluding gaps between cells). Hence it would appear that there is a very simple explanation for the observed cellular tropism. However, closer inspection of the data reveals that surface area is unlikely to be solely responsible, since one would predict an exponential relationship between DRGN diameter and frequency of GFP+ DRGN as opposed to the observed normal distribution of GFP+ DRGN diameters. Furthermore, it is likely that surface area to volume ratio is a more valid physical parameter than either measure alone. Within the parameters set out above, small diameter DRGN are seen to have surface area to volume ratios around 6 times greater than larger cells – so this would predict that smaller DRGN should be preferentially transduced. Hence, it seems unlikely that physical factors are solely responsible for the cellular tropism seen.

Probably the most likely explanation for the observed cellular tropism of AAV8 is the presence of specific surface molecules on a sub-population of DRGN that facilitate viral entry. The expression of such molecules is likely to be normally distributed on a particular subset of cells, which would explain the normal distribution of diameters of GFP+ DRGN. It is already known that one receptor exploited by AAV8 to transduce hepatocytes is LMR (Akache, Grimm et al. 2006), although a defining role for this has been excluded in this study since all DRGN were found to be LMR+. It must be emphasised, however, that this finding was qualitative – no quantification of LMR expression was performed, which may have revealed a small but statistically significant effect. Also, since histochemical detection of LMR in the DRG is novel, it

would have been ideal to fully validate the findings (see below in further work). Other, yet to be discovered, molecules are likely to be exploited by AAV8 to enter DRGN. This study has highlighted the potentially important role of ECM components in AAV8 transduction.

Finally, the contribution of experimental artefacts to the results obtained must be considered. The term 'artefact' describes an uncontrolled factor in an experiment, usually in the tissue processing, data capture and analysis stages. Great care was taken to ensure that tissue distortion during sample preparation and cryostat sectioning was minimised by examining selected sections under phase contrast microscopy to ensure that DRGN cell bodies were not artefactually distorted. Tissue blocks and sections were always stored appropriately and in the same conditions for all groups. Micrographs were taken using identical exposure settings where appropriate, and sections were stored in the dark to minimise bleaching of GFP. DRGN were counted using strict criteria by one experienced individual, described in Chapter 2.

Artefacts arising from technical factors are generally easier to control for than those due to unforeseen effects of an agent. In the experiments described above, it has already been noted that there was no formal assessment of DRGN survival *in vivo*. This deficiency is due to lack of experience of the author with stereological techniques and lack of time to become trained in these methods. It would have taken the author a number of months to become sufficiently competent in the theory and practice of stereological methods necessary for this study, and a lack of time prevented this. The specific problems caused by lack of survival data could include:

(i) AAV8$_{gfp}$ may have transduced small diameter DRGN, but these neurones may be highly susceptible to GFP toxicity. Their death would have led to an apparent shift in the GFP+ DRGN size distribution; (ii) AAV8 $_{gfp}$ may enter DRGN with large surface areas, but these cells may have died due to high viral loads, giving the appearance of a normally distributed GFP+ DRGN population, or (iii) some other, more subtle factor due to the inflammatory response in the DRG to AAV8 $_{gfp}$ inoculation may be at play, altering the size distribution of total DRGN. Furthermore, it may be possible that GFP+ DRGN are swollen by an as yet unidentified effect of GFP, although this seems unlikely since the central projections of these cells are consistent with large diameter DRGN. See Chapter 5 for more detail on inflammatory responses due to AAV8 $_{gfp}$.

### 4.4 Further work

The elucidation of molecular mechanisms determining the tropism of viral vectors is a growing and fruitful field. Identification of the ways in which viruses enter cells in order to transduce them allows one to pseudotype other viruses, thus targeting them to a cell of interest. Additionally, one may be able to increase the transducibility of cells that are refractory to viral transduction (e.g. by ECM manipulation). The work presented here is primarily phenomenological, showing that AAV8 is capable of preferentially transducing a particular sub-population of DRGN. However, if the precise mechanism of this phenomenon is to be found then more detailed experimental work must be undertaken.

### *Dose-response studies*

Due to constraints on time and resources, various doses of AAV8 were not use *in vitro* or *in vivo*. Such studies are necessary in order to find the optimum dose of AAV8 that gives the maximal transduction with minimal toxicity. It may be the case that the transduction rates of different sub-populations of DRGN are different at different doses of AAV8. Also, if a lower dose was found to give equivalent transduction rates as higher doses this would be preferred on both economical and ethical grounds.

### *Stereological assessment of DRGN death*

Due to reasons described above, it is necessary to accurately quantify DRGN survival after injection of AAV8. Without this, one cannot be fully convinced that the results shown were not confounded by toxicity.

### *The use of a labelled AAV8 particle*

In order to follow the route which AAV8 takes in order to access DRGN, it would be interesting to add a tag to the viral capsid (e.g. GFP or other fluorophore). This tagged virus could be injected and animals sacrificed at different time-points (short (minutes to days), medium (days to weeks) and long-term (weeks to months)) to see where the particles have travelled.

### *Studies to identify the molecular events in AAV8 transduction*

This study showed qualitatively that LMR has no role in transduction of DRGN by AAV8. Further, quantitative studies must be performed in order to confirm this and to show if any other molecules have a role to play. The methodology used to quantify parvalbumin expression could be used for other candidates (e.g. integrins). If a candidate was found, its role could be further confirmed by injecting AAV8 into the DRG alongside an antibody to the candidate molecule. It would be predicted that the antibody would lead to lower DRGN transduction rates compared to control injections using a neutral antibody (e.g. anti-GFP).

# Chapter 5

# Inflammatory and glial responses to AAV8-mediated transgene delivery

# Introduction

An important step that should ideally be included in the validation of viral vectors for gene therapy is the evaluation of immunological responses to (i), the vector particle itself and (ii), the transgene product that is to be delivered. This is vital not only from the point of view of translation into humans, but also with respect to experimental confounding – an issue that will be discussed below.

### 5.1.1 Basic immunology – a brief review

The mammalian immune system consists of a complex, interacting network of cellular and biochemical defences. The reader is referred to the excellent textbook by Murphy et al. for further information on generic aspects of immunology (Murphy, Travers et al. 2008). Unless an additional citation is provided, Murphy et al. was the source for the rest of this section.

One must consider immune responses both with respect to the mechanism of the response and the tissue in which the response is occurring. The immune system has two major ways in which it is able to deal with pathogens or other tissue insults (for the purposes of this section, AAV8 can be considered a 'pathogen' even though the wild-type virus has no known role in disease). A response can either be innate or adaptive, and each of these contains humoral and cellular elements. The innate immune response has ancient origins, and is found in most animals. It is able to act rapidly, in a non-specific way to clear pathogens or tissue debris. Humoral components of the innate immune system include complement (a protein network capable of binding to pathogens, marking them for destruction by cellular elements) and lytic enzymes such as lysozyme. Cellular elements of the innate immune system

include macrophages, neutrophils and mast cells. These cells are able to react to insults non-specifically by phagocytosing pathogens or tissue debris or releasing cytokines that serve to augment the response.

Components of the innate immune response are usually the first to arrive at the onset of an insult. They rapidly clear any pathogenic material, but their effects are relatively short-lived and they have no memory of previous insults. Adaptive immunity is required for a longer term response which is capable of being re-activated at short notice in the future by the same pathogen (immunological memory). As with innate immunity, the adaptive immune system consists of cellular and humoral elements. The major cellular elements include B-cells, T-cells and antigen presenting cells (APC). Adaptive immune responses are initiated by an APC phagocytosing an antigen, processing it and presenting it in a suitable form on its cell surface. Cells that behave as APCs include macrophages and B-cells, which present fragments of pathogen-derived antigen on the major histocompatibility complex class II molecule (MHCII).

Macrophages bind antigen *via* molecules expressed on their cell surface such as scavenger receptors (e.g. CD68). These receptors are non-specific and bind to a wide range of pathogenic material. B-cells are coated with a specific immunoglobulin (the B-cell receptor) which binds a single, specific antigen. Binding of antigen to either scavenger receptors or B-cell receptor leads to endocytosis of the resulting complex and intracellular proteolytic degradation. The resulting peptide fragments are loaded onto MHCII and displayed on the surface of the macrophage or B-cell.

APCs displaying antigen fragments on MHCII travel to lymph nodes where they are able to encounter T-helper cells, which recognise single, specific antigen fragments. Binding of the T-cell receptor to the displayed antigen fragment on a macrophage or B-cell leads to clonal expansion of the T cell (including production of some memory T-cells, primed for future insults) and a further cascade of events depending upon the APC. Activation of macrophages by T-helper cells leads to the release of macrophage activating signals such as interferon-ɣ (IFN-ɣ) that attract macrophages and augment their phagocytic abilities (including up-regulation of scavenger receptors). Activation of B-cells by T-helper cells leads to clonal expansion of the B-cell into a plasma cell population (cells which produce antibody – basically a soluble form of the B-cell receptor) and a memory B-cell population.

The pathways described above are effective in dealing with extracellular pathogens such as bacteria, which are bound by antibodies and cleared by phagocytes. Viruses pose a different challenge to the immune system, in that they are present *within* cells for a large part of their life-cycles. The immune system is capable of repelling viral attacks thanks to the presence of so-called cytotoxic T-cells. Most cells in the body (except neurones, see below) express the major histocompatibility complex class I molecule (MHCI). Much like MHCII, MHCI displays small peptides derived from antigens. The source of the antigens for MHCI is intracellular proteins that have been degraded by the proteasome, an intracellular proteolytic complex. The proteasome degrades most endogenous proteins, the resulting fragments of which are loaded onto MHCI and lead to no immune response. Exogenous intracellular proteins, such as those derived from viruses being manufactured within the cell, are

also expressed on MHCI. Cytotoxic T-cells bind MHCI and will kill the cell if it is displaying foreign proteins. Such cell killing will serve to halt the production of virus within that cell and so curb an infection.

### 5.1.2 The concept of immunological privilege

The events described above occur in most body regions that are accessible to the immune system. Certain tissues, however, have a specialised milieu that is capable of regulating (usually attenuating) the immune response that occurs following an insult. The classic model of immunological privilege arose from skin grafting experiments into the brain, performed by Medawar (Medawar 1948). In these experiments, Medawar noted that the implantation of a piece of skin from one animal into the brain of another failed to elicit an immune response. However, if skin was implanted into the brain and into the skin, an immune response to the skin within the brain was seen. The interpretation of these findings was that the brain was capable of being the recipient of an immune response (i.e. it had an efferent arm) but could not initiate an immune response itself (i.e. it did not have an afferent arm). An interpretation of these findings was that the BBB was regulating the activity of the immune response in the brain. The work of Medawar and many others both before and after him led to the formation of a number of erroneous interpretations about the properties of the BBB, many of which persist today (Bechmann, Galea et al. 2007). It is probably best to consider the CNS not as being devoid of an immune response, but as regulating inflammatory responses in such a way that damage to its precious neurones is minimised. The reader is reminded that frequently immune responses

are destructive, often leading to the death of many cells (consider the role of cytotoxic T cells in viral infections, see above).

Much less is known about the immune status of the PNS than the CNS. What can be said is that there is a blood-nerve barrier similar to that seen in the CNS, but probably not as 'hermetic' (Kieseier, Hartung et al. 2006). Most of what is known about PNS neuroimmunology comes from clinical studies or those using mice induced to develop so-called experimental acute neuritis. There is a paucity of reports examining the basic immunological processes occurring within PNS. One interesting feature of the PNS, however, is the relatively permeable environment of the DRG compared to peripheral nerves and roots. After injection of fluorescein, a small fluorescent molecule by routes including intravenous and intrathecal, the DRG was seen to contain a large amount of fluorescence whereas the sciatic nerve had minimal signal (Abram, Yi et al. 2006). The results of this experiment and a previous report using HRP support the idea that the DRG has permeable vessels, and is likely to be freely patrolled by elements of the immune system (Byrod, Rydevik et al. 2000). However, there are still many unknowns concerning PNS immunology, not least being the lack of data concerning lymphatic drainage of peripheral nerves and the DRG.

### 5.1.3 Why look for inflammatory responses to gene therapy vectors?

It must be stressed that the experiments described hereafter were not performed from a purely esoteric point of view. There are sound biological reasons why inflammatory responses to therapies need to be elucidated, particularly in the field of

CNS axon regeneration. The experiments employing injection of AAV8$_{gfp}$ were the necessary prequel to subsequent studies looking at the effect in animals receiving DC lesions of AAV8 vectors containing *nt-3* and/or shRNA$_{RhoA}$ (see Chapters 3 and 6).

The significance of inflammation in the study of spinal cord injury is a subject of much controversy (Chan 2008). Clearly, without inflammatory responses elements such as the glial scar would be unlikely to form. However, there is also a large body of evidence pointing to the ability of inflammation to stimulate axon regeneration. For example, it has been shown that initiation of an inflammatory response in the DRG can augment regeneration of DRGN central projections in the dorsal root (Lu and Richardson 1991). Conditioning lesions have some inflammatory features, and it is well documented that previous sciatic nerve injury can improve axon regeneration in the subsequently lesioned DC (Neumann and Woolf 1999). Furthermore, injection of pro-inflammatory molecules such as zymosan into the vitreous chamber of the eye leads to robust axon regeneration in the crushed optic nerve (Ahmed, Aslam et al. 2010). It seems from these data that inflammation at or near the cell body of a neurone can increase its regenerative capacity. Of course, this is beneficial and opens many avenues for therapies. However, it is a possibility that inflammation can be introduced into experiments as a consequence of viral vector delivery. This has the potential to confound experiments, particularly if the inflammatory characteristics of, say, the experimental viruses have not previously been examined in comparison to a control virus.

#### 5.1.4.1 Specific hypotheses

- The delivery of AAV8$_{gfp}$ does not lead to an appreciable inflammatory response after either intra-DRG or intrathecal injection
- The delivery of AAV8$_{gfp}$ does not lead to an appreciable change in the level of CNS glial activation after either intra-DRG or intrathecal injection
- The delivery of AAV8$_{gfp}$ does not lead to degeneration of DRGN central projections

#### 5.1.4.2 Specific aims

- To assess the inflammatory response in the DRG to intra-DRG and intrathecal injection of AAV8$_{gfp}$ compared with injection of PBS alone. Specifically, the responses of macrophages and satellite cells will be assessed using immunohistochemistry
- To assess the levels of microglial and astrocytic activation in various regions of the rostral lumbar spinal cord after intra-DRG and intrathecal injection of AAV8$_{gfp}$ using immunohistochemistry and image analysis
- To assess whether there is Wallerian degeneration of DRGN central projections in the DC after intra-DRG injection of AAV8$_{gfp}$ using Oil Red O staining

### 5.1.5 Brief description of methods

The tissue obtained from the animals used in the experiment described in Chapter 4 were analysed for evidence of glial activation and inflammatory responses. To re-iterate, a total of 18 animals (200-220g) were used in this study: 6 intra-DRG

injection of AAV8$_{gfp}$; 3 intra-DRG injection of PBS; 3 intrathecal injection of AAV8$_{gfp}$; 3 intrathecal injection of PBS; and 3 uninjected rats comprised controls.

The six animals receiving intra-DRG PBS or AAV8$_{gfp}$ received injections of 10µl PBS alone or $10^{10}$ vg in 10µl PBS to the left L4/L5 DRG using a glass micropipette inserted into the DRG under direct vision, and were sacrificed 28d later. Animals undergoing intrathecal injections received either 30µl PBS alone or $10^{12}$ vg AAV8$_{gfp}$ in 30µl PBS using a 25G needle inserted into the subarachnoid space in the lumbar spine.

The presence of inflammatory and glial cells in DRG and cord sections was assessed using standard immunohistochemical techniques. Glial (astrocytic and microglial) activation was quantified by taking photomicrographs of various regions white and grey matter in the rostral lumbar cord, using an exposure time that yielded no background in tissue from uninjected animals. A pixel-counting methodology was applied to fields of view taken from the various regions in animals injected with PBS and AAV8, allowing assessment of the level of glial activation.

# Results

### 5.2.1 Macrophages infiltrated the DRG after both intra-DRG and intrathecal delivery and satellite cells upregulated expression of CD68

The DRG from control, uninjected animals contained sparse $CD68^+$ macrophages, in contrast to DRG from animals receiving intrathecal PBS, where a few macrophages could be seen (Figure 5.1A). Intra-DRG (Figure 5.2) and intrathecal (Figure 5.1) injection of $AAV8_{gfp}$ resulted in high levels of $CD68^+$ immunoreactivity in the DRG, within morphologically identified haematogenous macrophages and satellite cells. Macrophages were not seen to enter the spinal cord after intrathecal injection of PBS or $AAV8_{gfp}$, their presence ending abruptly at the DREZ (Figure 5.3 C).

### 5.2.2 Microglia and astrocyte activation after $AAV8_{gfp}$ injection

After intra-DRG injection of $AAV8_{gfp}$, CD11b (a microglial marker) immunoreactivity in the ipsilateral deep dorsal horn was upregulated compared with PBS injected animals (t-test with Bonferroni correction (alpha=0.0083). p=0.0018; Fig. 5.4). Interestingly, there appeared to be a trend towards a reciprocal decrease in CD11b staining in white matter compared to grey matter. After intrathecal injection of either PBS, or $AAV8_{gfp}$, microglial activation in the cord was qualitatively no different from that of uninjected rats (Figure 5.5). A spatial correlation was observed between the presence of $AAV8_{gfp}$ within grey matter projection areas of the cord (such as Clarke's column) and CD11b expression.

Compared to intra-DRG PBS injected controls, after $AAV8_{gfp}$ delivery there was a quantitative increase in astrocyte activation in the rostral lumbar cord in all regions

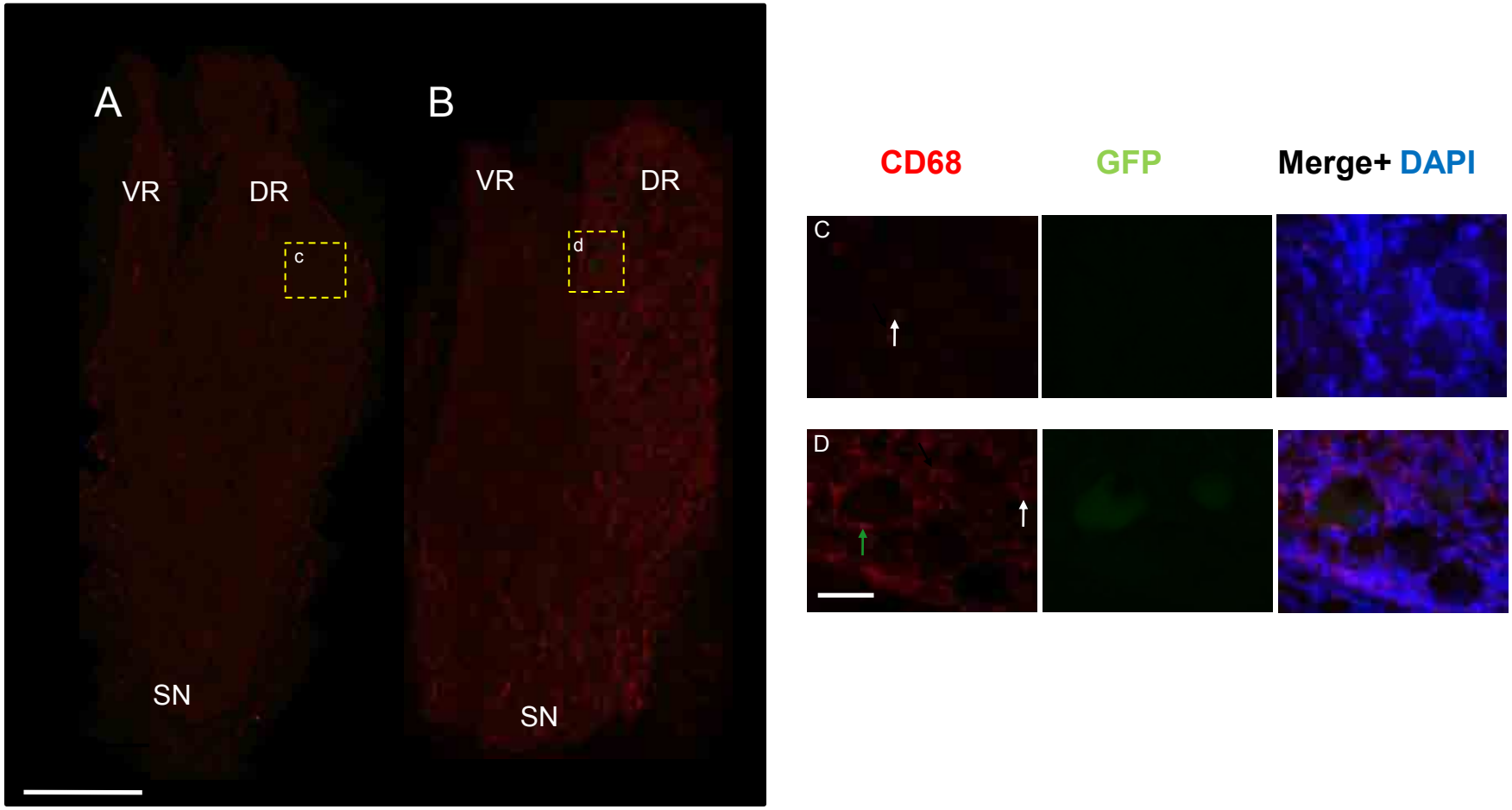


**Figure 5.1** CD68 staining in DRG sections from (A) intrathecal PBS injected controls and (B) intrathecal AAV8$_{gfp}$ injected animals. There is an increase in the number of CD68$^{+}$ macrophages (white arrows) in DRG from AAV8$_{gfp}$ injected animals (D) compared to control (C). Morphologically identified CD68$^{+}$ satellite cells (green arrow) are also present in the DRG from AAV8$_{gfp}$ injected animals. SN = spinal nerve, DR = dorsal root, VR = ventral root. Scale bar for composites (**A**+**B**) = 500μm. Scale bar for individual images (**C**+**D**) = 50μm.

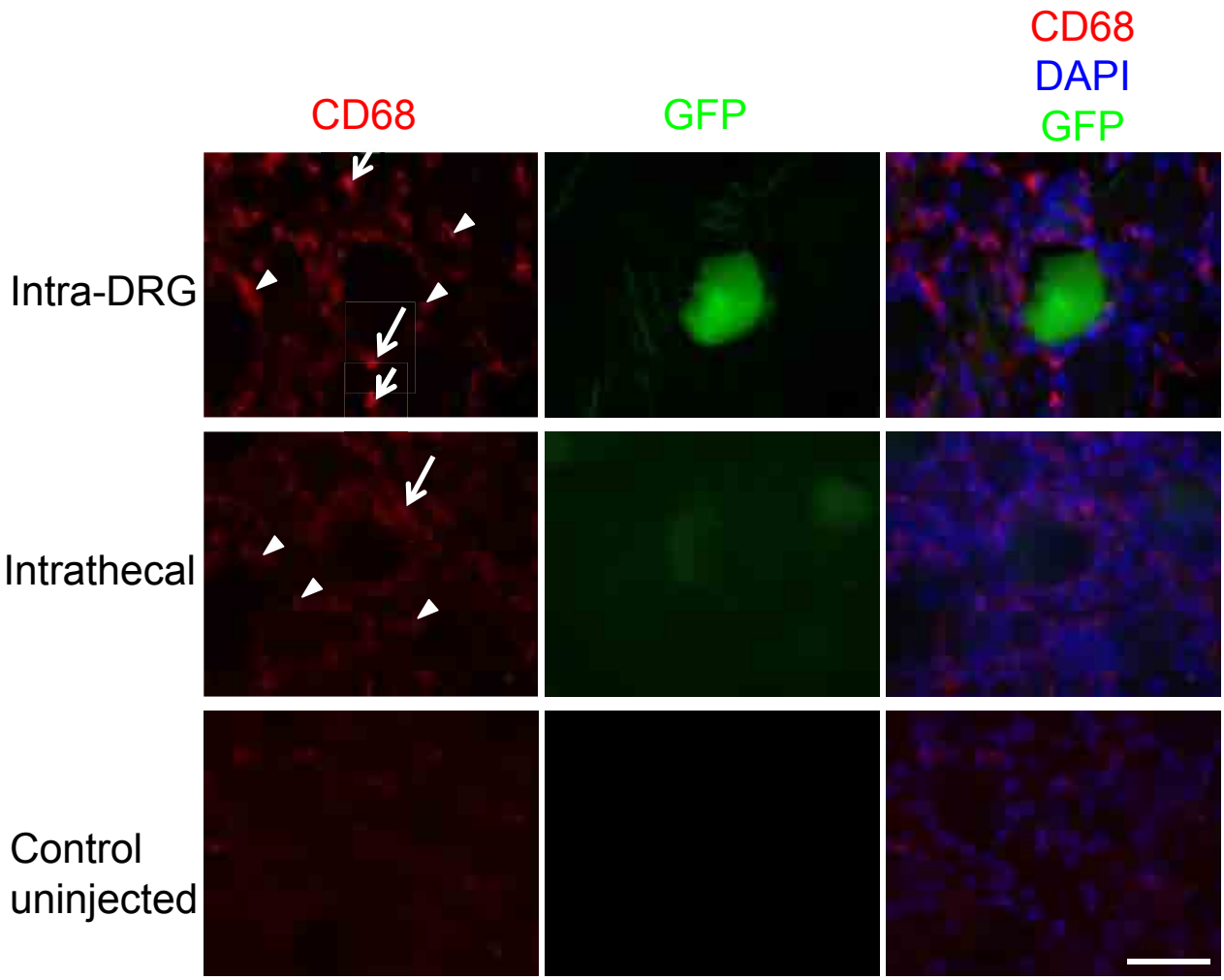


**Figure 5.2** CD68 immunoreactivity in the DRG after intra-DRG and intrathecal injection of AAV8$_{gfp}$. CD68+ macrophages (arrows) can be differentiated from CD68+ satellite cells (arrowheads) on morphological grounds. Scale bar = 50µm.

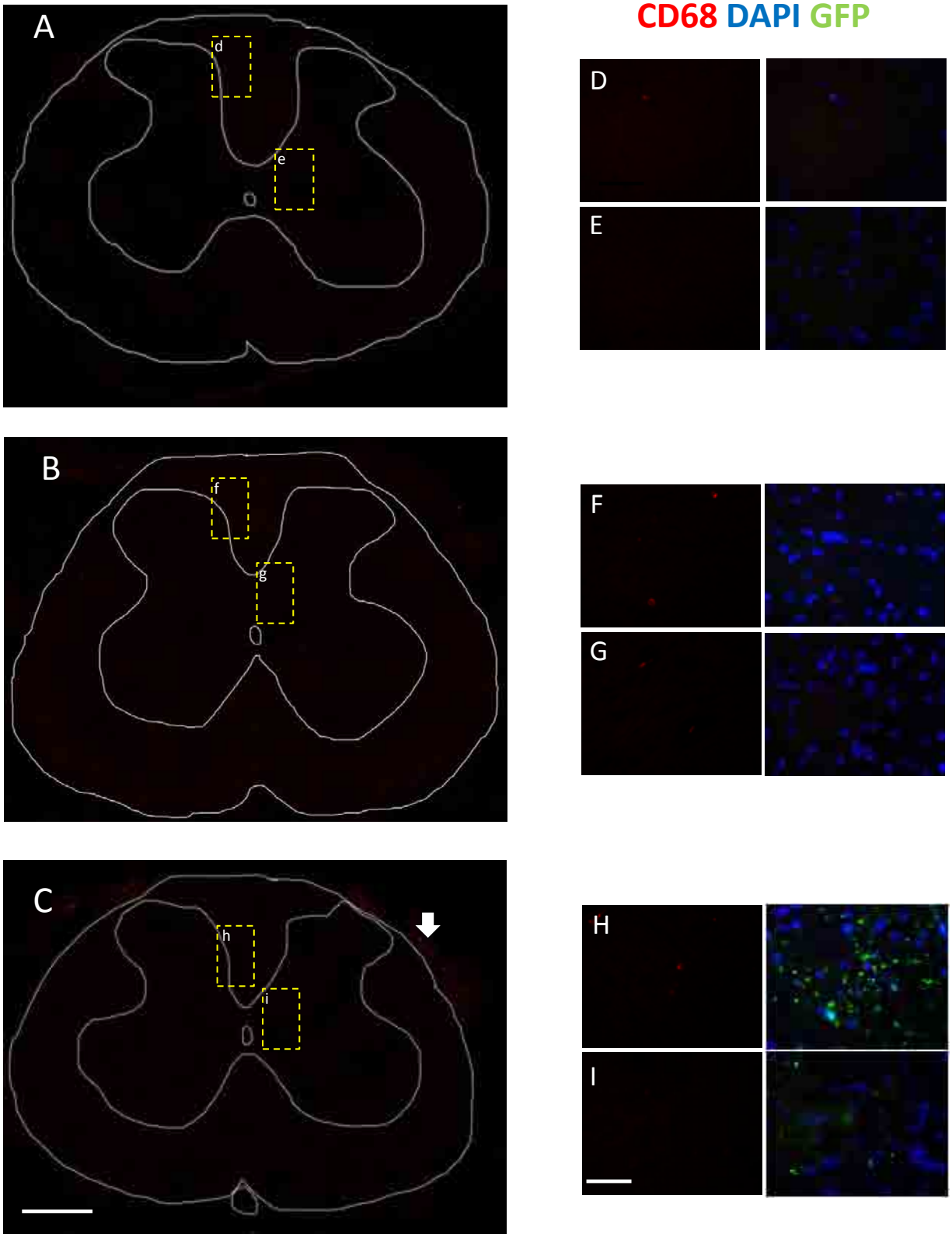


**Figure 5.3** CD68 staining in coronal lumbar spinal cord sections from (A) un-injected controls, (B) intrathecal PBS injected controls and (C) intrathecal AAV8$_{gfp}$ injected animals. Scale bar for composites **(A** – **C**) **=** 500µm. White arrow indicates CD68+ macrophages in the dorsal root. Scale bar for individual images (**D** – **I**) = 50µm.

**A**

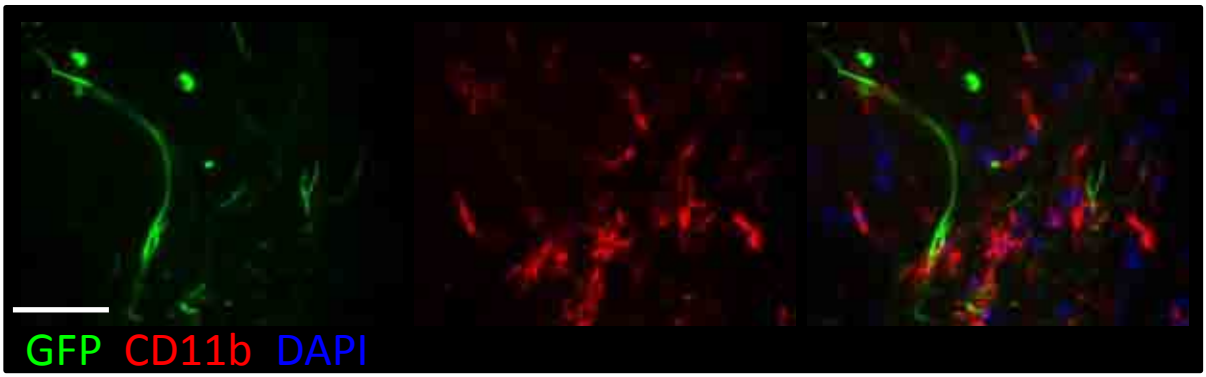


**B**

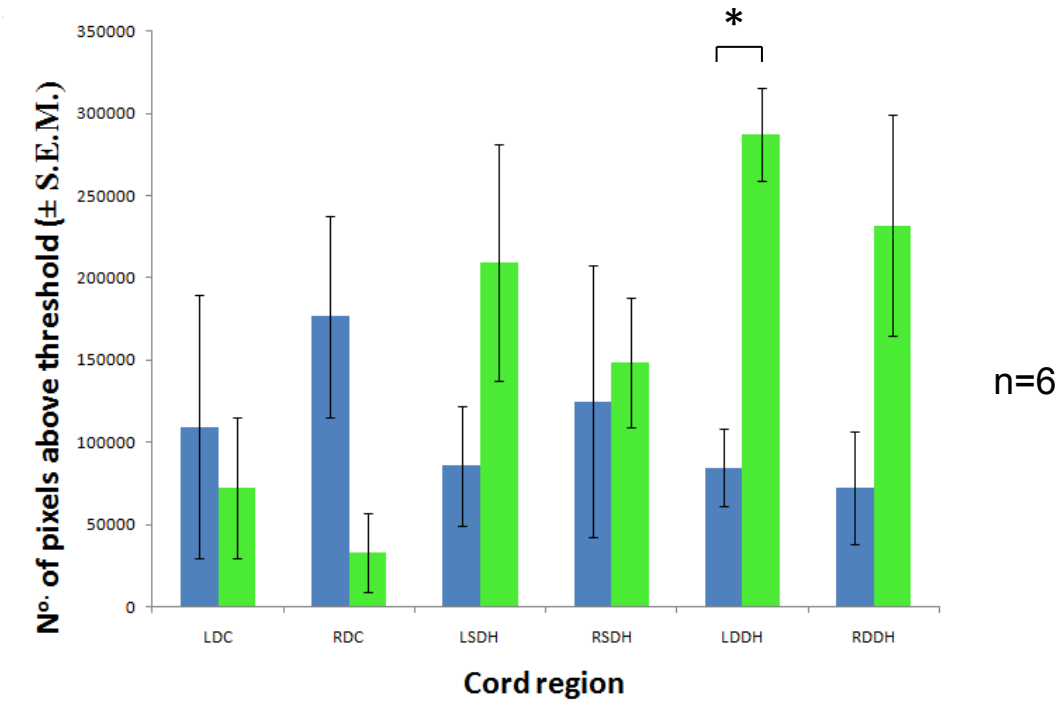


**Figure 5.4** Assessment of microglial activation by CD11b immunohistochemistry in various regions of the rostral lumbar cord after PBS *versus* AAV8$_{gfp}$ intra-DRG injection. **A**. Morphological appearance of activated microglia within Clarke's column ipsilateral to an L4/L5 intra-DRG injection of AAV8$_{gfp}$. Scale bar=50μm. **B**. Quantification of microglial activation in various regions of the rostral lumbar spinal cord after PBS (blue bars) and AAV8$_{gfp}$ (green bars) intra-DRG injection. LDC – left dorsal column, RDC – right dorsal column, LSDH – left superficial dorsal horn, RSDH – right superficial dorsal horn, LDDH – left deep dorsal horn, RDDH – right deep dorsal horn. t-test with Bonferroni correction (alpha=0.0083). *: p<0.0083

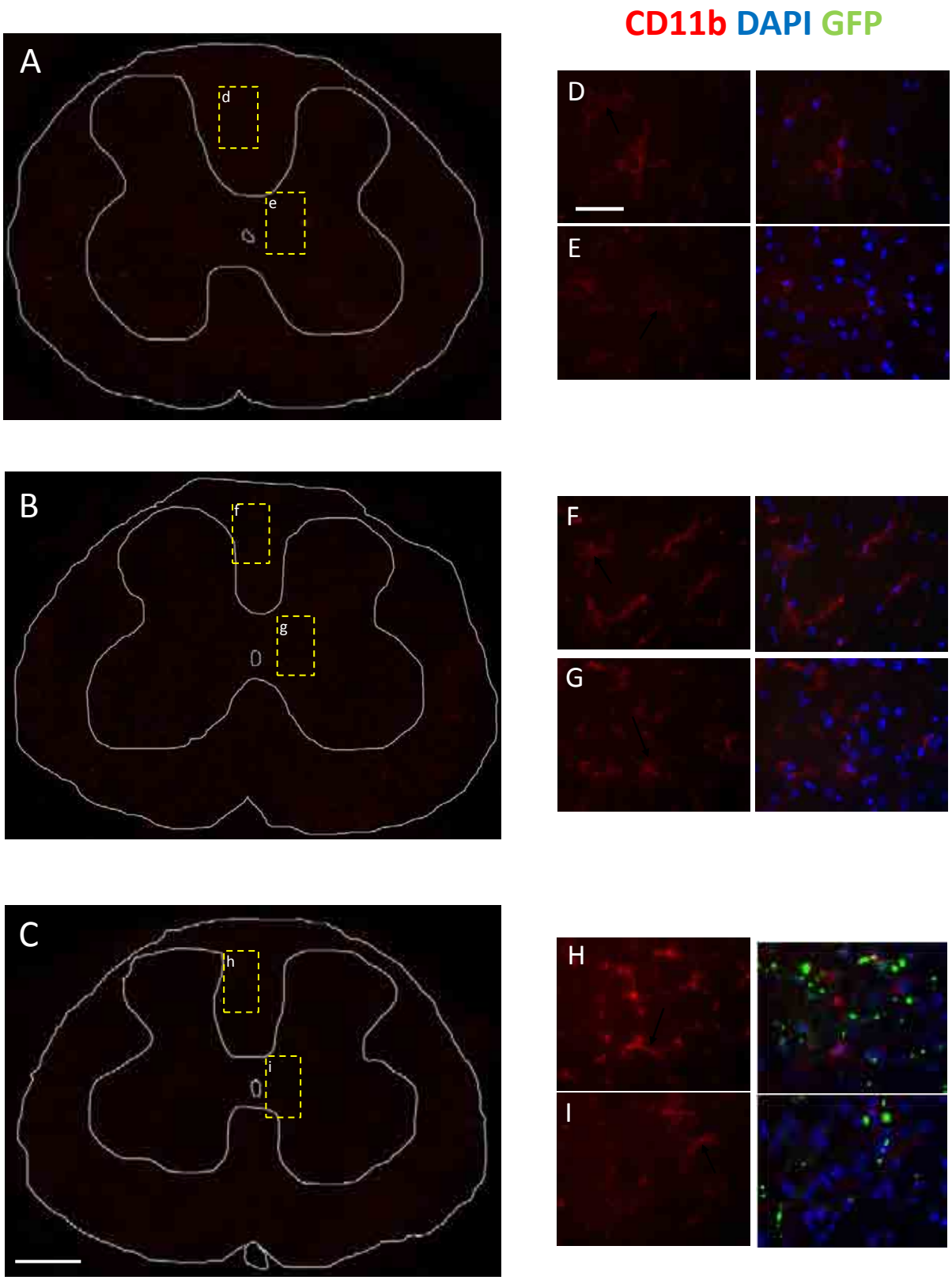


**Figure 5.5** CD11b staining in coronal lumbar spinal cord sections from (A) un-injected controls, (B) intra-DRG PBS injected controls and (C) intra-DRG AAV8$_{gfp}$ injected animals. Scale bar for composites (**A**-**C**) = 500µm. Scale bar for individual images (**D**-**I**) = 50µm.

examined (Fig. 5.6). However, only in the contralateral dorsal column did the increase in GFAP immunoreactivity reached significance (t-test with Bonferroni correction (alpha=0.0083) : p=0.0047). Intra-DRG PBS injection did not increase the level of astrocyte activation (not shown). Qualitatively, there was no evidence of astrocyte activation on the basis of GFAP immunohistochemistry after intrathecal injection of PBS or $AAV8_{gfp}$ compared with uninjected controls (Figure 5.7).

### 5.2.3 No degeneration of DRGN central axon projections after intra-DRG delivery of $AAV8_{gfp}$

Oil-Red-O staining revealed no evidence of myelin breakdown products within the dorsal columns after intra-DRG injection of $AAV8_{gfp}$ (Figure 5.8 A, B). A positive control using optic nerve sections 14d after an optic nerve crush injury that transects all axons (Berry, Carlile et al. 1996; Berry, Carlile et al. 1999) revealed clear Oil-Red-O staining in the distal optic nerve stump and lesion site (Figure 5.8, C-E).

**A**

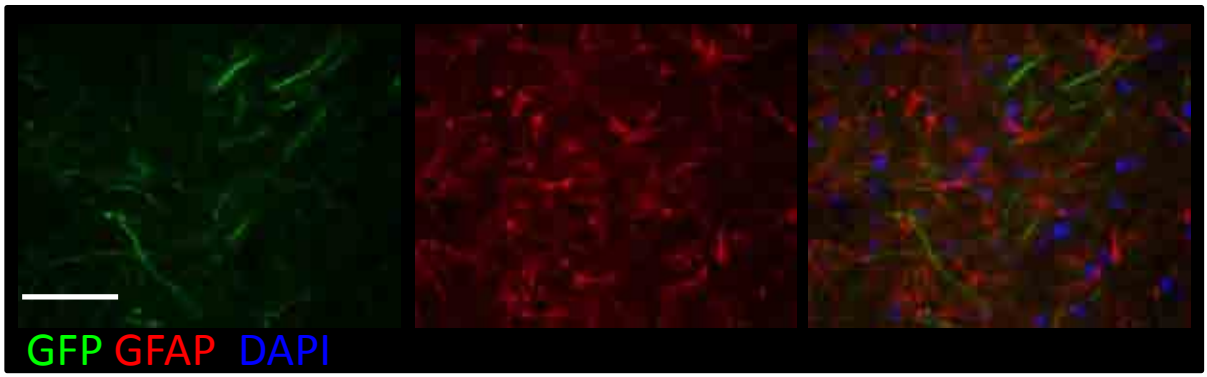


**B**

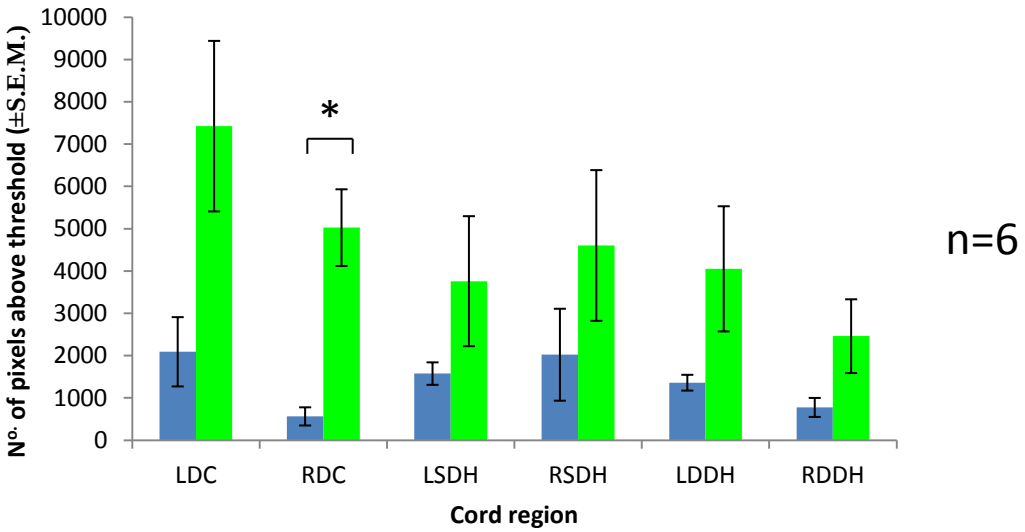


**Figure 5.6** Assessment of astrocytic activation by GFAP immunohistochemistry in various regions of the rostral lumbar cord after PBS *versus* AAV8$_{gfp}$ intra-DRG injection. **A**. Morphological appearance of activated astrocytes within Clarke's column ipsilateral to an L4/L5 intra-DRG injection of AAV8$_{gfp}$. Scale bar=50μm. **B**. Quantification of astrocytic activation in various regions of the rostral lumbar spinal cord after PBS (blue bars) and AAV8$_{gfp}$ injection. LDC – left dorsal column, RDC – right dorsal column, LSDH – left superficial dorsal horn, RSDH – right superficial dorsal horn, LDDH – left deep dorsal horn, RDDH – right deep dorsal horn. t-test with Bonferroni correction (alpha=0.0083). *: p<0.0083

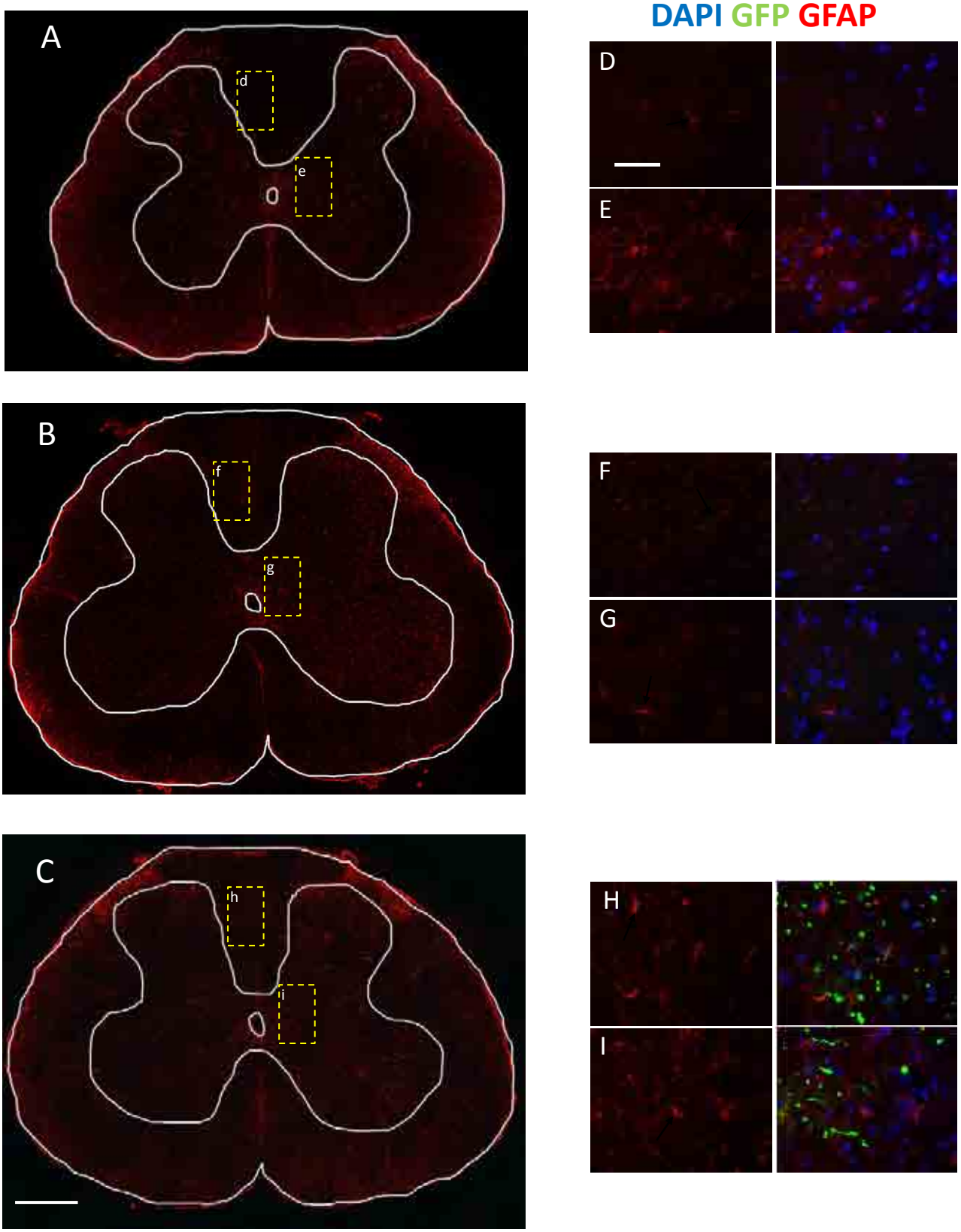


**Figure 5.7** GFAP staining in coronal spinal cord sections from (A) un-injected controls, (B) intrathecal PBS injected controls and (C) intrathecal AAV8$_{gfp}$ injected animals. Scale bar for composites (**A**-**C**) = 500µm. Scale bar for individual images (**D**-**I**) = 50µm.

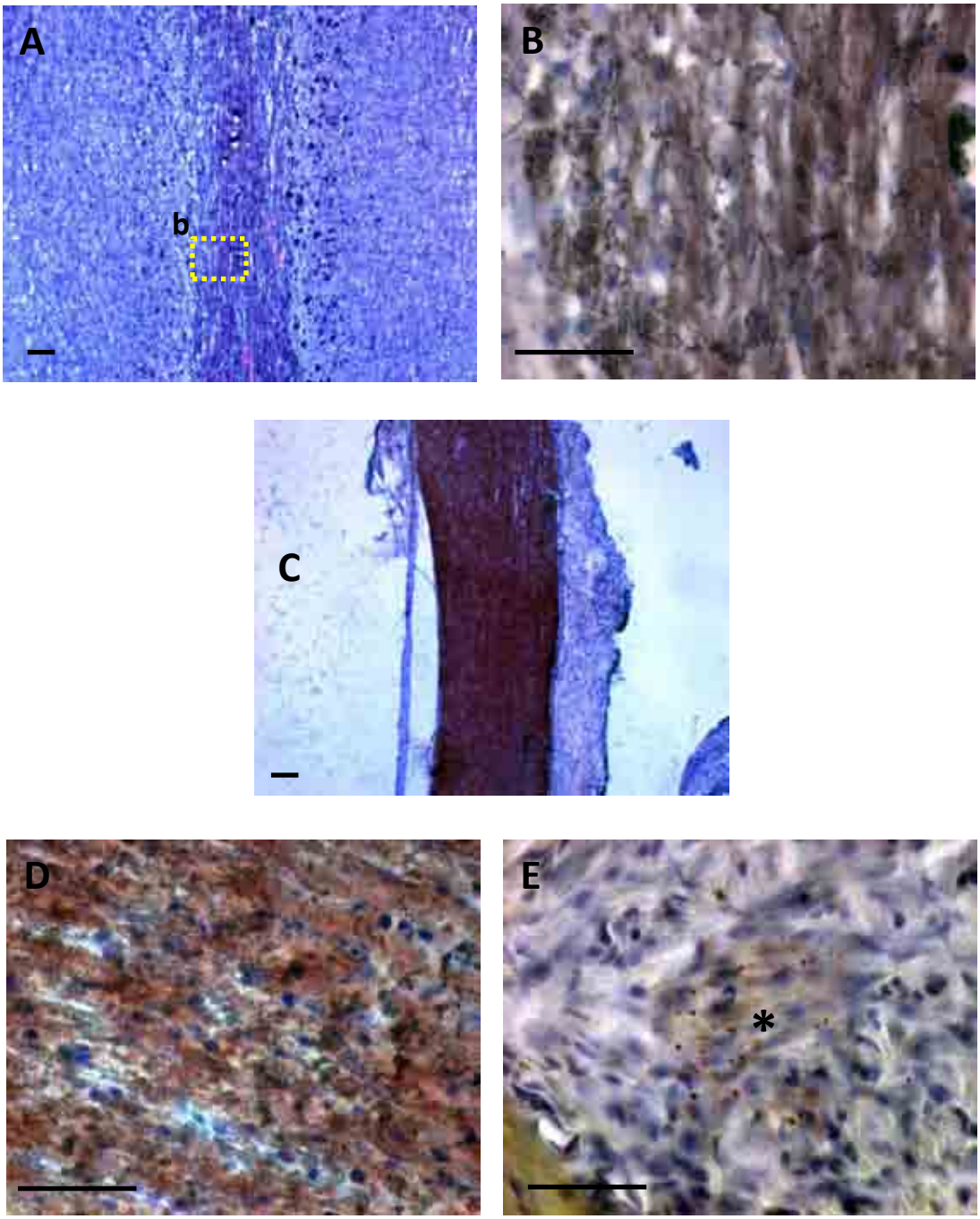


**Figure 5.8** Oil-Red-O staining reveals no evidence of Wallerian degeneration within the DC. A. Overview of horizontal section of cord at ~0.75mm depth from dorsal surface. B. High power view of left DC shown in A. C. Distal stump of optic nerve, crushed 14d previously, demonstrating strong red staining, indicative of axon degeneration. D, E. High power views of distal stump (D) and lesion site (E) demonstrating the expected appearance of Wallerian degeneration in the optic nerve including lipid droplets at the lesion site (asterisk). Scale bar = 50μm.

# Discussion

### 5.3.1 Why look for inflammatory responses?

At the onset of this study, it was felt that gene therapy vectors based on AAV8 were probably harmless due to the inability of AAV to cause any known disease. Additionally, fluorescent proteins were considered harmless and non-toxic due mainly to their widespread use as reporters in gene therapy studies and the 'received wisdom' from many workers that they were inert within the cell. However, some early results seemed to suggest that delivery of $AAV8_{gfp}$ to DRGN was not without problems. After intra-DRG injection, GFP+ axons of $AAV8_{gfp}$ transduced DRGN had grossly enlarged calibres, often seen as swellings between segments of apparently normal axon (see Figure 4.5). Normally, axons in the DC have diameters of around 1-2μm, whereas some of those seen in the transduced DC had diameters an order of magnitude higher at around 10-15μm (Nashmi and Fehlings 2001). This was clearly abnormal and prompted an effort to look for inflammatory responses to this vector in the DRG and cord. Interesting questions remained, however, concerning the mechanism of this axonal swelling and whether it could be a cause (or an effect) of an inflammatory response (see below).

### 5.3.2 The DRG contains a sparse resident macrophage population

The observation that the DRG contains occasional CD68+ macrophages is in keeping with a number of reports in the literature (Hu and McLachlan 2003; Hu, Bembrick et al. 2007; Kim and Moalem-Taylor 2011). The ED1 (anti-CD68) antibody, used to detect macrophages in this study, is known to detect up to 98% of macrophages in the rat (Dijkstra, Dopp et al. 1985). As with macrophages found in

other tissues, the function of these cells in the DRG is to act as part of the initial, innate immune response to tissue damage or infection. Around 35% of the macrophages within intact DRGs are also positive for MHCII, implying that they have a role in antigen presentation and possibly elicitation of T cell responses (Hu and McLachlan 2003). Additionally, it is known that these macrophages phagocytose neuronal debris within the DRG (Hu and McLachlan 2003).

An interesting question concerning the macrophages seen in naive DRGs relates to the proportion of them which are truly resident. The term 'resident' in this context refers to cells that stay within their tissue, and are not simply passing through. It has been shown using bone-marrow chimaeric mice that there is a turnover of macrophages in the DRG of around 80% (Muller, Leonhard et al. 2010). This implies that around 20% of the macrophages seen in the DRG are truly resident. It is likely that these resident macrophages have important roles as first-line defences, being capable of mobilising the migration of additional macrophages into the DRG following tissue insults. A richer knowledge of these resident macrophages may provide the potential for finer tuning of inflammatory responses in the DRG following insults.

### 5.3.3 Intrathecal and intra-DRG injection of AAV8*gfp* led to a robust macrophage response in the DRG

Regardless of delivery method, macrophages became activated and more numerous in the DRG 28d after injection of AAV8$_{gfp}$ but not after PBS injection. This observation strongly suggests that macrophages were activated as a consequence of

the viral vector and not due to direct trauma following intra-DRG injection. It is not appropriate to discuss the degree of macrophage activation seen in the two delivery paradigms due to essential differences between the two techniques – particularly the fact that the concentration of $AAV8_{gfp}$ particles in the DRG in either paradigm is unknown.

So how are DRG macrophages activated by $AAV8_{gfp}$? This question is ostensibly a simple one to answer, but further enquiry regarding the specifics of the immune response to AAV vectors leads one to the conclusion that AAV immunology is still in its infancy. A full explanation of the observed phenomenology is impossible without much further work.

In a tissue such as the DRG, whose immune response has not been extensively elucidated, one must be cautious when discussing immunological phenomena. If extrapolations are to be made from other tissues, it must be ascertained that the immunological components found in those tissues are also present within the DRG. Furthermore, available data must be used to determine whether those components behave in the same way as is seen in other tissues. A paucity of data on basic immunological responses in the PNS makes this a challenging task.

Before discussing immunology, it must be assumed that AAV particles are present in the DRG after injection by both routes. Clearly, this must be the case after intra-DRG

injection and it is reasonable to suppose that vector particles must access cell bodies to transduce DRGN after intrathecal injection (see Chapter 4). One must also be aware that it is possible that some AAV particles enter the lymph draining the DRG or the CSF, potentially leading to both local and systemic inflammatory responses. However, there is only very limited evidence demonstrating lymphatic drainage from the DRG, although it is known that CSF does drain to the cervical lymph nodes (Kuhlmann, Bitsch et al. 2001; Weller, Galea et al. 2010).

It is becoming increasingly recognised that components of the innate immune system known as Toll-like receptors (TLRs) are important in initiating immune responses to AAV vectors (Zhu, Huang et al. 2009). TLRs, of which around 10 have been identified in humans, are part of the innate immune response and are capable of detecting a wide range of pathogenic material (Murphy, Travers et al. 2008). TLRs are present both extracellularly on the plasma membrane and intracellularly within endosomes and respond to a diverse array of pathogen-derived ligands such as lipopolysaccharide, double-stranded RNA and DNA in various forms. Responses to TLR activation vary depending on the type of receptor activated.

In the paper by Zhu et al., various cell types including plasmacytoid dendritic cells (pDCs), conventional dendritic cells and macrophages were exposed to AAV2 encoding *LacZ*. Following exposure to AAV, cell medium was collected and analysed for a range of soluble inflammatory mediators. The only cell type which responded to the presence of AAV was pDCs, which displayed a strong Type-I

interferon response (a typical anti-viral cytokine response). pDCs taken from TLR9 double knockout mice showed no ability to mount a response. Additionally, if parts of the downstream signalling pathways for TLR9 were deleted, no response was initiated. No other cell type, including macrophages, was directly stimulated by AAV application.

The Type-I interferon response involves release of interferon-α and interferon-β predominantly. These cytokines are potent activators of macrophages, stimulating their phagocytic activity (Murphy, Travers et al. 2008). Additionally, the Type-I interferon response causes cells to up-regulate their endogenous anti-viral defences and activates other components of the innate immune response such as natural killer cells. If the mechanism elucidated by Zhu et al. (i.e. TLR9 mediated pDC activation followed by Type-I interferon response) is to be proposed as that which leads to macrophage activation in the DRG, then several criteria must be met. (i), are pDC present in the DRG? (ii) does the timescale described by Zhu et al. correspond to that seen in the experiments described above? (iii) is it likely that AAV8 leads to a similar response to AAV2? (iv) are there any other possible mechanisms that could be responsible for the observed phenomena?

No publications could be found describing the presence of pDCs in the DRG. However, this is not necessarily surprising since these cells are known to exist predominantly in the circulation, although they have been seen to migrate to virally infected tissues (Schuster, Boscheinen et al. 2011). If pDCs are to be implicated in DRG inflammation, then their attraction to the virally infected DRG must be

explained. So what else could be detecting the presence of AAV8, which could in turn lead to the ingress of pDCs? A recent publication has implicated TLR9 mediated cytokine release from DRGN as a possible mechanism for this (Qi, Buzas et al. 2011). Qi et al. demonstrated that human and murine DRGN express a variety of TLRs including TLR9. They showed that this neuronal TLR9 could be activated leading to the release of mediators such as CCL5 (RANTES), CXCL10 (IP-10), IL-1α, IL-1β, and PGE(2). Some of these molecules are known to be chemoattractants for leukocytes (e.g. CCL5) and to be capable of directly activating macrophages (e.g. IL-1α).

Although very difficult to reconcile with the results described in the present study, the experiments performed by Zhu et al. were analysed after a similar time point (Zhu et al. took samples after 36d, the present study took samples after 28d). Comparison of the two studies would have been less valid had the time points been considerably different, since different immune processes would be likely to predominate after, say, days compared with months.

When examining the literature concerning immune responses to viral vectors, it must be realised that it is probably not sufficient to assume that the immune response is the same across all serotypes of virus. This is because most of the antigenicity of a virus (particularly a viral vector) arises from the viral coat proteins, which are necessarily different between serotypes. With respect to AAV vectors, all rAAVs have the same basic genomic structure (ITRs derived from AAV2, see Introduction).

Thus, any differences between serotypes must be due to the capsid. Zhu et al. examined the effect of serotype on the responses of pDCs, and showed that there were predominantly quantitative rather than qualitative differences between AAV1, AAV2 and AAV9 (Zhu, Huang et al. 2009). From these data it seems reasonable to conclude that AAV8 leads to a Type-I interferon response.

As the reader will appreciate from the above discussion, immune responses to AAV vectors are complex and multifactorial. It is highly probable that there are other mechanisms at work that are responsible for macrophage activation in the DRG after AAV8 injection. This study has been hampered by the lack of any temporal data concerning DRG inflammatory responses. If a time-course for inflammation could be produced, then it may become apparent that different mechanisms predominated at different time points. For example, it may be that TLR9 mediated events predominate early (over days) followed by a more organised adaptive immune response driven by T cells. These issues cannot be addressed at present due to insufficient data.

### 5.3.4 Satellite cells were seen to express CD68 after delivery of AAV8*gfp*

Morphologically identified satellite cells that surrounded DRGN were seen to be CD68+. This is a novel finding in the rat, and contradicts one previous report that CD68+ cells in the DRG were not positive for known satellite cell markers such as GFAP and p75 (Hu and McLachlan 2003). It could indeed be the case that the cells that have been identified here as CD68+ satellite cells are in fact macrophages,

however two main points suggest that this may not be the case. Firstly, the location and frequency of these cells is highly suggestive of satellite cells, although it is known that macrophages can insinuate themselves between individual satellite cells to make contact with DRGN cell bodies (Lu and Richardson 1993). Secondly, it has been observed in human trigeminal ganglia that satellite cells have an antigen-presenting cell phenotype, including expression of CD68 detected by fluorescence activated cell sorting (van Velzen, Laman et al. 2009). Further co-localisation studies are needed to fully define the nature of these cells.

### 5.3.5 Macrophages were not seen to cross the DREZ from the dorsal root into the spinal cord

After intrathecal injection of AAV8$_{gfp}$, macrophages were seen in the dorsal root, but they were not seen in the spinal cord, their presence ending abruptly at the DREZ. This pattern of inflammation has been seen previously in chickens with acute neuroinflammation (Bader, Kothlow et al. 2010). Thus, it appears that the PNS/CNS boundary at the DREZ provides a barrier to macrophage migration. This could be due either to an inability of macrophages to cross the BBB or an inability of macrophages to enter the CNS from the PNS. Although the study of the BBB is undergoing considerable change, with regular paradigm shifts, it is clear that leukocytes (including macrophages) do not cross the BBB in large numbers (Bechmann, Galea et al. 2007). It is unknown whether the BBB is abnormal in animals injected with AAV8$_{gfp}$, although this seems unlikely.

A second, interesting mechanism that could be at play in restricting the migration of macrophages into the CNS from the dorsal root is the presence of the Fas ligand (FasL) on astrocytes of the glia limitans (Bechmann, Mor et al. 1999). FasL, through its binding to Fas found on leukocytes, leads to apoptosis. Macrophages have been shown to express Fas, possibly providing the mechanism whereby macrophage migration across the DREZ is inhibited (Richardson, Lalwani et al. 1994).

### 5.3.6 Intrathecal injection did not activate central glia whereas intra-DRG injection led to clear microglial and astrocytic activation

Although CNS glial activation was not quantified after intrathecal injection, it was qualitatively clear that delivery of PBS or AAV8$_{gfp}$ by this method failed to provoke astrogliosis or microgliosis in the rostral lumbar cord. Contrast this with intra-DRG injection, where a strong quantitative activation of microglia was observed, accompanied by a trend towards activation of astrocytes in all cord regions in rats receiving AAV8$_{gfp}$ compared with those receiving PBS alone. It must be stressed at this point that the method used to quantify glial activation did not allow statistical comparisons to be made between naive animals and those receiving an injection. Tissue from naive animals was used to derive a threshold value in order to perform pixel counts on tissue from injected animals. Also, naive tissue is probably not the best control in this situation, since the act of inserting a needle into the DRG or subarachnoid space without injecting is likely to result in an inflammatory response. Hence, a sham injected group would be useful to have. The rest of this discussion

will be based around comparisons between PBS injected animals and those receiving AAV8$_{gfp}$.

Two major differences exist between intra-DRG and intrathecal injection. First, intrathecal injection leads to a lower dose of vector being delivered to each DRGN (i.e. a lower multiplicity of infection) compared with intra-DRG injection where a high concentration of vector particles is delivered directly to DRGN. Secondly, intrathecal injection is not likely to lead to direct injury of DRGN cell bodies or axons within the DRG. Intra-DRG injection, using a glass micropipette inserted directly into the DRG parenchyma is likely to lead to considerable tissue disruption.

Dose-response studies have been performed using AAV vectors in the DRG, particularly looking at the level of transgene expression seen at various doses. It appears that, at least in the case of AAV5, increasing the dose of vector has a positive effect on the level of transgene expression (Klein, Hamby et al. 2002; Mason, Ehlert et al. 2010). This result, although intuitive, is not necessarily what was to be expected since previous studies on adenovirus have shown lower levels of transgene expression after injection of high titres compared with lower titres (Thomas, Birkett et al. 2001). Hence, it seems that in the DRG injected with AAV it is irrelevant whether it is the vector itself or the transgene that leads to an inflammatory response since higher titres lead to higher levels of transgene expression. Therefore, the results presented here are in keeping with what is currently known

(intrathecal injection leads to lower multiplicities of infection, lower levels of transgene expression and a lower level of glial activation).

If the stronger glial activation was solely due to trauma associated with intra-DRG injection, one would expect to see equal magnitudes of gliosis in the PBS and AAV8$_{gfp}$ injected animals. This is not the case – intra-DRG injection of AAV8$_{gfp}$ generally leads to higher levels of CNS glial activation. One possible explanation for this could be based around the idea of a double or even triple 'hit'. The three hits could come in the form of (i), trauma associated with injection; (ii), entry of viral particles with concomitant innate immune response and (iii), subsequent expression of transgene (*gfp*).

In the case of (i) it is clear that intra-DRG injection is much more traumatic than intrathecal injection for the target neurones. Indeed, in the present study it is likely that the volume injected into the DRG (10µl) was excessively high. This volume was selected as it was felt that it would be difficult to deliver smaller volumes accurately with this method. Other workers have used much smaller injection volumes and not reported any inflammatory responses (Mason, Ehlert et al. 2010; Fischer, Kostic et al. 2011) . However, in the case of Mason et al., only gross morphology of the DRG after haematoxylin and eosin staining was provided. After intra-DRG injection in the present study, no gross morphological abnormalities were observed. Macrophage infiltration and glial activation could still have been present in the animals injected by Mason et al.

What is the mechanism whereby DRG trauma could lead to CNS glial activation? The answer may lie in the extensive literature on neuropathic pain. Neuropathic pain often occurs after injuries to the PNS (and also the CNS) and is characterised by lowered pain thresholds and the perception of non-painful stimuli as being noxious (Scholz and Woolf 2007). The neurological basis of such pain states is believed to be extensive plastic change within the cord, associated with glial activation. It is known that damage to a peripheral nerve (this can include DRGN cell bodies and processes) leads to high frequency firing of the DRGN and release of mediators such as adenosine triphosphate (ATP), BDNF and nitric oxide at their central terminals (Vallejo, Tilley et al. 2010). ATP is chemoattractant for microglia and stimulates their activation. Nitric oxide is known to activate astrocytes (Brahmachari, Fung et al. 2006)s. Indeed, ATP can attract microglia from up to 100μm away from its site of release, and this does go some way to explaining the bilateral microglial activation seen in the deep dorsal horn (Vallejo, Tilley et al. 2010). This model provides an explanation for how direct DRG damage can lead to central glial activation, although three main criticisms arise. Firstly, if direct DRG damage after intra-DRG injection is responsible for these findings, why is the magnitude of the glial activation not equal after PBS and AAV8 injection? Secondly, behavioural measures of neuropathic pain in rats are not grossly affected 2 weeks after intra-DRG injection of 4μl PBS. Thirdly, there is no evidence of Wallerian degeneration in the DC after intra-DRG injection of $AAV8_{gfp}$. It is known that axotomy of the peripheral projection of DRGN leads to about 30% DRGN death (McKay Hart, Brannstrom et al. 2002). Surely, if intra-DRG injection axotomised DRGN then some CNS degeneration in the DC would be detectable? Thus it seems that, even if DRG injury has a role in the observed CNS

glial activation, it is likely that this is only sufficient at earlier time points. Something is presumably perpetuating the glial activation in animals receiving intra-DRG $AAV8_{gfp}$.

The factors responsible for the continuing glial activation seen in the cord after intra-DRG $AAV8_{gfp}$ may include the ongoing inflammatory response within the DRG (see above) or the onset of expression of GFP from transduced DRGN. At this point, it is worth re-iterating that intrathecal injection of $AAV8_{gfp}$ led to levels of transduction approximately an order of magnitude lower than seen after intra-DRG injection (see Chapter 4). Thus, if there is a threshold level of GFP expression that leads to CNS glial activation, this may not have been reached in animals receiving intrathecal injection.

Occasional GFP+ DRGN are seen at 1 week after intra-DRG injection of AAV5, with expression increasing to high levels after 4 weeks (Mason, Ehlert et al. 2010). It is believed that a major factor contributing to this time lag is the conversion of the ssDNA genome of AAV into a useable, transcriptionally-competent dsDNA molecule (Ferrari, Samulski et al. 1996). In the DRG it seems likely that high levels of GFP are seen from around 1-2 weeks post injection. So is it possible that GFP could be contributing to this scenario – is GFP neurotoxic?

There are a variety of fluorescent proteins currently used as reporter genes in many different branches of biological science. The two major forms are those derived from jellyfish (GFP, yellow fluorescent protein (YFP) and others) and those derived from

the sea pansy (hrGFP) (Shaner, Steinbach et al. 2005). Clearly, these molecules are extremely useful and enable visualisation of many diverse biological phenomena. If one speaks to researchers regularly using fluorescent proteins as reporters, they will frequently state that these molecules are non-toxic and essentially inert within the cell. However, the findings presented above led the author to question this dogma and to perform a thorough literature search looking for any evidence of toxicity associated with fluorescent proteins.

An early study discussing the toxicity of GFP actually used AAV8 to deliver this transgene to the rat striatum (Klein, Dayton et al. 2006). Klein et al. demonstrated that it was possible to kill neurones of the substantia nigra by delivering $AAV8_{gfp}$ alone. Furthermore, it was shown that no neuronal death occurred after injection of an equivalent amount of an empty AAV8 particle. This provided convincing evidence that GFP, when delivered in large quantities, was toxic to neurones. *In vitro* studies have also shown the capacity of GFP to form intracellular aggregates in HEK 293 cells (Link, Fonte et al. 2006) and neurones when co-expressed with other proteins (Krestel, Mihaljevic et al. 2004). Furthermore, axonal spheroids have been observed in aged mice of the YFP-H line (Bridge, Berg et al. 2009) and *Drosophila* expressing neuronal GFP have been shown to display neurological deficits (Mawhinney and Staveley 2011). Of course, the evidence presented above must be taken in the context of the many successful studies employing GFP. However, there is probably enough data to suggest that in certain contexts GFP can be toxic to neurones, or at least is capable of modulating inflammatory responses.

So to return to the original three hit hypothesis. After intra-DRG injection, there is a transient injury to DRGN cell bodies and axons (neuropraxia) followed by the influx of AAV8 particles. This sets up an inflammatory reaction in the DRG in the context of vulnerable neurones. As time progresses, GFP levels in transduced neurones increase leading to further neuronal toxicity. The level of insult to the neurone exceeds a threshold, beyond which inflammatory mediators are released from central terminals and CNS glia become activated. Intrathecal injection does not lead to any direct DRG damage, the levels of AAV8 particles in each DRG are lower and the amount of GFP expressed by individual DRGN is lower. Hence, DRGN do not exceed the threshold level after intrathecal injection and so do not release inflammatory mediators from their central terminals. Thus, intrathecal injection does not lead to CNS glial activation.

Clearly, much further work needs to be performed to confirm this intriguing hypothesis. However, the results as they stand should stimulate researchers working with fluorescent proteins in the nervous system to look for any signs of overt toxicity.

### 5.3.7 Astrocytes showed evidence of widespread activation after intra-DRG injection of AAV8$_{gfp}$

Although only one region of the cord displayed a statistically significant effect, it was still intriguing to see the consistent trend towards activation of astrocytes in all cord regions and on both sides after intra-DRG injection of AAV8$_{gfp}$. Clearly, in order to confirm this, additional animals need to be examined.

A phenomenon that may explain this global astrocyte activation arises from the literature on neuropathic pain. Some patients with neuropathic pain states arising from unilateral pathologies have been known to develop pain on the contralateral side, with no contralateral pathology (e.g. a nerve injury in the left arm leads to bilateral neuropathic pain). This is known as 'mirror-image' pain and has been extensively described in the literature (Hansson 2006). A number of theories have been proposed to explain this pattern of pain, the most compelling from the point of the present study being the propagation of calcium waves in astrocytes. Astrocytes are known to be connected to each other in what is known as a functional syncytium (Verkhratski and Butt 2007). The molecular basis for this arrangement is the presence of gap junctions between adjacent astrocytes, which are known to allow the propagation of calcium waves over long distances through the syncytium. It is possible that the widespread activation of astrocytes seen in this study is the result of syncytial interactions between activated astrocytes.

### 5.3.8 Central projections of DRGN did not show signs of degeneration after intra-DRG injection of AAV8*gfp*

As already discussed in Chapter 4, no stereological counts of DRGN in the various injection paradigms were made. This means that any comments regarding the survival of DRGN are based upon indirect measures. One such measure used was the assessment of Wallerian degeneration in the DC using the Oil Red O technique. Oil Red O exploits the fact that lipophilic dyes are less soluble in organised, laminar myelin than in the lipid droplets associated with degenerated myelin (Kiernan 2007).

Thus, a signal is obtained when degenerated myelin is present. In the present study, no signal was detected in the dorsal column of rats injected with AAV8$_{gfp}$. This was in the context of a positive control showing strong signal in the lesion site and distal stump of an optic nerve examined 14d post transection. Due to the fact that Wallerian degeneration is a very slow process in the CNS, taking months to years to complete, it is reasonable to assume that there will be detectable degenerating myelin after 28d (Vargas and Barres 2007). One must, however, be cautious in concluding that there was no axon degeneration present, due to the fact that only a small proportion (probably much fewer than 1%) of axons in the DC would have been transduced. Thus, it is possible that the signal to noise ratio would have been insufficient to detect any axonal degeneration. Indeed, there was high background in the tissues examined due to the high density of axons and the large number of haematoxylin stained nuclei. The signal to noise ratio could probably be increased by using thinner sections and omitting the haematoxylin counter-stain.

### 5.4 Further work

As the reader will undoubtedly have gathered from the preceding pages, the study of inflammatory responses to AAV8 in the nervous system is difficult, not helped by a paucity of data concerning both the specifics of AAV immune responses and neuroimmunology in general. Necessarily, much speculation has been included in the interpretation of the results obtained in this chapter, but most of the uncertainties raised could probably be addressed by the following additional experiments.

### *Assessment of the kinetics of AAV8 delivery to the DRG*

Due to a lack of time and resources, dose-response and time course experiments were not performed. Instead, the maximum reasonable dose of $AAV8_{gfp}$ was delivered in each injection paradigm. Dose-response studies may uncover an optimal amount of AAV to deliver in a minimum volume to effect the greatest amount of DRGN transduction in the context of minimal inflammation (although this seems unlikely from the work of Mason et al. on AAV5, see above). Time-course studies may uncover dynamic aspects of the inflammatory response to AAV8, possibly helping to answer some of the more difficult questions surrounding the 'three-hit hypothesis'.

### *Staining for additional components of the immune system*

It would be extremely interesting to look at the DRG (and spinal cord) for evidence of invasion by other cellular elements of the immune system such as T-cells, B-cells and dendritic cells. Additionally, immunohistochemistry could be performed to identify the presence of relevant cytokines and chemokines and to quantify their levels in the different injection paradigms. Introducing a quantitative element to the work on inflammatory responses would be very interesting. Furthermore, techniques such as microdialysis and serial sampling of CSF may be illuminating.

### *Sham injections*

As mentioned above, naive animals are probably not the ideal control for these experiments. Much more useful would be animals that had undergone the entire injection procedure but not the actual injection itself (i.e. insert the needle but don't inject). This would facilitate the estimation of the inflammatory response attributable to the procedure itself.

### *Quantification of axonal calibres in the DC*

The stimulus for assessing inflammatory responses to AAV8$_{gfp}$ came from the observation of axonal swelling in the DC. As mentioned above, this has been observed in YFP transgenic mice. It would be informative to measure the axonal diameters of the total population of DC axons compared with GFP+ axons and to correlate this with quantified parameters of the inflammatory response.

### *Test viral stocks for LPS*

Despite the fact that the viral vectors were prepared with *in vivo* experiments in mind, and obtained from reputable sources with good quality control systems, it would be ideal to test each batch for the presence of endotoxin, which is known to be a potent stimulant of inflammatory responses.

# Chapter 6

# A pilot experiment to examine the effect of AAV2/8 mediated delivery of NT-3 and shRNARhoA to DRGN on regeneration in the DC

# Introduction

The following introductory sections will specifically address studies employing viral vectors to deliver NT-3 and AGIL neutralisation strategies directly to components of the injured spinal cord. The reader is reminded that many other studies have delivered these therapeutics (particularly NT-3) by transducing cells, such as neural stem cells or olfactory ensheathing cells with a virus *ex vivo* and then injecting these cells into the cord (Liu, Himes et al. 1999; Ruitenberg, Levison et al. 2005).

### 6.1.1 Viral vector-mediated delivery of NT-3 to the spinal cord

The first demonstration that NT-3 delivered using a viral vector to the injured spinal cord can lead to regeneration of sensory axons came from a collaboration between the laboratories of Patrick Anderson and Joost Verhaagen (Zhang, Dijkhuizen et al. 1998). In the study by Zhang et al., NT-3 was delivered to motor neurone cell bodies in the ventral horn using an adenoviral vector (Ad-NT3). Being the natural target for many large diameter TrkC+ DRGN central projections, it was hypothesised that overexpression of NT-3 in motor neurones would lead to chemotaxis of avulsed DRGN projections in the re-anastomosed dorsal root towards the ventral horn. In order to maximise regenerative potential, a preconditioning sciatic nerve lesion was also performed. It was found that many regenerating axons penetrated into the spinal cord grey matter as deep as lamina V in Ad-NT3 treated animals. No axons were seen to enter the cord after application of a control vector, Ad-LacZ.

The study by Zhang et al. demonstrated a phenomenon that has been repeated a number of times – namely, that NT-3 is capable of guiding lesioned axons through

the CNS parenchyma. However, it must be stressed that in the study by Zhang et al. there was not significant damage done to the spinal cord itself, which is likely to liberate a high concentration of soluble AGIL. A study by Blits et al., where AAV-NT3 was injected caudal to a complete transection filled with a Schwann cell graft, showed numerous axons entering the graft but none were seen to regenerate into the caudal spinal cord (Blits, Oudega et al. 2003).

A second interesting property of NT-3 is that it is capable of stimulating plasticity in the injured spinal cord. Zhou et al. showed that, after unilateral corticospinal tract lesion at the level of the medulla, adenovirally-mediated delivery of NT-3 to ventral horn motor neurones stimulated midline crossing of intact CST projections to the lesioned side (Zhou, Baumgartner et al. 2003).

It seems that NT-3 mediated chemotaxis is not sufficient to stimulate regeneration of axons in the spinal cord. Have studies delivering NT-3 directly to cell bodies of axotomised neurones fared any better? It was demonstrated in 1997 that AAV-mediated delivery of NT-3 to DRG explants *in vitro* resulted in a robust neurite outgrowth response (Dijkhuizen, Hermens et al. 1997). However, in the study by Dijkhuizen et al., AGIL were not present. At the time of writing, no publications could be found reporting the effect of virally-delivered NT-3 directly to neuronal cell bodies *in vivo*. It is known from other studies, however, that application of neurotrophins including NT-3 to neurones *in vitro* can activate their growth state as evidenced by their up-regulation of growth-associated protein 43 (Mohiuddin, Fernandez et al.

1995). It must, however, be acknowledged that NT-3 application to the neuronal cell body alone has no effect on neurite outgrowth (Kimpinski, Campenot et al. 1997). The reader is reminded that in the present study it is an *nt-3*-encoding virus that has been applied to neuronal cell bodies. The fate of the synthesised NT-3 protein is currently unknown, although it seems likely that much of it will be released at both peripheral and central terminals, as well as into the DRG itself from the cell body. Such release from terminals provides a rationale for this approach and allows the current study to be compared with previous work where NT-3 was applied directly to the lesion site (Bradbury, Khemani et al. 1999).

To conclude this section, it is known that NT-3 is beneficial for neuronal plasticity and regeneration and it seems reasonable to expect that AAV-mediated delivery of NT-3 to DRGN cell bodies will augment the regenerative capacity of their axons. However, it is also known that single therapies often fail, so a combined approach employing the delivery of an AGIL neutralisation therapy is likely to be more fruitful (see Introduction for more details).

### 6.1.2 Viral vector-mediated delivery of AGIL neutralisation therapies to the spinal cord

In 2004, Fischer et al. demonstrated that AAV-mediated delivery of a dominant-negative form of NgR to RGC resulted in significant amounts of axon regeneration in the optic nerve, only when combined with activation of the RGC growth state (Fischer, He et al. 2004). Most of the literature reporting effects of virally-mediated knockdown of NgR is from China and shows encouraging results suggesting that

adenoviral and lentiviral delivery of RNAi against NgR results in functional improvements in animal models of stroke and SCI (Lu, Yuan et al. 2010; Wang, Wang et al. 2010; Xu, Liu et al. 2011).

Other studies have looked at the effects of virally-delivered inhibitors of RhoA and its downstream effectors. A recent study described positive effects on peripheral nerve regeneration after delivery of an adenovirus expressing dominant-negative forms of RhoA and Rac1 to the proximal nerve stump (Kusano, Enomoto et al. 2011). Similarly, a dominant-negative form of ROCK was administered to the red nucleus using a lentiviral vector followed by lesioning of the rubrospinal tract (Wu, Yang et al. 2009). This single therapy resulted in improved functional recovery and enhanced regeneration of rubrospinal axons caudal to the lesion. In this study, the authors themselves state that it is likely that combinatorial therapies including ROCK inhibition are likely to give higher levels of axon regeneration.

At the time of writing, no published reports describing the effect of virally delivered RNAi targeted at RhoA were available. However, this approach has been convincingly validated *in vitro* using both transfection of siRNA against RhoA into primary retinal cultures (Suggate, Ahmed et al. 2009) and delivery of a plasmid encoding $shRNA_{RhoA}$ to PC12 cells (Fan, Pang et al. 2008). Both of these studies demonstrated significant levels of disinhibited neurite outgrowth.

A final, cautionary note must be included regarding a recent paper from the lab of Joost Verhaagen (Ehlert, Eggers et al. 2010). In the paper by Ehlert et al., neuronal toxicity was noted when therapeutic and control shRNAs were delivered using an AAV1-based vector to the red nucleus. A significant inflammatory response accompanied by neuronal degeneration in the red nucleus was observed. Fortunately, from the point of view of the present study, minimal toxicity was seen in the DRG after intra-DRG injection of the same shRNAs using AAV5. However, this study serves to highlight that caution must be exercised when over-expressing therapeutic genes in neurones.

### 6.1.3 Combining viral delivery of growth factors with neutralisation of AGIL in the injured spinal cord

The present study is, to the best of the author's knowledge, the first account of the use of a single viral vector containing both a growth factor and an AGIL neutralisation therapy (i.e. $AAV8_{hrgfp\text{-}nt3\text{-}shrnarhoa}$). Indeed, it is the first study to specifically look at the effect of combining NT-3 administration with RhoA knockdown *in vivo*. The rationale for the production of this vector is founded upon an established evidence base emphasising the need for activation of a neurone's growth state and inactivation of myelin-derived inhibitors to effect CNS axon regeneration.

### 6.1.4 How can previous findings inform experimental design?

The results presented in Chapters 4 had great significance with respect to the design of the experiment described in this chapter. The discovery that AAV8 preferentially transduces large-diameter proprioceptive DRGN projecting to Clarke's column led to the requirement for the DC lesion to be performed at the L1 spinal level (see Figure 2.2). It is known that the Clarke's column projections of the sciatic nerve terminate in the caudal half of the thoracic cord (LaMotte, Kapadia et al. 1991). Thus, a T8 lesion (the 'traditional' level for DC lesions in the Molecular Neuroscience Group) would be likely to fail to transect the vast majority of central projections of transduced DRGN. A lesion at a level too caudal (e.g. L5 cord level) would not be conducive to axonal tracing using intra-sciatic nerve CTB, since the sciatic nerve in the rat takes its origin predominantly from the L4 and L5 spinal nerves (Craigie, Innes et al. 1963). Thus, it was decided to perform the lesion at L1. Furthermore, a DC lesion at L1 is much less likely to interfere with the function of other nerves (L2 may affect the femoral nerve) or the locomotor function of the animal (mid-lumbar may affect the sciatic nerve or circuitry involved in the regulation of the central pattern generator for gait).

#### 6.1.5.1 Specific hypothesis

$AAV8_{hrgfp\text{-}nt3\text{-}shrna\text{-}rhoa}$ and $AAV8_{hrgfp\text{-}nt3}$ transduction of DRGN *in vivo* mediates neurone disinhibited regeneration of DC axons

### 6.1.5.2 Specific aims

- To confirm that AAV8$_{hrgfp\text{-}nt3\text{-}shrnarhoa}$ and AAV8$_{hrgfp\text{-}nt3}$ transduce DRGN *in vivo* and that these neurones are also CTB+ using immunohistochemistry
- To examine the gross pathological appearance of DC lesion sites from animals receiving AAV8$_{gfp}$, AAV8$_{hrgfp\text{-}nt3\text{-}shrna\text{-}rhoa}$ and AAV8$_{hrgfp\text{-}nt3}$
- To assess the completeness of DC lesions using CTB immunohistochemistry in a selected animal from each group
- To qualitatively examine the characteristics of the DC lesion site in a selected animal from each group using GFAP immunohistochemistry
- To use CTB immunohistochemistry to evaluate the extent of axon regeneration across the DC lesion site in a selected animal from each group

## Section 6.1.6 Brief description of methods

The experimental design comprised three groups with a total of 14 animals (200-220g). At day 0, animals received intra-DRG injections to the left L4 and L5 DRG of AAV8$_{gfp}$ ("GFP": n=4, $10^{11}$ viral genomes per DRG in 10µl); AAV8$_{hrgfp\text{-}nt3}$ (NT-3": n=5, $10^{11}$ viral genomes per DRG in 10µl) and AAV8$_{hrgfp\text{-}nt3\text{-}shrnarhoa}$ ("NT3-shRNA": n=5, $10^{11}$ viral genomes per DRG in 10µl). At 28d post injection, animals received bilateral DC crush lesions at the L1 spinal cord level. Professor Martin Berry, who performed the lesions, was blinded with respect to which group each animal belonged to. At 26dpl, animals received intra-neural injections of 2µl 1% CTB to the left sciatic nerve. At 28dpl animals were sacrificed, perfused with 4% formaldehyde

and dissected, harvesting the lesion sites, left L4/L5 DRG and medulla. DRG were cut into 15μm sections, those from the centre of each ganglion being selected for CTB immunohistochemistry. Medullas were cut into 15μm sections, those at the level of the obex were selected for CTB immunohistochemistry. Lesion sites were cut into 25μm sections in the parasagittal plane – immunohistochemistry for GFAP and CTB was performed on sections taken approximately 200μm to the left of the mid-line.

DRG and lesion sites were examined using standard immunohistochemical techniques.

Unfortunately, due to a lack of time, only tissues from one animal from each group were analysed immunohistochemically. The reader is reminded at this stage, therefore, that only preliminary conclusions can be drawn from the results described below. Much further work is required.

# Results

### 6.2.1 GFP was present in large-diameter DRGN, co-localising with CTB

CTB immunoreactivity was seen in the cell bodies of many DRGN within the DRG from all animals examined (Figure 6.1). Expression appeared maximal in cell bodies of large diameter DRGN. GFP expression, as previously observed, was also predominantly seen in cell bodies of large diameter DRGN. Additionally, GFP was seen in axons within the DRG. No co-localisation of GFP with CTB in axons was observed in the DRG (Figure 6.1) or the spinal cord (Figure 6.7 D).

### 6.2.2 No differences were observed in the gross pathological appearance of lesion sites from animals in different treatment groups

Qualitatively, no differences were observed in the gross appearance of the lesion sites from all of the animals studied. Lesions frequently appeared cystic (by their dark appearance), located at the rostral end of the lumbar enlargement (Figure 6.2, arrow). All lesions were localised to within approximately 1mm of their epicentre, with no evidence of rostral cavitation.

### 6.2.3 GFP+/CTB+ terminals were seen in the medullas from the three animals that were analysed

In the gracile nuclei from the three animals studied, GFP+ terminals were seen to co-localise with CTB (Figure 6.3 arrows and arrowheads, repectively). The animals in the NT3-shRNA$_{RhoA}$ group displayed the highest level of expression of GFP and CTB.

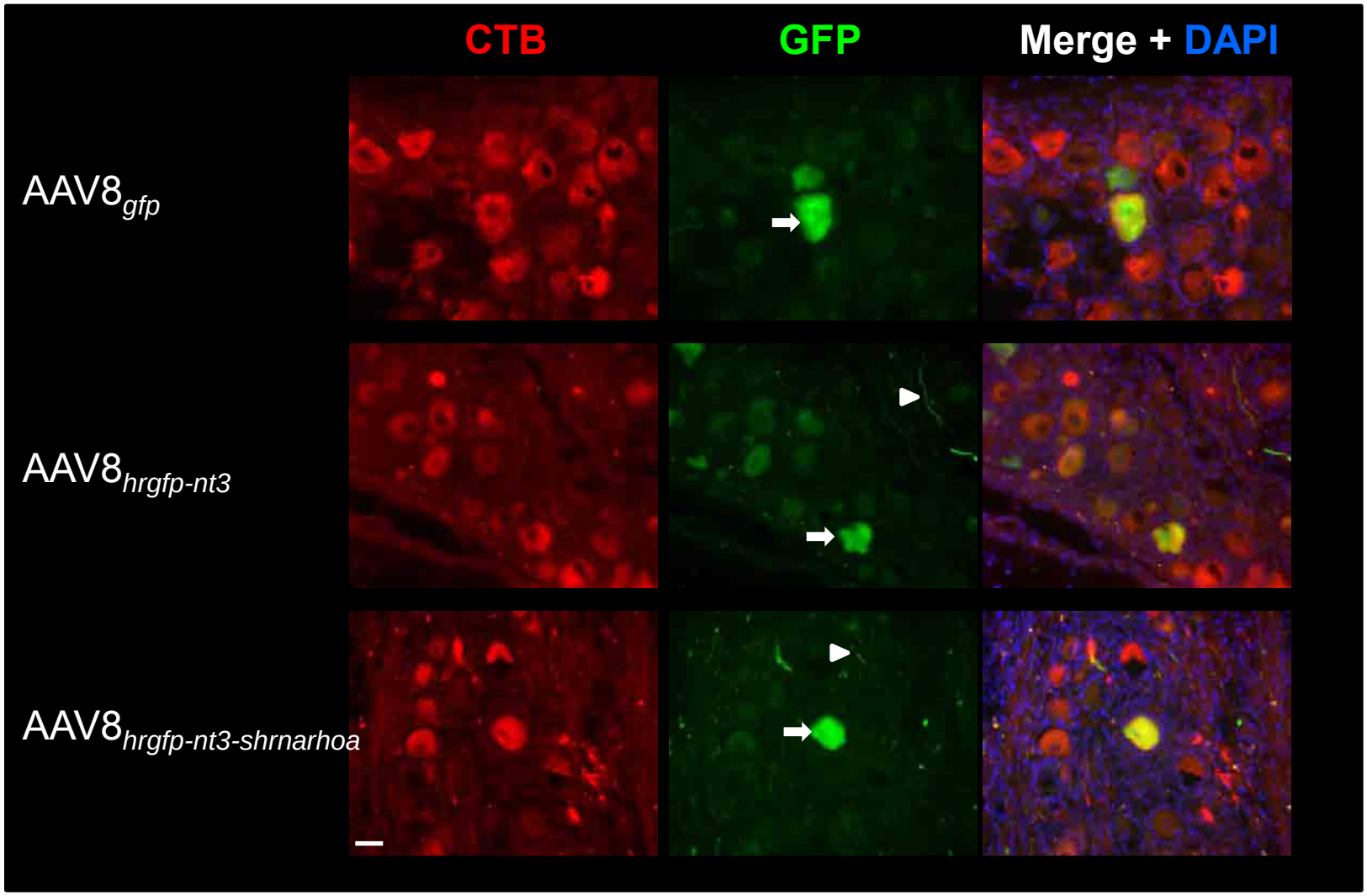


**Figure 6.1** Co-localisation of CTB and GFP in the DRG. Large diameter GFP+ DRGN (arrows) are seen in particular to co-express CTB. GFP+ axons (arrowheads) display minimal CTB immunoreactivity in the DRG. Scale bar = 50μm.

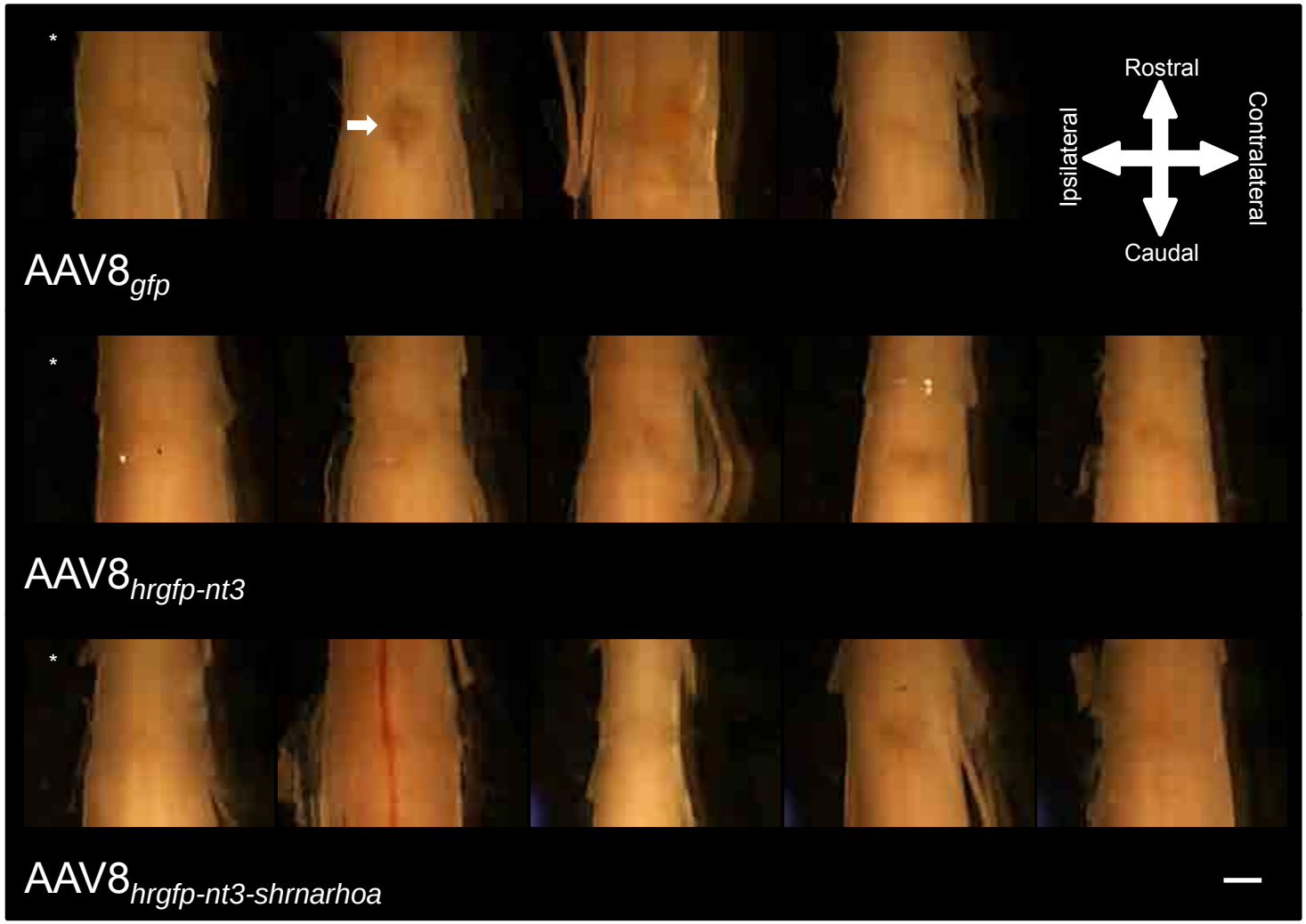


**Figure 6.2** Gross pathological appearances of L1 DC crush sites 28dpl. AAV8 vectors were administered to the left (ipsilateral) L4 and L5 DRG 28d prior to lesioning. Note typical cystic lesion sites (e.g. arrow) extending between the left and right dorsal root entry zones. The lesions labelled with a (*) were subjected to further histological analysis. Scale bar = 1mm.

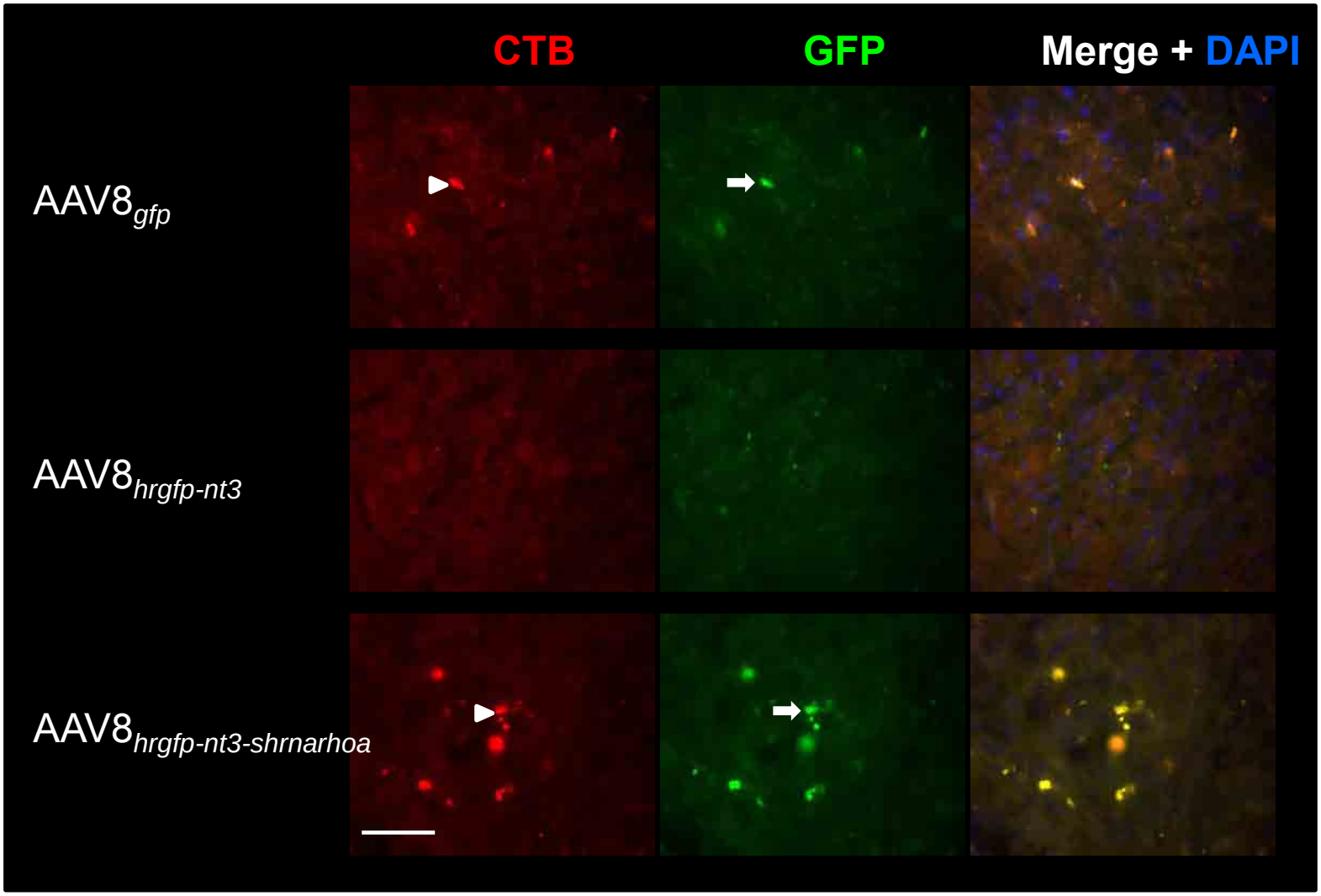


**Figure 6.3** CTB and GFP expression in the gracile nucleus at the level of the obex in AAV8-injected, DC lesioned animals. In most cases, GFP+ terminals (arrows) are seen to co-express CTB (arrowheads). Scale bar = 50µm.

The animal from the NT3 group showed only very low levels of GFP and CTB in the gracile nucleus.

### 6.2.4 Differences were seen in the appearance of the lesions and surrounding cord in the three animals that were analysed using GFAP immunohistochemistry

The lesion site from the animal analysed in the GFP group was cystic, extending approximately 1mm into the dorsal spinal cord, with a clearly defined accessory glia limitans (Figure 6.4 A, white arrowhead). Occasional morphologically identified macrophages were seen in the core of the lesion, but many were seen in the white matter 1mm rostral to the lesion (Figure 6.7 arrows). Additionally, there was what appeared to be GFP+ debris occasionally within and caudal to the lesion, but mostly in the 1mm rostral to the lesion (Figure 6.7, arrowheads). Very infrequent GFP+ axons in the DC were seen rostral (Figure 6.4 C) and caudal (Figure 6.4 D) to the lesion.

The lesion site from the animal in the NT-3 group was cystic, extending approximately 750μm into the dorsal spinal cord with a relatively weakly GFAP+ accessory glia limitans (Figure 6.5 A, 6.7). The lesion core was filled with macrophages and GFP+ debris. There was a large amount of hrGFP in the grey matter deep to the lesion. Much of this hrGFP seemed to be present within neurones, identified by their large DAPI+ nuclei. What were presumed to be hrGFP+ axons were seen caudal to the lesion in the DC, although the pattern of hrGFP

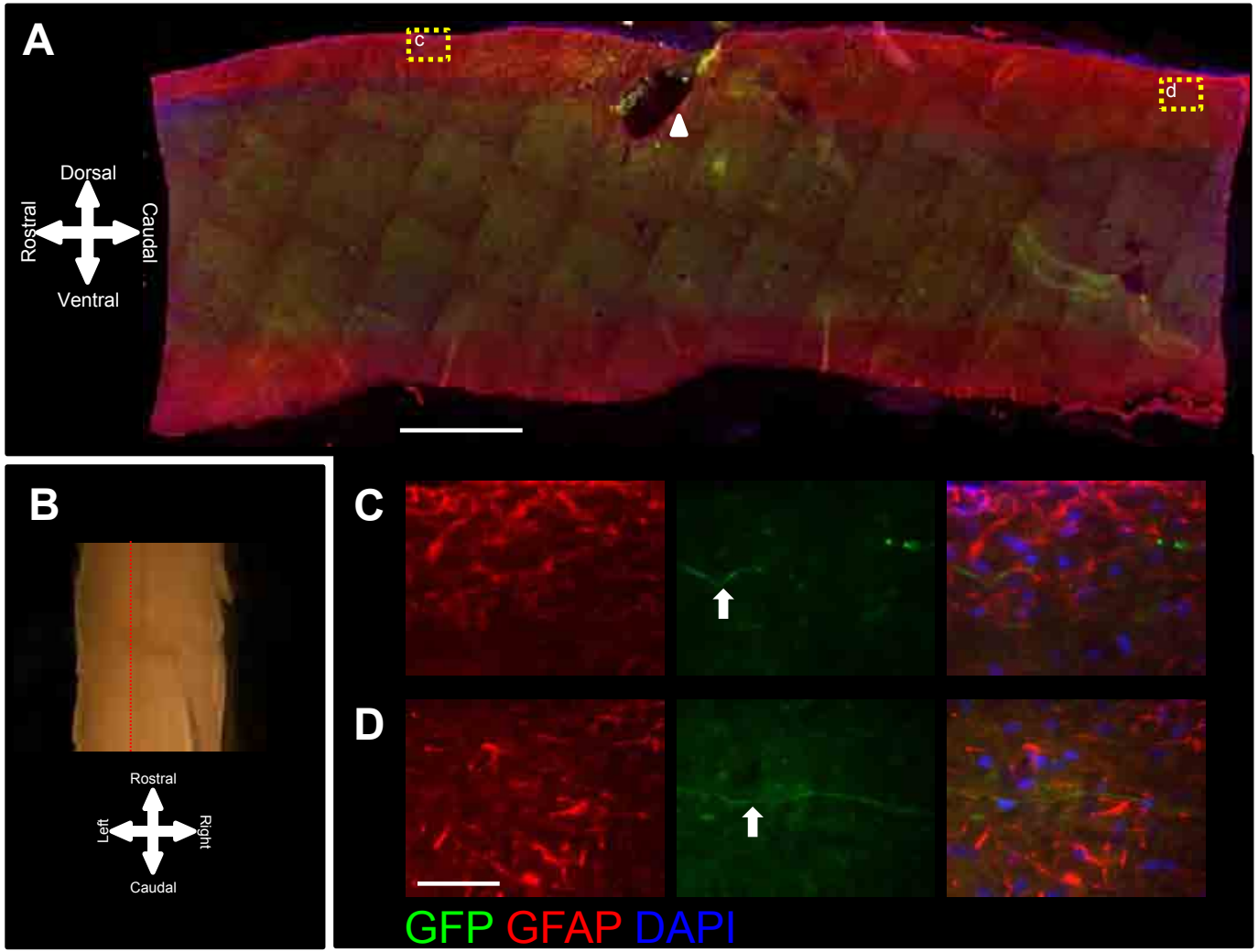


**Figure 6.4** Expression of GFP and GFAP after DC lesion in an animal receiving intra-DRG AAV8$_{gfp}$ to the left L4/L5 DRG 28d prior to lesioning. **A**. Composite image of a parasagittal section from approximately 200µm to the left of the midline (depicted in **B**). White arrowhead indicates accessory glia limitans. **C**. High magnification view of a GFP+ axon (arrow) rostral to the lesion in region in **Ac**. **D**. High magnification view of a GFP+ axon (arrow) caudal to the lesion in region **Ad**. Scale bar for **A** = 1mm, **C**, **D** = 50µm.

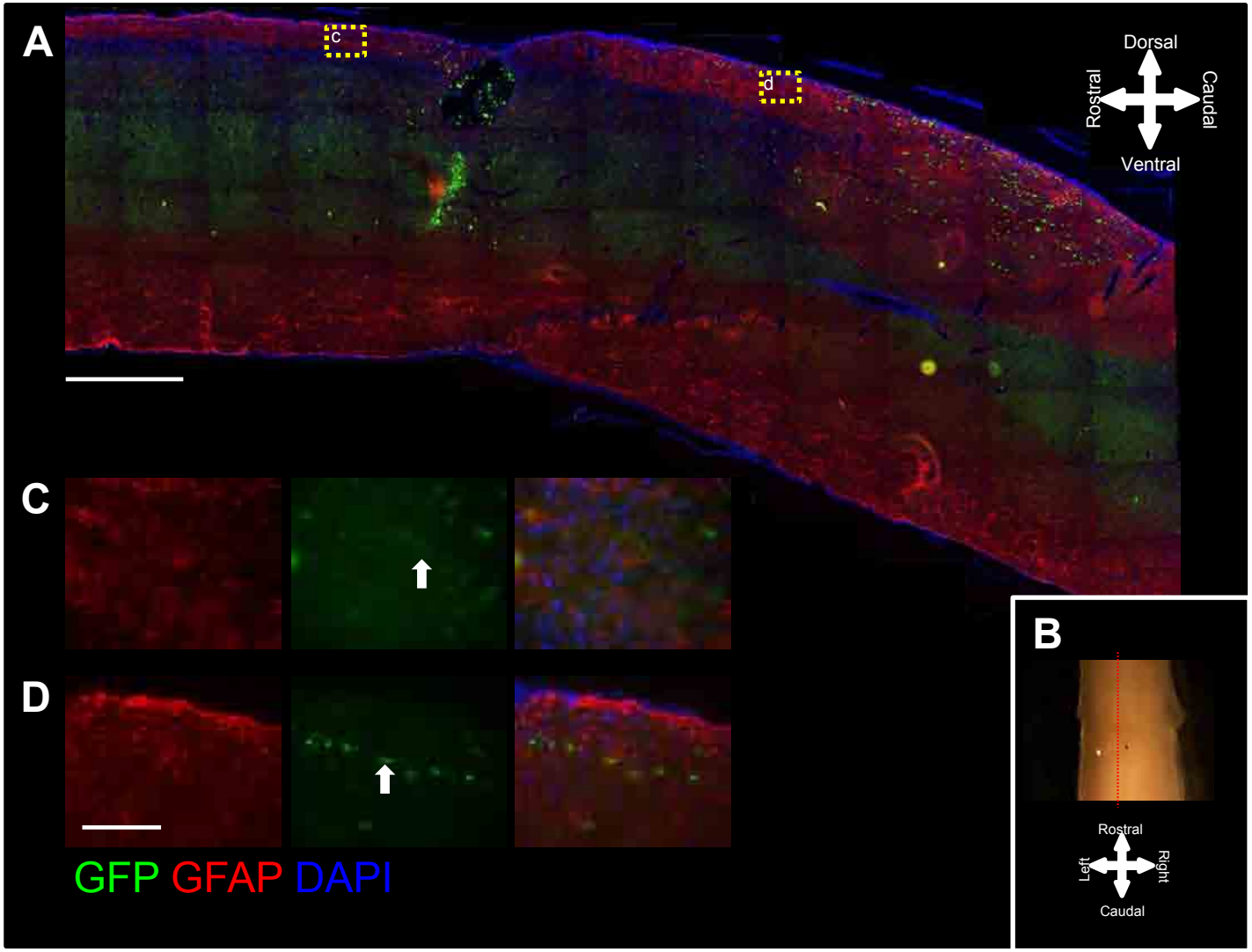


**Figure 6.5** Expression of hrGFP and GFAP after DC lesion in an animal receiving intra-DRG AAV8$_{hrgfp\text{-}nt3}$ to the left L4/L5 DRG 28d prior to lesioning. **A**. Composite image of a parasagittal section from approximately 200µm to the left of the midline (depicted in **B**). **C**. High magnification view of an hrGFP+ axon (arrow) rostral to the lesion in region in **Ac**. **D**. High magnification view of an hrGFP+ axon (arrow) caudal to the lesion in region **Ad**. Scale bar for **A** = 1mm, **C**, **D** = 50µm

expression was predominantly linearly punctuate, with few very obvious, intact axons (Figure 6.5 D). Rostral to the lesion, extremely infrequent axons were seen, expressing low levels of hrGFP (Figure 6.5 C).

In the NT3-shRNA$_{RhoA}$ animal, the lesion site had a different morphology compared to the other groups. The lesion cavity appeared to be smaller and there was a poorly defined accessory glia limitans making assessment of its extent difficult (Figure 6.6 A). The lesion core contained macrophages and occasional hrGFP+ debris. The number of macrophages in the lesion and rostrally were much higher than in the other two groups. Also, there was much more hrGFP+ debris rostral to the lesion (Figure 6.7). Caudal to the lesion, many intact hrGFP+ axons were seen as well as hrGFP in a linear punctuate arrangement (Figure 6.6 D). At the level of the lesion in the DC, occasional intact hrGFP+ axons were seen, following the familiar trajectory of DC axons (Figure 6.6 E), whereas rostral to the lesion some hrGFP+ axons possessing terminal swellings were observed in the DC (Figure 6.6 C).

### 6.2.5 CTB immunostaining failed to demonstrate axons adequately

CTB immunohistochemistry proved disappointing, leading to very high background levels and consequent poor signal-to-noise ratios (Figure 6.8). CTB was predominantly seen in terminals ending in the dorsal horn (Figure 6.8 A, C), and never seen to be present in axons (Figure 6.8 D). This is to be contrasted with GFP expression, which does label axons and terminals with a high signal-to-noise ratio.

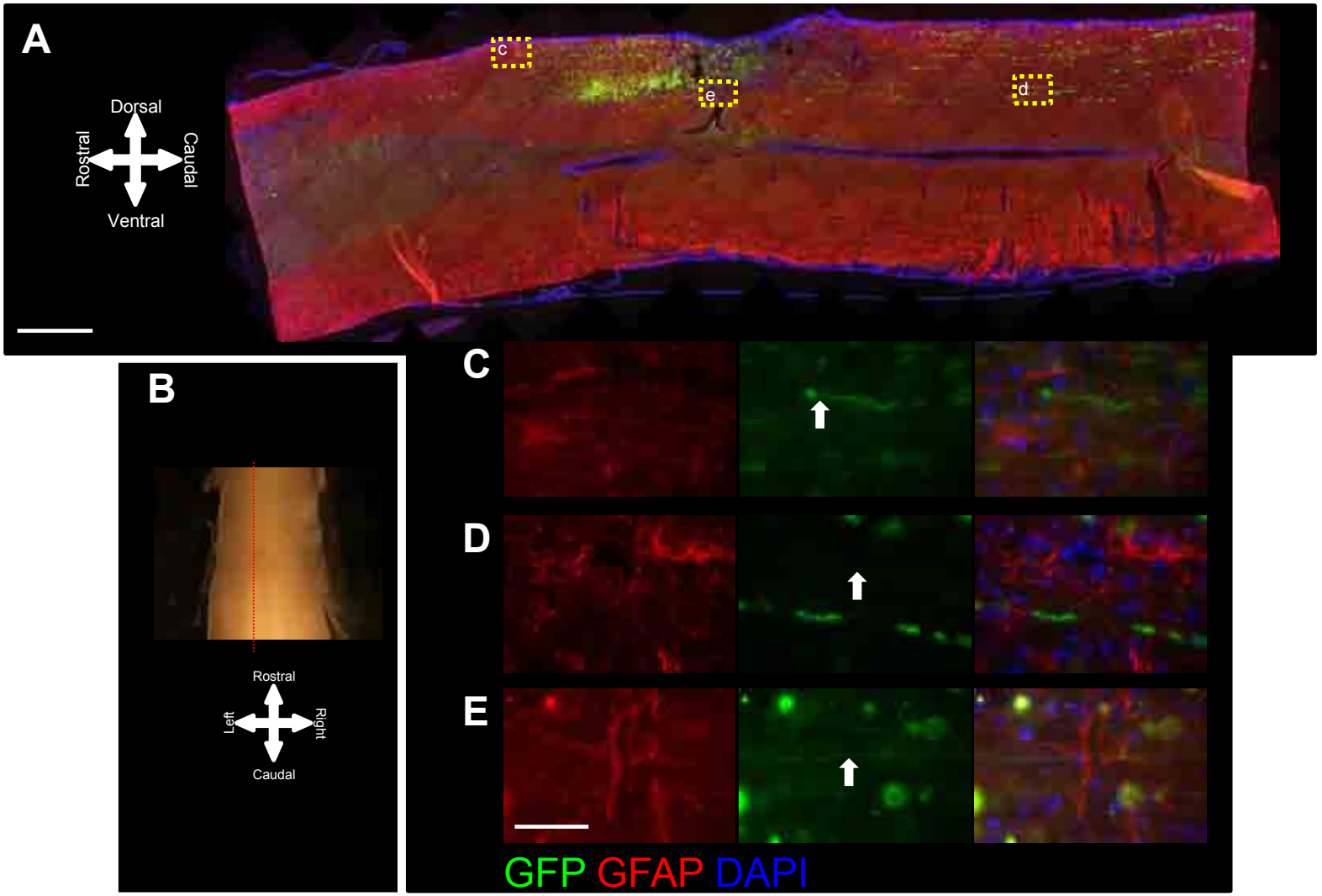


**Figure 6.6** Expression of hrGFP and GFAP after DC lesion in an animal receiving intra-DRG AAV8$_{hrgfp\text{-}nt3\ \text{-}shrnarhoa}$ to the left L4/L5 DRG 28d prior to lesioning. **A**. Composite image of a parasagittal section from approximately 200µm to the left of the midline (depicted in **B**). **C**. High magnification view of an hrGFP+ axon (arrow) rostral to the lesion in region in **Ac**. **D**. High magnification view of an hrGFP+ axon (arrow) caudal to the lesion in region **Ad**. **E**. High magnification view of an hrGFP+ axon (arrow) at the level of the lesion site. Scale bar for **A** = 1mm, **C**, **D** = 50µm

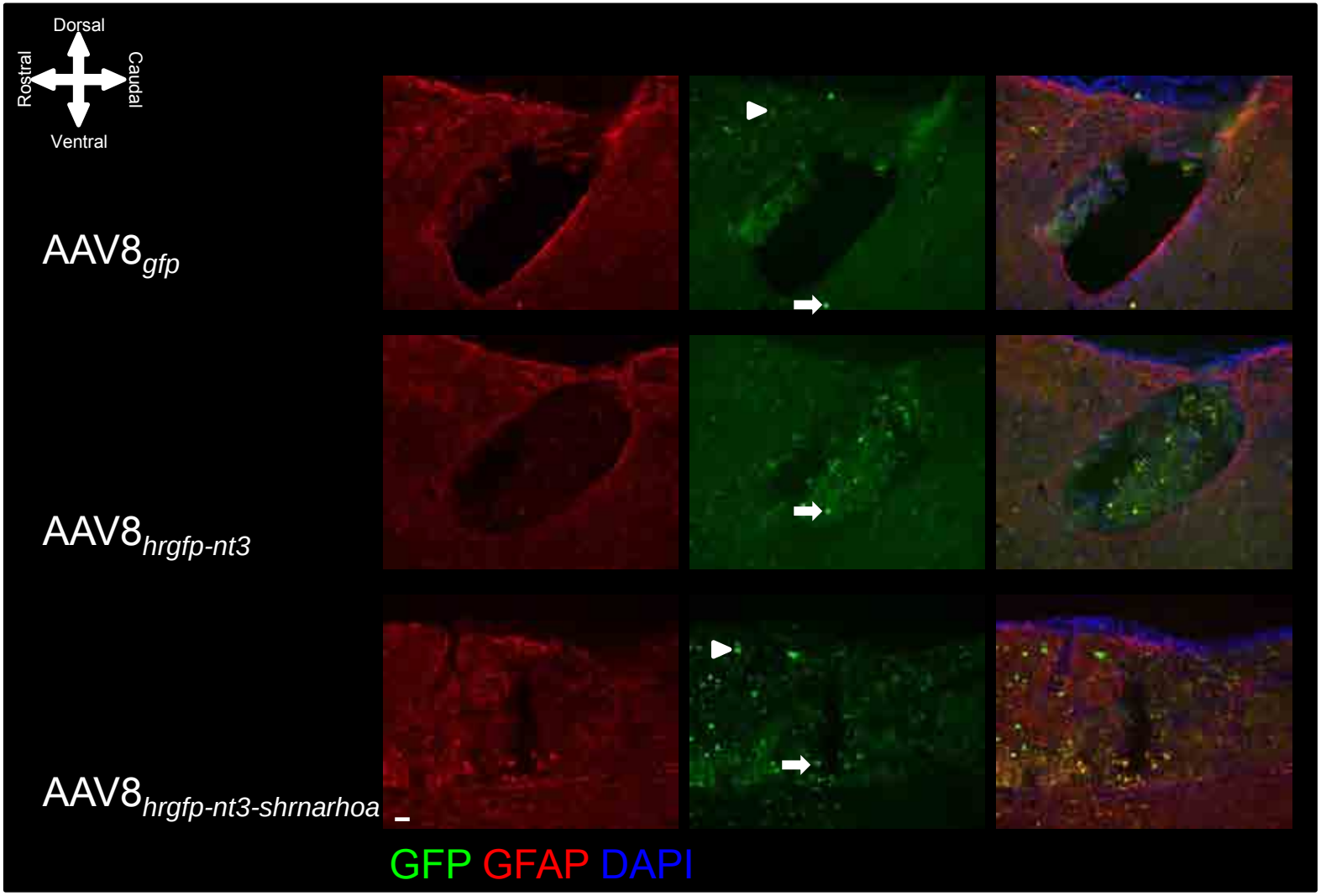


**Figure 6.7** GFAP immunohistochemistry on parasagittal sections of lesion sites showing more detailed morphology. Morphologically identified macrophages (arrows) can be seen within and occasionally rostral to the lesion site. Additionally, GFP+debris (arrowheads) can frequently be seen rostral to the lesion. Scale bar = 50μm.

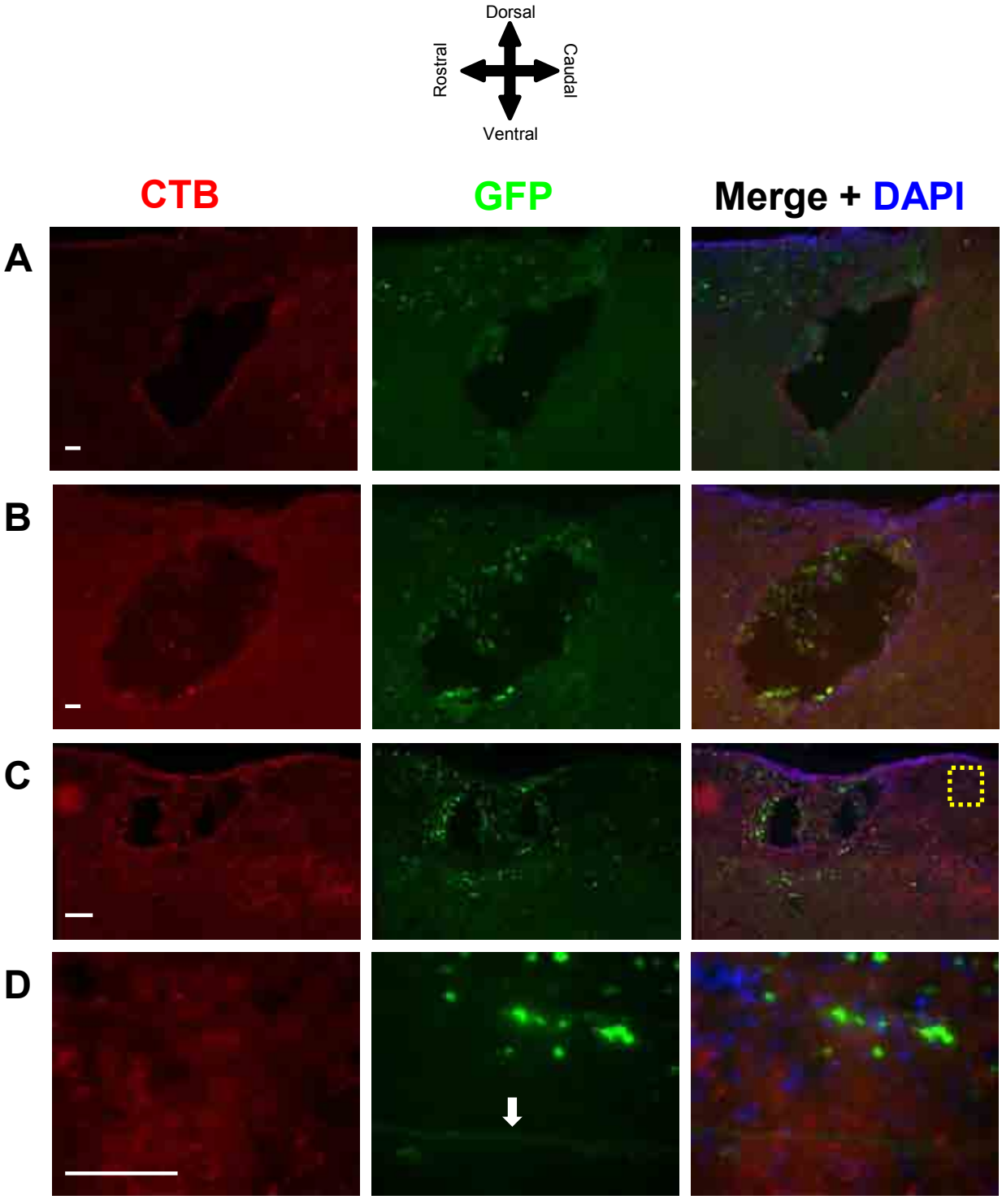


**Figure 6.8** The appearance of CTB immunostaining in DC lesion sites from animals injected with AAV8$_{gfp}$ (**A**), AAV8$_{hrgfp\text{-}nt3}$ (**B**) and AAV8$_{hrgfp\text{-}nt3\text{-}shrnarhoa}$ (**C, D**). **D** is a high power view of the region demarcated by the yellow box in **C**, showing a GFP+ axon (arrow). Scale bar = 50μm.

# Discussion

### 6.3.1 CTB and GFP were found to co-localise

That CTB preferentially labels large-diameter DRGN is corroborated in the literature (Liu, Llewellyn-Smith et al. 1995). The mechanism of this is probably differential expression of the ganglioside GM1 between different classes of DRGN (Gong, Tagawa et al. 2002). The above observation, combined with the fact that AAV8 has a tropism for large diameter DRGN, makes CTB a promising tool for assessing axon regeneration in AAV8-treated animals.

### 6.3.2 The gracile nuclei contained GFP and CTB

The gracile nuclei were examined in order to assess the completeness of the lesion in each animal. The presence of CTB and GFP in the gracile nuclei of all animals examined probably suggests that the lesions were incomplete. The background to this was discussed in the Introduction, but it is worth re-iterating at this point. When performing partial lesions, it is always a possibility that some axons may be spared – either missed or not completely transected (Steward, Zheng et al. 2003). In order to account for this, one must take a number of precautions. Firstly, the lesion must be planned carefully taking into account the species and age of animals and the necessary dimensions of the lesion. Secondly, the lesion must be performed carefully and as accurately as possible to maximise the probability of transecting all of the axons in the region of interest. Finally, one must ensure that lesioned animals are left for an appropriate amount of time before sacrificing. These three points will be discussed below with respect to the present study.

The lesion was planned so as to transect the DC of adult rats bilaterally to a depth of 1.5mm, medial to the dorsal root entry zones at the L1 spinal cord level. Referring to a rat spinal cord atlas confirms that the depth and width of the planned lesion in adult animals was more than adequate to transect all of the axons in the DC (Watson 2009).

The lesion was performed by Professor Martin Berry, an expert in the field of CNS regeneration. Fine jeweller's forceps were used, marked to a depth of 1.5mm. The lesions were performed by hand under direct vision using operating microscope. Despite these rigorous precautions, it is likely that the fact that the lesions were performed by hand, along with other factors, contributed to their being incomplete. During the operation, the meninges were left intact. This combined with the presence of blood and CSF within the wound may have led to the forceps being inserted to an inadequate depth since the 'surface' of the cord would have been misjudged. Additionally, any lesions performed by hand naturally will result in a higher variability than those performed using mechanical devices due to inherent human error.

Animals were left for 28d after lesioning. Although it is not known what the rate of regeneration in the spinal cord is, this is probably a reasonable period of time based on the estimates found in the literature (Steward, Zheng et al. 2003). The work of Steward et al. postulates that the theoretical maximum rate of axon regeneration in the CNS is 1mm per day. It is probably reasonable to assume that axon

regeneration occurs more slowly than this in the CNS due to the inhibitory environment. Additionally, severed axons probably take some time to recover from transection. In rats the distance from the L1 cord segment to the medulla is approximately 5cm, meaning that any CTB seen in the medulla 28dpl is extremely likely to represent spared axons and not regeneration.

Thus, it seems likely that a high proportion of the lesions performed in the present study were incomplete. However, one must also be mindful that treatments themselves may modulate the level of axon sparing, for example the possible conditioning effect of intra-DRG injection and the direct effects of NT-3 administration and RhoA antagonisation (see below for further discussion).

### 6.3.3 The lesioned spinal cord in the animal from the GFP group manifested features consistent with the literature

Consistent with the present findings, Lagord et al. observed axonal debris within macrophages within and rostral to the lesion 28d after a DC crush (Lagord, Berry et al. 2002). Additionally, in agreement with the present study, Lagord et al. noted a GFAP+ accessory glia limitans had formed by the first week post lesion.

The presence of morphologically identified macrophages rostral to the lesion probably correlates with a high level of phagocytic activity, necessary for the removal of degenerating axonal components. It must be noted that on morphological grounds

it is very difficult to differentiate activated macrophages from fully activated microglia (David and Kroner 2011).

### 6.3.4 Much more GFP+ material was seen in the animals from the NT-3 and NT3-shRNA groups than the animal in the GFP group

Before making any further comments on comparative aspects of the morphology of the lesions examined in this study, the author would like to emphasise a technical point. In preparing the tissues for this study, it was impossible to get the same orientation of the tissue specimens across all of the groups. Specifically, it may be the case that lesion sites that were sectioned were angulated slightly differently leading to subtle differences in the appearance of the tissue. This can be assessed by looking at the organisation of white and grey matter within each section. Despite this, the reader is reassured that lesion sites are all from the same place (approximately 200μm to the left of the midline – this was achieved by taking the fourth section that came off after the central canal was seen at the level of the lesion), allowing reasonably valid comparisons to be made at lesion sites and the perilesional area.

Hardly any GFP+ axons or debris was seen around the lesion in the animal from the GFP group. This could be due to a number of reasons. It may have been the case that the intra-DRG injections in this animal were unsatisfactory compared with those performed on the other animals. The animal looked at in the GFP group was the first to be injected in this experiment. Intra-DRG injections are not performed regularly by

Professor Berry, and it may be that a 'training effect' occurred, as the operator performed more injections. However, this seems unlikely since for every intra-DRG injection, the DRG is directly seen to swell. However, it is worth reminding the reader of the inherent variability of this injection technique (see Chapter 4, Table 1).

A second possibility is that a DC lesion provided a fourth 'hit' to already damaged DRGN (see Chapter 5 for the 'triple hit hypothesis'). The additional insult of a DC lesion may have led to catastrophic loss of DRGN and subsequent clearance of the GFP+ axonal debris. Could the large amount of GFP seen in the animals injected with $AAV8_{hrgfp\text{-}nt3}$ and $AAV8_{hrgfp\text{-}nt3\text{-}shrnarhoa}$ be due to neuroprotective effects of their therapeutic payloads? The answer to this question is impossible to address without examining the other animals in each group.

A final, vital point to consider is the fact that in this experiment two different types of GFP were delivered. $AAV8_{gfp}$ gave expression of eGFP – a modified form of *Aequorea* GFP (Zhang, Gurtu et al. 1996). $AAV8_{hrgfp\text{-}nt3}$ and $AAV8_{hrgfp\text{-}nt3\text{-}shrnarhoa}$ give expression of hrGFP, derived from the sea pansy *Renilla* (Lorenz, Cormier et al. 1996). In the present study, only the inflammatory characteristics of eGFP delivered by AAV8 have been studied. Nothing is known about inflammatory responses to hrGFP. It may be the case that hrGFP is less toxic than eGFP, meaning that DRGN in animals injected with $AAV8_{gfp}$ may be under less cellular stress than those in the other two groups. This issue cannot be resolved with the data available presently.

An interesting observation in the animal from the NT-3 group was the presence of large numbers of what may have been GFP+ neurones deep to the lesion site. Without further characterisation, it is possible that these could have been macrophages although their deep location and minimal auto-fluorescence seems to preclude this. It is likely that after intra-DRG injection of AAV8 vectors, some particles enter the CSF, and are capable of transducing contralateral DRGN (see Chapter 4). In the case of the result described above, it is possible that AAV8$_{hrgfp\text{-}nt3}$ present in the CSF could have been able to access neurones in the spinal cord grey matter following tissue disruption caused by the DC lesion. It is known that AAV8 cannot normally cross the spinal cord pia mater, so the above explanation seems plausible (see Chapter 4 Discussion).

### 6.3.5 Animals from the NT-3 and NT3-shRNA groups showed features consistent with axonal degeneration

Irrespective of whether differences exist between the inflammatory characteristics of eGFP and hrGFP, the issue of the high levels of axonal fragmentation must be addressed. The morphology of the vast majority of axons in animals receiving AAV8$_{hrgfp\text{-}nt3}$ and AAV8$_{hrgfp\text{-}nt3\text{-}shrnarhoa}$ was of linearly arranged, discontinuous GFP+ blebs. This is clearly not normal, and contrasting to the situation seen in unlesioned animals, where many axons do display swellings, but often as part of an intact axon (see Chapters 4 and 5).

The phenomenon of axon dieback, where axon terminals are seen sometimes up to several millimetres from the lesion site is already recognised after SCI (Ramon y Cajal 1991; McPhail, Stirling et al. 2004). Frequently these axons display abnormal morphologies including swellings, usually at or near their terminals. The pattern of hrGFP expression seen in lesioned animals injected with AAV8$_{hrgfp\text{-}nt3}$ and AAV8$_{hrgfp\text{-}nt3\text{-}shrnarhoa}$ is not wholly consistent with simple axonal dieback, since GFP+ swellings are seen throughout the length of the axon both rostral and caudal to the lesion. The picture is much more consistent with anterograde and retrograde axonal degeneration.

The presence of features of anterograde (or Wallerian) axonal degeneration rostral to the lesion site does not come as a surprise in this study, since this is a phenomenon that has been observed repeatedly over at least the last century (Ramon y Cajal 1991). At the time of the lesion (28d post injection), many axons in the DC would have been GFP+, and their distal stumps would have undergone degeneration regardless of whether they eventually regenerated or not. The fact that there is a large amount of GFP+ axonal debris rostral to the lesion even at 28dpl is consistent with the extremely slow rate of Wallerian degeneration in the CNS (Vargas and Barres 2007). Studies of axonal degeneration in the spinal cord using mice stably expressing fluorescent proteins in neurones have shown similar appearances of axons undergoing anterograde degeneration to that found here, although at earlier time points (Kerschensteiner, Schwab et al. 2005). Wallerian degeneration has also been studied in the PNS of YFP mice, displaying virtually identical features of

anterograde axonal degeneration seen in the present study, but occurring much more quickly (Beirowski, Adalbert et al. 2005).

The observation of features consistent with retrograde degeneration in animals from the NT-3 and NT3-shRNA groups is interesting, and somewhat unexpected. The mechanism of this phenomenon may be (i) the lesioned, transduced DRGN survive but the remnants of the proximal portions of their axons degenerate or (ii) the lesioned, transduced DRGN die and as a consequence all of their projections degenerate. Unfortunately, the data available do not allow this issue to be resolved. In support of (i), it has been observed that axons proximal to a lesion can degenerate distances of up to 3mm (Wang, Hu et al. 2009). However, in the present study, features of axon degeneration were seen throughout the proximal DC. It is not clear what the proximal extent of retrograde axonal degeneration in the DC is. Furthermore, there were no features in the DRG consistent with DRGN death or degeneration of axons (e.g. GFP+ debris). Thus, it would appear from this very preliminary study that transduced, axotomised DRGN do survive but undergo considerable levels of retrograde degeneration. It must not be forgotten, however, that there were still intact axons observed caudal, rostral and in some cases at the level of the lesion.

### 6.3.6 Did axon regeneration occur in any of the animals?

Firstly, it must be emphasised that it appears that none of the lesions were complete as evidenced by the presence of GFP and CTB in the gracile nuclei of lesioned

animals. Does this preclude any comment on axon regeneration? The answer is 'not necessarily', although extreme caution must be exercised. For a full analysis it is necessary to examine all of the lesioned animals in all groups and to repeat the experiment using a different protocol if lesions are consistently incomplete.

Before discussing axon regeneration, it is worth considering any alternative explanations for the presence of GFP and CTB in the gracile nuclei of lesioned animals. Could it be that the lesions were incomplete not as a consequence of technical factors, but because of some effect of the treatments? In other words, could the treatments have protected axons from being damaged? There are insufficient data to confirm or refute this idea, although feasible biological mechanisms exist related to both the viral vectors and their therapies. For example, as shown in Chapter 5, $AAV8_{gfp}$ generates an inflammatory response in the DRG. It is reasonable to assume that the therapeutic vectors also generate a similar response, and it is known that the presence of macrophages around neuronal cell bodies can have anti-apoptotic effects (Ahmed, Aslam et al. 2010). Since axon degeneration shares many features with apoptosis, could it be possible that axons are protected from the effects of lesions by inflammation (Vargas and Barres 2007)? It does, however, seem difficult to accept that neuroprotective therapies could protect axons from direct physical damage.

With respect to the therapeutic vectors, it is possible that NT-3 delivery could also have a protective effect on axons *via* the mechanism described above since NT-3 is

known to be anti-apoptotic (Kuo, Simpson et al. 2005). Knockdown of RhoA may even be predicted to have an adverse effect on axonal resilience after injury, since this treatment may adversely affect cytoskeletal dynamics.

Examination of the morphology of non-degenerating axons in the three groups reveals that the overwhelming majority look like normal DC axons. This is consistent with an incomplete lesion. The only axon with a morphology consistent with regeneration was seen in the animal treated with AAV8$_{hrgfp\text{-}nt3\text{-}shrnarhoa}$ (Figure 6.6 C). This axon, found in the DC rostral to the lesion had what appeared to be a hrGFP+ terminal growth cone. This is unlikely to represent a dystrophic end-bulb as it lies approximately 1mm distal to the lesion. It is of course possible that this could be an axonal swelling on an intact axon, the distal segment of which was not present in the section. However, no other intact axons with swellings were seen in this region.

### 6.3.7 CTB immunostaining failed to demonstrate axons adequately

Disappointingly, CTB immunohistochemistry did not demonstrate axons adequately due to its high level of background staining and absence in axons. The high background was probably due to the use of thick sections (25µm) and inadequate blocking. Thick sections were used to give the best chance of preserving tissue morphology (thin sections fold on themselves and distort easily).

CTB staining was restricted to terminals of sensory neurones. Indeed, CTB has frequently been used to label projection areas in grey matter (LaMotte, Kapadia et al. 1991). However, many other workers have used CTB to successfully demonstrate axons in tracts such as the DC (Bradbury, Khemani et al. 1999). No essential differences existed between the protocol for CTB tracing used in the present study compared with the consensus in the literature, resulting in a frustrating situation (Zhang, Dijkhuizen et al. 1998; Bradbury, Khemani et al. 1999; Kadoya, Tsukada et al. 2009). It is worthwhile attempting to optimise CTB delivery by altering parameters such as the batch or brand of toxin used, the quantity injected, the technique of injection and length of time before sacrificing animals. Additionally, detection may be improved by increasing the concentration of blocking reagents, maximising tissue penetration of antibodies by increasing the concentration of detergents, using a different antibody or different detection technique (e.g. HRP *versus* immunofluorescence) or using thinner (or even thicker) sections. From a recent discussion at the International Spinal Research Trust Network Meeting, it seems highly likely that protocols employing free-floating sections will be successful (Ann Logan, personal communication).

### 6.4 Further work

This Chapter has dealt with only very preliminary data from a pilot experiment. The further work can be split into categories, namely: completion of replicates, further characterisation of the therapeutic vectors, confirmation of therapeutic bioactivity, further assessment of lesion characteristics and addition of further experimental groups.

***Completion of replicates***

Clearly, in order to provide a full characterisation of the axon regenerative effects of the therapeutic vectors, all animal in each group must be subjected to immunohistochemical analysis

***Further characterisation of therapeutic vectors***

It is necessary to confirm that the transduction rates and tropisms of the therapeutic vectors are comparable to that seen for the control vector $AAV8_{gfp}$ in order to make valid comparisons between treatment and control groups. Furthermore, it must be shown that the glial and inflammatory responses of the therapeutic vectors are comparable to the control.

***Confirmation of therapeutic bioactivity***

It is important to confirm that what was seen *in vitro* (see Chapter 3) was also present *in vivo* – namely, production of NT-3 in the DRG and knockdown of RhoA in DRGN. This could be shown by quantitative immunohistochemistry for NT-3 and RhoA on DRG sections. Furthermore, the reader is reminded that the NT-3 that was delivered in these experiments was human. Human and rat NT-3 share the same primary sequence but have differences in their signal peptides (Maisonpierre, Belluscio et al. 1990; Maisonpierre, Le Beau et al. 1991). It would be possible to show by quantitative PCR the relative amounts of human (exogenous) and rat (endogenous) NT-3 present in the DRG.

***Further assessment of lesion characteristics***

If, upon completion of replicates, it was found that the majority of lesions were incomplete, it would be necessary to attempt to optimise the lesioning protocol. This may involve calibration of lesion depth or even necessitate changing the lesioning technique, for example using a mechanical or stereotactic device.

It would be informative to further characterise the lesions histologically and immunohistochemically, namely by measuring lesion volumes and staining for macrophages, activated microglia and oligodendrocytes. Additionally, immunohistochemical amplification of the GFP signal may demonstrate more axons around the lesion site.

***Further experimental groups***

Ideally, a number of additional control groups should be added to the experiment. These were not included originally due to time and financial constraints. He additional groups should include sham injected, lesioned animals; PBS injected lesioned animals; a group receiving AAV8$_{hrgfp}$ (this vector was not available) and a lesion and also a group receiving AAV8$_{hrgfp\text{-}shrnarhoa}$ (this vector was not available). Furthermore, it is necessary to ascertain whether the therapeutic vectors have any effects on the normal, uninjured spinal cord (e.g. increased sprouting, neuronal death etc.).

# General Discussion

In this Chapter, the major findings of the present study will be presented followed by a distillation of these results, putting them into context and highlighting any important general principles. The author hopes that the reader will some key 'take-home' messages from the following pages.

## 7.1 Summary of findings

### Chapter 3 – Production and validation of AAV constructs

Specific hypotheses

- Delivery of NT-3 to adult rat DRGN *in vitro* augments survival and stimulates neurite outgrowth
- Knockdown of RhoA by transfection of an shRNA against RhoA will lead to disinhibited neurite outgrowth and diminution of RhoA protein levels

Major findings

- rhNT-3 supported survival but not neurite outgrowth of dissociated rat DRGN *in vitro*
- High concentrations of FLAG-tagged NT-3 were detected by Western blotting and ELISA in conditioned medium from COS-1 cells transfected with pAAV-CMV-NT3-FLAG-IRES-hrGFP

- NT3-FLAG was not amenable to assessment of its biological activity, so it was decided to produce plasmids containing untagged NT-3
- pFBGR-IRES-hrGFP-MCS was generated by overlap extension PCR of a NotI site in pAAV-IRES-hrGFP followed by sub-cloning of its IRES-spanned region into pFBGR
- A human NT-3 sequence was obtained, and its sequence confirmed (hNT-3)
- The hNT-3 sequence was inserted into pFBGR-IRES-hrGFP-MCS yielding pFBGR-CMV-NT3-IRES-hrGFP
- An shRNA sequence was identified that was capable of maximally knocking down the expression of RhoA ($shRNA_{RhoA}$)
- The $shRNA_{RhoA}$ sequence was inserted into pFBGR-CMV-NT3-IRES-hrGFP yielding pFBGR-IRES-hrGFP-NT3-$shRNA_{RhoA}$
- pFBGR-CMV-NT3-IRES-hrGFP and pFBGR-IRES-hrGFP-NT3-$shRNA_{RhoA}$ were sent to the University of Iowa's Gene Transfer Vector Core for production of $AAV8_{hrgfp\text{-}nt3}$ and $AAV8_{hrgfp\text{-}nt3\text{-}shrnarhoa}$, respectively

Hypothesis 1 was partially supported, hypothesis 2 was not conclusively supported or refuted.

## Chapter 4 - Assessment of the cellular tropism of AAV8 in the DRG using two different delivery methods

Specific hypotheses

- AAV8 transduces all subtypes of DRGN with equal frequency *in vitro* and *in vivo* regardless of delivery route – there is no cellular tropism
- Transduction of DRGN will correlate with the level of expression of LMR
- The central projections of DRGN will be completely filled with GFP

Major findings

- $AAV8_{gfp}$ was capable of transducing DRGN after both intra-DRG and intrathecal injection
- $AAV8_{gfp}$ preferentially transduced large-diameter, parvalbumin$^{+}$ DRGN
- All DRGN were LMR$^{+}$
- The central projections of $AAV8_{gfp}$ transduced DRGN were labelled with GFP
- Preferential transduction of large diameter DRGN is lost *in vitro*

Hypothesis 1 was refuted, hypothesis 2 was refuted, hypothesis 3 was supported.

## Chapter 5 - Inflammatory and glial responses to AAV8 mediated transgene delivery

Specific hypotheses

- The delivery of $AAV8_{gfp}$ does not lead to an appreciable inflammatory response after either intra-DRG or intrathecal injection
- The delivery of $AAV8_{gfp}$ does not lead to an appreciable change in the level of CNS glial activation after either intra-DRG or intrathecal injection
- The delivery of $AAV8_{gfp}$ does not lead to degeneration of DRGN central projections

Major findings

- Macrophages infiltrated the DRG after intra-DRG and intrathecal delivery of $AAV8_{gfp}$
- Satellite cells upregulated expression of CD68 after intra-DRG and intrathecal delivery of $AAV8_{gfp}$
- Microglia and astrocytes were activated in the spinal cord after intra-DRG delivery of $AAV8_{gfp}$
- Microglia and astrocytes were not activated in the cord after intrathecal delivery of $AAV8_{gfp}$

- No degeneration of DRGN central axon projections occurred after intra-DRG delivery of AAV8$_{gfp}$
- There was no evidence of DRGN death after intra-DRG or intrathecal delivery of AAV8$_{gfp}$

Hypotheses 1 and 2 were refuted, hypothesis 3 was supported.

## Chapter 6 - A pilot experiment to examine the effect of AAV8 mediated delivery of NT-3 and shRNARhoA to DRGN on axon regeneration in the DC

Specific hypothesis

- AAV8$_{hrgfp\text{-}nt3\text{-}shrna\text{-}rhoa}$ and AAV8$_{hrgfp\text{-}nt3}$ transduction of DRGN *in vivo* mediates neurone survival and disinhibited regeneration of DC axons

Major findings

- After intra-DRG injection of AAV8$_{hrgfp\text{-}nt3\text{-}shrna\text{-}rhoa}$ and AAV8$_{hrgfp\text{-}nt3}$, GFP was present in large-diameter DRGN, co-localising with CTB
- No differences were observed in the gross pathological appearance of lesion sites from animals in different treatment groups
- GFP+/CTB+ terminals were seen in the medullas from the three animals that were analysed

- Hints of axon regeneration were observed in the animal injected with AAV8$_{hrgfp\text{-}nt3\text{-}shrna\text{-}rhoa}$

It was not possible to state whether the hypothesis for this chapter was either supported or refuted.

### 7.2 NT-3 is a worthwhile growth factor to use in SCI

A large proportion of this study focussed on demonstrating that NT-3 was an appropriate growth factor to stimulate regeneration of DRGN axons. Despite the fact that the present study failed to demonstrate any effect of NT-3 on neurite outgrowth in dissociated DRG cultures, it is very convincing from the literature that NT-3 is neuritogenic and activates the neurone's intrinsic growth state *in vitro* (Mohiuddin, Fernandez et al. 1995; Gavazzi, Kumar et al. 1999). Furthermore, a number of reports have shown NT-3 bioactivity in the injured spinal cord *in vivo*, both as a chemotropic agent as well as a stimulant of regenerative axon growth (Bradbury, Khemani et al. 1999; Alto, Havton et al. 2009).

The rationale for the delivery of an NT-3 expressing AAV vector to cell bodies in the DRG was to avoid the so-called 'neurotrophic sink' phenomenon observed when a neurotrophin is applied at lesion sites. Also, it was hoped that the long-term and stable levels of transgene expression provided by AAV vectors would provide a

strong and sustained trophic stimulus for axotomised DRGN. Only further analysis will show if this is an effective strategy in the injured DC.

### 7.3 The assessment of viral vector tropism both in vitro and in vivo should be an essential part of any gene therapy study

The fact that viral vectors display varying cellular tropisms is not unexpected and actually extremely welcome, especially in the case of AAV vectors, which have many natural serotypes. Only in recent years, however, has the detailed study of AAV tropism found prevalence in the literature (Vulchanova, Schuster et al. 2010; Fischer, Kostic et al. 2011). The significance of viral vector tropism is particularly profound in the nervous system, which contains discrete collections of neurones, which are not necessarily functionally identical. For example, the DRG houses a highly diverse population of sensory neurones that are known to project to CNS regions such as the dorsal horn, ventral horn, thoracic cord and medulla. It becomes immediately obvious that problems may arise if one were to deliver a viral vector directed at 'sensory neurones' without any prior knowledge of its cellular tropism. Of course, there may be a place for widespread transduction of sensory neurones but this is unlikely to become a recognised treatment modality of the future due to the diverse trophic needs of sensory neurones (Gavazzi, Kumar et al. 1999; Huang and Reichardt 2001). Aberrant stimulation of sprouting in, say, nociceptive neurones could lead to potentially disastrous consequences such as neuropathic pain (Eriksdotter Jonhagen, Nordberg et al. 1998; Nauta, Wehman et al. 1999).

A second, important observation from the present study was that the observed tropism of a viral vector can be modulated by the neuronal environment. The fact that AAV8 does not target large diameter DRGN *in vitro* points to the importance of not assuming that *in vitro* results can be translated to the *in vivo* situation. Clearly, this is a caveat that most biological scientists are aware of but it did come as something of a surprise to see this effect with AAV8 since it was assumed that viral tropism was predominantly determined by receptors on the cell surface. This should be the subject of much further study since it offers the potential for further 'fine-tuning' of viral tropism, maybe by modulating the extracellular matrix.

## 7.4 Potential inflammatory responses and neurotoxicity of viral vectors and transgenes must be taken seriously and be an essential part of any gene therapy study

It was not expected that AAV8$_{gfp}$ would generate an inflammatory response in the DRG or spinal cord since previous reports had shown that AAV vectors (and GFP) were relatively immunologically inert (Daya and Berns 2008). However, the results obtained in this study strongly pointed towards potential inflammatory responses to AAV8$_{gfp}$, and a subsequent literature search produced a number of reports describing neurotoxicity of GFP overexpression in neurones (see Chapter 5 for more). It is the author's opinion that there is significant publication bias in the literature concerning GFP neurotoxicity since many research groups rely extensively on animals that stably express fluorescent proteins. Also, studies employing Cre-Lox technology frequently use GFP-expressing viral vectors as controls (Park, Liu et al. 2008). Could

GFP-related neurotoxicity or inflammatory responses to viral vectors be confounding their results?

## 7.5 Combinatorial strategies for the treatment of SCI are effective and hold much promise for the future

Disappointingly, due to lack of time, the final analysis of axon regeneration in animals treated with the therapeutic viruses was not completed. However, there were a number of promising features present in the animals treated with AAV8$_{hrgfp\text{-}nt3\text{-}shrna\text{-}rhoa}$ and AAV8$_{hrgfp\text{-}nt3}$ – definitely enough to necessitate complete analysis of all the animals in the experiment in Chapter 6. It seems highly likely that combinatorial therapies will prove useful in the future. The majority of the most successful studies on axon regeneration have used combinations of therapies to elicit convincing anatomical restitution of damaged neural pathways. Recent work from Tuszynski's laboratory provides a particularly good example of this approach (Alto, Havton et al. 2009; Kadoya, Tsukada et al. 2009).

## 7.6 Final conclusion

The vast majority of scientific endeavour occurs as an incremental, often frustratingly slow progression of ideas. The study of CNS axon regeneration is no exception, although its history has been punctuated by a number of paradigm shifts, e.g. the works of Windle and Raisman (Windle and Chambers 1950; Raisman, Cowan et al. 1966). The author is under no illusion about the modest import of the ideas

contained in the previous pages, but hopes that the data collected during the course of his three years in the laboratory will at least stimulate other workers who read this to think about the implications of the results presented. For it is only by independent repetition and confirmation (or refutation) of experimental results that science can progress.

# References


Abram, S. E., J. Yi, et al. (2006). "Permeability of injured and intact peripheral nerves and dorsal root ganglia." Anesthesiology **105**(1): 146-53.

Aguayo, A. J., M. Vidal-Sanz, et al. (1987). "Growth and connectivity of axotomized retinal neurons in adult rats with optic nerves substituted by PNS grafts linking the eye and the midbrain." Ann N Y Acad Sci **495**: 1-9.

Agudo, M., M. Robinson, et al. (2005). "Regulation of neuropilin 1 by spinal cord injury in adult rats." Mol Cell Neurosci **28**(3): 475-84.

Ahmed, Z., M. Aslam, et al. (2010). "Optic nerve and vitreal inflammation are both RGC neuroprotective but only the latter is RGC axogenic." Neurobiol Dis **37**(2): 441-54.

Ahmed, Z., M. Berry, et al. (2009). "ROCK inhibition promotes adult retinal ganglion cell neurite outgrowth only in the presence of growth promoting factors." Mol Cell Neurosci **42**(2): 128-33.

Ahmed, Z., R. G. Dent, et al. (2005). "Matrix metalloproteases: degradation of the inhibitory environment of the transected optic nerve and the scar by regenerating axons." Molecular & Cellular Neurosciences **28**(1): 64-78.

Ahmed, Z., R. G. Dent, et al. (2005). "Disinhibition of neurotrophin-induced dorsal root ganglion cell neurite outgrowth on CNS myelin by siRNA-mediated knockdown of NgR, p75NTR and Rho-A." Molecular & Cellular Neurosciences **28**(3): 509-23.

Ahmed, Z., S. J. Jacques, et al. (2009). "Epidermal growth factor receptor inhibitors promote CNS axon growth through off-target effects on glia." Neurobiology of Disease **36**(1): 142-150.

Ahmed, Z., G. Mazibrada, et al. (2006). "TACE-induced cleavage of NgR and p75NTR in dorsal root ganglion cultures disinhibits outgrowth and promotes branching of neurites in the presence of inhibitory CNS myelin." FASEB Journal **20**(11): 1939-41.

Ahmed, Z., E. L. Suggate, et al. (2006). "Schwann cell-derived factor-induced modulation of the NgR/p75NTR/EGFR axis disinhibits axon growth through CNS myelin in vivo and in vitro." Brain **129**(Pt 6): 1517-33.

Akache, B., D. Grimm, et al. (2006). "The 37/67-kilodalton laminin receptor is a receptor for adeno-associated virus serotypes 8, 2, 3, and 9." J Virol **80**(19): 9831-6.

Almad, A., F. R. Sahinkaya, et al. (2011). "Oligodendrocyte fate after spinal cord injury." Neurotherapeutics **8**(2): 262-73.

Alto, L. T., L. A. Havton, et al. (2009). "Chemotropic guidance facilitates axonal regeneration and synapse formation after spinal cord injury." Nat Neurosci **12**(9): 1106-13.

Angeletti, R. H. and R. A. Bradshaw (1971). "Nerve growth factor from mouse submaxillary gland: amino acid sequence." Proc Natl Acad Sci U S A **68**(10): 2417-20.

Atwal, J. K., J. Pinkston-Gosse, et al. (2008). "PirB is a functional receptor for myelin inhibitors of axonal regeneration." Science **322**(5903): 967-70.

Bader, S. R., S. Kothlow, et al. (2010). "Acute paretic syndrome in juvenile White Leghorn chickens resembles late stages of acute inflammatory demyelinating polyneuropathies in humans." J Neuroinflammation **7**: 7.

Barde, Y. A., D. Edgar, et al. (1982). "Purification of a new neurotrophic factor from mammalian brain." Embo J **1**(5): 549-53.

Barrett, L. B., M. Berry, et al. (2004). "CTb targeted non-viral cDNA delivery enhances transgene expression in neurons." Journal of Gene Medicine **6**(4): 429-38.

Bechmann, I., I. Galea, et al. (2007). "What is the blood-brain barrier (not)?" Trends Immunol **28**(1): 5-11.

Bechmann, I., G. Mor, et al. (1999). "FasL (CD95L, Apo1L) is expressed in the normal rat and human brain: evidence for the existence of an immunological brain barrier." Glia **27**(1): 62-74.
Beirowski, B., R. Adalbert, et al. (2005). "The progressive nature of Wallerian degeneration in wild-type and slow Wallerian degeneration (WldS) nerves." BMC Neurosci **6**: 6.
Berkelaar, M., D. B. Clarke, et al. (1994). "Axotomy results in delayed death and apoptosis of retinal ganglion cells in adult rats." J Neurosci **14**(7): 4368-74.
Berry, M. (1982). "Post-injury myelin-breakdown products inhibit axonal growth: an hypothesis to explain the failure of axonal regeneration in the mammalian central nervous system." Bibl Anat(23): 1-11.
Berry, M., J. Carlile, et al. (1996). "Peripheral nerve explants grafted into the vitreous body of the eye promote the regeneration of retinal ganglion cell axons severed in the optic nerve." J Neurocytol **25**(2): 147-70.
Berry, M., J. Carlile, et al. (1999). "Optic nerve regeneration after intravitreal peripheral nerve implants: trajectories of axons regrowing through the optic chiasm into the optic tracts." J Neurocytol **28**(9): 721-41.
Berry, M., A. M. Gonzalez, et al. (2001). "Sustained effects of gene-activated matrices after CNS injury." Molecular & Cellular Neurosciences **17**(4): 706-16.
Berry, M. and A. Logan (1999). CNS injuries : cellular responses and pharmacological strategies. Boca Raton ; London, CRC Press.
Blight, A. R. (1985). "Delayed demyelination and macrophage invasion: a candidate for secondary cell damage in spinal cord injury." Cent Nerv Syst Trauma **2**(4): 299-315.
Blits, B., M. Oudega, et al. (2003). "Adeno-associated viral vector-mediated neurotrophin gene transfer in the injured adult rat spinal cord improves hind-limb function." Neuroscience **118**(1): 271-281.
Blochl, A. and R. Blochl (2007). "A cell-biological model of p75NTR signaling." Journal of Neurochemistry **102**(2): 289-305.
Boudreau, R. L. and B. L. Davidson (2010). "RNAi therapeutics for CNS disorders." Brain Res **1338**: 112-21.
Boyd, J. G. and T. Gordon (2003). "Neurotrophic factors and their receptors in axonal regeneration and functional recovery after peripheral nerve injury." Mol Neurobiol **27**(3): 277-324.
Bradbury, E. J., S. Khemani, et al. (1999). "NT-3 promotes growth of lesioned adult rat sensory axons ascending in the dorsal columns of the spinal cord." Eur J Neurosci **11**(11): 3873-83.
Brahmachari, S., Y. K. Fung, et al. (2006). "Induction of glial fibrillary acidic protein expression in astrocytes by nitric oxide." J Neurosci **26**(18): 4930-9.
Bridge, K. E., N. Berg, et al. (2009). "Late onset distal axonal swelling in YFP-H transgenic mice." Neurobiol Aging **30**(2): 309-21.
Brodbelt, A. R. and M. A. Stoodley (2003). "Post-traumatic syringomyelia: a review." J Clin Neurosci **10**(4): 401-8.
Broekman, M. L. D., L. A. Comer, et al. (2006). "Adeno-associated virus vectors serotyped with AAV8 capsid are more efficient than AAV-1 or -2 serotypes for widespread gene delivery to the neonatal mouse brain." Neuroscience **138**(2): 501-10.
Byrod, G., B. Rydevik, et al. (2000). "Transport of epidurally applied horseradish peroxidase to the endoneurial space of dorsal root ganglia: a light and electron microscopic study." J Peripher Nerv Syst **5**(4): 218-26.
Cafferty, W. B. J., A. W. McGee, et al. (2008). "Axonal growth therapeutics: regeneration or sprouting or plasticity?" Trends in Neurosciences **31**(5): 215-220.
Cannon, J. R., T. Sew, et al. (2011). "Pseudotype-dependent lentiviral transduction of astrocytes or neurons in the rat substantia nigra." Exp Neurol **228**(1): 41-52.
Caroni, P. and M. E. Schwab (1988). "Antibody against myelin-associated inhibitor of neurite growth neutralizes nonpermissive substrate properties of CNS white matter." Neuron **1**(1): 85-96.

Chamberlin, N. L., B. Du, et al. (1998). "Recombinant adeno-associated virus vector: use for transgene expression and anterograde tract tracing in the CNS." Brain Research **793**(1-2): 169-175.

Chan, C. C. (2008). "Inflammation: beneficial or detrimental after spinal cord injury?" Recent Pat CNS Drug Discov **3**(3): 189-99.

Chao, M. V. (1994). "The p75 neurotrophin receptor." J Neurobiol **25**(11): 1373-85.

Chew, D. J., V. H. Leinster, et al. (2008). "Cell death after dorsal root injury." Neurosci Lett **433**(3): 231-4.

Chierzi, S., G. M. Ratto, et al. (2005). "The ability of axons to regenerate their growth cones depends on axonal type and age, and is regulated by calcium, cAMP and ERK." Eur J Neurosci **21**(8): 2051-62.

Chiu, W. T., H. C. Lin, et al. (2010). "Review paper: epidemiology of traumatic spinal cord injury: comparisons between developed and developing countries." Asia Pac J Public Health **22**(1): 9-18.

Chivatakarn, O., S. Kaneko, et al. (2007). "The Nogo-66 receptor NgR1 is required only for the acute growth cone-collapsing but not the chronic growth-inhibitory actions of myelin inhibitors." J Neurosci **27**(27): 7117-24.

Cohen, S. (1960). "PURIFICATION OF A NERVE-GROWTH PROMOTING PROTEIN FROM THE MOUSE SALIVARY GLAND AND ITS NEURO-CYTOTOXIC ANTISERUM." Proc Natl Acad Sci U S A **46**(3): 302-11.

Craigie, E. H., J. R. M. Innes, et al. (1963). Craigie's neuroanatomy of the rat. New York, Academic Press.

Curtis, R., J. R. Tonra, et al. (1998). "Neuronal Injury Increases Retrograde Axonal Transport of the Neurotrophins to Spinal Sensory Neurons and Motor Neurons via Multiple Receptor Mechanisms." Molecular and Cellular Neuroscience **12**(3): 105-118.

David, S. and A. Kroner (2011). "Repertoire of microglial and macrophage responses after spinal cord injury." Nat Rev Neurosci **12**(7): 388-99.

Davies, S. J., M. T. Fitch, et al. (1997). "Regeneration of adult axons in white matter tracts of the central nervous system." Nature **390**(6661): 680-3.

Daya, S. and K. I. Berns (2008). "Gene therapy using adeno-associated virus vectors." Clin Microbiol Rev **21**(4): 583-93.

De la Calle, J. L. and C. L. Paíno (2002). "A procedure for direct lumbar puncture in rats." Brain Research Bulletin **59**(3): 245-250.

Dergham, P., B. Ellezam, et al. (2002). "Rho signaling pathway targeted to promote spinal cord repair." J Neurosci **22**(15): 6570-7.

Dijkhuizen, P. A., W. T. Hermens, et al. (1997). "Adenoviral vector-directed expression of neurotrophin-3 in rat dorsal root ganglion explants results in a robust neurite outgrowth response." Journal of Neurobiology **33**(2): 172-84.

Dijkstra, C. D., E. A. Dopp, et al. (1985). "The heterogeneity of mononuclear phagocytes in lymphoid organs: distinct macrophage subpopulations in the rat recognized by monoclonal antibodies ED1, ED2 and ED3." Immunology **54**(3): 589-99.

Dijkstra, S., E. J. Geisert, et al. (2000). "Up-regulation of CD81 (target of the antiproliferative antibody; TAPA) by reactive microglia and astrocytes after spinal cord injury in the rat." J Comp Neurol **428**(2): 266-77.

Dou, F., L. Huang, et al. (2009). "Temporospatial expression and cellular localization of oligodendrocyte myelin glycoprotein (OMgp) after traumatic spinal cord injury in adult rats." J Neurotrauma **26**(12): 2299-311.

Douglas, M. R., K. C. Morrison, et al. (2009). "Off-target effects of epidermal growth factor receptor antagonists mediate retinal ganglion cell disinhibited axon growth." Brain **132**(Pt 11): 3102-21.

Du, C., D. M. Yang, et al. (2010). "Neuronal differentiation of PC12 cells induced by sciatic nerve and optic nerve conditioned medium." Chin Med J (Engl) **123**(3): 351-5.
Duan, D., Y. Yue, et al. (2000). "Endosomal processing limits gene transfer to polarized airway epithelia by adeno-associated virus." J Clin Invest **105**(11): 1573-87.
Duffy, P., A. Schmandke, et al. (2009). "Rho-associated kinase II (ROCKII) limits axonal growth after trauma within the adult mouse spinal cord." J Neurosci **29**(48): 15266-76.
Dusart, I. and M. E. Schwab (1994). "Secondary cell death and the inflammatory reaction after dorsal hemisection of the rat spinal cord." Eur J Neurosci **6**(5): 712-24.
Dyck, P. J., S. Peroutka, et al. (1997). "Intradermal recombinant human nerve growth factor induces pressure allodynia and lowered heat-pain threshold in humans." Neurology **48**(2): 501-5.
Ehlert, E. M., R. Eggers, et al. (2010). "Cellular toxicity following application of adeno-associated viral vector-mediated RNA interference in the nervous system." BMC Neurosci **11**: 20.
Elsabahy, M., A. Nazarali, et al. (2011). "Non-viral nucleic acid delivery: key challenges and future directions." Curr Drug Deliv **8**(3): 235-44.
Eriksdotter Jonhagen, M., A. Nordberg, et al. (1998). "Intracerebroventricular infusion of nerve growth factor in three patients with Alzheimer's disease." Dement Geriatr Cogn Disord **9**(5): 246-57.
Fan, Y.-M., C.-P. Pang, et al. (2008). "Marked effect of RhoA-specific shRNA-producing plasmids on neurite growth in PC12 cells." Neuroscience Letters **440**(2): 170-175.
Farhadi, H. F., S. J. Mowla, et al. (2000). "Neurotrophin-3 sorts to the constitutive secretory pathway of hippocampal neurons and is diverted to the regulated secretory pathway by coexpression with brain-derived neurotrophic factor." J Neurosci **20**(11): 4059-68.
Fehlings, M. G., N. Theodore, et al. (2011). "A Phase I/IIa Clinical Trial of a Recombinant Rho Protein Antagonist in Acute Spinal Cord Injury." J Neurotrauma **28**(5): 787-96.
Ferrari, F. K., T. Samulski, et al. (1996). "Second-strand synthesis is a rate-limiting step for efficient transduction by recombinant adeno-associated virus vectors." J Virol **70**(5): 3227-34.
Fischer, D., Z. He, et al. (2004). "Counteracting the Nogo receptor enhances optic nerve regeneration if retinal ganglion cells are in an active growth state." Journal of Neuroscience **24**(7): 1646-51.
Fischer, G., S. Kostic, et al. (2011). "Direct injection into the dorsal root ganglion: Technical, behavioral, and histological observations." J Neurosci Methods **199**(1): 43-55.
Fitch, M. T. and J. Silver (2008). "CNS injury, glial scars, and inflammation: Inhibitory extracellular matrices and regeneration failure." Exp Neurol **209**(2): 294-301.
Fleming, J., S. L. Ginn, et al. (2001). "Adeno-associated virus and lentivirus vectors mediate efficient and sustained transduction of cultured mouse and human dorsal root ganglia sensory neurons." Hum Gene Ther **12**(1): 77-86.
Fortun, J., R. Puzis, et al. (2009). "Muscle injection of AAV-NT3 promotes anatomical reorganization of CST axons and improves behavioral outcome following SCI." J Neurotrauma **26**(7): 941-53.
Fournier, A. E., G. C. Gould, et al. (2002). "Truncated soluble Nogo receptor binds Nogo-66 and blocks inhibition of axon growth by myelin." J Neurosci **22**(20): 8876-83.
Fournier, A. E., T. GrandPre, et al. (2001). "Identification of a receptor mediating Nogo-66 inhibition of axonal regeneration." Nature **409**(6818): 341-6.
Foust, K. D., A. Poirier, et al. (2008). "Neonatal intraperitoneal or intravenous injections of recombinant adeno-associated virus type 8 transduce dorsal root ganglia and lower motor neurons." Human Gene Therapy **19**(1): 61-69.
Funakoshi, H., J. Frisen, et al. (1993). "Differential expression of mRNAs for neurotrophins and their receptors after axotomy of the sciatic nerve." Journal of Cell Biology **123**(2): 455-65.
Galtrey, C. M. and J. W. Fawcett (2007). "The role of chondroitin sulfate proteoglycans in regeneration and plasticity in the central nervous system." Brain Res Rev **54**(1): 1-18.

Gaudet, A. D., S. J. Williams, et al. (2004). "Regulation of TRPV2 by axotomy in sympathetic, but not sensory neurons." Brain Research **1017**(1-2): 155-162.
Gavazzi, I., R. D. Kumar, et al. (1999). "Growth responses of different subpopulations of adult sensory neurons to neurotrophic factors in vitro." Eur J Neurosci **11**(10): 3405-14.
Geraldo, S. and P. R. Gordon-Weeks (2009). "Cytoskeletal dynamics in growth-cone steering." J Cell Sci **122**(Pt 20): 3595-604.
Gharabaghi, A. and M. Tatagiba (2005). "Functional regeneration of the axotomized auditory nerve with combined neurotrophic and anti-inhibitory strategies." Acta Neurochir Suppl **93**: 89-91.
Gillani, R. L., S. Y. Tsai, et al. (2010). "Cognitive recovery in the aged rat after stroke and anti-Nogo-A immunotherapy." Behav Brain Res **208**(2): 415-24.
Glover, D. J., H. J. Lipps, et al. (2005). "Towards safe, non-viral therapeutic gene expression in humans." Nat Rev Genet **6**(4): 299-310.
Gluzman, Y. (1981). "SV40-transformed simian cells support the replication of early SV40 mutants." Cell **23**(1): 175-82.
Goncalves, M. A. F. V. (2005). "Adeno-associated virus: from defective virus to effective vector." Virology Journal **2**: 43.
Gong, Y., Y. Tagawa, et al. (2002). "Localization of major gangliosides in the PNS: implications for immune neuropathies." Brain **125**(Pt 11): 2491-506.
Gonzalez, A. M., M. Berry, et al. (2006). "Matrix-mediated gene transfer to brain cortex and dorsal root ganglion neurones by retrograde axonal transport after dorsal column lesion." Journal of Gene Medicine **8**(7): 901-9.
GrandPre, T., S. Li, et al. (2002). "Nogo-66 receptor antagonist peptide promotes axonal regeneration." Nature **417**(6888): 547-51.
Guo, Q., S. Li, et al. (2007). "Expression of oligodendrocyte myelin glycoprotein and its receptor NgR after the injury of rat central nervous system." Neurosci Lett **422**(2): 103-8.
Hallbook, F., C. F. Ibanez, et al. (1991). "Evolutionary studies of the nerve growth factor family reveal a novel member abundantly expressed in Xenopus ovary." Neuron **6**(5): 845-58.
Haller, F. R., C. Haller, et al. (1972). "The fine structure of cellular layers and connective tissue space at spinal nerve root attachments in the rat." Am J Anat **133**(1): 109-23.
Hamburger, V. (1934). "The effects of wing bud extirpation on the development of the central nervous system in chick embryos." Journal of Experimental Zoology **68**(3): 449-494.
Hanani, M. (2005). "Satellite glial cells in sensory ganglia: from form to function." Brain Res Brain Res Rev **48**(3): 457-76.
Hansson, E. (2006). "Could chronic pain and spread of pain sensation be induced and maintained by glial activation?" Acta Physiol (Oxf) **187**(1-2): 321-7.
Harper, A. A. and S. N. Lawson (1985). "Conduction velocity is related to morphological cell type in rat dorsal root ganglion neurones." J Physiol **359**: 31-46.
Harvey, A. R., M. Hellstrom, et al. (2009). "Gene therapy and transplantation in the retinofugal pathway." Prog Brain Res **175**: 151-61.
Heumann, R., D. Lindholm, et al. (1987). "Differential regulation of mRNA encoding nerve growth factor and its receptor in rat sciatic nerve during development, degeneration, and regeneration: role of macrophages." Proc Natl Acad Sci U S A **84**(23): 8735-9.
Hiltunen, J. O., A. Laurikainen, et al. (2005). "Neurotrophin-3 is a target-derived neurotrophic factor for penile erection-inducing neurons." Neuroscience **133**(1): 51-8.
Himango, W. A. and F. N. Low (1971). "The fine structure of a lateral recess of the subarachnoid space in the rat." Anat Rec **171**(1): 1-19.
Hu, P., A. L. Bembrick, et al. (2007). "Immune cell involvement in dorsal root ganglia and spinal cord after chronic constriction or transection of the rat sciatic nerve." Brain Behav Immun **21**(5): 599-616.

Hu, P. and E. M. McLachlan (2003). "Distinct functional types of macrophage in dorsal root ganglia and spinal nerves proximal to sciatic and spinal nerve transections in the rat." Exp Neurol **184**(2): 590-605.

Huang, E. J. and L. F. Reichardt (2001). "NEUROTROPHINS: Roles in Neuronal Development and Function1." Annual Review of Neuroscience **24**(1): 677-736.

Huang, E. J. and L. F. Reichardt (2003). "TRK RECEPTORS: ROLES IN NEURONAL SIGNAL TRANSDUCTION *." Annual Review of Biochemistry **72**(1): 609-642.

Huber, A. B., O. Weinmann, et al. (2002). "Patterns of Nogo mRNA and protein expression in the developing and adult rat and after CNS lesions." J Neurosci **22**(9): 3553-67.

Huebner, E. A. and S. M. Strittmatter (2009). "Axon regeneration in the peripheral and central nervous systems." Results Probl Cell Differ **48**: 339-51.

Hunt, D., R. S. Coffin, et al. (2002). "The Nogo receptor, its ligands and axonal regeneration in the spinal cord; a review." J Neurocytol **31**(2): 93-120.

ICCP. (2010). "www.campaignforcure.org accessed on 9/4/2010."

Jamieson, S. M. F., J. Liu, et al. (2005). "Oxaliplatin causes selective atrophy of a subpopulation of dorsal root ganglion neurons without inducing cell loss." Cancer Chemotherapy and Pharmacology **56**(4): 391-399.

Jing, S., P. Tapley, et al. (1992). "Nerve growth factor mediates signal transduction through trk homodimer receptors." Neuron **9**(6): 1067-1079.

Kadoya, K., S. Tsukada, et al. (2009). "Combined intrinsic and extrinsic neuronal mechanisms facilitate bridging axonal regeneration one year after spinal cord injury." Neuron **64**(2): 165-72.

Kaisho, Y., K. Yoshimura, et al. (1990). "Cloning and expression of a cDNA encoding a novel human neurotrophic factor." FEBS Lett **266**(1-2): 187-91.

Kashiba, H., K. Noguchi, et al. (1995). "Coexpression of trk family members and low-affinity neurotrophin receptors in rat dorsal root ganglion neurons." Molecular Brain Research **30**(1): 158-164.

Kashiba, H., Y. Ueda, et al. (1996). "Coexpression of preprotachykinin-A, [alpha]-calcitonin gene-related peptide, somatostatin, and neurotrophin receptor family messenger RNAs in rat dorsal root ganglion neurons." Neuroscience **70**(1): 179-189.

Kerschensteiner, M., M. E. Schwab, et al. (2005). "In vivo imaging of axonal degeneration and regeneration in the injured spinal cord." Nat Med **11**(5): 572-7.

Kiernan, J. A. (1979). "Hypotheses concerned with axonal regeneration in the mammalian nervous system." Biol Rev Camb Philos Soc **54**(2): 155-97.

Kiernan, J. A. (2007). "Histochemistry of Staining Methods for Normal and Degenerating Myelin in the Central and Peripheral Nervous Systems." The Journal of Histotechnology **30**(2).

Kieseier, B. C., H. P. Hartung, et al. (2006). "Immune circuitry in the peripheral nervous system." Curr Opin Neurol **19**(5): 437-45.

Kim, C. F. and G. Moalem-Taylor (2011). "Detailed characterization of neuro-immune responses following neuropathic injury in mice." Brain Res **1405**: 95-108.

Kim, J. E., B. P. Liu, et al. (2004). "Nogo-66 receptor prevents raphespinal and rubrospinal axon regeneration and limits functional recovery from spinal cord injury." Neuron **44**(3): 439-51.

Kimpinski, K., R. B. Campenot, et al. (1997). "Effects of the neurotrophins nerve growth factor, neurotrophin-3, and brain-derived neurotrophic factor (BDNF) on neurite growth from adult sensory neurons in compartmented cultures." Journal of Neurobiology **33**(4): 395-410.

Klein, R. L., R. D. Dayton, et al. (2006). "Efficient Neuronal Gene Transfer with AAV8 Leads to Neurotoxic Levels of Tau or Green Fluorescent Proteins." Mol Ther **13**(3): 517-527.

Klein, R. L., M. E. Hamby, et al. (2002). "Measurements of vector-derived neurotrophic factor and green fluorescent protein levels in the brain." Methods **28**(2): 286-92.

Koprivica, V., K.-S. Cho, et al. (2005). "EGFR activation mediates inhibition of axon regeneration by myelin and chondroitin sulfate proteoglycans.[see comment]." Science **310**(5745): 106-10.

Krestel, H. E., A. L. Mihaljevic, et al. (2004). "Neuronal co-expression of EGFP and beta-galactosidase in mice causes neuropathology and premature death." Neurobiol Dis **17**(2): 310-8.

Krewson, C. E. and W. M. Saltzman (1996). "Transport and elimination of recombinant human NGF during long-term delivery to the brain." Brain Res **727**(1-2): 169-81.

Kuhlmann, T., A. Bitsch, et al. (2001). "Macrophages are eliminated from the injured peripheral nerve via local apoptosis and circulation to regional lymph nodes and the spleen." J Neurosci **21**(10): 3401-8.

Kuo, L.-T., A. Simpson, et al. (2005). "Effects of systemically administered NT-3 on sensory neuron loss and nestin expression following axotomy." Journal of Comparative Neurology **482**(4): 320-32.

Kusano, K., M. Enomoto, et al. (2011). "Enhancement of sciatic nerve regeneration by adenovirus-mediated expression of dominant negative RhoA and Rac1." Neurosci Lett **492**(1): 64-9.

Kwon, B. K., T. R. Oxland, et al. (2002). "Animal models used in spinal cord regeneration research." Spine (Phila Pa 1976) **27**(14): 1504-10.

Lagord, C., M. Berry, et al. (2002). "Expression of TGFbeta2 but not TGFbeta1 correlates with the deposition of scar tissue in the lesioned spinal cord." Molecular & Cellular Neurosciences **20**(1): 69-92.

LaMotte, C. C., S. E. Kapadia, et al. (1991). "Central projections of the sciatic, saphenous, median, and ulnar nerves of the rat demonstrated by transganglionic transport of choleragenoid-HRP (B-HRP) and wheat germ agglutinin-HRP (WGA-HRP)." J Comp Neurol **311**(4): 546-62.

Landon, D. N. (1976). The peripheral nerve. London, Chapman and Hall [etc.].

Leclere, P. G., A. Panjwani, et al. (2005). "Effective gene delivery to adult neurons by a modified form of electroporation." J Neurosci Methods **142**(1): 137-43.

Lee, R., P. Kermani, et al. (2001). "Regulation of cell survival by secreted proneurotrophins." Science **294**(5548): 1945-8.

Levi-Montalcini, R. (1987). "The nerve growth factor: thirty-five years later.[erratum appears in EMBO J 1987 Sep;6(9):2856]." EMBO Journal **6**(5): 1145-54.

Levi-Montalcini, R., H. Meyer, et al. (1954). "In vitro experiments on the effects of mouse sarcomas 180 and 37 on the spinal and sympathetic ganglia of the chick embryo." Cancer Res **14**(1): 49-57.

Li, S., B. P. Liu, et al. (2004). "Blockade of Nogo-66, myelin-associated glycoprotein, and oligodendrocyte myelin glycoprotein by soluble Nogo-66 receptor promotes axonal sprouting and recovery after spinal injury." J Neurosci **24**(46): 10511-20.

Link, C. D., V. Fonte, et al. (2006). "Conversion of Green Fluorescent Protein into a Toxic, Aggregation-prone Protein by C-terminal Addition of a Short Peptide." Journal of Biological Chemistry **281**(3): 1808-1816.

Liot, G., C. Gabriel, et al. (2004). "Neurotrophin-3-induced PI-3 kinase/Akt signaling rescues cortical neurons from apoptosis." Exp Neurol **187**(1): 38-46.

Liu, H., I. J. Llewellyn-Smith, et al. (1995). "Co-injection of wheat germ agglutinin-HRP and choleragenoid-HRP into the sciatic nerve of the rat blocks transganglionic transport." J Histochem Cytochem **43**(5): 489-95.

Liu, K., A. Tedeschi, et al. (2011). "Neuronal Intrinsic Mechanisms of Axon Regeneration." Annu Rev Neurosci.

Liu, Y., B. T. Himes, et al. (1999). "Intraspinal delivery of neurotrophin-3 using neural stem cells genetically modified by recombinant retrovirus." Exp Neurol **158**(1): 9-26.

Llorens, F., V. Gil, et al. (2011). "Emerging functions of myelin-associated proteins during development, neuronal plasticity, and neurodegeneration." FASEB J **25**(2): 463-75.

Lo, W. D., G. Qu, et al. (1999). "Adeno-associated virus-mediated gene transfer to the brain: duration and modulation of expression." Hum Gene Ther **10**(2): 201-13.

Logan, A., Z. Ahmed, et al. (2006). "Neurotrophic factor synergy is required for neuronal survival and disinhibited axon regeneration after CNS injury." Brain **129**(Pt 2): 490-502.
Logan, A., J. Green, et al. (1999). "Inhibition of glial scarring in the injured rat brain by a recombinant human monoclonal antibody to transforming growth factor-beta2." European Journal of Neuroscience **11**(7): 2367-74.
Lord-Fontaine, S., F. Yang, et al. (2008). "Local inhibition of Rho signaling by cell-permeable recombinant protein BA-210 prevents secondary damage and promotes functional recovery following acute spinal cord injury." J Neurotrauma **25**(11): 1309-22.
Lorenz, W. W., M. J. Cormier, et al. (1996). "Expression of the Renilla reniformis luciferase gene in mammalian cells." J Biolumin Chemilumin **11**(1): 31-7.
Lu, B. T., W. Yuan, et al. (2010). "Lentiviral vector-mediated RNA interfere gene Nogo receptor to repair spinal cord injury." Zhonghua Wai Ke Za Zhi **48**(20): 1573-6.
Lu, P., L. L. Jones, et al. (2005). "BDNF-expressing marrow stromal cells support extensive axonal growth at sites of spinal cord injury." Exp Neurol **191**(2): 344-60.
Lu, P. and M. H. Tuszynski (2008). "Growth factors and combinatorial therapies for CNS regeneration." Experimental Neurology **209**(2): 313-320.
Lu, S.-G., X. Zhang, et al. (2006). "Intracellular calcium regulation among subpopulations of rat dorsal root ganglion neurons." The Journal of Physiology **577**(1): 169-190.
Lu, X. and P. M. Richardson (1991). "Inflammation near the nerve cell body enhances axonal regeneration." J Neurosci **11**(4): 972-8.
Lu, X. and P. M. Richardson (1993). "Responses of macrophages in rat dorsal root ganglia following peripheral nerve injury." J Neurocytol **22**(5): 334-41.
Maisonpierre, P. C., L. Belluscio, et al. (1990). "Neurotrophin-3: A Neurotrophic Factor Related to NGF and BDNF." Science **247**(4949): 1446-1451.
Maisonpierre, P. C., M. M. Le Beau, et al. (1991). "Human and rat brain-derived neurotrophic factor and neurotrophin-3: gene structures, distributions, and chromosomal localizations." Genomics **10**(3): 558-68.
Marks Jr, W. J., J. L. Ostrem, et al. (2008). "Safety and tolerability of intraputaminal delivery of CERE-120 (adeno-associated virus serotype 2-neurturin) to patients with idiopathic Parkinson's disease: an open-label, phase I trial." The Lancet Neurology **7**(5): 400-408.
Mason, M. R., E. M. Ehlert, et al. (2010). "Comparison of AAV serotypes for gene delivery to dorsal root ganglion neurons." Mol Ther **18**(4): 715-24.
Mawhinney, R. M. and B. E. Staveley (2011). "Expression of GFP can influence aging and climbing ability in Drosophila." Genet Mol Res **10**(1): 494-505.
McCarty, D. M., P. E. Monahan, et al. (2001). "Self-complementary recombinant adeno-associated virus (scAAV) vectors promote efficient transduction independently of DNA synthesis." Gene Ther **8**(16): 1248-54.
McDonald, J. W. and C. Sadowsky (2002). "Spinal-cord injury." The Lancet **359**(9304): 417-425.
McFadden, G., M. R. Mohamed, et al. (2009). "Cytokine determinants of viral tropism." Nat Rev Immunol **9**(9): 645-55.
McKay Hart, A., T. Brannstrom, et al. (2002). "Primary sensory neurons and satellite cells after peripheral axotomy in the adult rat: timecourse of cell death and elimination." Exp Brain Res **142**(3): 308-18.
McLachlan, E. M., W. Janig, et al. (1993). "Peripheral nerve injury triggers noradrenergic sprouting within dorsal root ganglia." Nature **363**(6429): 543-6.
McPhail, L. T., D. P. Stirling, et al. (2004). "The contribution of activated phagocytes and myelin degeneration to axonal retraction/dieback following spinal cord injury." Eur J Neurosci **20**(8): 1984-94.
McQuarrie, I. G. and B. Grafstein (1973). "Axon outgrowth enhanced by a previous nerve injury." Arch Neurol **29**(1): 53-5.

Medawar, P. B. (1948). "Immunity to homologous grafted skin; the fate of skin homografts transplanted to the brain, to subcutaneous tissue, and to the anterior chamber of the eye." Br J Exp Pathol **29**(1): 58-69.

Mendell, L. M., J. B. Munson, et al. (2001). "Neurotrophins and synaptic plasticity in the mammalian spinal cord." J Physiol **533**(Pt 1): 91-7.

Merajver, S. D. and S. Z. Usmani (2005). "Multifaceted role of Rho proteins in angiogenesis." J Mammary Gland Biol Neoplasia **10**(4): 291-8.

Mi, S., X. Lee, et al. (2004). "LINGO-1 is a component of the Nogo-66 receptor/p75 signaling complex." Nat Neurosci **7**(3): 221-8.

Miyagoe-Suzuki, Y. and S. Takeda (2010). "Gene therapy for muscle disease." Exp Cell Res **316**(18): 3087-92.

Mohiuddin, L., K. Fernandez, et al. (1995). "Nerve growth factor and neurotrophin-3 enhance neurite outgrowth and up-regulate the levels of messenger RNA for growth-associated protein GAP-43 and T alpha 1 alpha-tubulin in cultured adult rat sensory neurones." Neuroscience Letters **185**(1): 20-3.

Mukhopadhyay, G., P. Doherty, et al. (1994). "A novel role for myelin-associated glycoprotein as an inhibitor of axonal regeneration." Neuron **13**(3): 757-67.

Muller, M., C. Leonhard, et al. (2010). "On the longevity of resident endoneurial macrophages in the peripheral nervous system: a study of physiological macrophage turnover in bone marrow chimeric mice." J Peripher Nerv Syst **15**(4): 357-65.

Murata, Y., B. Rydevik, et al. (2005). "Incision of the intervertebral disc induces disintegration and increases permeability of the dorsal root ganglion capsule." Spine (Phila Pa 1976) **30**(15): 1712-6.

Murphy, K. P., P. Travers, et al. (2008). Janeway's immunobiology. New York, Garland Science ; London : Taylor & Francis [distributor].

Nakahara, Y., F. H. Gage, et al. (1996). "Grafts of fibroblasts genetically modified to secrete NGF, BDNF, NT-3, or basic fgf elicit differential responses in the adult spinal cord." Cell Transplantation **5**(2): 191-204.

Nashmi, R. and M. G. Fehlings (2001). "Changes in axonal physiology and morphology after chronic compressive injury of the rat thoracic spinal cord." Neuroscience **104**(1): 235-51.

Natalie, J. G., B. J. C. William, et al. (2002). "Expression of gp130 and leukaemia inhibitory factor receptor subunits in adult rat sensory neurones: regulation by nerve injury." Journal of Neurochemistry **83**(1): 100-109.

Nauta, H. J., J. C. Wehman, et al. (1999). "Intraventricular infusion of nerve growth factor as the cause of sympathetic fiber sprouting in sensory ganglia." J Neurosurg **91**(3): 447-53.

Neumann, S. and C. J. Woolf (1999). "Regeneration of dorsal column fibers into and beyond the lesion site following adult spinal cord injury.[see comment]." Neuron **23**(1): 83-91.

Olejniczak, M., P. Galka, et al. (2010). "Sequence-non-specific effects of RNA interference triggers and microRNA regulators." Nucleic Acids Res **38**(1): 1-16.

Pajusola, K., M. Gruchala, et al. (2002). "Cell-type-specific characteristics modulate the transduction efficiency of adeno-associated virus type 2 and restrain infection of endothelial cells." J Virol **76**(22): 11530-40.

Pannese, E. (1994). Neurocytology : fine structure of neurons, nerve processes, and neuroglial cells. Stuttgart, Thieme.

Park, J. B., G. Yiu, et al. (2005). "A TNF receptor family member, TROY, is a coreceptor with Nogo receptor in mediating the inhibitory activity of myelin inhibitors." Neuron **45**(3): 345-51.

Park, K. K., K. Liu, et al. (2010). "PTEN/mTOR and axon regeneration." Exp Neurol **223**(1): 45-50.

Park, K. K., K. Liu, et al. (2008). "Promoting axon regeneration in the adult CNS by modulation of the PTEN/mTOR pathway." Science **322**(5903): 963-6.

Patapoutian, A. and L. F. Reichardt (2001). "Trk receptors: mediators of neurotrophin action." Current Opinion in Neurobiology **11**(3): 272-280.
Petruska, J. C., B. Kitay, et al. (2010). "Intramuscular AAV delivery of NT-3 alters synaptic transmission to motoneurons in adult rats." Eur J Neurosci **32**(6): 997-1005.
Pille, J. Y., C. Denoyelle, et al. (2005). "Anti-RhoA and anti-RhoC siRNAs inhibit the proliferation and invasiveness of MDA-MB-231 breast cancer cells in vitro and in vivo." Mol Ther **11**(2): 267-74.
Properzi, F., R. A. Asher, et al. (2003). "Chondroitin sulphate proteoglycans in the central nervous system: changes and synthesis after injury." Biochem Soc Trans **31**(2): 335-6.
Qi, J., K. Buzas, et al. (2011). "Painful pathways induced by TLR stimulation of dorsal root ganglion neurons." J Immunol **186**(11): 6417-26.
Raisman, G., W. M. Cowan, et al. (1966). "An experimental analysis of the efferent projection of the hippocampus." Brain **89**(1): 83-108.
Ramon y Cajal, S. (1890). "À quelle époque apparaissent les expansions des cellules nerveuses de la moëlle épinière du poulet? ." Anatomomischner Anzeiger **21**: 609-639.
Ramon y Cajal, S. (1991). Cajal's degeneration and regeneration of the nervous system. New York ; Oxford, Oxford University Press.
Ransohoff, R. M. and V. H. Perry (2009). "Microglial Physiology: Unique Stimuli, Specialized Responses." Annual Review of Immunology **27**(1): 119-145.
Raper, S. E., N. Chirmule, et al. (2003). "Fatal systemic inflammatory response syndrome in a ornithine transcarbamylase deficient patient following adenoviral gene transfer." Mol Genet Metab **80**(1-2): 148-58.
Reichardt, L. F. (2006). "Neurotrophin-regulated signalling pathways." Philosophical Transactions of the Royal Society of London - Series B: Biological Sciences **361**(1473): 1545-64.
Richardson, B. C., N. D. Lalwani, et al. (1994). "Fas ligation triggers apoptosis in macrophages but not endothelial cells." Eur J Immunol **24**(11): 2640-5.
Richardson, P. M. and V. M. Issa (1984). "Peripheral injury enhances central regeneration of primary sensory neurones." Nature **309**(5971): 791-3.
Richardson, P. M., U. M. McGuinness, et al. (1980). "Axons from CNS neurons regenerate into PNS grafts." Nature **284**(5753): 264-5.
Ruitenberg, M. J., D. B. Levison, et al. (2005). "NT-3 expression from engineered olfactory ensheathing glia promotes spinal sparing and regeneration." Brain **128**(Pt 4): 839-53.
Sandvig, A., M. Berry, et al. (2004). "Myelin-, reactive glia-, and scar-derived CNS axon growth inhibitors: expression, receptor signaling, and correlation with axon regeneration." GLIA **46**(3): 225-51.
Schmalbruch, H. (1987). "The number of neurons in dorsal root ganglia L4-L6 of the rat." Anat Rec **219**(3): 315-22.
Schmandke, A. and S. M. Strittmatter (2007). "ROCK and Rho: biochemistry and neuronal functions of Rho-associated protein kinases." Neuroscientist **13**(5): 454-69.
Schnell, L., R. Schneider, et al. (1994). "Neurotrophin-3 enhances sprouting of corticospinal tract during development and after adult spinal cord lesion." Nature **367**(6459): 170-3.
Scholz, J. and C. J. Woolf (2007). "The neuropathic pain triad: neurons, immune cells and glia." Nat Neurosci **10**(11): 1361-8.
Schuster, P., J. B. Boscheinen, et al. (2011). "The Role of Plasmacytoid Dendritic Cells in Innate and Adaptive Immune Responses against Alpha Herpes Virus Infections." Advances in Virology **2011**.
Shaner, N. C., P. A. Steinbach, et al. (2005). "A guide to choosing fluorescent proteins." Nat Methods **2**(12): 905-9.
Shi, T. J., T. Tandrup, et al. (2001). "Effect of peripheral nerve injury on dorsal root ganglion neurons in the C57 BL/6J mouse: marked changes both in cell numbers and neuropeptide expression." Neuroscience **105**(1): 249-63.

Silver, J. (2009). "CNS regeneration: only on one condition." Curr Biol **19**(11): R444-6.
Sims, K., Z. Ahmed, et al. (2009). "In vitro evaluation of a 'stealth' adenoviral vector for targeted gene delivery to adult mammalian neurones." J Gene Med **11**(4): 335-44.
Snider, W. D. and I. Silos-Santiago (1996). "Dorsal root ganglion neurons require functional neurotrophin receptors for survival during development." Philos Trans R Soc Lond B Biol Sci **351**(1338): 395-403.
Standring, S. and H. A. Gray (2008). Gray's anatomy : the anatomical basis of clinical practice. Edinburgh, Churchill Livingstone.
Steward, O., B. Zheng, et al. (2003). "False resurrections: Distinguishing regenerated from spared axons in the injured central nervous system." The Journal of Comparative Neurology **459**(1): 1-8.
Storek, B., M. Reinhardt, et al. (2008). "Sensory neuron targeting by self-complementary AAV8 via lumbar puncture for chronic pain." Proc Natl Acad Sci U S A **105**(3): 1055-60.
Storek, B., M. Reinhardt, et al. (2008). "Sensory neuron targeting by self-complementary AAV8 via lumbar puncture for chronic pain." Proceedings of the National Academy of Sciences of the United States of America **105**(3): 1055-60.
Suggate, E. L., Z. Ahmed, et al. (2009). "Optimisation of siRNA-mediated RhoA silencing in neuronal cultures." Mol Cell Neurosci **40**(4): 451-62.
Tandrup, T., C. J. Woolf, et al. (2000). "Delayed loss of small dorsal root ganglion cells after transection of the rat sciatic nerve." J Comp Neurol **422**(2): 172-80.
Tanis, K. Q., S. S. Newton, et al. (2007). "Targeting neurotrophic/growth factor expression and signaling for antidepressant drug development." CNS & Neurological Disorders Drug Targets **6**(2): 151-60.
Tatagiba, M., S. Rosahl, et al. (2002). "Regeneration of auditory nerve following complete sectioning and intrathecal application of the IN-1 antibody." Acta Neurochir (Wien) **144**(2): 181-7.
Taylor, M. D., A. S. Holdeman, et al. (2005). "Modulation of muscle spindle innervation by neurotrophin-3 following nerve injury." Exp Neurol **191**(1): 211-22.
Taylor, M. D., R. Vancura, et al. (2001). "Postnatal regulation of limb proprioception by muscle-derived neurotrophin-3." J Comp Neurol **432**(2): 244-58.
Taylor, M. D., R. Vancura, et al. (2001). "Overexpression of neurotrophin-3 in skeletal muscle alters normal and injury-induced limb control." Somatosens Mot Res **18**(4): 286-94.
Teng, F. Y. and B. L. Tang (2005). "Why do Nogo/Nogo-66 receptor gene knockouts result in inferior regeneration compared to treatment with neutralizing agents?" J Neurochem **94**(4): 865-74.
Teng, H. K., K. K. Teng, et al. (2005). "ProBDNF induces neuronal apoptosis via activation of a receptor complex of p75NTR and sortilin." Journal of Neuroscience **25**(22): 5455-63.
Terpe, K. (2003). "Overview of tag protein fusions: from molecular and biochemical fundamentals to commercial systems." Appl Microbiol Biotechnol **60**(5): 523-33.
Thomas, C. E., D. Birkett, et al. (2001). "Acute direct adenoviral vector cytotoxicity and chronic, but not acute, inflammatory responses correlate with decreased vector-mediated transgene expression in the brain." Mol Ther **3**(1): 36-46.
Tremblay, M. (1995). "The Canadian revolution in the management of spinal cord injury." Can Bull Med Hist **12**(1): 125-55.
Tsoulfas, P., D. Soppet, et al. (1993). "The rat trkC locus encodes multiple neurogenic receptors that exhibit differential response to neurotrophin-3 in PC12 cells." Neuron **10**(5): 975-90.
Tuszynski, M. H. and J. H. Kordower (2008). CNS regeneration : basic science and clinical advances. London, Academic.
Urabe, M., C. Ding, et al. (2002). "Insect cells as a factory to produce adeno-associated virus type 2 vectors." Hum Gene Ther **13**(16): 1935-43.
Vallejo, R., D. M. Tilley, et al. (2010). "The role of glia and the immune system in the development and maintenance of neuropathic pain." Pain Pract **10**(3): 167-84.

van Velzen, M., J. D. Laman, et al. (2009). "Neuron-interacting satellite glial cells in human trigeminal ganglia have an APC phenotype." J Immunol **183**(4): 2456-61.
Vargas, M. E. and B. A. Barres (2007). "Why is Wallerian degeneration in the CNS so slow?" Annu Rev Neurosci **30**: 153-79.
Verkhratski, A. N. and A. Butt (2007). Glial neurobiology : a textbook. Chichester, Wiley.
Verma, I. M. and M. D. Weitzman (2005). "Gene therapy: twenty-first century medicine." Annu Rev Biochem **74**: 711-38.
von Meyenburg, J., C. Brosamle, et al. (1998). "Regeneration and sprouting of chronically injured corticospinal tract fibers in adult rats promoted by NT-3 and the mAb IN-1, which neutralizes myelin-associated neurite growth inhibitors." Exp Neurol **154**(2): 583-94.
Vulchanova, L., D. J. Schuster, et al. (2010). "Differential adeno-associated virus mediated gene transfer to sensory neurons following intrathecal delivery by direct lumbar puncture." Mol Pain **6**: 31.
Wang, K. C., J. A. Kim, et al. (2002). "P75 interacts with the Nogo receptor as a co-receptor for Nogo, MAG and OMgp." Nature **420**(6911): 74-8.
Wang, K. C., V. Koprivica, et al. (2002). "Oligodendrocyte-myelin glycoprotein is a Nogo receptor ligand that inhibits neurite outgrowth." Nature **417**(6892): 941-4.
Wang, L., B. Hu, et al. (2009). "Glial and axonal responses in areas of Wallerian degeneration of the corticospinal and dorsal ascending tracts after spinal cord dorsal funiculotomy." Neuropathology **29**(3): 230-41.
Wang, T., J. Wang, et al. (2010). "Down-regulation of Nogo receptor promotes functional recovery by enhancing axonal connectivity after experimental stroke in rats." Brain Res **1360**: 147-58.
Wang, T. H., Q. S. Meng, et al. (2008). "NT-3 expression in spared DRG and the associated spinal laminae as well as its anterograde transport in sensory neurons following removal of adjacent DRG in cats." Neurochem Res **33**(1): 1-7.
Watson, C. (2009). The spinal cord : a Christopher and Dana Reeve Foundation text and atlas. London, Academic.
Weller, R. O., I. Galea, et al. (2010). "Pathophysiology of the lymphatic drainage of the central nervous system: Implications for pathogenesis and therapy of multiple sclerosis." Pathophysiology **17**(4): 295-306.
White, A. F., M. Mazur, et al. (2008). "Genetic modification of adeno-associated viral vector type 2 capsid enhances gene transfer efficiency in polarized human airway epithelial cells." Hum Gene Ther **19**(12): 1407-14.
Willis, W. D. and R. E. Coggeshall (2004). Sensory mechanisms of the spinal cord. New York ; London, Kluwer Academic/Plenum.
Windle, W. F. and W. W. Chambers (1950). "Regeneration in the spinal cord of the cat and dog." J Comp Neurol **93**(2): 241-57.
Windle, W. F. e. (1955). Regeneration in the central nervous system. Springfield, Charles C Thomas.
Winton, M. J., C. I. Dubreuil, et al. (2002). "Characterization of new cell permeable C3-like proteins that inactivate Rho and stimulate neurite outgrowth on inhibitory substrates." Journal of Biological Chemistry **277**(36): 32820-9.
Wright, D. E., J. M. Williams, et al. (2002). "Muscle-derived neurotrophin-3 reduces injury-induced proprioceptive degeneration in neonatal mice." J Neurobiol **50**(3): 198-208.
Wu, D., P. Yang, et al. (2009). "Targeting a dominant negative rho kinase to neurons promotes axonal outgrowth and partial functional recovery after rat rubrospinal tract lesion." Mol Ther **17**(12): 2020-30.
Wu, K., E. M. Meyer, et al. (2005). "AAV2/5-mediated NGF gene delivery protects septal cholinergic neurons following axotomy." Brain Res **1061**(2): 107-13.
Xu, S., M. Liu, et al. (2011). "Effect of lentiviral shRNA of Nogo receptor on rat cortex neuron axon outgrowth." Can J Neurol Sci **38**(1): 133-8.

Xu, Y., Y. Gu, et al. (2003). "Efficiencies of transgene expression in nociceptive neurons through different routes of delivery of adeno-associated viral vectors." Hum Gene Ther **14**(9): 897-906.

Xu, Z. L., H. Mizuguchi, et al. (2005). "Approaches to improving the kinetics of adenovirus-delivered genes and gene products." Adv Drug Deliv Rev **57**(5): 781-802.

Yiu, G. and Z. He (2006). "Glial inhibition of CNS axon regeneration." Nat Rev Neurosci **7**(8): 617-27.

Yurek, D. M., A. M. Fletcher, et al. (2009). "Long-term transgene expression in the central nervous system using DNA nanoparticles." Mol Ther **17**(4): 641-50.

Zeilig, G., M. Dolev, et al. (2000). "Long-term morbidity and mortality after spinal cord injury: 50 years of follow-up." Spinal Cord **38**(9): 563-6.

Zhang, G., V. Gurtu, et al. (1996). "An enhanced green fluorescent protein allows sensitive detection of gene transfer in mammalian cells." Biochem Biophys Res Commun **227**(3): 707-11.

Zhang, Y., P. A. Dijkhuizen, et al. (1998). "NT-3 delivered by an adenoviral vector induces injured dorsal root axons to regenerate into the spinal cord of adult rats." J Neurosci Res **54**(4): 554-62.

Zhao, Z. S. and E. Manser (2005). "PAK and other Rho-associated kinases--effectors with surprisingly diverse mechanisms of regulation." Biochem J **386**(Pt 2): 201-14.

Zheng, B., J. Atwal, et al. (2005). "Genetic deletion of the Nogo receptor does not reduce neurite inhibition in vitro or promote corticospinal tract regeneration in vivo." Proc Natl Acad Sci U S A **102**(4): 1205-10.

Zheng, H., C. Qiao, et al. (2009). "Efficient Retrograde Transport of AAV8 to Spinal Cord and Dorsal Root Ganglion after Vector Delivery in Muscle." Hum Gene Ther.

Zhou, L., B. J. Baumgartner, et al. (2003). "Neurotrophin-3 expressed in situ induces axonal plasticity in the adult injured spinal cord." J Neurosci **23**(4): 1424-31.

Zhou, X. F. and R. A. Rush (1994). "Localization of neurotrophin-3-like immunoreactivity in the rat central nervous system." Brain Res **643**(1-2): 162-72.

Zhu, J., X. Huang, et al. (2009). "The TLR9-MyD88 pathway is critical for adaptive immune responses to adeno-associated virus gene therapy vectors in mice." J Clin Invest **119**(8): 2388-98.

Zorner, B. and M. E. Schwab (2010). "Anti-Nogo on the go: from animal models to a clinical trial." Ann N Y Acad Sci **1198 Suppl 1**: E22-34.